Mikronährstoffprofile der Gerste (*Hordeum vulgare* L.): eine Analyse der natürlichen Variation, der räumlichen Verteilung und der Beladungsmechanismen

Dissertation

zur Erlangung des akademischen Grades einer

Doktorin der Naturwissenschaften (Dr. rer. nat.)

in der Bayreuther Graduiertenschule für Mathematik und Naturwissenschaften (BayNAT)

der Universität Bayreuth

vorgelegt von

Amelie Sophie Detterbeck (geb. Betzlbacher)
aus Regensburg

Bayreuth, 2019

Die vorliegende Arbeit wurde in der Zeit von April 2013 bis Juni 2019 in Bayreuth am Lehrstuhl für Pflanzenphysiologie unter Betreuung von Herrn Professor Dr. Stephan Clemens angefertigt.

Vollständiger Abdruck der von der Bayreuther Graduiertenschule für Mathematik und Naturwissenschaften (BayNAT) der Universität Bayreuth genehmigten Dissertation zur Erlangung des akademischen Grades einer Doktorin der Naturwissenschaften (Dr. rer. nat.).

Dissertation eingereicht am: 27.06.2019

Zulassung durch das Leitungsgremium: 09.07.2019

Wissenschaftliches Kolloquium: 30.10.2019

Amtierender Direktor: Prof. Dr. Markus Lippitz

Prüfungsausschuss:

Prof. Dr. Stephan Clemens (Gutachter)

Prof. Dr. Angelika Mustroph (Gutachterin)

Prof. Dr. Klaus Ersfeld (Vorsitz)

PD Dr. Alfons Weig

Publikationsliste

Publikationen dieser Doktorarbeit

Detterbeck, A, Nagel, M, Rensch, S, Weber, M, Börner, A, Persson, DP, Schjoerring, JK, Christov, V, Clemens, S. 2019. The search for candidate genes associated with natural variation of grain Zn accumulation in barley. *The Biochemical journal*. DOI: 10.1042/BCJ20190181. (Status: online veröffentlicht am 04.06.2019)

Detterbeck, A, Pongrac, P, Rensch, S, Reuscher, S, Pecovnik, M, Vavpetic, P, Pelicon, P, Holzheu, S, Kramer, U, Clemens, S. 2016. Spatially resolved analysis of variation in barley (*Hordeum vulgare*) grain micronutrient accumulation. *The New phytologist* 211: 1241–1254. DOI:10.1111/nph.13987.

Detterbeck, A, Pongrac, P, Persson. DP, Vogel-Mikuš, K, Mitja, K, Vavpetic, P, Pelicon, P, Arčon, I, Husted, S, Schjoerring, JK, Clemens, S (-). Temporal and spatial pattern of zinc and iron accumulation during barley (*Hordeum vulgare*) grain development. (Status: Manuskript)

Weitere Publikationen

Farooq, MA, Detterbeck, A, Clemens, S, Dietz, K-J. 2016. Silicon-induced reversibility of cadmium toxicity in rice. *Journal of experimental botany* 67: 3573–3585. DOI: 10.1093/jxb/erw175.

Weig, AR, Peršoh, D, Werner, S, Betzlbacher, A, Rambold, G. 2013. Diagnostic assessment of mycodiversity in environmental samples by fungal ITS1 rDNA length polymorphism. *Mycological Progress* 12: 719–725. DOI: 10.1007/s11557-012-0883-1.

Inhaltsverzeichnis

I Zusammenfassung

Mikronährstoffmangel, auch bekannt als verborgener Hunger, betrifft schätzungsweise ein Drittel der Weltbevölkerung. In besonderem Maße sind Kinder unter fünf Jahren betroffen, die durch den Mangel an lebenswichtigen Mikronährstoffen wie Zink an systemischen Beeinträchtigungen wie Wachstumsverzögerungen, Dysfunktionen des Immunsystems und kognitiven Störungen leiden. Da Grundnahrungsmittel wie Getreide einen maßgeblichen Anteil zur Mikronährstoffaufnahme insbesondere in Ländern des globalen Südens beitragen, können sowohl ackerbauliche Maßnahmen als auch die Prozessierung von Lebensmitteln Lösungsansätze liefern. Diese sind jedoch häufig kostenintensiv, weshalb die Biofortifikation von Nahrungsmitteln eine nachhaltigere Reduktion von Mikronährstoffmangel erreichen kann. Hierbei ist von Bedeutung, dass für eine erfolgreiche Biofortifikation aus züchterischer Sicht diverse Prädispositionen, wie eine genetisch verankerte Variation der Mikronährstoff-Gehalte und die mechanistische Kenntnis der Mikronährstoff-Akkumulation, vorhanden sein müssen. Ziel dieser Doktorarbeit war es daher, anhand der ackerbaulichen Modellpflanze Gerste (*Hordeum vulgare* L.) grundlegende Fragestellungen zur Verwirklichung von Biofortifikationsstrategien zu beantworten.

Hierbei lagen die Schwerpunkte auf drei verschiedenen Themenblöcken: der natürlichen Variation von Mikronährstoffen, der räumlichen Verteilung innerhalb des Korns und den zugrundeliegenden Beladungs- und Distributionsmechanismen. Zunächst wurde das Züchtungspotential, das maßgeblich von der vorhandenen genetischen Variabilität bestimmt wird, für mikronährstoffreiche Körner ermittelt. Dementsprechend wurde die natürliche Diversität der Mikronährstoff-Akkumulation in zwei weltweit gesammelten Gerstekollektionen in verschiedenen Jahren und Umwelten untersucht. Die Analysen ergaben eine ausgeprägte genetische Komponente der Mikronährstoff-Akkumulation insbesondere für Zink und Eisen. Hieraus lässt sich schlussfolgern, dass eine Züchtungsbasis für mikronährstoffreichere Getreide vorhanden ist. Neben der Analyse von Genotyp-Umwelt-Interaktionen lag ein weiteres Augenmerk auf der Variation von für den Menschen toxischen Schwermetallen wie Cadmium. Die Ergebnisse ließen auf ähnliche Transport- und Beladungsmechanismen von Zink und Cadmium schließen, da eine hohe Zink-Akkumulation häufig mit einer höheren Cadmium-Akkumulation im Korn einherging. Aus diesem Grund stellt eine Kulturführung im Rahmen einer guten landwirtschaftlichen Praxis, mit genauer Kenntnis der bewirtschafteten Böden, eine grundlegende Voraussetzung im Anbau von biofortifiziertem Getreide dar.

Der zweite Block umfasste die Frage der detaillierten räumlichen Verteilung der Mikronährstoffe im Korn. Dies ist in besonderem Maße für etwaige Verzehrempfehlungen für biofortifiziertes Getreide von Bedeutung. Um Einblick in die räumliche Verteilung der Mikroelement-Gehalte zu erlangen, wurden reife Samen von ausgewählten, kontrastierenden Linien zerlegt und mit Hilfe verschiedener qualitativer und quantitativer Verfahren charakterisiert. Hoch Zink-akkumulierende Linien wiesen in nahezu allen analysierten Geweben, inklusive dem Endosperm, höhere Zink-Konzentrationen auf. Hieraus kann man schließen, dass auch der Konsum von biofortifiziertem weißem Mehl einen wichtigen Beitrag zur Verbesserung der Mikronährstoffaufnahme leisten kann. Um Hinweise auf verschiedene Bindungsumgebungen im Endosperm-Gewebe zu erhalten und eine potentielle Aussage über die Bioverfügbarkeit von Zink in hoch Zink-akkumulierenden Linien treffen zu können, wurden Proben extrahiert und mittels chromatographischer und massenspektrometrischer Methoden vermessen. Hierbei konnte dokumentiert werden, dass lösliches Zink nicht mit Phosphor oder Schwefel co-eluierte. Dies deutet darauf hin, dass andere Bindungspartner als Proteine oder Phytat in die Zink-Bindung involviert sein könnten. Da der Anteil des löslichen Zinks jedoch mit zunehmender Reife deutlich abnahm, müssen weiterführende Analysen die Speziierung von unlöslich gebundenem Zink charakterisieren.

Die molekularen Mechanismen der Mikronährstoff-Akkumulation waren Hauptbestandteil des dritten Arbeitsschwerpunktes dieser Dissertation. Für moderne, biotechnologische Züchtungsmethoden ist ein mechanistisches Verständnis der Aufnahme- und Verteilungswege von Mikronährstoffen von zentraler Bedeutung. Hierbei kann beispielsweise die Entwicklung molekularer Marker zur Beschleunigung des Züchtungsprozesses beitragen. Für die Suche nach Kandidatengenen wurden zwei niedrig und zwei hoch Zink-akkumulierende Linien ausgewählt, um Marker-Merkmals-Assoziationen und Transkriptom-Unterschiede zu analysieren. Hierbei konnten mit Hilfe einer genomweiten Assoziationsstudie erhöhte Zink-Konzentrationen im Korn mit einem Marker assoziiert werden, in dessen Nähe zwei Gene der „Yellow Stripe-Like“ (YSL)-Transporterfamilie liegen. Des Weiteren wurden unter den stringenten Analysebedingungen weder Unterschiede in der Transkript-Häufigkeit von bekannten Transportgenen noch von Genen, die Zink-Bindungspartner wie Nicotianamin oder Metallothioneinen codieren, als Faktoren für die erhöhte Zink-Akkumulation identifiziert. In den Ähren von hoch Zink-akkumulierenden Linien war insbesondere eine putative α-Amylase/Trypsin CMb Inhibitor Vorstufe höher exprimiert als in niedrig Zink-akkumulierenden Linien. Bei einem weniger stringenten Vergleich näher verwandter Linien konnte ein Kandidatengen für die Zink-Akkumulation im Korn identifiziert werden, das Ähnlichkeit zu einem „*Metal Tolerance Protein 5*“ (*MTP5*) in Gerste aufweist. Weiterer Forschungsbedarf ergibt sich insbesondere aus der Notwendigkeit zur zellulären

Lokalisation und zur näheren funktionellen Beschreibung der Kandidatengene. Darüber hinaus stellt die hohe Zahl bisher noch nicht näher charakterisierter Gene, die Unterschiede in der Transkript-Häufigkeit zeigten, Grund für weitere Forschungen in diesem Bereich dar.

Die in dieser Doktorarbeit bearbeiteten Fragestellungen und Ergebnisse geben einen detaillierten und umfassenden Überblick der Mikronährstoff-Akkumulation in Gerstekörnern wieder. Hierbei wurden insbesondere die natürliche Diversität, die räumliche Verteilung und die zugrundeliegenden Beladungsmechanismen erforscht und diskutiert. Außerdem konnten bisher ungeklärte Fragen zur Konzentration und Speziierung von Zink während der Entwicklung und zu Transkript-Unterschieden in unterschiedlich hoch Zink-akkumulierenden Gerstelinien beantwortet werden. Weiterer Forschungsbedarf besteht jedoch zur Aufklärung der Hauptbindungsformen von unlöslichem Zink im Endosperm und zur weiterführenden Charakterisierung von Kandidatengenen. Darüber hinaus bieten die Ergebnisse dieser Doktorarbeit eine wichtige Grundlage insbesondere für Fragen der genetischen Prädisposition der Mikronährstoff-Akkumulation und ebnen somit den Weg für eine züchterische Herangehensweise bei der Bekämpfung von verstecktem Hunger.

II Abstract

Micronutrient deficiencies, also known as Hidden Hunger, affect approximately 1/3 of the population worldwide with children under the age of five being especially susceptible. The lack of vital micronutrients such as zinc can lead to growth retardation, immune dysfunctions and cognitive disorders. Especially in the global south, staple crops are the main source of micronutrients in the diet. Therefore, both agronomic and food processing measures can provide solutions to solve micronutrient deficiencies. However, these procedures are often cost intensive, whereas the biofortification of plants can provide a more cost efficient and therefore more sustainable solution to reduce micronutrient deficiencies. For breeding biofortified crops, diverse predispositions, such as a genetically determined variation and a mechanistic understanding of micronutrient accumulation, are needed. Therefore, the goal of this thesis was to answer basic questions about the implementation of biofortification strategies with the agricultural model crop barley (*Hordeum vulgare* L.).

The emphasis laid on three thematic blocks: First, on the natural variation of micronutrients, second, on their spatial distribution within the grain, and third, on the underlying loading and distribution mechanisms. Initially, the breeding potential, which is mainly determined by the genetic variability, of micronutrient-dense grains was analyzed. The natural diversity of micronutrient accumulation was assessed in different years and environments of two worldwide-sampled barley collections. There was a pronounced genetically determined variation for zinc and iron found, which can build a breeding basis for micronutrient-dense cereals. Besides the analysis of genotype-environment interactions, the variation of cadmium, which is toxic for humans, was evaluated. High zinc accumulation was found to be associated with higher cadmium accumulation in the grain to a considerable degree, indicating similar transport and loading mechanisms for zinc and cadmium. Therefore, it is essential to follow the guidelines for good agricultural practice and analyze the soil of sites where biofortified crops are intended to be grown.

In the second part of this dissertation, a focus lay on the spatial distribution of micronutrients within the grain. This is especially important for giving recommendations on the consumption of biofortified cereals. Mature grains of barley lines with contrasting zinc accumulation were dissected and analyzed with qualitative and quantitative methods. High zinc-accumulating lines contained more zinc in nearly all analyzed tissues, including the endosperm. Therefore, the consumption of biofortified white flour can contribute to improved micronutrient intake. Knowledge about binding partners can help to evaluate the bioavailability of zinc in high zinc-accumulating lines. To identify binding partners of zinc in the endosperm,

samples were extracted and analyzed with chromatographic and mass-spectrometric methods. Soluble zinc did not co-elute with phosphorus or sulfur, which indicated other binding environments than proteins or phytate. However, as the portion of soluble zinc was decidedly decreasing during grain maturation, additional studies need to characterize the binding species of insoluble zinc in the grain.

The third section of this thesis elucidates the molecular mechanisms involved in micronutrient accumulation. For modern, biotechnological breeding techniques, a mechanistic understanding of the uptake and distribution mechanisms for micronutrients is crucial. Here, the development of molecular markers can accelerate the breeding process. In the search for candidate genes, two low and high zinc-accumulating lines were chosen for assessment of marker-trait-associations and transcript analysis. Results of a genome-wide association mapping showed that high zinc accumulation in the grain was associated with a marker on 2H at 82.8 cM in close vicinity to two genes belonging to the family of yellow stripe-like (YSL) transporters. Furthermore, the stringent parameters for transcript analysis revealed no differences in transcript abundance of genes known to be involved in metal transport or metal binding such as nicotianamine or metallothioneins. In ears of high zinc-accumulating lines, a putative α-amylase/trypsin inhibitor CMb precursor was decidedly higher expressed than in low zinc-accumulating lines. Following a less stringent comparison of more related lines, a candidate gene for grain zinc accumulation showing similarity to *metal tolerance protein 5* (*HvMTP5*) was identified. Hence, more detailed analysis is needed for a cellular localization and functional description of the candidate genes. Furthermore, the number of unidentified, not-yet-assigned and characterized genes showing differences in transcript abundance provides reason for further in-depth study.

This thesis comprises a detailed and comprehensive overview on micronutrient accumulation in barley grains. In particular, the natural diversity, spatial distribution and underlying loading mechanisms were analyzed and discussed. Furthermore, questions on zinc concentration and speciation during grain development and differences in transcript abundance leading to low or high zinc accumulation in the grain were answered. However, further research is needed to identify the main binding partners of insoluble zinc in the endosperm and to characterize candidate genes. Providing knowledge about the genetic predisposition of micronutrient accumulation, the results of this thesis facilitate breeding approaches to fight Hidden Hunger.

1 Synopsis

1.1 Tabellen- und Abbildungsverzeichnis Synopsis

1.2 Forschungsstand zum Thema Mikronährstoffmangel

Mikronährstoffmangel, auch bekannt als verborgener Hunger („Hidden Hunger“), betrifft schätzungsweise zwei Milliarden Menschen weltweit (WHO, 2002; Tulchinsky, 2010; Muthayya *et al.*, 2013; Ruel-Bergeron *et al.*, 2015). Unter Mikronährstoffmangel versteht man die Unterversorgung mit Vitaminen und essentiellen Mikroelementen wie Iod (I), Zink (Zn), Eisen (Fe), Mangan (Mn) und Kupfer (Cu), die zu einer Beeinträchtigung der normalen Körperfunktionen bis hin zum Tod führen kann. Insbesondere der Mangel an Zink betrifft Menschen jeden Geschlechts und Alters weltweit, vor allem jedoch Kinder unter fünf Jahren in „less developed countries“ (LDCs) (WHO, 2002; Black, 2003). Eine Unterversorgung mit Zink führt zu systemischen Beeinträchtigungen wie Wachstumsverzögerungen, Dysfunktionen des Immunsystems und kognitiven Beeinträchtigungen (Prasad, 2013). Die Versorgung mit Zink spielt durch dessen Beteiligung am Proteinmetabolismus, an der Aufrechterhaltung der Membranstabilität sowie an Zellteilungs- und zahlreichen weiteren Prozessen eine bedeutende biologische Rolle. Insbesondere als Cofaktor bestimmt Zink die Aktivität von über 300 Proteinen und über 1000 Transkriptionsfaktoren (Waters & Sankaran, 2011; Prasad, 2013).

Geographisch gesehen decken sich Regionen mit einem erhöhten Risiko für Zink-Mangel innerhalb der Bevölkerung häufig mit Regionen, in denen es Anzeichen von Zink-Mangel in Pflanzen gibt (Abb. 1). Dies ist in besonderem Maß auf ein geringes Pro-Kopf-Einkommen zurückzuführen, das zum einem mit einer kleinbäuerlich geprägten Gesellschaftsstruktur als auch mit einem einseitigen Konsum von pflanzlichen Grundnahrungsmitteln wie Getreide verbunden ist. Hierbei wird die gesamte Zink-Aufnahme durch eine vergleichsweise geringe Mikronährstoffdichte dieser Grundnahrungsmittel limitiert (Sandstead, 1991; Clemens, 2014).

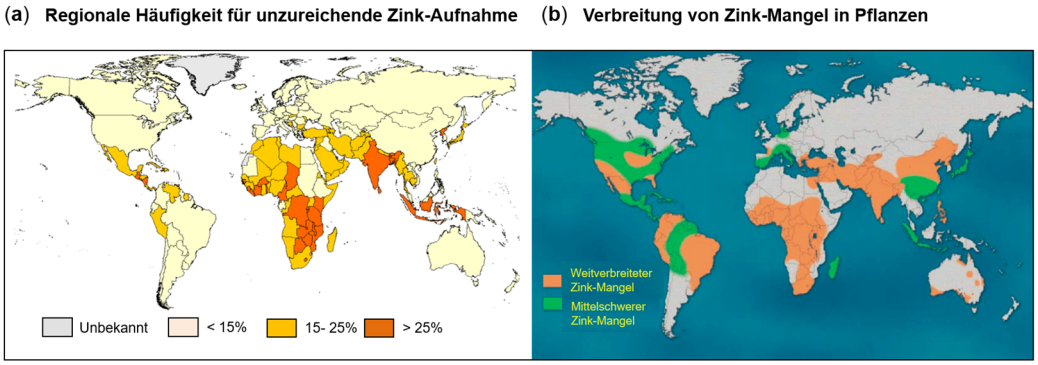

Abb. 1 Geographische Überlappung von Zink-Mangel in der menschlichen Bevölkerung und in Pflanzen. (**a**) Dargestellt ist der Vergleich der geographischen Verteilung von regionalen Häufigkeiten von Zink-Mangel bei Menschen (mod. nach Wessells & Brown, 2012) und (**b**) von Zink-Mangel in Pflanzen (Alloway, 2008).

Durch steigende CO_2-Konzentrationen in der Atmosphäre könnte sich der Mikronährstoffmangel zusätzlich verschärfen. So konnten Studien zeigen, dass Zink-Konzentrationen in Weizen bei erhöhten CO_2-Konzentrationen um 9,3 % niedriger lagen als bei aktuellen atmosphärischen Konzentrationen (Myers *et al.*, 2014; Dietterich *et al.*, 2015; Smith & Myers, 2018). Die Notwendigkeit zur Lösung jeglicher Form von Mangelernährung wurde in der „Rome Declaration on Nutrition“ von 170 teilnehmenden Ländern 2014 festgehalten (Second International Conference on Nutrition, 2014). Im „European Food and Nutrition Action Plan 2015-2020“ der WHO Europa wird ebenso eine signifikante Reduktion der Mangelernährung durch eine Verbesserung der Nahrungsqualität gefordert, was einen zügigen Handlungsbedarf weiter unterstreicht (WHO, 2015).

Eine Herausforderung bei der Lösung des verborgenen Hungers stellt dar, geeignete Maßnahmen zur Verbesserung von Grundnahrungsmitteln zu identifizieren (Gómez-Galera *et al.*, 2010; Murgia *et al.*, 2013). Eine Rolle spielen hierbei Ansätze zur Nahrungsmittel-Prozessierung, wie die Supplementation von Nahrungsmitteln mit Mikronährstoffen oder eine veränderte Nahrungsmittelaufbereitung (Mayo-Wilson *et al.*, 2014; Liberato *et al.*, 2015). Auf der Erzeugerseite können ackerbauliche Maßnahmen, wie eine gezielte Düngung, Erfolge versprechen (Cakmak, 2008; Cakmak & Kutman, 2018). Die nachhaltigste und auf Dauer kostengünstigste Form der Anreicherung von Grundnahrungsmitteln mit Mikronährstoffen stellt jedoch die genetische Biofortifikation dar, die eine Erhöhung des bioverfügbaren Mikronährstoff-Gehalts mit Hilfe der Pflanzenzucht beschreibt (White & Broadley, 2005; Bouis & Welch, 2010). Hierbei führen sowohl klassische Züchtungsmethoden, Marker-assistierte Methoden als auch gentechnische Verfahren zum Erfolg (Borrill *et al.*, 2014). Die Wissenschaft kann hierbei einen grundlegenden Beitrag zum Verständnis der Zusammenhänge und Beladungsmechanismen der Mikronährstoff-Akkumulation, insbesondere in essbaren Teilen von Pflanzen, leisten (Palmgren *et al.*, 2008; Waters & Sankaran, 2011; Xu *et al.*, 2011; Shahzad *et al.*, 2014).

Für die angewandte Grundlagenforschung ist es zum einen wichtig, an ackerbaulichen Kulturen zu forschen, zum anderen sollten diese für wissenschaftliche Fragestellungen gewisse Voraussetzungen erfüllen. Hierbei bringt Gerste (*Hordeum vulgare* L.) als Modellpflanze für grundlagenorientierte Fragestellungen zahlreiche Vorteile mit sich. Gerste ist nach Mais, Weizen und Reis mit circa 141 Millionen Tonnen Gesamtproduktion im Jahr 2016 (FAOSTAT, 2018) das viertwichtigste Getreide weltweit. Neben ihrer weltweiten Verbreitung sprechen sowohl die diploide Genomstruktur als auch das Inzucht-basierte Fortpflanzungssystem für die Eignung der Gerste als Modellpflanze. Ein bedeutender Grundstein zur Erforschung molekularer Mechanismen wurde durch die Genomsequenzierung von *Hordeum vulgare* L. gelegt (International Barley Genome Sequencing *et al.*, 2012;

Mascher *et al.*, 2017). Mit Hilfe des komplett sequenzierten Genoms und einer großen Anzahl verschiedener Genbanken können nunmehr unterschiedlichste molekulare Fragestellungen adressiert werden. Ein Beispiel für diese Genbanken stellt die „Barley Core Collection“ (BCC) dar, die 1989 zusammengestellt wurde und mit über 1600 Akzessionen einen weltweiten Gerste-Genpool widerspiegelt (Bothmer, 2003). Die darin enthaltenen Landrassen und Sorten wurden ausgewählt, um die gesamte genetische Vielfalt der globalen Gerstepopulation zu repräsentieren. Diese natürliche Variation bietet das Potential zur Identifikation von Linien, die Unterschiede in ihren Zink-Gehalten im Korn zeigen und somit vielversprechende Kandidaten für die Analyse der Distribution von Zink in Gerste darstellen. Ebenso von Bedeutung ist in diesem Zusammenhang die ICARDA („International Center for Agricultural Research in the Dry Areas“)-Sammlung verschiedener Landrassen und Kultivare, die Teil eines Zucht-programms für Gerste ist (Jilal *et al.*, 2008). Speziell aus Sicht moderner Züchtungsmethoden sind Linien interessant, deren bekannter genetischer Hintergrund neben der Analyse der Metallgehalte zu einer Marker-basierten Selektion führen kann. Diese Grundlage wird durch die für die ICARDA-Linien vorhandene Marker-Datenbasis geschaffen. Hierdurch kann die Charakterisierung von verschiedenen Eigenschaften durch die Identifikation von Regionen, die an der Ausprägung eines quantitativen Merkmals („Quantitative Trait Loci“, QTL) beteiligt sind, und in Folge dessen durch die Identifikation der für den entsprechenden Phänotyp verantwortlichen Gene, erleichtert werden.

Die Basis für die Züchtung von ernährungsphysiologisch wertvollen Grund-nahrungsmitteln stellt das Züchtungspotential dar, das maßgeblich durch die natürliche Diversität des jeweiligen Züchtungsmerkmals, wie z.B. der Mikronährstoff-Akkumulation, bestimmt wird (Huang & Han, 2014). Die genetischen Ressourcen einer Pflanzenart können am effektivsten über eine vergleichende Anzucht einer Genbank-Kollektion, die die gesamte genetische Variabilität der Art darstellen soll, unter kongruenten Umweltbedingungen ermittelt werden. Diverse Studien konnten die natürliche Variation der Akkumulation von Zink, Eisen und weiteren Mikronährstoffen in den weltweit wichtigsten Getreidearten Mais, Weizen, Reis und Gerste zeigen (Ma *et al.*, 2004; Shi *et al.*, 2009; White & Broadley, 2009; Zhao *et al.*, 2009; Xu *et al.*, 2011; Baxter *et al.*, 2014; Mamo *et al.*, 2014; Pinson *et al.*, 2015). Bisherige Züchtungsprogramme wie HarvestPlus basieren vorwiegend auf der Ausschöpfung dieser natürlichen Diversität mit Hilfe klassischer Züchtungsmethoden (Pfeiffer & McClafferty, 2007; Bouis & Welch, 2010). Ein Schwerpunkt liegt hierbei auf der Erhöhung des Zink-, Eisen- und Provitamin A-Anteils in verschiedenen Getreidearten sowie in Süßkartoffel, Bohnen und Maniok. Aus dieser Züchtungsarbeit sind über 150 Sorten von 12 biofortifizierten Kulturarten in 30 Ländern hervorgegangen (Bouis, 2018). Diese Züchtungsarbeit stellt einen ersten großen Erfolg zur Bekämpfung der weltweiten Mangelernährung dar. Ohne das detaillierte

Verständnis der Aufnahme-, Distributions- und Akkumulationsprozesse von Mikronährstoffen ist eine gezielte, und somit weniger zeitaufwendige, Züchtung jedoch nicht möglich.

Ein besonderes Augenmerk muss hierbei zunächst auf die räumliche Verteilung und Bioverfügbarkeit der Mikroelemente gelegt werden. Der Distribution von Mikroelementen kommt vor allem durch den potentiellen Mikronährstoffverlust bei der Prozessierung der Körner, z.B. durch das Mahlen zu Mehl, eine Bedeutung zu (Hansen *et al.*, 2012; Atungulu & Pan, 2014). Mit Hilfe hochauflösender Röntgenfluoreszenz-Spektroskopie konnten Lombi *et al.* (2011) eine Übersicht über die Lokalisation von Makro- und Mikroelementen im Korn von Gerste erstellen. Hierbei zeigte sich, dass der Embryo und die äußeren Gewebe des Korns reich an Nährstoffen waren. Anhand von Weizen konnte gezeigt werden, dass eine Zink-Düngung zu einer Erhöhung des Zink-Gehalts im Aleuron, Scutellum und Embryo führte (Pongrac *et al.*, 2013). Ob und inwiefern jedoch eine natürliche genetische Disposition zur höheren Akkumulation von Zink im Korn einen Einfluss auf die räumliche Verteilung von Mikroelementen hat, ist bisher nicht untersucht. Neben der räumlichen Verteilung der Mikronährstoffe ist es zudem von zentraler Bedeutung, dass diese in einer für den Menschen bioverfügbaren Form im Korn vorliegen (Clemens, 2014; La Frano *et al.*, 2014). Die Möglichkeit zur Aufnahme von Mikroelementen über den menschlichen Gastrointestinaltrakt ist abhängig von der Bindung von z.B. Zink und Eisen mit Phosphor in Form von Phytat (IP_6) oder Schwefel in Form von Proteinen. Es wurde lange Zeit vermutet, dass Mikroelemente vorwiegend in Form von Phytat, welches von Menschen durch den Mangel an Phytasen nicht verdaut werden kann, in Samen gebunden sind (Oatway *et al.*, 2007; Gupta *et al.*, 2015). Mit Hilfe von massen-spektrometrischen Techniken konnte jedoch ein differenzierterer Einblick in die Speziierung von Metallen in verschiedenen Pflanzenfamilien gewonnen werden (Clemens, 2014). So konnte Persson *et al.* (2009) in einer simultanen Analyse von Zink, Eisen, Phosphor und Schwefel zeigen, dass Zink in Embryonen von Weizen mit Schwefel und nicht mit Phosphor co-eluierte. Diese Ergebnisse legten nahe, dass Zink im Gegensatz zu Eisen vorwiegend an Peptide gebunden war. In einer weiteren Studie an Weizenkörnern konnte dargelegt werden, dass für Eisen und Zink unterschiedliche Bindungspartner im Endosperm-Gewebe vorliegen (Eagling *et al.*, 2014). Als potentielle Bindungspartner kommen hierbei, neben IP_6, chelat-bildende Verbindungen wie Nicotianamin (NA) oder 2'-Desoxymuginsäure in Betracht. Über dieses grundlegende Verständnis hinaus ist jedoch bisher noch wenig über einen potentiellen Unterschied in der Zusammensetzung verschiedener Bindungspartner in niedrig und hoch Zink-akkumulierenden Linien bekannt.

Um neben Züchtungszielen wie der Anpassung unserer Kulturarten an Umwelt-veränderungen eine züchterische Rolle spielen zu können, müssen des Weiteren die molekularen Mechanismen der Mikronährstoff-Akkumulation als Basis für eine schnelle,

kosteneffiziente und gerichtete Züchtung erforscht werden. So ist zum Beispiel die Beladung der Samenhülle, dem maternalen Gewebe des Korns, aus dem Phloem und der Transport von Zink von maternalem zu filialem Gewebe (Embryo, Endosperm, Aleuron) über den apoplastischen Raum bisher nicht genau geklärt. Tauris *et al.* (2009) gelang es mittels Laser-Mikrodissektion Zellen verschiedener Korngewebe aus Gerste (*Hordeum vulgare* L.) zu isolieren und deren spezifische Expressionsmuster bezüglich diverser Metallhomöostase-Gene zu identifizieren. Dabei konnten, differentiell nach Korngewebe, unterschiedlich erhöhte Expressionsmuster der Genfamilien HMA („Heavy Metal ATPase"), ZIP („Zrt-, Irt-like Protein"), MTP („Metal Tolerance Protein"), Nramp („Natural Resistance-Associated Protein"), NAS („Nicotianamine Synthase") und YSL („Yellow Stripe-Like") nachgewiesen werden. Außerdem können Mutationsstudien dazu beitragen, den Einfluss verschiedener Transporter auf das Metallallokationssystem zu beschreiben. So konnten in *Arabidopsis thaliana* zwei P1B-ATPasen nachgewiesen werden, die aktiv Zink von der Mutterpflanze in Filialgewebe transportieren. Die Mutation dieser Transporter resultierte in deutlich geringeren Zink-Konzentrationen innerhalb des Samens (Olsen *et al.*, 2016). Diese Studien sind Beispiele für die Erforschung des Zusammenspiels von Transportprozessen in Körnern, die sich vornehmlich auf potentielle Unterschiede verschiedener Metalltransporter konzentrierten. Ein wichtiges Augenmerk muss jedoch ebenso auf das komplexe System aus potentiellen Liganden, sink-source-Mechanismen und die Speicherungsfähigkeit der Mikronährstoffe innerhalb des Korns gelegt werden. Einen zusätzlichen Beitrag zur Identifikation von Kandidatengenen, die mit einer erhöhten Mikronährstoff-Akkumulation in Verbindung gebracht werden können, leisten des Weiteren genomweite Assoziations-Studien („Genome-wide association studies", GWAS) (Alomari *et al.*, 2018; Yang *et al.*, 2018). Hierbei werden genetische Informationen mit phänotypischen Eigenschaften in Verbindung gebracht. Darüber hinaus kann die Verknüpfung von genomweiten Assoziations-Studien und Transkriptom-Analysen dazu beitragen, die molekularen Unterschiede der natürlichen Diversität der Mikronährstoff-Akkumulation zu erklären und grundlegende physiologische Mechanismen aufzudecken.

Ziel dieser Doktorarbeit war es, die Mikronährstoff-Akkumulation im Korn anhand von Gerste als ackerbaulicher Modellpflanze detailliert zu beschreiben und einen Einblick in die grundlegenden molekularen Mechanismen der Zink-Akkumulation zu gewinnen. Hierbei lag das Hauptaugenmerk auf drei Themengebieten: I Der Erforschung des genetischen Potentials der Mikronährstoff-Akkumulation in Gerste, II der Beschreibung der räumlichen Verteilung von Mikronährstoffen im Korn sowie deren Speziierung während der Kornentwicklung und III der Aufklärung molekularer Mechanismen der Zink-Akkumulation in niedrig und hoch Zink-akkumulierenden Gerstelinien.

1.3 Bearbeitete Fragestellungen und Hypothesen

Als Basis jeglicher Züchtung dient ein hohes Züchtungspotential, das maßgeblich von der vorhandenen genetischen Variabilität bestimmt wird. Für die Züchtung biofortifizierter Nutzpflanzen ist daher die Erfassung dieser Variabilität ein wichtiger erster Schritt. Dementsprechend wurde in dieser Doktorarbeit zunächst die natürliche Diversität der Zink-Akkumulation in zwei weltweit gesammelten Gerstekollektionen untersucht. Hierzu dienten Linien der BCC-Kollektion, die im Rahmen des von der europäischen Union geförderten PHIME („Public health impact of long-term, low-level mixed element exposure in susceptible population strata“)-Projekts ausgewählt wurden, als auch Kultivare und Landrassen der ICARDA-Kollektion (Abb. 2). Das Hauptaugenmerkt lag hierbei vor allem auf den Mikroelementen Zink, Eisen, Mangan und Kupfer und der Frage, ob sich die Gehalte dieser Mikroelemente im Korn von verschiedenen Gerstelinien unterscheiden. Anschließend sollte durch die Analyse von Genotyp-Umwelt-Interaktionen eine genetische Disposition der Mikronährstoff-Akkumulation analysiert werden. Hierbei war die Hypothese, dass die Mikronährstoff-Akkumulation aufgrund der streng regulierten Prozesse der Metallhomöostase in Zellen genetisch kontrolliert und somit Raum für genetische Anpassung vorhanden ist. Konsekutiv wurden Korrelationen verschiedener Mikronährstoffe untereinander untersucht, um hierdurch mögliche analoge Transportprozesse zu identifizieren. Aufgrund ihrer häufig zweifach positiven Ladung können Mikroelemente wie z.B. Zink und Eisen durch Transportmoleküle oder Bindungspartner oftmals nicht selektiv unterschieden werden. Dies führt zu der Hypothese, dass bei gleichzeitig hoher Zink- und Eisen-Akkumulation ähnliche Transport- und Verteilungsprozesse beeinflusst sein könnten. Dies kann wiederum bei der Züchtung neuer Linien berücksichtigt werden. Die chemische Ähnlichkeit von Mikroelementen und somit der Aufnahmeprozesse spielt jedoch auch bei der Aufnahme von nicht-essentiellen Metallen, die bereits in geringen Konzentrationen giftig sind, eine Rolle. Aufgrund der oben genannten Parallelität von Mechanismen muss bei biofortifiziertem Getreide deshalb insbesondere auf schwermetallbelasteten Böden die Aufnahme von toxischen Metallen in essbare Teile der Pflanze reduziert werden. Dazu wurde eine Auswahl an Linien in schwermetallbelasteten Böden im Gewächshaus herangezogen und auf deren Cadmium- und Mikroelement-Gehalte untersucht. Hierbei wäre es wünschenswert, Pflanzen zu identifizieren, bei denen die Transportprozesse von erwünschten Mikroelementen und unerwünschten Schwermetallen möglichst selektiv vorliegen.

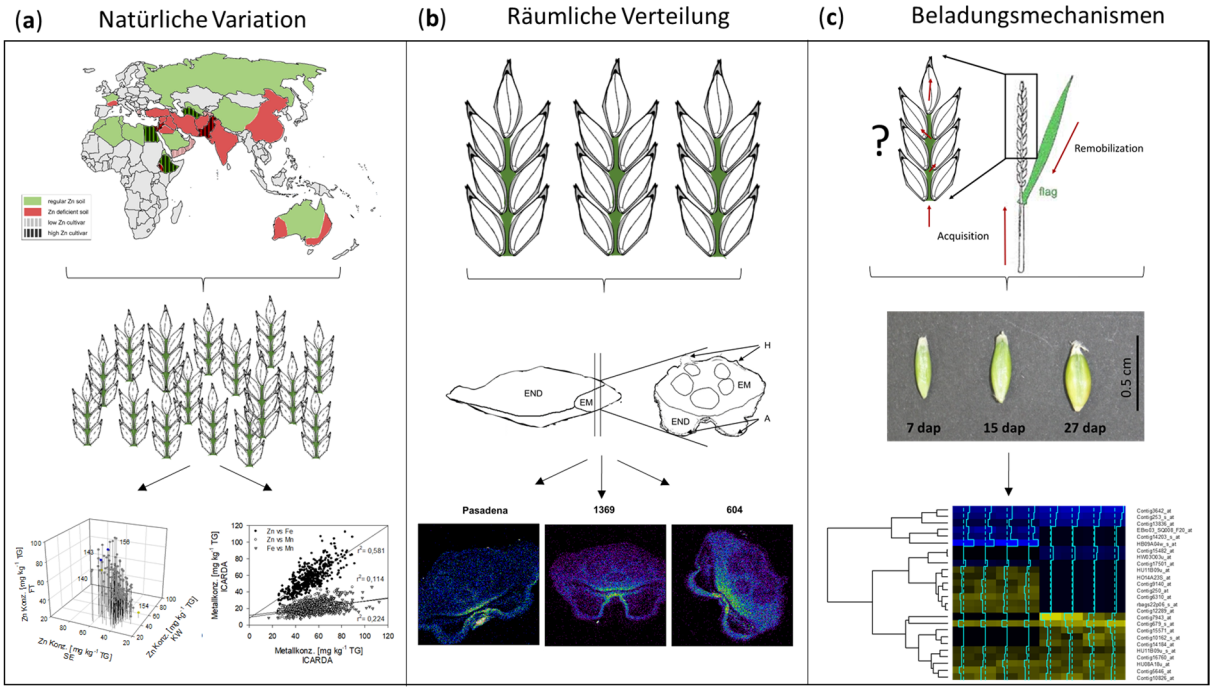

Abb. 2 Schematische Darstellung der bearbeiteten Themengebiete und Vorgehensweise. (**a**) Übersicht über die Vorgehensweise zur Erfassung der natürlichen Variation, (**b**) der räumlichen Verteilung und (**c**) der Beladungsmechanismen von Mikronährstoffen in den Körnern von Gerste.

Die Frage der detaillierten räumlichen Verteilung der Mikronährstoffe im Korn ist vor allem für Verzehrempfehlungen von Bedeutung. Sollte ein Großteil der Mikroelemente im Korn in der Hüll- und Aleuron-Schicht, also in äußeren Bestandteilen des Samens, vorhanden sein, sollten vor allem Vollkornprodukte verzehrt werden. Da die Getreide-Prozessierung jedoch häufig das Mahlen zu weißem Mehl beinhaltet, das aus stärkehaltigem Endosperm besteht, ist es wichtig, die Konzentrationen in den einzelnen Geweben zu quantifizieren. Um eine Aufschlüsselung der Verteilung der Mikroelement-Gehalte zu erreichen, wurden reife Samen von ausgewählten Linien zerlegt und analysiert. Mit Hilfe verschiedener qualitativer und quantitativer bildgebender Verfahren wurde zudem während der Kornentwicklung die Akkumulation von Mikro- und Makroelementen in ausgewählten Linien charakterisiert. Da nicht nur die Konzentration der Mikroelemente, sondern insbesondere auch deren Bindungsform für die Bioverfügbarkeit von Belang ist, wurden die Ergebnisse der bildgebenden Verfahren unter diesem Aspekt untersucht. So kann nicht nur eine Aussage über die Verteilung der Elemente im Korn getroffen werden, sondern über Co-Lokalisationsanalysen auch eine weitere Annäherung an die potentiellen Bindungspartner erfolgen. Da es sich sowohl bei Korrelations- als auch Lokalisationsanalysen um indirekte Analyseverfahren handelt, wurden Proben zusätzlich extrahiert und über chromatographisch und massenspektrometrisch basierte Methoden vermessen, um potentielle Bindungspartner zu identifizieren. Diese Speziierungs-

analysen wurden sowohl bei einer niedrig als auch einer hoch Zink-akkumulierenden Linie durchgeführt. Hierbei war die Hypothese, dass bei der hoch Zink-akkumulierenden Linie potentiell unterschiedliche Bindungspartner eine Rolle spielen, was wiederum einen Effekt auf die Bioverfügbarkeit haben könnte.

Neben der genauen Kenntnis um die Verteilung der Mikroelemente im Korn ist für die moderne Züchtung ein mechanistisches Verständnis der Aufnahme- und Verteilungswege von zentraler Bedeutung. Daher war eine weitere Fragestellung dieser Doktorarbeit, wie sich niedrig und hoch Zink-akkumulierende Linien auf Genom- und Transkriptomebene unterscheiden. Die Hypothese war hierbei, dass Unterschiede in der Gensequenz oder unterschiedlich starke Expression von Transporter-Genen die Zink-Akkumulation im Korn beeinflussen könnten. Die Analyse von Marker-Eigenschaft-Assoziationen wurde genutzt, um Gene zu identifizieren, die bei der Akkumulation von Mikronährstoffen eine Rolle spielen könnten. Mit Hilfe einer vergleichenden Transkriptom-Analyse wurden zudem ganze Ähren und Fahnenblätter untersucht, um sowohl Prozesse des Zink-Transports von der Mutterpflanze zum Korn als auch der Verteilung innerhalb des Kornes erfassen zu können. Ein wichtiger Bestandteil der Untersuchung war hierbei, dass die Pflanzen weder unter Zink-Mangel noch -Überschuss kultiviert wurden, um grundlegende Mechanismen der natürlichen Variation von Zink-Gehalten im Korn zu untersuchen.

Die bearbeiteten Fragestellungen sollten ein detailliertes und umfassendes Bild der Akkumulation von Mikroelementen in den Körnern von Gerste aufzeigen. Dies beinhaltet die Darstellung der weltweit vorhandenen natürlichen Variation der Mikronährstoff-Gehalte im Korn, die räumliche Verteilung und Speziierung der Mikronährstoffe und die vergleichende Untersuchung Marker-basierter und transkriptioneller Unterschiede in niedrig und hoch Zink-akkumulierenden Linien.

1.4 Material und Methoden

1.4.1 Pflanzenmaterial und Anzucht

Zwei verschiedene Gerstekollektionen wurden untersucht, die zum einen im Rahmen des EU-Forschungsprojekts „Public health impact of long-term, low-level mixed element exposure in susceptible population strata“ (PHIME) aus der „Barley Core Collection“ (BCC) und zum anderen aus der „International Center for Agricultural Research in the Dry Areas“ (ICARDA)-Sammlung zusammengestellt wurden. Alle Samen wurden von der bundeszentralen Ex-situ-Genbank für landwirtschaftliche und gartenbauliche Kulturpflanzen des IPK Gatersleben (Deutschland) zur Verfügung gestellt.

Die Anzucht der Linien zur Ermittlung der natürlichen Variation der Mikronährstoff-Gehalte erfolgte für die ICARDA-Kollektion durch die Genbank-Abteilung in Gatersleben in drei verschiedenen Anzuchten, um den Einfluss verschiedener Umwelten auf die Metall-Akkumulation im Korn zu testen. Die Linien der BCC-Kollektion wurden unter kontrollierten Bedingungen im Gewächshaus unter Langtagbedingungen (16h: 8h, Licht: Dunkel) mit Zusatzbeleuchtung (absolute Lichtintensität 100-150 µmol s^{-1} m^{-2}) über drei verschiedene Jahre angezogen. Der Zink-Gehalt der Erde lag bei den Gewächshausanalysen der BCC-Kollektion vergleichbar dem Durchschnitt des europäischen Mutterbodens (68,1 mg kg^{-1} Trockengewicht (TG), FOREGS Geochemical Atlas of Europe, http://weppi.gtk.fi/publ/foregsatlas/) bei 82 mg kg^{-1}. Die Zink-Gehalte der verschiedenen Anzuchten in Gatersleben lagen im Bereich von 4,3-16,6 mg kg^{-1} TG (AGROLAB Boden- und Pflanzenberatungsdienst GmbH, Oberdorla). Zur Analyse der Metallgehalte der BCC wurden je Pflanze fünf reife Samen von verschiedenen Ähren und Positionen innerhalb der Ähre vereinigt und bei 60 °C für 3 Tage getrocknet.

Für detaillierte Analysen der Metall-Akkumulation und -distribution im Korn wurden aus beiden Kollektionen Linien mit kontrastierenden Zink-Akkumulationsmustern ausgewählt. Diese waren für die BCC-Kollektion *Hordeum vulgare* 'Pasadena' als Referenzlinie sowie Linien 1369 (niedrig), Linien 32, 35, 54, 434 (intermediär) und Linien 431, 601, 604 und 605 (hoch). Diese Linien wurden zusätzlich in Töpfen in ackerbaulich genutzter, leicht Cadmium-kontaminierter Erde in Töpfen unter Langtagbedingungen (16h: 8h, Licht: Dunkel) mit Zusatzbeleuchtung (absolute Lichtintensität 80-110 µmol s^{-1} m^{-2}) im Gewächshaus kultiviert. Die Pflanzen zeigten hierbei keine Anzeichen von Toxizität.

Im Rahmen der ICARDA-Kollektion wurden zwei niedrig (140, 154) und zwei hoch Zink-akkumulierende Linien (143, 156) für die Analyse von Transkript-Daten und für die Analyse

verschiedener Entwicklungsstadien ausgewählt. Hierzu wurden diese Linien zusätzlich in bis zu fünf Anzuchtrunden in der Anzuchtkammer oder im Gewächshaus wie zuvor beschrieben kultiviert. Der Zink-Gehalt der Erde lag bei den Gewächshausanalysen vergleichbar dem Durchschnitt des europäischen Mutterbodens bei 89,7 mg kg^{-1} TG. Um einen Einfluss auf die Genexpression zu vermeiden, wurden die Pflanzen nicht mit Pestiziden oder Fungiziden behandelt. Für die Analyse wurden ausschließlich gesunde Pflanzen verwendet. Für die Microarray-Analyse wurden ganze Ähren ohne Grannen und Fahnenblätter 15 Tage nach der Befruchtung (TnB) beprobt. Die Beprobung fand immer zur gleichen Tageszeit statt, um einen Einfluss der circadianen Rhythmik auf die Analyseergebnisse auszuschließen. Die Proben wurden nach der Ernte unverzüglich in flüssigen Stickstoff eingefroren, anschließend in Porzellanschalen mit Hilfe von flüssigem Stickstoff zermahlen und bis zur weiteren Verarbeitung bei -80 °C gelagert.

1.4.2 Samenzerlegung

Reife Samen wurden in destilliertem Wasser für vier Stunden bei 4 °C eingeweicht, bevor sie unter einem Stereomikroskop in die äußere Schale (inklusive Spelzen, epidermale Zellschichten und Testa), Endosperm (inklusive Teile der Aleuron-Schicht) und Embryo mit Scutellum zerlegt wurden. Hierfür wurden zur Vermeidung von Metall-Kontaminationen Plastikpinzetten verwendet. Anschließend wurden Gewebe von je fünf zerlegten Körnern vereinigt und bei 60 °C für drei Tage getrocknet.

1.4.3 Analyse der Mikronährstoffprofile durch optische Emissionsspektrometrie mittels induktiv gekoppelten Plasmas (ICP-OES) und Massenspektrometrie (ICP-MS)

Zur Analyse der Mikroelement-Gehalte wurden ofen-getrocknete Samen in einer START 1500 Mikrowellen-Anlage (MLS GmbH) nassverdaut. Hierfür wurden die Proben mit 2 ml destilliertem Wasser, 2 ml 30 % H_2O_2 (w/w) und 4 ml 65 % HNO_3 (w/w) für 12 Minuten bei 180 °C unter Druck aufgeschlossen. Endosperm-Gewebe wurde auf die gleiche Weise verdaut, wohingegen Embryo- und Schalengewebe lediglich mit 1 ml destilliertem Wasser, 1 ml 30 % H_2O_2 (w/w) und 2 ml 65 % HNO_3 (w/w) in kleineren Gefäßen verdaut wurden. Ebenso wurde mit dem gemahlenen und gefriergetrocknetem Ähren- und Fahnenblattmaterial verfahren, das für die Bestimmung der Metallgehalte während der Pflanzenentwicklung geerntet wurde.

Die Gesamtkonzentration an Metallen in den zur Anzucht verwendeten Erden wurde durch Zugabe von 2,25 ml konzentrierter 37 % HCl (w/w) und 0,75 ml 65 % HNO_3 (w/w) zu 0,25 g getrockneter Erde ermittelt. Vor dem Druckaufschluss in einer START 1500 Mikrowellen-Anlage wurden die Gefäße 30 Minuten offen unter einem Abzug verwahrt, um gebildete Gase entweichen zu lassen. Der Aufschluss fand bei einem initialen 15-minütigen Anstieg auf 160 °C statt, der bei dieser Temperatur für 15 Minuten gehalten wurde. Das finale Volumen wurde mit destilliertem Wasser auf 10 ml aufgefüllt.

Metall-Konzentrationen wurden mittels ICP-OES (iCAP 6500, Thermo Scientific) bei den Wellenlängen 213,8 nm (Zink, Zn), 238,2 nm (Eisen, Fe), 257,6 nm (Mangan, Mn), 324,7 nm (Kupfer, Cu) und 226,5 nm (Cadmium, Cd) ermittelt.

1.4.4 Proton-induzierte Röntgenemissionsanalyse („Micro-proton-induced X-ray emission“, µ-PIXE)

Für die Lokalisation von Metallen wurden reife Körner sowie Körner während der Kornentwicklung 7, 15 und 27 Tage nach der Befruchtung (TnB) geerntet. Dies geschah bei Genotypen mit kontrastierenden Zink-Akkumulationen. Für die BCC-Kollektion wurden drei Genotypen (*H. vulgare* 'Pasadena', Linie 1369 und 604) ausgewählt, deren reife Körner untersucht wurden. *H. vulgare* 'Pasadena' diente hierbei als Referenzlinie. Für die ICARDA-Kollektion wurden je zwei kontrastierende Linien ausgewählt (niedrig Zink-akkumulierend: 140 und 154 sowie hoch Zink-akkumulierend: 143 und 156), die in vier verschiedenen Entwicklungsstadien beprobt wurden.

Die unreifen Körner wurden während der Ernte bei 4 °C gekühlt und nach der Ernte unverzüglich in mit flüssigem Stickstoff gekühlten Isopenten eingefroren. Anschließend wurden die Körner in flüssigem Stickstoff gefroren und drei Tage bei einem Temperaturgradienten (-180 °C auf -25 °C, 0.08 mbar) gefriergetrocknet (Alpha 2-4, Christ). Das sukzessive Einfrieren in Isopenten und flüssigem Stickstoff vermindert die Bildung von Eiskristallen, die die Zellstrukturen nachhaltig schädigen und somit die Analyse der Metallgehalte beeinträchtigen können. Vor der Präparation der zu analysierenden Schnitte wurden die Körner in destilliertem Wasser bei 4 °C für vier Stunden (reife Körner), drei Stunden (27 TnB), zwei Stunden (15 TnB) und eine Stunde (7 TnB) eingeweicht, um eine leichtere Schnittführung und somit ebene Analyseflächen zu erzielen. Je drei bis vier Körner pro Linie und Entwicklungsstadium wurden anschließend unter einem Stereomikroskop per Hand mit neuen rostfreien Stahl-Rasierklingen (Science Services GmbH) geschnitten, unverzüglich in flüssigen Stickstoff eingefroren und wie zuvor beschrieben gefriergetrocknet. Die Schnitte

wurden transversal gewählt, sodass möglichst viele verschiedene Korngewebe in einem Schnitt vertreten waren. Hierbei wurde der Embryo halbiert, sodass die Querschnitte den Embryo mit Wurzelprimordien, Scutellum sowie Endosperm mit Aleuron und Perikarp enthielten. Für Körner 7 TnB wurden zusätzlich, wie in Vogel-Mikuš *et al.* (2014) beschrieben, Schnitte mittels Gefriermikrotom angefertigt, um eine genauere Schnittführung im Bereich des sich entwickelnden Embryogewebes zu ermöglichen.

Für die Analyse wurden die Schnitte anschließend, wie von Vogel-Mikuš *et al.* (2008), Klančnik *et al.* (2014) und Villafort Carvalho *et al.* (2015) beschrieben, auf speziellen Halterungen zur Messung befestigt. Die Pixelgröße lag bei 7,81 µm und die Strahlengröße bei 0,8 µm. Mithilfe von PyMca vers. 5.0.0 (Solé *et al.*, 2007) wurden basierend auf mit GEOPIXE II generierten numerischen Matrices (Ryan, 2000) quantitative räumliche Verteilungskarten erstellt. Anschließend wurden mithilfe des ImageJ Werkzeugs ROI Manager mittlere Konzentrationen anhand spezifisch ausgewählter Bereiche des Schnittes ermittelt (Abràmoff *et al.*, 2004). Für jeden Schnitt wurden sowohl die ganze Schnittebene des Korns, Aleuron, Endosperm, sich entwickelnder bzw. entwickelter Embryo mit Scutellum und Hüllgewebe/Perikarp differenziert. Für die Schnitte 7 TnB konnten aufgrund des frühen Entwicklungsstadiums noch keine Aleuron-Schicht oder differenzierten Embryogewebe definiert werden.

1.4.5 Genomweite Assoziationsstudie („Genome-wide association study“, GWAS)

DArT™ Marker und ihre chromosomale Position wurden von Triticarte Pty Ltd., Yarralumla, ACT, Australien, bezogen. Das Marker-Set bestand aus 703 Markern mit durchschnittlichen Abständen von 1,6 Centimorgan (cM) und einer „minor allele frequency“ von 16,6 %. Für die Marker-Assoziations-Analyse wurden phänotypische Daten mittels REML („Residual Maximum Likelihood“)-Methode in GenStat 18 (VSN International, 2013) analysiert. Der beste unverzerrte lineare Schätzer („Best linear unbiased estimates“, BLUEs) wurde für alle Genotypen unter Annahme von determinierten genotypischen und zufälligen Umwelt-Effekten unter Berücksichtigung der Genotyp-Umwelt-Varianz hergeleitet. Ein gemischtes lineares Modell wurde zur Kalkulation der Marker-Eigenschaft-Assoziationen herangezogen. Assoziationen wurden bei einem Grenzwert von -log(PM) ≥ 2,5 als signifikant eingestuft. Zur Identifikation von putativen Kandidatengenen wurden nicht-DArT™ Marker verwendet, die innerhalb von 0,5 cM (LD bei $P \leq 0{,}001$) und 2,5 cM (LD bei $P \leq 0{,}05$) zu beiden Seiten der mittels Marker-Eigenschaft assoziierten Loci lokalisiert waren. Hierfür wurde der IPK BLAST Server, Gatersleben, (http://webblast.ipk-gatersleben.de/barley_ibsc/) verwendet.

1.4.6 RNA-Extraktion, cDNA-Synthese und Microarray-Analyse

Für die RNA-Extraktion wurden circa 100 mg gemahlenes Ähren- oder Fahnenblattmaterial verwendet, die eine Vereinigung aus drei bis fünf verschiedenen Pflanzen pro Probe darstellte. Zur Extraktion von RNA aus den stärkereichen Körnern wurde eine Methode entwickelt, die aus einer kombinierten Nutzung von TRIzol (Life Technologies GmbH) und RNeasy Mini Kit (Qiagen) bestand. Hierdurch wurde ein Verkleben der in den Säulen integrierten Silikamembran durch stärkehaltiges Material verhindert und somit eine deutliche Verbesserung der RNA-Qualität erzielt. Dementsprechend wurde das gemahlene Pflanzenmaterial mit 1 ml TRIzol für 3 Minuten vermengt und anschließend 5 Minuten bei Raumtemperatur inkubiert. Anschließend wurden die Proben bei 4 °C und 12.000 x g für 10 Minuten zentrifugiert, um überschüssiges Pflanzenmaterial inklusive Stärkeanteile von der flüssigen Phase zu trennen. Der Überstand wurde mit 0,2 ml Chloroform und 1 ml TRIzol für 15 Sekunden per Hand geschüttelt und anschließend bei 4 °C und 12.000 x g für 10 Minuten zentrifugiert. Ab diesem Schritt wurde entsprechend des Qiagen RNeasy Mini Protokolls für Pflanzen und Pilze verfahren, indem 1 ml RLC Puffer zum Überstand hinzugefügt und invertiert wurden. Nachdem eine weitere TRIzol Phasenseparierung (Schritt 5 des Qiagen Protokolls) durchgeführt wurde, wurde in Höhe der Hälfte des Volumens Ethanol zur flüssigen Phase hinzugegeben. RNA-Integrität und -Qualität wurden mit Hilfe von Agarosegelen und NanoPhotometer-Messungen (Implen GmbH) durchgeführt. Erfüllten die RNA-Proben die Reinheitskriterien von mindestens 1,8 (260/280) oder 1,6 (260/230) nicht, wurden sie einem weiteren Reinigungsschritt gemäß des RNeasy Mini Kit (Qiagen) Protokolls unterzogen. Anschließend wurden 500 ng RNA mit DNase-I (Life Technologies GmbH) behandelt und gemäß Herstellerangaben mit PrimeScript RT MasterMix (Perfect Realtime) (Takara Bio Inc.) in cDNA umgeschrieben.

Zur Transkriptanalyse wurde entsprechend der Herstellerangaben des GeneChip 3' IVT Express Kits (Affymetrix Inc.) aRNA amplifiziert. Die aRNA-Aufreinigung erfolgte mit Hilfe des RNeasy Mini Kits (Qiagen) gemäß des RNA-Aufreinigungs-Protokolls des Herstellers. Die Hybridisierung und Signaldetektion der Proben auf GeneChip Barley Genome Arrays (Affymetrix Inc.) erfolgte in Kooperation mit dem Zentrum für Medizinische Grundlagenforschung des Universitätsklinikums Halle (Saale) gemäß Herstellerangaben.

Die Auswertung der Daten erfolgte mittels RobiNA Software, Version 1.2.4_build656, (Lohse *et al.*, 2012) im Basismodus und der Nutzung von GcRMA als Normalisierungsmethode. Der *P*-Grenzwert lag bei 0,05 und ein minimaler logarithmischer „fold change" von 1 wurde festgesetzt. *P*-Wert Korrektur erfolgte mittels der Bonferroni-Hochberg-Methode und multiples

Testen wurde mit nested-F durchgeführt. Heatmaps wurden mit Hilfe von R (R Core Team, vers. 3.0.1) und dem Paket „gplots“ (Warnes *et al.*, 2016) und Dendrogramme mit der Funktion „hclust“ erstellt.

1.4.7 Speziierungsanalyse

Für die Speziierungsanalyse wurden Ähren 7, 15 und 27 Tage nach Befruchtung (TnB) und reife Körner einer hoch Zink-akkumulierenden Linie (156) der ICARDA-Kollektion analysiert. Aus unreifen Körnern wurde Endosperm-Gewebe entnommen und, wie die reifen Körner, gefriergetrocknet. Anschließend wurden je 30 mg homogenisiertes Probenmaterial nach Persson *et al.* (2016) extrahiert und entsprechend mittels SEC-ICP-MS vermessen.

1.4.8 Statistische Analyse

Zur Darstellung der Mikronährstoff-Variation in den Körnern von Gerste wurden Box-Plot-Diagramme erstellt, die den Median, das untere und obere Quartil und Ausreißer darstellen. Mit Hilfe des Pearson-Korrelationskoeffizienten und Regressionsanalysen (SigmaPlot, vers. 11.0) wurden Zusammenhänge zwischen den verschiedenen Mikronährstoffen auf Basis der verschiedenen Anzuchtrunden ermittelt. Hierfür wurden die Pearson-Korrelationskoeffizienten quadriert, um den Determinationskoeffizienten (r^2) zu bestimmen. Um Genotyp-Runden-Effekte bzw. die Genotyp-Umwelt-Einflüsse zu differenzieren und deren Beitrag zur Gesamtvarianz einordnen zu können, wurde eine Zwei-Wege ANOVA mit R (vers. 3.0.1) durchgeführt (R Core Team, 2013). Hierfür wurde das Paket „multcomp“ verwendet (Hothorn *et al.*, 2008). Es wurden nur Linien in die Analyse der Einflüsse auf die Mikronährstoffe inkludiert, die in allen drei unabhängigen Anzuchtrunden wuchsen (BCC: n=87, ICARDA: n=130). Signifikanztests ($P \leq 0{,}05$) wurden mit Hilfe von ANOVA und Tukey’s HSD posthoc Test mit R (R Core Team, vers. 3.0.1) ausgeführt. Hierbei wurden die Pakete „multcomp“ (Hothorn *et al.*, 2008) und „agricolae“ (Mendiburu, 2013) verwendet. Paarweise Vergleiche wurden mittels t-Test mit SigmaPlot (vers. 11.0) durchgeführt ($P \leq 0{,}05$).

1.5 Ergebnisse

1.5.1 Zusammenstellung der Gerstekollektionen

Um eine möglichst umfassende Bandbreite der natürlichen Metall-Akkumulation widerspiegeln zu können, wurden die Linien der BCC- und ICARDA-Kollektion hinsichtlich einer größtmöglichen Vielfalt bezüglich ihrer Herkunft, der an der Sammelstelle vorherrschenden Bodeneigenschaften, Ährenform und Repräsentation von Kultivaren und Landrassen ausgewählt. So wurden für die BCC-Kollektion 136 Linien aus fünf verschiedenen Kontinenten und 21 Ländern, darunter 98 Kultivare und 38 Landrassen sowie zwei- und sechszeilige *H. vulgare* L. mit 15 verschiedenen *subtaxa* ausgewählt. Die ausgewählten Linien der ICARDA-Kollektion bieten zusätzlich zur BCC den Vorteil, dass DArT^{TM} Marker generierte Populationsstrukturen vorhanden und somit eine genetische Einordnung der Pflanzen möglich ist. Die ICARDA-Kollektion, bestehend aus 180 Linien, repräsentiert jedes der verschiedenen Cluster der Populationsstruktur und setzt sich aus 111 Landrassen und 65 Kultivaren aus 30 verschiedenen Ländern zusammen. Hierbei waren unter anderem die Unterarten und Varietäten *H. vulgare subsp. vulgare convar. vulgare* sowie *H. vulgare subsp. vulgare convar. distichon* vertreten.

1.5.2 Variation von Zink im Korn von Gerste

Da die Variation von Merkmalen eine züchterische Grundlage darstellt, wurden zwei verschiedene Gerstekollektionen (BCC, ICARDA) auf deren Mikronährstoff-Gehalt im Korn untersucht. Hierbei wurde für die BCC sowohl Genbankmaterial (IPK) untersucht als auch Pflanzen im Gewächshaus in drei verschiedenen Jahren angezogen, um die natürliche Variation von Zink zu dokumentieren. Ein weiteres Set an Pflanzen der ICARDA-Kollektion wurde im Freiland innerhalb eines Jahres an drei verschiedenen Standorten angezogen, um zusätzlich den Einfluss von unterschiedlichen Standort- und Umweltfaktoren auf die Mikronährstoff-Akkumulation zu ermitteln. Mediane Zink-Konzentrationen lagen bei den Samen, die direkt aus Genbankmaterial vermessen wurden, bei 24,8 mg kg^{-1} Trockengewicht (TG). Die medianen Konzentrationen der einzelnen Anzuchten lagen bei der BCC bei 48,1, 63,4 und 46,1 mg kg^{-1} TG sowie bei der ICARDA-Kollektion bei 56,5, 45,9 und 50,1 mg kg^{-1} TG (FT, SE, KW) (Abb. 3a, b). Minimale und maximale Zink-Konzentrationen wurden für die BCC in den Probensets IPK (15,1 mg kg^{-1} TG) und Runde II (92,3 mg kg^{-1} TG) sowie für die ICARDA-Kollektion in Umwelt FT (24,8 mg kg^{-1} TG und 91,1 mg kg^{-1} TG)

gemessen. Hierdurch ergab sich ein möglicher Unterschied in der Zink-Akkumulation von circa 3,7 in den verschiedenen Linien als Basis für verschiedene Züchtungsmethoden.

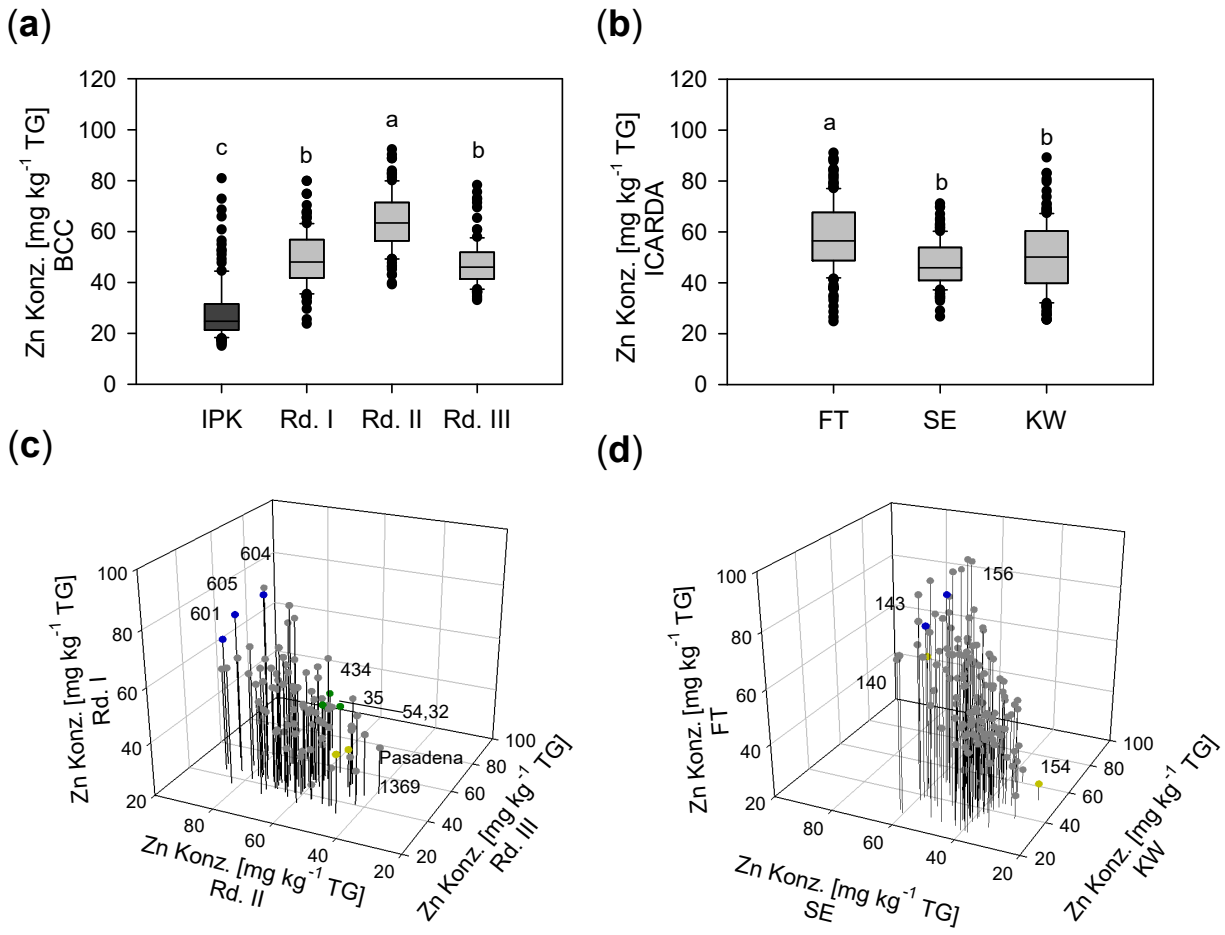

Abb. 3 Variation des Zink-Gehalts in Körnern von Gerste. (**a**) Zink (Zn)-Konzentrationen in Körnern von Gerste (*Hordeum vulgare* L.) der „Barley Core Collection“ (BCC) in einzelnen Jahren und (**b**) der „International Center for Agricultural Research in the Dry Areas“ (ICARDA)-Kollektion in einzelnen Umwelten. Für die BCC wurden Körner direkt nach dem Erhalt aus dem Material der Genbank des IPK in Gatersleben (IPK) oder nach Anzucht im Gewächshaus in drei verschiedenen Jahren (Rd. I, Rd. II, Rd. III) analysiert. Für die ICARDA-Kollektion wurden die Pflanzen in drei verschiedenen Umwelten (FT, SE, KW) innerhalb eines Jahres kultiviert und die Körner anschließend vermessen. Die Boxplots stellen den Median, die oberen und unteren Quartile sowie Extreme von min. 102 (BCC) und 150 (ICARDA) Linien dar. Statistische Unterschiede wurden mittels ANOVA/Tukey's HSD post hoc Test berechnet und sind mit Kleinbuchstaben gekennzeichnet ($P \leq 0{,}05$). (**c**) Zink-Konzentration der einzelnen Linien verglichen über die verschiedenen Anzuchten der BCC- und (**d**) der ICARDA-Kollektion. Linien, die als repräsentativ für unterschiedliche Akkumulationsmuster ausgewählt wurden, sind farblich markiert (gelb: niedrig, grün: intermediär, blau: hoch Zink-akkumulierend). Für die BCC wurden 87, für die ICARDA-Kollektion 130 Linien für die Darstellung in 3D-Punktwolken herangezogen. TG: Trockengewicht.

Eine weitere Komponente zur Ermittlung der Züchtungsbasis ist die Stabilität einer gewünschten Eigenschaft über verschiedene Umwelten und extrinsische Einflussfaktoren hinaus. Um die Stabilität der Zink-Akkumulation der einzelnen Linien zu ermitteln und Linien für weiterführende Untersuchungen auszuwählen, wurden die Ergebnisse der Zink-Akkumulation in 3D-Punktwolken dargestellt (Abb. 3c, d). Hierbei zeigte sich, dass die Linien 601, 604 und 605 (BCC) und 156, 143 (ICARDA) stabil hoch Zink-akkumulierend sowie die Referenzlinie Pasadena und 1369 (BCC) sowie 140 und 154 (ICARDA) niedrig akkumulierend waren. Linie 431 der BCC, die lediglich in zwei Anzuchten geerntet und daher nicht in Abbildung 3c repräsentiert ist, wurde ebenso zur Gruppe der hoch Zink-akkumulierenden Linien hinzugefügt. Für die BCC wurden zusätzlich intermediäre Linien (32, 35, 54 und 434) ausgewählt.

1.5.3 Korrelation von Mikronährstoffen und Genotyp-Umwelt-Interaktionen

Die Analyse von Korrelationen verschiedener Mikroelemente zueinander kann wichtige Hinweise auf ähnliche Verteilungs- und Akkumulationsmechanismen während der Kornbeladung liefern. Daher wurden die ermittelten Zink-, Eisen-, Mangan- und Kupfer-Konzentrationen der Körner korreliert und der Determinationskoeffizient bestimmt. In beiden untersuchten Kollektionen konnten die stärksten Korrelationen zwischen Zink und Eisen mit einem Determinationskoeffizienten von 0,465 (BCC) und 0,581 (ICARDA) ermittelt werden, gefolgt von Zink und Kupfer mit 0,337 (BCC) und 0,446 (ICARDA) (Abb. 4). Die Korrelationen zwischen Zink und Mangan, Eisen und Mangan sowie Kupfer und Eisen waren mit Werten zwischen 0,114 (ICARDA, Zink und Mangan) und 0,284 (ICARDA, Kupfer und Eisen) geringer. Keine signifikante Korrelation konnte innerhalb der ICARDA-Kollektion für Kupfer und Mangan ermittelt werden.

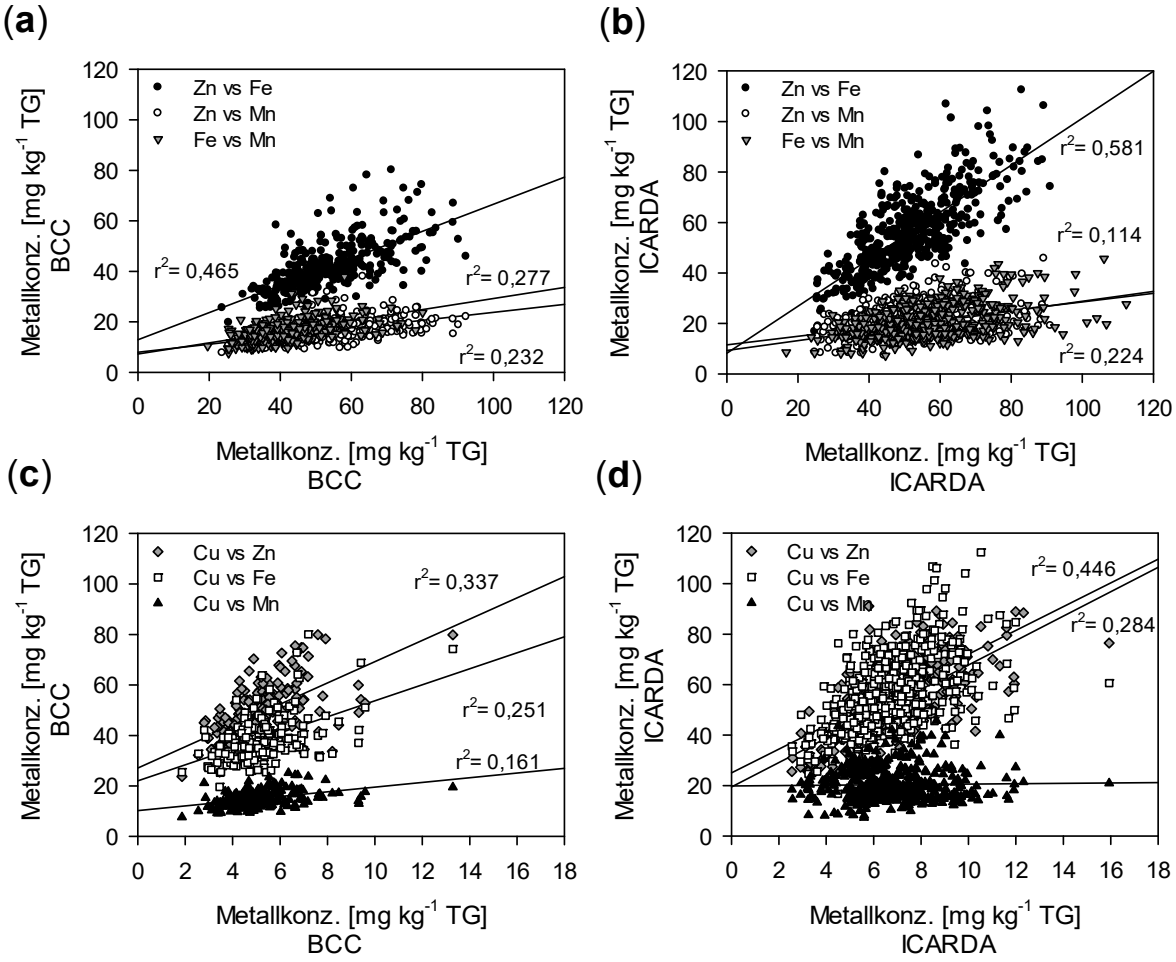

Abb. 4 Regression von Mikronährstoff-Konzentrationen im reifen Korn von Gerste (**a**) Regression von Zink (Zn) vs Eisen (Fe), Zn vs Mangan (Mn) und Fe vs Mn in Linien der BCC- und (**b**) ICARDA-Kollektion. (**c**) Regression von Kupfer (Cu) vs Zn, Fe und Mn in Linien der BCC- und (**d**) ICARDA-Kollektion. Die Gesamtzahl der einbezogenen Linien bezieht sich für die BCC auf alle drei Anzuchtrunden mit 321 Proben in (**a**) und die erste und dritte Anzuchtrunde mit 219 Proben in (**c**). Für die drei verschiedenen Umwelten der ICARDA-Kollektion wurden 473 Proben einbezogen (**b**, **d**). r^2: Determinationskoeffizient. Alle dargestellten Determinationskoeffizienten waren signifikant ($P \leq 0,05$). TG: Trockengewicht.

Die Ausprägung eines bestimmten Phänotyps folgt unter Vereinfachung der Annahme, dass er vom Genotyp, der die Pflanze umgebenden Umwelt sowie einer Interaktion aus beiden Faktoren bestimmt wird. Um züchterisch auf ein Merkmal Einfluss nehmen zu können, ist es bedeutend, dass der Genotyp die Merkmalsausprägung maßgeblich beeinflusst. Um eine Einschätzung des Einflusses der unterschiedlichen Faktoren auf die Zink-Akkumulation im Korn geben zu können, wurde eine ANOVA durchgeführt. Hierbei wurde bei der BCC der Einfluss des Genotyps als auch der Einfluss der verschiedenen Anzuchtrunden unter kontrollierten Gewächshausbedingungen analysiert (Tab. 1), wohingegen für die ICARDA-Kollektion der Einfluss des Genotyps und der Einfluss der drei verschiedenen Umwelten

(FT, SE, KW) ermittelt wurden (Tab. 2). Hierbei zeigte sich bei beiden Kollektionen, dass für Zink und Eisen der Genotyp eine signifikante Rolle in der Merkmalsausprägung spielt. Besonders deutlich war dieser Einfluss mit 58,1 % für Zink und 64,5 % für Eisen bei der ICARDA-Kollektion. Der Umwelteinfluss war hierbei mit 13,4 % (Zink) und 9,3 % (Eisen) relativ gering. Für Kupfer ergaben sich unterschiedliche Ergebnisse in den beiden Kollektionen, die jedoch durch stark schwankende Kupfer-Konzentrationen der Anzuchterde in der BCC zumindest zum Teil überzeichnet sein können. In beiden Kollektionen wurden insbesondere die Mangan-Konzentrationen in den Körnern mit bis zu 50,8 % stärker durch die Umwelt beeinflusst als durch den Genotyp.

Tab. 1 Genotyp- und Anzuchtrunden-Effekte auf Zink (Zn), Eisen (Fe), Mangan (Mn) und Kupfer (Cu) in den Körnern von Gerste der „Barley Core Collection“ (BCC). 87 Genotypen wurden in drei verschiedenen Anzuchtrunden im Gewächshaus kultiviert und Mikronährstoff-Konzentrationen mittels ANOVA analysiert ($P \leq 0{,}05$).

Mikroelement	Quelle	FG	QS	MQ	F Wert	*P* Wert	Beitrag zur Varianz [%]
Zn	Genotyp	86	18404,6	214,0	3,3	< 0,001	41,5
	Runde	2	14694,7	7347,4	112,8	< 0,001	33,2
	Residuum	172	11202,3	65,1			
Fe	Genotyp	86	7577,8	88,1	1,4	< 0,05	29,3
	Runde	2	7557,6	3778,8	60,8	< 0,001	29,3
	Residuum	172	10695,1	62,2			
Mn	Genotyp	86	1086,1	12,6	1,4	< 0,05	24,0
	Runde	2	1887,5	943,7	104,9	< 0,001	41,7
	Residuum	172	1548,2	9			
Cu	Genotyp	86	170,3	2,0	2,0	< 0,001	13,2
	Runde	2	956,0	478,0	492,8	< 0,001	73,9
	Residuum	172	166,8	1,0			

FG: Freiheitsgrad, QS: Quadratsumme, MQ: Mittlere Quadratsumme

Tab. 2 Genotyp- und Umwelt-Effekte auf Zink (Zn), Eisen (Fe), Mangan (Mn) und Kupfer (Cu) in den Körnern von Gerste der „International Center for Agricultural Research in the Dry Areas“ (ICARDA)-Kollektion. 130 Genotypen wurden in drei verschiedenen Umwelten kultiviert und Mikronährstoff-Konzentrationen mittels ANOVA analysiert ($P \leq 0{,}001$).

Mikroelement	Quelle	FG	QS	MQ	F Wert	*P* Wert	Beitrag zur Varianz [%]
Zn	Genotyp	129	38892,0	301,5	4,1	< 0,001	58,1
	Umwelt	2	8985,4	4492,7	60,7	< 0,001	13,4
	Residuum	258	19109,3	74,1			
Fe	Genotyp	129	65839,2	510,4	4,9	< 0,001	64,5
	Umwelt	2	9515,1	4757,5	46,0	< 0,001	9,3
	Residuum	258	26667,8	103,4			
Mn	Genotyp	129	5190,8	40,2	3,6	< 0,001	31,6
	Umwelt	2	8346,9	4173,5	372,5	< 0,001	50,8
	Residuum	258	2890,9	11,2			
Cu	Genotyp	129	592,6	4,6	3,1	< 0,001	46,3
	Umwelt	2	306,9	153,5	103,9	< 0,001	24,0
	Residuum	258	381,1	1,5			

FG: Freiheitsgrad, QS: Quadratsumme, MQ: Mittlere Quadratsumme

1.5.4 Cadmium-Akkumulation in ausgewählten Linien der „Barley Core Collection“ (BCC)

Da zahlreiche Kationentransportsysteme auf der Grundlage des negativen Membranpotentials der Pflanzenzelle beruhen, werden nicht nur für die Pflanze wichtige, sondern auch zum Teil phytotoxische Ionen aufgenommen (Palmgren *et al.*, 2008). Da durch eine erhöhte Zink-Aufnahme die Gefahr einer Cadmium-Akkumulation im Korn besteht, muss unter anderem Cadmium als phyto- und humantoxisches Metall in Biofortifikationsbestrebungen Beachtung finden (Clemens *et al.*, 2013). Aus diesem Grund wurde ein ausgewähltes Set an Pflanzen der BCC auf einer durch Bergbau kontaminierten landwirtschaftlichen Erde angezogen. Die Linien wurden aufgrund ihrer Zink-Akkumulationsmuster während der drei Anzuchtrunden im Gewächshaus ausgewählt und spiegelten die Bandbreite der Zink-Akkumulation wider (s. Abschnitt 1.5.2). Alle ausgewählten

Linien zeigten auf kontaminierter Erde deutlich erhöhte Zink-Konzentrationen von 68±15,6 und 166,7±29 mg kg^{-1} TG (Abb. 5a). Hierbei spiegelten die Konzentrationen unter höheren Schwermetallverfügbarkeiten nicht in allen Linien die vorherige Klassifizierung ihrer Zink-Akkumulation wider. So wies Linie 434 die höchsten Zink-Konzentrationen (166,7±29 mg kg^{-1} TG) auf, die zuvor unter den intermediären Linien zu finden war. Die Analyse der Cadmium-Konzentrationen in den Körnern konnte zeigen, dass mit einem mehr als 8-fachen Unterschied eine deutliche Variation in der Cadmium-Akkumulation vorhanden war. Mit einer Konzentration von 0,07±0,03 mg kg^{-1} TG lag nur das Referenzkultivar *H. vulgare* 'Pasadena' unterhalb des Grenzwertes von 0,1 mg kg^{-1} TG, der vom Codex Alimentarius für Getreide (mit Ausnahme von Weizen und Reis mit je 0,2 mg kg^{-1} TG und 0,4 mg kg^{-1} TG) festgelegt ist (Joint FAO/WHO Codex Alimentarius Commission, 1995). Die höchsten Cadmium-Konzentrationen wurden in Linie 604 mit 0,6±0,3 mg kg^{-1} TG detektiert, die unter den hoch Zink-akkumulierenden Linien zu finden war.

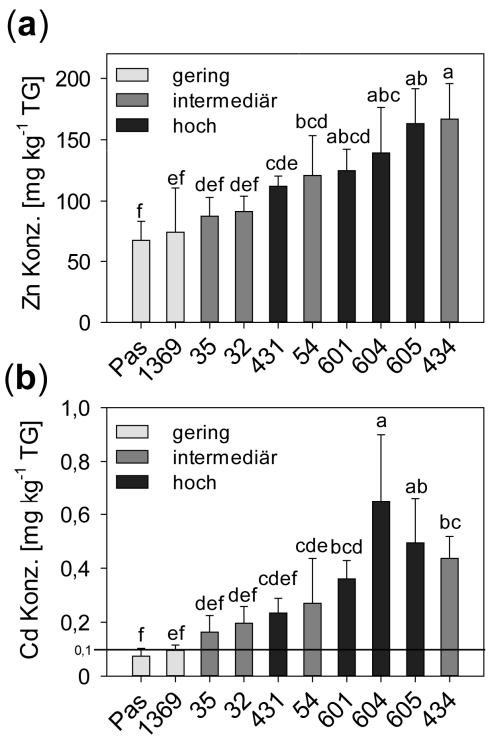

Abb. 5 Zink (Zn)- und Cadmium (Cd)-Konzentrationen in ausgewählten Linien der „Barley Core Collection“ (BCC) nach Anzucht auf kontaminierter Erde. (**a**) Zn- und (**b**) Cd-Konzentrationen von Körnern ausgewählter BCC Linien (32, 35, 54, 431, 434, 601, 604, 605, 1369) sowie des Referenzkultivars *Hordeum vulgare* 'Pasadena' (Pas) nach Anzucht in metallkontaminierter landwirtschaftlicher Erde. Zuvor wurden die Linien nach Anzucht auf nicht-kontaminierter Erde entsprechend der Zink-Konzentrationen im Korn als niedrig (Pas, 1369), intermediär (32, 35, 54 und 434) und hoch (431, 601, 604, 605) Zink-akkumulierend eingestuft. Der Grenzwert von 0,1 mg kg^{-1} TG, der vom Codex Alimentarius (Joint FAO/WHO Codex Alimentarius Commission, 1995) festgesetzt wurde, ist durch eine schwarze Linie angezeigt. Dargestellt sind Mittelwerte + Standardabweichung (n = 7). Statistische Unterschiede wurden mittels ANOVA/Tukey's HSD post hoc Test berechnet und sind mit Kleinbuchstaben gekennzeichnet ($P \leq 0,05$). TG: Trockengewicht.

1.5.5 Lokalisation von Zink in unterschiedlichen Korngeweben

Getreide wird häufig zu Mehl weiterverarbeitet, wobei je nach Mahlgrad die äußeren Bestandteile des Korns und der Embryo entfernt werden. Dies kann jedoch je nach Verteilung der Mikronährstoffe im Korn einen erheblichen Einfluss auf die ernährungsphysiologische Güte des Mehls haben. Um mögliche Unterschiede in der Zink-Akkumulation in verschiedenen Korngeweben zu analysieren, wurden Kornzerlegungen an ausgewählten Linien der BCC- und ICARDA-Kollektion durchgeführt (Abb. 6a, b).

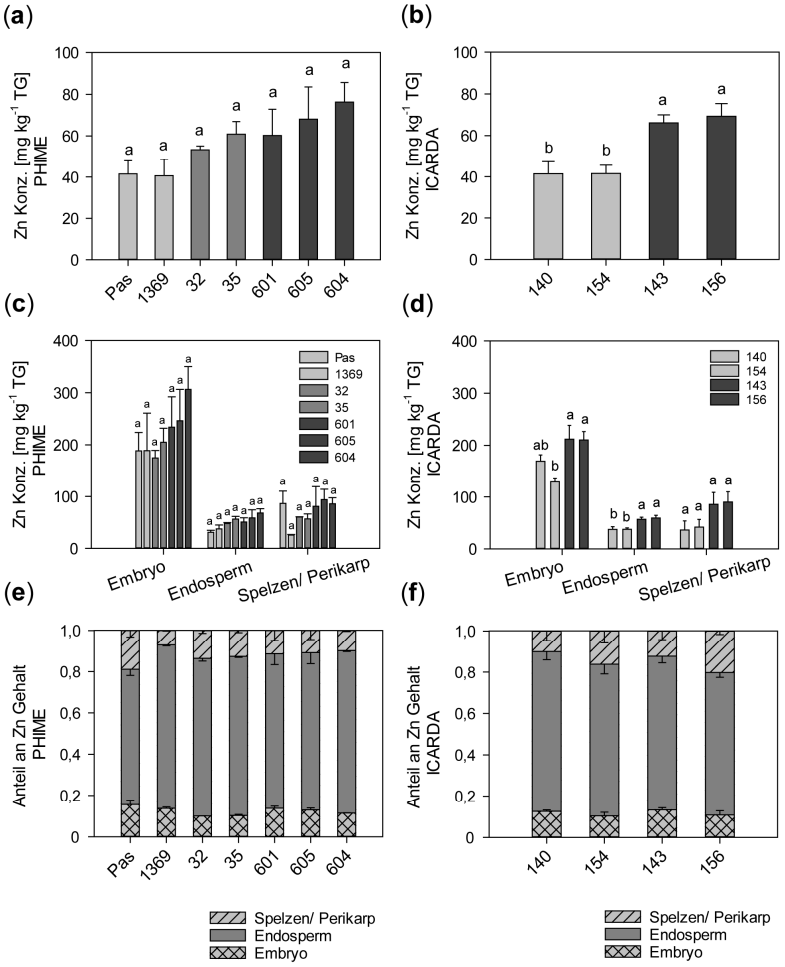

Abb. 6 Mikronährstoff-Gehalte in unterschiedlichen Korngeweben von Gerste. (**a**) Zink (Zn)-Konzentrationen in den reifen Körnern ausgewählter Linien der BCC- und (**b**) ICARDA-Kollektion. Hierbei wurden für die BCC niedrig Zn-akkumulierende (*Hordeum vulgare* 'Pasadena' (Pas), 1369), intermediäre (32, 35) und hoch Zn-akkumulierende Linien (601, 605, 604) und für die ICARDA-Kollektion zwei niedrig (140, 154) und zwei hoch Zn-akkumulierende Linien (143, 156) ausgewählt. (**c**) und (**d**) Zn-Konzentrationen einzelner Korngewebe (Embryo, Endosperm und Spelzen/ Perikarp) für die in (**a**) und (**b**) beschriebenen Linien. (**e**) und (**f**) Anteil der einzelnen Gewebe (Embryo, Endosperm und Spelzen/ Perikarp) am Gesamtgehalt von Zn im Korn. Für jede Probe wurden fünf Körner pro Linie und Anzuchtrunde vereinigt. Dargestellt sind Mittelwerte + Standardabweichung (n = 2-3). Statistische Unterschiede wurden mittels ANOVA/Tukey's HSD post hoc Test berechnet und sind mit Kleinbuchstaben gekennzeichnet ($P \leq 0{,}05$). TG: Trockengewicht.

In beiden Kollektionen und den analysierten Geweben konnte in überwiegend allen Linien ein ähnliches Zink-Akkumulationsmuster entsprechend ihrer vorherigen Einordnung in niedrig und hoch akkumulierend ermittelt werden. Es gab somit keinen Hinweis auf spezifische Akkumulationsfähigkeiten in einzelnen Geweben der hoch akkumulierenden Linien. Außerdem zeigte sich, dass die höchsten Konzentrationen an Zink im Embryogewebe zu finden waren (BCC: 174,9±14,3 bis 306,4±43,7 mg kg^{-1} TG, ICARDA: 129,0±7,9 mg kg^{-1} TG bis 211,8±26,6 mg kg^{-1} TG) (Abb. 6c, d). Betrachtet man jedoch den Gewichtsbeitrag der einzelnen Gewebe zum gesamten Zink-Gehalt im Korn, decken sich die Ergebnisse der beiden Kollektionen. Das Endosperm-Gewebe hatte mit 65,5 bis 79,3 % (BCC) und 69,0 bis 77,5 % (ICARDA) den größten Anteil am Zink-Gehalt des Korns. Embryo- und Hüllgewebe trugen hierbei zu einem vergleichbar geringeren Anteil zum gesamten Zink-Gehalt bei (10 bis 15,6 % und 7 bis 18,9 % für die BCC und 10,4 bis 13,3 % und 10 bis 20,2 % für die ICARDA-Kollektion).

1.5.6 Konzentration und Lokalisation von Zink während der Kornentwicklung

Die Aufnahme und Verteilung von Zink im Korn von Gerste ist insbesondere während der Kornentwicklung bisher kaum erforscht. Hierbei ist auch noch wenig bekannt, inwieweit die Remobilisierungsprozesse aus dem Fahnenblatt oder direkte Aufnahme über die Wurzeln und Transport zum Korn eine Bedeutung spielen. Um ein genaueres Bild der Zink-Akkumulation während der Kornentwicklung zu gewinnen, wurden ganze Ähren 7, 15 und 27 Tage nach der Befruchtung (TnB) und Körner bei Reife analysiert (Abb. 7a). Dazu wurden zwei niedrig (140, 154) und zwei hoch (143, 156) Zink-akkumulierende Linien der ICARDA-Kollektion ausgewählt. Ein signifikanter Unterschied in den Zink-Konzentrationen der Körner der niedrig und hoch akkumulierenden Linien wurde lediglich im letzten analysierten Stadium, der Reife, detektiert. Steigende Zink-Konzentrationen während der Entwicklung konnten kaum beobachtet werden, wohingegen dennoch eine nicht statistisch nachweisbare Tendenz zu niedrigeren oder höheren Konzentrationen in den jeweiligen Linien sichtbar war. Zur Ermittlung etwaiger Einflüsse oder Korrelationen der Zink-Konzentrationen in den Fahnenblättern wurden diese während der Entwicklung beprobt (Abb. 7b). Hierbei konnte jedoch kein Muster detektiert werden, das dem der entsprechend niedrigen oder hohen Zink-Akkumulationen im Korn entsprach.

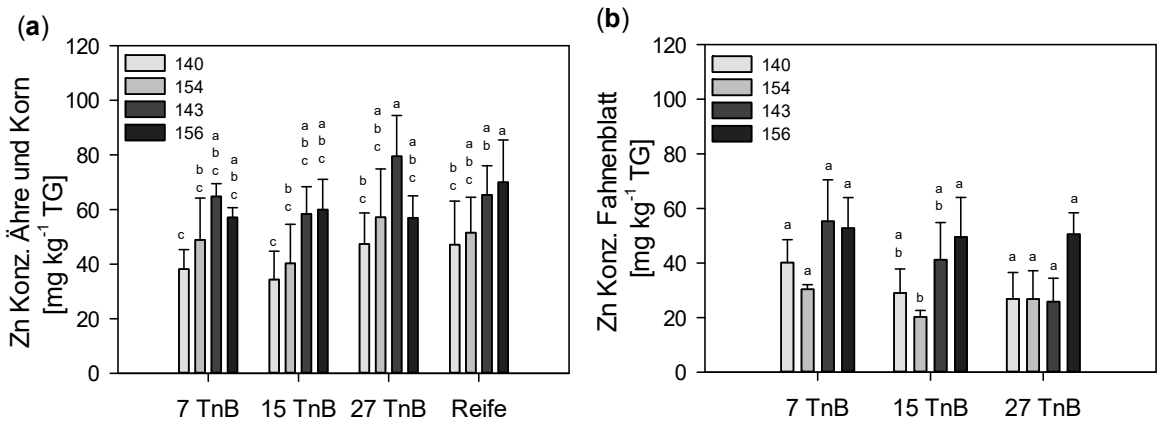

Abb. 7 Zink (Zn)-Konzentrationen in ganzen Ähren und den Fahnenblättern von Gerste während der Kornentwicklung. (**a**) Zn-Konzentrationen in ganzen Ähren oder Körnern und (**b**) Fahnenblättern von niedrig (140, 154) und hoch Zink-akkumulierenden Linien (143, 156) der ICARDA-Kollektion. Pflanzen wurden 7, 15 und 27 Tage nach der Befruchtung (TnB) und bei Reife beprobt. Drei bis fünf Pflanzen wurden in drei (7, 27 TnB) oder fünf (15 TnB, Reife) Runden im Gewächshaus oder in der Kulturkammer angezogen. Bei den Proben 7, 15 und 27 TnB wurden drei bis fünf Ähren zu einer Probe pro Runde vereinigt. Im Reifezustand wurden je Runde fünf Körner einer Pflanze zu einer Probe vereinigt (drei bis fünf Pflanzen pro Runde). Dargestellt sind Mittelwerte + Standardabweichung (n = 3-20). Statistische Analysen wurden mittels ANOVA/Tukey's HSD post hoc Test durchgeführt und sind mit Kleinbuchstaben gekennzeichnet ($P \leq 0{,}05$). TG: Trockengewicht.

Um einen detaillierten Einblick in die Zink-Akkumulation innerhalb der Körner während der Entwicklung gewinnen zu können, wurden zwei kontrastierende Linien (140 und 156) ausgewählt und mittels µ-PIXE untersucht. Hierfür wurden von den Körnern Schnitte angefertigt, die sowohl den sich entwickelnden oder entwickelten Embryo, das Endosperm-Gewebe, Aleuron und Perikarp enthielten (Abb. 8).

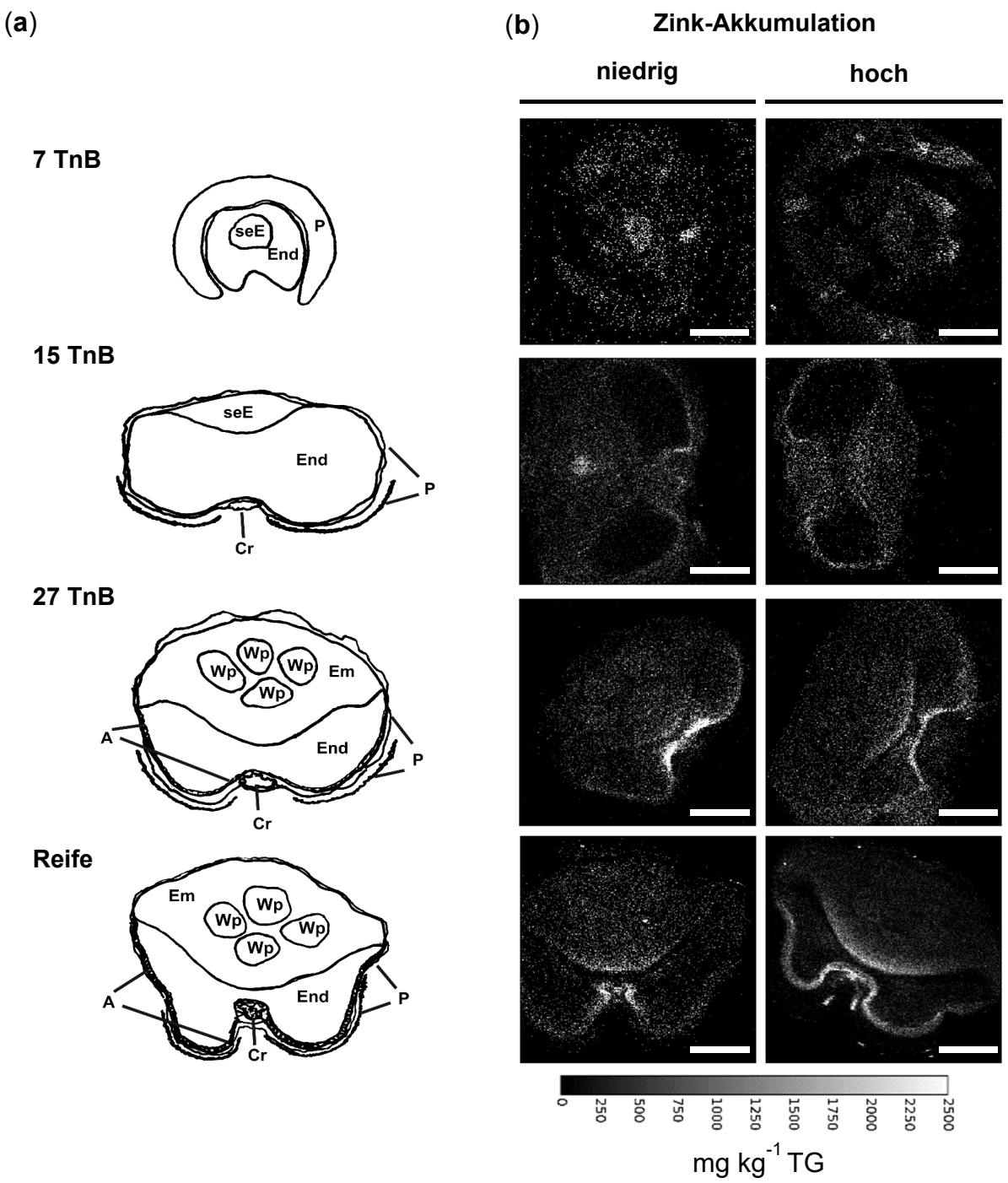

Abb. 8 Darstellung der analysierten Korngewebe und Verbreitungskarten von Zink (Zn) basierend auf µ-PIXE Messungen von zwei kontrastierenden Gerstelinien während der Kornentwicklung. (**a**) Skizze der analysierten Schnitte 7, 15 und 27 Tage nach Befruchtung (TnB) und bei Reife. Körner wurden an der Position des (sich entwickelnden) Embryos transversal geschnitten, sodass Embryo, Endosperm, Aleuron und Perikarp zu sehen waren. seE: sich entwickelnder Embryo, End: Endosperm, P: Perikarp, Cr: Crease, Wp: Wurzelprimordien, Em: Embryo, A: Aleuron. (**b**) µ-PIXE Karten von einer niedrig (140) und hoch (156) Zink-akkumulierenden Linie der ICARDA-Kollektion während vier verschiedener Entwicklungszeitpunkte (7, 15, 27 TnB und zum Zeitpunkt der Reife). Die Skalenleisten der µ-PIXE Verbreitungskarten zeigen 62,5 µm (7 TnB) und 500 µm (15, 27 TnB und bei Reife) an. TG: Trockengewicht.

Die Verbreitungskarten der µ-PIXE Analyse zeigten insbesondere ab 27 TnB höhere Zink-Konzentrationen einer Übergangszone zwischen Aleuron, Endosperm und Embryo, in der eine verstärkte Beladung des Korns mit Zink augenscheinlich wirkt. Ab 27 TnB erhöhen sich die Zink-Konzentrationen im Endosperm, die bis ins Reifestadium anhalten. Ein signifikanter Unterschied der Linien ist, entsprechend der vorherigen Ergebnisse, die in ganzen Ähren ermittelt wurden, erst ab Reife sichtbar. Eine quantitative Analyse der Verteilungsmappen zeigte entsprechend der Ergebnisse der Samendissektion bei reifen Körnern höhere Zink-Gehalte insbesondere im Endosperm und Aleuron-Gewebe in der hoch Zink-akkumulierenden Linie im Vergleich zur niedrig Zink-akkumulierenden Linie (Daten nicht gezeigt).

1.5.7 Speziierung im Endosperm während der Kornentwicklung

Für die Aufnahme von Mikroelementen über den Gastrointestinaltrakt des Menschen ist nicht lediglich die Gesamtmenge an Mikroelementen in den konsumierten Nahrungsmitteln bedeutend, sondern in besonderem Maße auch deren Bindungsform. So können zum Beispiel Eisen oder Zink, die in Form von Phytat gebunden sind, nicht aufgenommen werden, da der menschliche Organismus keine Phytasen zum Aufschluss der Verbindung bilden kann. Um einen Eindruck der Bindungsumwelt von Zink in sich entwickelndem Endosperm-Gewebe zu gewinnen, wurden deshalb Proben der hoch Zink-akkumulierenden Linie 156 via SEC-ICP-MS während der Kornentwicklung vermessen (Abb. 9).

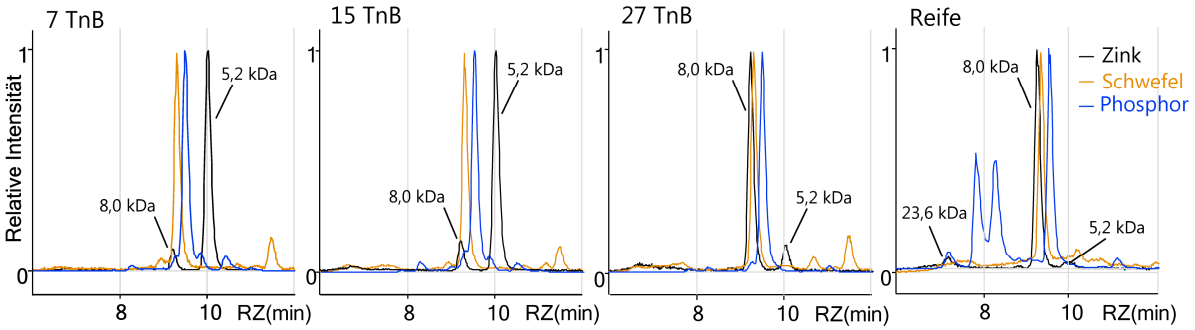

Abb. 9 SEC-ICP-MS Chromatogramme von Zink, Schwefel und Phosphor Spezies aus Endosperm von Gerstekörnern während der Entwicklung. Endosperm einer hoch Zink-akkumulierenden Linie (156) der ICARDA-Kollektion wurde 7, 15 und 27 Tage nach der Befruchtung (TnB) und das ganze Korn bei Reife extrahiert und mittels SEC-ICP-MS analysiert. Die Chromatogramme wurden auf das höchste Signal je Entwicklungsstadium normalisiert. Die korrespondierenden Molekulargewichte der jeweiligen Zink-Peaks sind in kDa in der Abbildung indiziert. Retentionszeiten (RZ) sind in Minuten (min) angegeben.

Die Analyse der löslichen Extrakte ergab drei verschiedene Zink-Spezies mit Molekulargewichten von 5,2, 8,0 und 23,6 kDA. Die beiden kleineren Zink-Spezies konnten während aller Entwicklungsstadien detektiert werden, wobei ein Wechsel der relativen Intensität ab 27 TnB zu sehen war. Keiner dieser Peaks co-eluierte mit Phosphor oder Schwefel, was auf eine andere als Phytat- oder Protein-basierte Bindungsumgebung hindeutete. Die größere Zink-Spezies von 23,6 kDA schien mit Phosphor zu co-eluieren, was eine mögliche Verbindung zu einem Phytat-Polymer indiziert. Die Extraktion mittels NH_4OAc resultierte jedoch mit voranschreitender Entwicklung in immer geringeren Extraktionseffizienzen (45 % bei 7 TnB bis 7 % bei Reife, Daten nicht gezeigt). Dies deutet darauf hin, dass Zink mit zunehmender Reife in unlöslicher Form gebunden war.

1.5.8 Genomweite Assoziationsstudie und Transkriptom-Analyse von Ähren und Fahnenblättern kontrastierender Linien

Für die Züchtung biofortifizierter Kulturpflanzen mit Hilfe moderner Züchtungsmethoden ist die Kenntnis von molekularen Translokations- und Akkumulations-prozessen von Zink während der Kornentwicklung notwendig. Um Kandidatengene zu identifizieren, wurde anhand der für die ICARDA-Kollektion vorhandenen Marker eine genomweite Assoziationsstudie durchgeführt. Mit Hilfe der Zink-Konzentrationen von Körnern aus drei verschiedenen Umwelten wurden für Zink 13 Marker-Eigenschaft-Assoziationen ermittelt (BLUEs). Innerhalb von ±2,5 cM Abstand zum signifikant assoziierten Marker 2H-bPb9754 (82,77 cM) konnten zwei Gene der „Yellow Stripe-Like“ (YSL)-Familie identifiziert werden. Eines dieser Gene zeigt Homologie zu *AtYSL2* (*MLOC_40066.1*, Position 80,89 cM) und das zweite ist als Gerste *YSL9* (*MLOC_61170.4*, Position 80,95 cM) annotiert.

Des Weiteren wurden sowohl ganze Ähren als auch Fahnenblätter von zwei niedrig (140, 154) und hoch (143, 156) Zink-akkumulierenden Linien der ICARDA-Kollektion 15 TnB beprobt und auf Transkriptomebene analysiert. Um grundlegende Mechanismen der unterschiedlichen Zink-Akkumulation zu erforschen, wurden paarweise Vergleiche durchgeführt und nur Gene in Betracht gezogen, die in allen Vergleichen zwischen hoch und niedrig akkumulierenden Linien (156 vs 140 und 154 sowie 143 vs 140 und 154) unter-schiedlich exprimiert waren. Diese strenge Gruppierung führte zu einer relativ geringen Anzahl niedriger oder höher exprimierter Gene (Abb. 10).

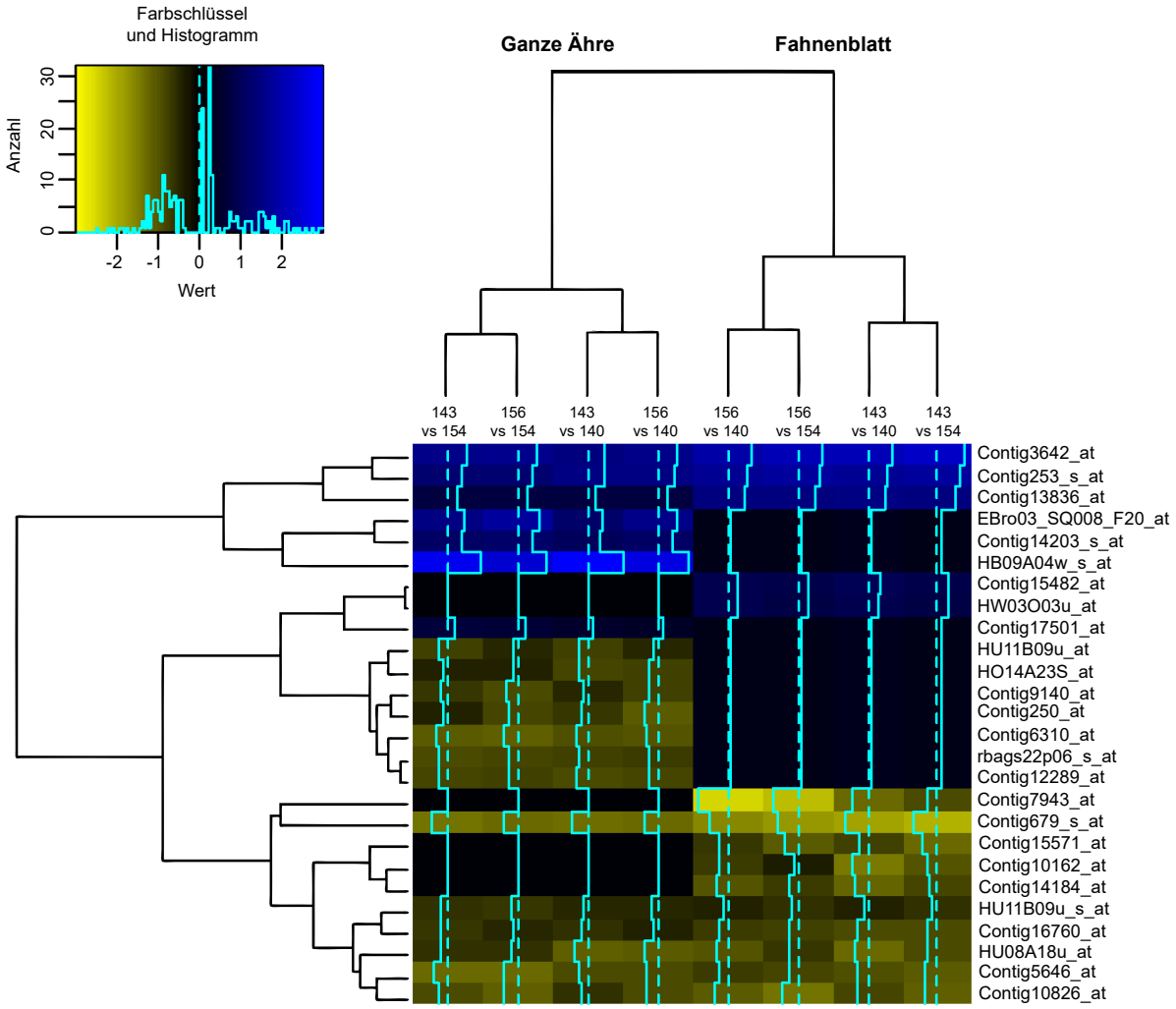

Abb. 10 Signifikant niedriger oder höher exprimierte Gene in niedrig und hoch Zink-akkumulierenden Linien in Ähren und Fahnenblättern von Gerste. Von je zwei niedrig (140, 154) und hoch (143, 156) Zink-akkumulierenden Linien wurden 15 Tage nach Befruchtung (TnB) ganze Ähren und Fahnenblätter geerntet und mittels Microarray-Analyse untersucht. Nur Gene, die in allen Vergleichen 143 vs 140 und 154 sowie 156 vs 140 und 154 als signifikant niedriger oder höher exprimiert erschienen, sind dargestellt. $P \leq 0{,}05$, „fold-change“ >1. Clustering wurde mit Hilfe von Hclust (gplots) durchgeführt.

Sieben bzw. 13 Gene waren in ganzen Ähren und 5 bzw. 11 in Fahnenblättern höher oder niedriger exprimiert. Neunzehn von 26 Genen waren keiner spezifischen funktionellen Kategorie (bin) zugewiesen. Die weiteren Gene waren unter anderem an Prozessen der DNA- und Proteinsynthese, des mitochondrialen Elektronentransports/ATP Synthese, der Entwicklungsinhibierung sowie der Pathogenabwehr beteiligt. Eine putative α-Amylase/Trypsin Inhibitor CMb Vorstufe war in hoch Zink-akkumulierenden Linien 8,5-fach höher exprimiert als in niedrig Zink-akkumulierenden Linien (HB09A04w_s_at). Unter den signifikant unterschiedlich exprimierten Genen waren keine bekannten Metalltransporter oder Gene zu finden, die mit Zink-Bindungspartnern wie Metallothioneine (MTs) und Nicotianamin

(NA) in Verbindung gebracht werden. Aus diesem Grund wurden zusätzliche Datenbank-recherchen durchgeführt, um weitere Nukleotidsäure-Proben des Microarrays mit metallbezogenen Genen in Verbindung zu bringen. Diese Suche resultierte in 383 Genen, die bekannten Metallhomöostase-Genen zugeordnet werden konnten. Da unter den stringenten Analysebedingungen jedoch in Fahnenblättern und in Ähren keines dieser Gene unterschiedlich exprimiert war, wurden die Analysebedingungen gelockert und einzelne Vergleiche näher verwandter Linien in Betracht gezogen (143 und 140 oder 156 und 154). Hierbei konnte in Ähren ein Kandidatengen identifiziert werden, das Ähnlichkeit zu „*Metal Tolerance Protein 5*“ (*HvMTP5*: *HORVU1Hr1G071930*, Expect = 7^{e-66}, Ähnlichkeiten = 208/252 [82 %]) in Gerste aufweist.

1.6 Diskussion und Schlussfolgerung

Versteckter Hunger ist ein weltweit verbreitetes Phänomen, das circa ein Drittel der Weltbevölkerung betrifft (Grebmer *et al.*, 2014). Da ein Großteil des Mikronährstoffbedarfs durch pflanzliche Nahrung gedeckt wird, kann die Pflanzenzüchtung bedeutend zur Lösung dieses Problems beitragen. Insbesondere gilt dies im Hinblick auf klimatische Veränderungen, die einen zunehmenden Einfluss auf die Nährstoffzusammensetzung unserer Nahrungsmittel haben können (Myers *et al.*, 2014; Dietterich *et al.*, 2015). Aus diesem Grund sollte die Thematik der Mikronährstoff-Akkumulation ein Bestandteil zukünftiger Züchtungsbestrebungen sein. Als Grundvoraussetzung für die klassische Züchtung von ernährungsphysiologisch wertvolleren Lebensmitteln dient insbesondere die natürliche Variation der Mikronährstoffe in den essbaren Teilen der Pflanzen. Um zudem mit Hilfe modernster Methoden wie der Genom-Editierung, z.B. durch CRISPR/CAS9, Pflanzen züchten zu können, muss das grundlegende Wissen über molekulare Mechanismen der Mikronährstoff-Akkumulation erweitert werden (Palmgren *et al.*, 2008; Murgia *et al.*, 2013). Gerste (*Hordeum vulgare* L.) ist hierfür als Modellpflanze insbesondere geeignet, da sie weltweit verbreitet, an verschiedenste Umweltbedingungen angepasst und das Genom sequenziert ist (Bothmer, 2003; International Barley Genome Sequencing *et al.*, 2012; Dawson *et al.*, 2015). Für die Aufklärung der natürlichen Variation und von mechanistischen Zusammenhängen der Mikronährstoff-Akkumulation besteht jedoch noch Forschungsbedarf. Aus diesem Grund wurde in dieser Doktorarbeit erforscht, inwieweit Mikronährstoffe im Korn der Gerste variieren und zueinander in Verbindung stehen, wie verschiedene Mikronährstoffe während der Kornentwicklung verteilt und gebunden sind und wie sich das molekulare Netzwerk der Akkumulation von Zink im Korn gestaltet.

Um die natürliche Variation der Mikronährstoff-Akkumulation zu untersuchen, wurde auf Basis des FAO Bodenatlasses eine Auswahl an Kulturgerste und Landrassen getroffen. Hierbei wurden aus zwei Gerstekollektionen je 136 (BCC) und 180 (ICARDA) Linien ausgewählt, in je drei verschiedenen Anzuchtrunden kultiviert und die Körner auf deren Mikronährstoff-Gehalt analysiert (Abb. 3). Über verschiedene Jahre und Umwelten hinweg konnte eine Variation um den Faktor 1,3 bis 1,5 (BCC) und 3,7 (ICARDA) im Zink-Gehalt detektiert werden. Die Konzentrationen streuten hierbei von minimal 15,1 mg kg^{-1} TG und maximal 92,3 mg kg^{-1} TG. Die Medianwerte entsprachen mit 30,7 bis 48,5 mg kg^{-1} TG bereits publizierten Ergebnissen für Landrassen aus Äthiopien und Eritrea (Mamo *et al.*, 2014). Im Vergleich zu Analysen von Weizen und Reis zeigt sich, dass Gerste mehr Zink im Korn anreichert (White & Broadley, 2009; Xu *et al.*, 2011; Norton *et al.*, 2014; Pinson *et al.*, 2015). Des Weiteren kann die Analyse von Korrelationen verschiedener Mikronährstoffe zueinander

wertvolle Hinweise über deren Verteilungswege liefern. So konnten die stärksten Korrelationen zwischen Zink und Eisen ermittelt werden (Abb. 4). Innerhalb der ICARDA-Kollektion konnten knapp 60% der Variation der Eisen-Konzentration im Korn durch die Zink-Konzentration erklärt werden. Vergleichbare Korrelationen wurden zuvor in Weizen (Cakmak *et al.*, 2004; Morgounov *et al.*, 2007; Peleg *et al.*, 2008; Zhao *et al.*, 2009; Chatzav *et al.*, 2010; Guttieri *et al.*, 2015), Reis (Jiang *et al.*, 2007) und Hirse (Bashir *et al.*, 2014; Phuke *et al.*, 2017) berichtet. Diese Ergebnisse lassen darauf schließen, dass Zink und Eisen zumindest partiell ähnlichen Aufnahme- und Distributionsprozessen unterliegen. Am schwächsten war die Korrelation von Zink und Mangan ausgeprägt, was mit der Analyse der Genotyp-Runden- bzw. Genotyp-Umwelt-Interaktionen kongruierte. Durch statistische Analysen wurde der Anteil der auf genetischen Determinanten beruhenden Variation errechnet. Ein Großteil der analysierten phänotypischen Variation der Zink- und Eisen-Konzentration wurde durch den Genotyp bestimmt (Tab. 1 und 2). Außerdem waren deutliche Unterschiede zwischen den analysierten Mikronährstoffen erkennbar. So lag der Genotypeinfluss für Zink bei bis zu 58,1 %, wohingegen die Mangan-Konzentrationen mit 50,8 % deutlich stärker von Umwelteinflüssen geprägt waren. Aus züchterischer Sicht ist wichtig, dass durch einen prägnanten genetischen Einfluss die Stabilität der Zink-Akkumulation im Korn verschiedener Linien über verschiedene Umwelten und Jahre hinweg gewährleistet ist. Die Ergebnisse dieser Arbeit decken sich mit der Identifizierung mehrerer QTLs für Zink im Korn innerhalb einer doppelhaploiden Kartierungspopulation durch Lonergan und Kollegen (2009) sowie mit der in einer äthiopischen und eritreischen Population identifizierten Heritabilität (Mamo *et al.*, 2014). Diese Ergebnisse verdeutlichen, dass für die Züchtung hoch Zink-akkumulierender Kultivare geeignetes genetisches Material, sowohl in Bezug auf die Variation der Zink-Gehalte als auch auf deren genetische Determination, vorhanden ist.

Da der Konsum von pflanzlichen Nahrungsmitteln die Hauptaufnahmequelle für Cadmium in den menschlichen Organismus darstellt, ist eine mögliche Korrelation von erhöhten Zink-Gehalten mit erhöhten Cadmium-Gehalten im Korn für die Biofortifikation von Bedeutung (Clemens *et al.*, 2013; Meharg *et al.*, 2013). Hierbei wird die Akkumulation von Cadmium durch die Versorgung der Pflanze mit Mikroelementen beeinflusst und zum Teil durch ähnliche Transportwege wie für Zink, Eisen und Mangan vermittelt (Clemens, 2006; Khan *et al.*, 2014; Slamet-Loedin *et al.*, 2015). Daher wurde für diese Arbeit ein ausgewähltes Set an Linien in niedrig Cadmium-kontaminierter, ackerbaulich genutzter Erde angezogen und Körner auf deren Zink- und Cadmium-Konzentrationen untersucht (Abb. 5). Hierbei lag die Cadmium-Konzentration der Erde mit 10 mg kg^{-1} TG innerhalb der für europäische Oberböden von FORGES Geochemical Atlas of Europe dokumentierten Spannbreite von bis zu 14 mg kg^{-1} TG (Pan *et al.*, 2010). Die Cadmium-Konzentrationen in den Körnern der

analysierten Linien überstiegen die Grenzwerte des Codex Alimentarius von 0,1 mg kg^{-1} TG (Joint FAO/WHO Codex Alimentarius Commission, 1995) mit Ausnahme einer Linie. Entsprechend der vorhandenen Variation der Zink-Akkumulationsfähigkeit wurde eine circa 8-fache Variation der Cadmium-Konzentration im Korn detektiert. Vergleichend hierzu konnte eine Untersuchung von hundert Gerste-Akzessionen der BCC in verschiedenen Umwelten weitaus höhere, bis zu 64-fache, Variation von Cadmium im Korn detektieren (Wu *et al.*, 2015). Hierbei wurde, ähnlich zur Zink-Akkumulation in dieser Arbeit, eine hohe genetische Determination der Cadmium-Akkumulation festgestellt. Die Ergebnisse dieser Doktorarbeit legen nahe, dass höhere Zink-Konzentrationen im Korn mit höheren Cadmium-Konzentrationen assoziiert sind. Diese Ergebnisse verdeutlichen, dass die Berücksichtigung der potentiellen Akkumulation von Schwermetallen in Biofortifikations-Bestrebungen unabdingbar ist. Trotz der deutlichen Korrelation von Zink und Cadmium im Korn gab es jedoch eine Variation in der Zink/Cadmium Ratio, wodurch dennoch Potential zur Züchtung von niedrig Cadmium-akkumulierenden und hoch Zink-akkumulierenden Gerstelinien gegeben ist. Gleichwohl sollten insbesondere im Anbau biofortifizierter Getreide die jeweiligen Bodeneigenschaften im Rahmen einer guten landwirtschaftlichen Praxis berücksichtigt werden.

Höhere Zink-Gehalte im Korn können nur zu einer Verbesserung der Ernährungssituation beitragen, wenn diese nach Prozessierung der Körner, zum Beispiel zu Mehl, weiterhin vorhanden sind (Hansen *et al.*, 2012). Daher ist ein detailliertes Wissen über die Zink-Lokalisation, insbesondere in hoch Zink-akkumulierenden Linien, für diese Beurteilung und für spätere Verzehrempfehlungen grundlegend (Pongrac *et al.*, 2013). Entsprechend wurden in dieser Arbeit reife Gerstekörner ausgewählter Linien der BCC und ICARDA-Kollektion in einzelne Kornbestandteile zerlegt und analysiert (Abb. 6). Hierbei wurde deutlich, dass die höchsten Konzentrationen an Zink im Embryo zu finden waren. Vorherige Analysen in Gerstekörnern konnten ähnliche Ergebnisse dokumentieren (Lombi *et al.*, 2011). Zudem konnte für Weizen gezeigt werden, dass die Konzentrationen im Embryo im Vergleich zum Endosperm um das circa 8-Fache erhöht waren (Zhang *et al.*, 2010; Eagling *et al.*, 2014; Liu *et al.*, 2017). Da das Embryogewebe mit circa 10-15 % zum gesamten Zink-Gehalt im Korn einen geringfügigen Teil beiträgt, ist insbesondere die Zink-Konzentration im Endosperm von Bedeutung. Das Endosperm liefert einen ausschlaggebenden Anteil von bis zu 80 % des gesamten Zink-Gehalts im Korn. Die vergleichenden Analysen dieser Doktorarbeit von niedrig und hoch Zink-akkumulierenden Linien konnten darlegen, dass die Unterschiede in der Zink-Akkumulation nahezu alle untersuchten Gewebe, inklusive des Endosperms, betrafen und kein Gewebe spezifisch in hoch Zink-akkumulierenden Linien angereichert wurde. Ähnliche Ergebnisse sind aus agronomisch Zink-biofortifiziertem Weizen bekannt, in dem das

Endosperm-Gewebe ebenso höhere Zink-Konzentrationen als in der Kontrolle aufwies (Pongrac *et al.*, 2013). Aus den Ergebnissen lässt sich schlussfolgern, dass Zink in hoch Zink-akkumulierenden Linien nicht im Aleuron oder Hüll-Geweben zurückgehalten, sondern zum Endosperm transferiert wird. Dem liegt womöglich ein unterschiedlicher Zink-Transport oder eine effizientere Beladung mit Zink von maternalem zu filialem Gewebe zugrunde. Eine Alternativhypothese wäre, dass hoch Zink-akkumulierende Linien eine unterschiedliche Speicherungsfähigkeit oder sink-Stärke besitzen (Tauris *et al.*, 2009; Xue *et al.*, 2014; Guttieri *et al.*, 2015). Weiterführend stellt sich die Frage, inwieweit Zink im Endosperm gleichmäßig oder in Form eines Gradienten verteilt ist. Dies wäre insbesondere in Hinblick auf verschiedene Mahlgrade des Mehles und eines damit einhergehenden Verlustes von Zink-reichem Gewebe von Bedeutung. In einer kürzlich veröffentlichten Studie konnte ein abnehmender Gradient von Zink von außen nach innen in Weizenkörnern dokumentiert werden (Singh *et al.*, 2018). Interessant wäre für weiterführende Forschungsfragen daher, ob bei unterschiedlich hoch Zink-akkumulierenden Linien unterschiedliche Gradienten vorhanden sind. Zusammenfassend kann hinsichtlich züchterischer und ernährungsphysiologischer Sicht aus den Ergebnissen dieser Arbeit geschlussfolgert werden, dass in hoch Zink-akkumulierenden Linien auch das stärkereiche Endosperm-Gewebe, das den Haupt-bestandteil von Mehl ausmacht, mehr Zink enthält und somit eine potentielle Erhöhung der Gesamt-Zinkaufnahme erzielt werden kann.

Weitestgehend unbekannt war bisher, wie sich Zink während der Entwicklung im Korn anreichert und wo Zink vorrangig im Korn von Gerste lokalisiert ist. Aus diesem Grund wurden zwei niedrig und zwei hoch Zink-akkumulierende Linien ausgewählt und 7, 15 und 27 TnB sowie bei Reife auf die Zink-Konzentration in der ganzen Ähre und in reifen Körnern untersucht (Abb. 7). Höchste Zink-Konzentrationen wurden in reifen Körnern sowohl in der niedrig als auch in der hoch Zink-akkumulierenden Linie detektiert. Während der Entwicklung blieb die Konzentration von Zink in den Ähren auf einem vergleichbaren Niveau, wobei die niedrig akkumulierenden Linien tendenziell niedrigere Konzentrationen während der Entwicklung aufwiesen als die hoch Zink-akkumulierenden Linien. Die Lokalisation von Zink veränderte sich während der Kornentwicklung im Vergleich zum reifen Korn nicht maßgeblich, wobei jedoch die Gesamtkonzentrationen in allen Geweben am Ende der Reife am höchsten waren (Abb. 8). Auch in den analysierten Schnitten konnten in der hoch Zink-akkumulierenden Linie im reifen Korn in allen analysierten Geweben höhere Zink-Gehalte detektiert werden als in der niedrig Zink-akkumulierenden Linie. Demgegenüber ergaben Analysen in Weizen, dass die höchsten Zink-Konzentrationen im frühen Milchstadium von *Triticum aestivum* L. 'Balatilla' detektiert werden konnten (Ozturk *et al.*, 2006). Ebenso konnte in einer anderen Studie während der Kornentwicklung, vor allem im Endosperm, eine Zink-Reduktion um bis zu 7-45 %

zwischen 7 und 34 Tagen nach der Blüte ermittelt werden (Stomph *et al.*, 2011). Interessanterweise wurde hierbei jedoch während der Kornentwicklung ein 5- bis 9-facher Anstieg der Zink-Konzentrationen in der Crease-Region gemessen, weshalb die Autoren einer Limitierung der Abgabe-Kapazität von Crease zu Endosperm als Einflussfaktor eine Rolle zuschrieben. Untersuchungen mittels µ-XRF in Reis konnten zeigen, dass zwar die höchsten Zink-Konzentrationen in der Aleuron-Schicht vorhanden waren, dass Zink jedoch auch innerhalb des Endosperms verbreitet war (Iwai *et al.*, 2012). Die Verteilung von Zink bis ins Endosperm begann circa 10 Tage nach der Blüte und erreichte 21 Tage nach der Blüte ein Plateau. Weitere Untersuchungen in drei verschiedenen Reis-Kultivaren konnten in ähnlicher Weise durch die Analyse verschiedener Mahlfraktionen feststellen, dass Zink in einem abnehmenden Gradienten bis ins innere Endosperm-Gewebe verteilt war (Wang *et al.*, 2011). Diese Ergebnisse decken sich mit höheren mittleren Zink-Gehalten und der breiteren Variabilität der Zink-Konzentrationen in Gerste im Vergleich zu Weizen und Reis (White & Broadley, 2009; Xu *et al.*, 2011; Norton *et al.*, 2014; Pinson *et al.*, 2015). Da die Ergebnisse dieser Arbeit eine Zunahme der Zink-Konzentrationen speziell in reifen Körnern dokumentieren, könnte in Gerste im Vergleich zu Weizen und Reis eine effektivere Beladung mit und Verteilung von Zink innerhalb des Korns oder eine höhere Zink-Speicherkapazität im Endosperm vorliegen. Eine unterschiedliche Ausprägung dieser Akkumulationsfähigkeit war auch in den untersuchten Linien 140 und 156 zu sehen. Interessant ist hierbei jedoch insbesondere, dass beide Linien während ihrer Entwicklung einem ähnlichen Akkumulations-Muster folgten, das insbesondere in seiner Höhe unterschiedlich ausgeprägt war.

Höhere Zink-Gehalte im Korn können einen entscheidenden Beitrag zur Bekämpfung von Mikronährstoffmangel leisten. Von zentraler Bedeutung für die Aufnahme über den Verdauungstrakt ist jedoch, in welcher Form Zink im Korn und insbesondere im Endosperm gebunden ist. Aus diesem Grund wurden Speziierungsanalysen mittels SEC-ICP-MS an Endosperm-Extrakten zweier kontrastierender Gerstelinien durchgeführt (Abb. 9). Die Ergebnisse deuten an, dass Zink in löslicher Form nicht an Phosphor- oder Schwefel-Liganden gebunden zu sein scheint. Dies lässt auf eine andere Bindungsumwelt als Phytat schließen. Lange Zeit wurde vermutet, dass Zink und Eisen in Getreidekörnern überwiegend in für den Menschen unverdaulicher Form an Phytat gebunden sind (Oatway *et al.*, 2007; Schlemmer *et al.*, 2009; Gupta *et al.*, 2015). Durch SEC-ICP-MS Analysen konnte jedoch in Erbsen- und Gerstesamen herausgestellt werden, dass ein durchaus komplexeres Zusammenspiel an Ligandenformen vorhanden ist (Clemens, 2014). So konnte Persson *et al.* (2009) zeigen, dass im Embryo von Gerstesamen Zink vor allem mit Schwefel co-eluierte. Dies lässt auf eine Bindung an Peptide und somit auf eine bessere Bioverfügbarkeit für den Menschen schließen. Auch Analysen von Endosperm-Gewebe zweier kontrastierender

Weizenlinien ergaben, dass lösliches Zink im weißen Mehl vermutlich vorwiegend als bioverfügbarer Zink-Nicotianamin-Komplex vorliegt (Eagling *et al.*, 2014). Die Ergebnisse dieser Arbeit zeigen jedoch auch, dass Zink während der Reife zunehmend in unlöslicher Form gebunden ist. Hierbei können, im Gegensatz zu den Analysen von löslichem Zink mittels chromatographischer Verfahren, K-edge XANES Analysen Hinweise über die Speziierung von unlöslich gebundenem Zink liefern. In Weizen ergaben entsprechende Analysen, dass circa 70-80 % des im Korn vorhandenen Zinks als Zinkphosphat und 20-30 % in anderer Form gebunden waren (Zhang *et al.*, 2018). µ-XRF Analysen in sich entwickelnden Körnern von Reis ließen vermuten, dass Zink aufgrund seiner Verteilung hin bis ins Innere des Endosperms nicht nur an $InsP_6$ gebunden ist, sondern auch in anderen Bindungsformen vorliegt (Iwai *et al.*, 2012). Weiterführende Analysen anhand kontrastierender Linien sollten sich daher auf eine weitere Charakterisierung der unlöslichen Zink-Spezies fokussieren. Dies kann zum Beispiel in einem ersten Schritt mit Hilfe enzymatischer Assays im Vergleich zu spektroskopischen Analysen ohne großen Zeit- und Kostenaufwand durchgeführt werden. Konsekutiv wäre für eine weiterführende Aussage eine in vitro Permeabilitätsanalyse mit Caco-2 Zelllinien aufschlussreich, um eine Aussage über die potentielle Aufnahme von Zink aus Mehl der kontrastierenden Gerstelinien im Verdauungstrakt des Menschen treffen zu können. Nichtsdestotrotz geben die Analysen dieser Arbeit einen ersten Einblick in die Speziierung verschieden hoch Zink-akkumulierender Gerstelinien. Hierbei ist besonders hervorzuheben, dass sich die Linien nicht grundlegend in der Art, sondern vielmehr in der Ausprägung ihrer Speziierung von löslichem Zink während der Entwicklung unterschieden.

Für biotechnologische Züchtungsmethoden ist die Kenntnis der molekularen Prozesse der Metallhomöostase von ausschlaggebender Bedeutung. Insbesondere die molekularen Mechanismen einer unterschiedlichen Zink-Akkumulierungsfähigkeit im Korn von Gerste sind jedoch bisher wenig untersucht. Um Kandidatengene zu ermitteln, die zur natürlichen Variation der Zink-Akkumulation in den Körnern beitragen, wurde zunächst eine genomweite Assoziationsanalyse anhand der für die ICARDA-Kollektion ermittelten Zink-Konzentrationen durchgeführt. Über die verschiedenen Umwelten hinweg wurden sieben Marker-Eigenschaft-Assoziationen detektiert, die mit der Zink-Akkumulation assoziiert werden konnten. Innerhalb eines Bereichs von ±2,5 cM um den Marker bPb9754 (82,77 cM) auf Chromosom 2 konnten zwei Kandidatengene der „Yellow Stripe-Like“ (YSL)-Transporterfamilie identifiziert werden. Bisherige Studien konnten zeigen oder deuten darauf hin, dass YSL-Proteine Metalle transportieren, die an Nicotianamin oder Phytosiderophore gebunden sind (Waters *et al.*, 2006; Conte & Walker, 2012; Senoura *et al.*, 2017). Verschiedene Studien konnten die Bedeutung von YSL-Transportern bei der Beladung von Zink und Eisen im Korn zeigen, wie z.B. *AtYSL1* und *AtYSL3*, die für eine erfolgreiche Reproduktion benötigt werden (Waters *et al.*, 2006;

Chu *et al.*, 2010). In Reis spielt YSL9 eine Rolle in der Translokation von Eisenkomplexen vom Endosperm-Gewebe zum Embryo (Senoura *et al.*, 2017). Unterschiede in der Transport-Kapazität von maternalem zu filialem Gewebe könnten die höheren Zink-Konzentrationen in den hoch Zink-akkumulierenden Linien dieser Arbeit erklären. Weitere Studien müssen jedoch zeigen, ob Unterschiede wie etwaige Polymorphismen der *YSL*-Gene zwischen den unterschiedlichen Linien bestehen und ob sie direkt mit unterschiedlichen Zink-Konzentrationen in Verbindung gebracht werden können.

Um zu untersuchen, ob transkriptionelle Unterschiede zu unterschiedlichen Zink-Konzentrationen im Korn führen, wurden je zwei hoch und zwei niedrig Zink-akkumulierende Linien kultiviert und sowohl ganze Ähren als auch Fahnenblätter mittels Microarray-Analysen untersucht (Abb. 10). Das Hauptaugenmerk dieser Transkriptomanalyse lag auf der Aufdeckung grundlegender Metallhomöostase-Unterschiede zwischen hoch und niedrig akkumulierenden Linien, weshalb die Linien gruppiert und die Ergebnisse aus den Vergleichen stringent auf unterschiedlich exprimierte Gene gefiltert wurden. Hierbei war eine relativ geringe Zahl an Genen in hoch Zink-akkumulierenden Linien im Vergleich zu niedrig Zink-akkumulierenden Linien niedriger oder höher exprimiert. Inkludiert waren Gene, die in basale DNA- und Proteinsynthese-Prozesse, der mitochondrialen Elektronentransport/ATP Synthese, die Entwicklungsinhibierung sowie in die Pathogenabwehr involviert sind. Weitere Studien konnten bereits in Reis und *Arabidopsis* zeigen, dass Unterschiede in Protein- und DNA-Modifizierung eine Rolle in der Metallhomöostase spielen. Insbesondere Gene, die in die Pathogenabwehr involviert sind, wurden zudem in zahlreichen Untersuchungen mit der Metallhomöostase in Verbindung gebracht (Zhao *et al.*, 2009; Aznar *et al.*, 2015; Kühnlenz *et al.*, 2015; Zschiesche *et al.*, 2015; Fischer *et al.*, 2017; Peris-Peris *et al.*, 2017). Die direkte Implikation von Abwehrgenen in die höhere Akkumulation von Zink in Körnern ist jedoch noch nicht eindeutig geklärt, weshalb weiterer Forschungsbedarf zur Aufklärung der zugrundeliegenden Mechanismen besteht. In ganzen Ähren hoch akkumulierender Linien war in dieser Analyse insbesondere eine putative α-Amylase/Trypsin Inhibitor CMb Vorstufe deutlich stärker exprimiert als in niedrig akkumulierenden Linien. Hierbei sind zwei potentielle regulatorische Einflüsse auf die Zink-Akkumulation denkbar. α-Amylase Inhibitoren verhindern eine frühzeitige Aufspaltung der Stärke im Korn, wie sie erst während der Keimung benötigt wird (Sales *et al.*, 2012). Eine Regulierung des Stärke-Gehalts unter Zink-Defizienz wurde in mehreren Studien in Reis und *Arabidopsis* nachgewiesen (Suzuki *et al.*, 2012; Chen *et al.*, 2016; Nanda *et al.*, 2017). Hierbei vermuteten die Autoren einen Effekt erhöhter Stärke-Gehalte in Form eines verminderten osmotischen Stresses oder als Signalmolekül. In dieser Studie waren die Pflanzen jedoch nicht Zink-defizient, weshalb weitere Funktionen von α-Amylase Inhibitoren in der Pathogenabwehr oder als Speicherproteine eine Rolle spielen

könnten (Täufel *et al.;* Franco *et al.*, 2002; Altenbach *et al.*, 2011). Verwunderlich war bei der Analyse der Micorarray-Ergebnisse zunächst, dass in den unterschiedlich regulierten Genen keine bekannten Metalltransporter oder Zink-Bindungspartner wie Metallothioneine (MTs) oder Nicotianaminsynthase-Gene (NA) zu finden waren. Aus diesem Grund wurden zusätzliche Datenbanksuchen durchgeführt, um weitere Gene des Microarrays mit bekannten metallbezogenen Genen verknüpfen zu können. Diese Suche resultierte in 383 Genen, welche jedoch ebenso anhand der gewählten stringenten Kriterien unter natürlichen Bedingungen nur eine untergeordnete Rolle für die unterschiedliche Zink-Akkumulationsfähigkeit zu spielen schienen. Aus diesem Grund wurde die Stringenz der Analyse gelockert und näher verwandte Linien miteinander verglichen. Hierbei wurde ein Kandidatengen in Ähren detektiert, das Ähnlichkeit zu „*Metal Tolerance Protein 5*“ (*HvMTP5*) in Gerste aufweist und in hoch Zink-akkumulierenden Linien niedriger exprimiert war als in niedrig Zink-akkumulierenden Linien. Proteine der MTP-Familie sind membranständige Transporter, die in den Efflux von Zink vom Cytoplasma in zelluläre Bestandteile, wie z.B. der Vakuole, beteiligt sind (Ricachenevsky *et al.*, 2013). Eine Hypothese zur Beteiligung von MTP5 an der Zink-Akkumulation in den Körnern könnte sein, dass Zink durch MTP5 auf dem Transportweg von maternalem zu filialem Gewebe in die Vakuole transportiert wird und somit nicht mehr für den Transfer in filiales Gewebe zur Verfügung steht. Zur Überprüfung dieser Theorie sind jedoch weitere Analysen nötig, um aufzuklären, wo *MTP5* exprimiert wird und inwieweit es zur Zink-Akkumulation im Korn beiträgt.

Die in dieser Doktorarbeit dargestellten Ergebnisse liefern einen grundlegenden Beitrag zur Beschreibung und Aufklärung der natürlichen Diversität, der räumlichen Verteilung und der entwicklungsbezogenen Anreicherung von Zink in kontrastierenden Gerstelinien. Außerdem konnten bisher ungeklärte Fragen zur Konzentration und Speziierung von Zink während der Entwicklung und zu Transkriptunterschieden in unterschiedlich hoch Zink-akkumulierenden Gerstelinien beantwortet werden. Es bedarf jedoch weiterer Forschung zur Aufklärung der Hauptbindungsformen von unlöslichem Zink im Endosperm und der weiterführenden Charakterisierung von bisher nicht funktionell zugeordneten Genen. Darüber hinaus bieten die Ergebnisse dieser Doktorarbeit eine wichtige Grundlage insbesondere für Fragen der genetischen Prädispositionen der Mikronährstoff-Akkumulation und ebnen somit den Weg für eine züchterische Herangehensweise zur Bekämpfung von verstecktem Hunger.

1.7 Literaturverzeichnis

Abràmoff, MD, Magalhães, PJ, Ram, SJ. 2004. Image Processing with ImageJ. *Biophotonics International* 11: 36–42.

Alloway, BJ. 2008. Zinc in soils and crop nutrition. Brüssel, Belgien und Frankreich: IZA; IFA.

Alomari, DZ, Eggert, K, Wirén, N von, Alqudah, AM, Polley, A, Plieske, J, Ganal, MW, Pillen, K, Röder, MS. 2018. Identifying Candidate Genes for Enhancing Grain Zn Concentration in Wheat. *Frontiers in plant science* 9: 390.

Altenbach, SB, Vensel, WH, Dupont, FM. 2011. The spectrum of low molecular weight alpha-amylase/protease inhibitor genes expressed in the US bread wheat cultivar Butte 86. *BMC research notes* 4: 242.

Atungulu, GG, Pan, Z. 2014. Rice industrial processing worldwide and impact on macro- and micronutrient content, stability, and retention. *Annals of the New York Academy of Sciences* 1324: 15–28.

Aznar, A, Chen, NWG, Thomine, S, Dellagi, A. 2015. Immunity to plant pathogens and iron homeostasis. *Plant Sci.* 240: 90–97.

Bashir, EMA, Ali, AM, Ali, AM, Ismail, MI, Parzies, HK, Haussmann, BIG. 2014. Patterns of pearl millet genotype-by-environment interaction for yield performance and grain iron (Fe) and zinc (Zn) concentrations in Sudan. *Field Crops Research* 166: 82–91.

Bashir, EMA, Ali, AM, Ali, AM, Melchinger, AE, Parzies, HK, Haussmann, BIG. 2014. Characterization of Sudanese pearl millet germplasm for agro-morphological traits and grain nutritional values. *Plant Genetic Resources* 12: 35–47.

Baxter, I. 2009. Ionomics: studying the social network of mineral nutrients. *Current opinion in plant biology* 12: 381–386.

Baxter, I, Ziegler, G, Lahner, B, Mickelbart, MV, Foley, R, Danku, J, Armstrong, P, Salt, DE, Hoekenga, OA. 2014. Single-kernel ionomic profiles are highly heritable indicators of genetic and environmental influences on elemental accumulation in maize grain (*Zea mays*). *PLoS ONE* 9: e87628.

Black, RE. 2003. Zinc deficiency, infectious disease and mortality in the developing world. *The Journal of nutrition* 133: 1485S-9S.

Black, RE, Allen, LH, Bhutta, ZA, Caulfield, LE, Onis, M de, Ezzati, M, Mathers, C, Rivera, J. 2008. Maternal and child undernutrition: global and regional exposures and health consequences. *The Lancet* 371: 243–260.

Borrill, P, Connorton, JM, Balk, J, Miller, AJ, Sanders, D, Uauy, C. 2014. Biofortification of wheat grain with iron and zinc. Integrating novel genomic resources and knowledge from model crops. *Frontiers in Plant Science* 5. 53.

Bothmer, Rv. 2003. Diversity in barley. (*Hordeum vulgare*). Amsterdam, Boston: Elsevier.

Bouis, H. 2018. Reducing Mineral and Vitamin Deficiencies through Biofortification. Progress Under HarvestPlus. *World review of nutrition and dietetics* 118: 112–122.

Bouis, HE, Welch, RM. 2010. Biofortification—A Sustainable Agricultural Strategy for Reducing Micronutrient Malnutrition in the Global South. *Crop Science* 50: 20-32.

Brenchley, R, Spannagl, M, Pfeifer, M, Barker, GLA, D'Amore, R, Allen, AM, McKenzie, N, Kramer, M, Kerhornou, A, Bolser, D, Kay, S, Waite, D, Trick, M, Bancroft, I, Gu, Y, Huo, N, Luo, M-C, Sehgal, S, Gill, B, Kianian, S, Anderson, O, Kersey, P, Dvorak, J, McCombie, WR, Hall, A, Mayer, KFX, Edwards, KJ, Bevan, MW, Hall, N. 2012. Analysis of the bread wheat genome using whole-genome shotgun sequencing. *Nature* 491: 705–710.

Cakmak, I. 2008. Enrichment of cereal grains with zinc. Agronomic or genetic biofortification? *Plant and Soil* 302: 1–17.

Cakmak, I, Kutman, UB. 2018. Agronomic biofortification of cereals with zinc: a review. *European Journal of Soil Science* 69: 172–180.

Cakmak, I, Turun, A, Millet, E, Feldman, M, Fahima, T, Korol, A, Nevo, E, Braun, HJ, Ozkan, H. 2004. *Triticum dicoccoides*. An important genetic resource for increasing zinc and iron concentration in modern cultivated wheat. *Soil Science and Plant Nutrition* 50: 1047–1054.

Chatzav, M, Peleg, Z, Ozturk, L, Yazici, A, Fahima, T, Cakmak, I, Saranga, Y. 2010. Genetic diversity for grain nutrients in wild emmer wheat. Potential for wheat improvement. *Annals of botany* 105: 1211–1220.

Chen, F, Dong, J, Wang, F, Wu, F, Zhang, G, Li, G, Chen, Z, Chen, J, Wei, K. 2007. Identification of barley genotypes with low grain Cd accumulation and its interaction with four microelements. *Chemosphere* 67: 2082–2088.

Chen, X, Yuan, L, Ludewig, U. 2016. Natural Genetic Variation of Seed Micronutrients of *Arabidopsis thaliana* Grown in Zinc-Deficient and Zinc-Amended Soil. *Frontiers in Plant Science* 7: 1070.

Chu, H-H, Chiecko, J, Punshon, T, Lanzirotti, A, Lahner, B, Salt, DE, Walker, EL. 2010. Successful reproduction requires the function of *Arabidopsis* Yellow Stripe-Like1 and Yellow Stripe-Like3 metal-nicotianamine transporters in both vegetative and reproductive structures. *Plant physiology* 154: 197–210.

Clemens, S. 2006. Toxic metal accumulation, responses to exposure and mechanisms of tolerance in plants. *Biochimie* 88: 1707–1719.

Clemens, S. 2014. Zn and Fe biofortification. The right chemical environment for human bioavailability. *Plant Sci.* 225: 52–57.

Clemens, S, Aarts, MGM, Thomine, S, Verbruggen, N. 2013. Plant science. The key to preventing slow cadmium poisoning. *Trends in plant science* 18: 92–99.

Conte, SS, Walker, EL. 2012. Genetic and biochemical approaches for studying the yellow stripe-like transporter family in plants. *Current topics in membranes* 69: 295–322.

Dawson, IK, Russell, J, Powell, W, Steffenson, B, Thomas, WTB, Waugh, R. 2015. Barley. A translational model for adaptation to climate change. *New Phytologist* 206: 913–931.

Dietterich, LH, Zanobetti, A, Kloog, I, Huybers, P, Leakey, ADB, Bloom, AJ, Carlisle, E, Fernando, N, Fitzgerald, G, Hasegawa, T, Holbrook, NM, Nelson, RL, Norton, R, Ottman, MJ, Raboy, V, Sakai, H, Sartor, KA, Schwartz, J, Seneweera, S, Usui, Y, Yoshinaga, S, Myers, SS. 2015. Impacts of elevated atmospheric CO_2 on nutrient content of important food crops. *Scientific data* 2: 150036.

Eagling, T, Neal, AL, McGrath, SP, Fairweather-Tait, S, Shewry, PR, Zhao, F-J. 2014. Distribution and Speciation of Iron and Zinc in Grain of Two Wheat Genotypes. *Journal of Agricultural and Food Chemistry* 62: 708–716.

European Food Safety Authority. 2009. Scientific Opinion of the Panel on Contaminants in the Food Chain on a request from the European Commission on cadmium in food. *EFSA J.*: 1–139.

FAOSTAT. 2018. FAOSTAT Statistics Database. http://faostat.fao.org/.

Fischer, S, Spielau, T, Clemens, S. 2017. Natural variation in *Arabidopsis thaliana* Cd responses and the detection of quantitative trait loci affecting Cd tolerance. *Scientific reports* 7: 3693.

Food and Agriculture Organization of the United Nations. 2012. FAO GEONETWORK. Digital Soil Map of the World (GeoLayer). http://www.fao.org/soils-portal/soil-survey/soil-maps-and-databases/faounesco-soil-map-of-the-world/en.

Franco, OL, Rigden, DJ, Melo, FR, Grossi-de-Sá, MF. 2002. Plant α-amylase inhibitors and their interaction with insect α-amylases. *European Journal of Biochemistry* 269: 397–412.

Gómez-Galera, S, Rojas, E, Sudhakar, D, Zhu, C, Pelacho, AM, Capell, T, Christou, P. 2010. Critical evaluation of strategies for mineral fortification of staple food crops. *Transgenic research* 19: 165–180.

Grebmer, Kv, Saltzman, A, Birol, E, Wiesmann, D, Prasai, N, Yin, S, Yohannes, Y, Menon, P, Thompson, J, Sonntag, A. 2014. 2014 Global Hunger Index: The challenge of hidden hunger. Bonn, Washington, D.C., Dublin: International Food Policy Research Institute, Concern Worldwide, Welthungerhilfe.

Gupta, RK, Gangoliya, SS, Singh, NK. 2015. Reduction of phytic acid and enhancement of bioavailable micronutrients in food grains. *Journal of food science and technology* 52: 676–684.

Guttieri, MJ, Baenziger, PS, Frels, K, Carver, B, Arnall, B, Waters, BM. 2015. Variation for Grain Mineral Concentration in a Diversity Panel of Current and Historical Great Plains Hard Winter Wheat Germplasm. *Crop Science* 55: 1035.

Hansen, TH, Lombi, E, Fitzgerald, M, Laursen, KH, Frydenvang, J, Husted, S, Boualaphanh, C, Resurreccion, A, Howard, DL, de Jonge, Martin D., Paterson, D, Schjoerring, JK. 2012. Losses of essential mineral nutrients by polishing of rice differ among genotypes due to contrasting grain hardness and mineral distribution. *Journal of Cereal Science* 56: 307–315.

Hothorn, T, Bretz, F, Westfall, P. 2008. Simultaneous inference in general parametric models. *Biometrical journal. Biometrische Zeitschrift* 50: 346–363.

Huang, X, Han, B. 2014. Natural variations and genome-wide association studies in crop plants. *Annual review of plant biology* 65: 531–551.

International Barley Genome Sequencing, Mayer, KF, Waugh, R, Brown, JWS, Schulman, A, Langridge, P, Platzer, M, Fincher, GB, Muehlbauer, GJ, Sato, K, Close, TJ, Wise, RP, Stein, N. 2012. A physical, genetic and functional sequence assembly of the barley genome. *Nature* 491: 711–716.

International Nutritional Anemia Consultative Group (INACG), World Health Organization (WHO), United Nations Childrens Fund (UNICEF). 1998. Guidelines for the use of iron supplements to prevent and treat iron deficiency anemia. Washington, DC: ILSI Pr.

Iwai, T, Takahashi, M, Oda, K, Terada, Y, Yoshida, KT. 2012. Dynamic changes in the distribution of minerals in relation to phytic acid accumulation during rice seed development. *Plant Physiology* 160: 2007–2014.

Jiang, SL, Wu, JG, Feng, Y, Yang, XE, Shi, CH. 2007. Correlation analysis of mineral element contents and quality traits in milled rice (*Oryza sativa* L.). *Journal of Agricultural and Food Chemistry* 55: 9608–9613.

Jilal, A, Grando, S, Henry, RJ, Lee, LS, Rice, N, Hill, H, Baum, M, Ceccarelli, S. 2008. Genetic diversity of ICARDA's worldwide barley landrace collection. *Genetic Resources and Crop Evolution* 55: 1221–1230.

Joint FAO/WHO Codex Alimentarius Commission. 1995. General Standard For Contaminants And Toxins In Food And Feed (CODEX STAN 193-1995). Adopted in 1995. Revised in 1997, 2006, 2008, 2009. Amendment 2010, 2012, 2013, 2014.

Khan, MA, Castro-Guerrero, N, Mendoza-Cozatl, DG. 2014. Moving toward a precise nutrition: preferential loading of seeds with essential nutrients over non-essential toxic elements. *Frontiers in Plant Science* 5: 51.

Klančnik, K, Vogel-Mikuš, K, Kelemen, M, Vavpetič, P, Pelicon, P, Kump, P, Jezeršek, D, Gianoncelli, A, Gaberščik, A. 2014. Leaf optical properties are affected by the location and type of deposited biominerals. *Journal of photochemistry and photobiology. B, Biology* 140: 276–285.

Kodkany, BS, Bellad, RM, Mahantshetti, NS, Westcott, JE, Krebs, NF, Kemp, JF, Hambidge, KM. 2013. Biofortification of pearl millet with iron and zinc in a randomized controlled trial increases absorption of these minerals above physiologic requirements in young children. *The Journal of nutrition* 143: 1489–1493.

Kühnlenz, T, Westphal, L, Schmidt, H, Scheel, D, Clemens, S. 2015. Expression of *Caenorhabditis elegans PCS* in the AtPCS1-deficient *Arabidopsis thaliana cad1-3* mutant separates the metal tolerance and non-host resistance functions of phytochelatin synthases. *Plant, cell & environment* 38: 2239–2247.

Kyriacou, B, Moore, KL, Paterson, D, Jonge, MD, Howard, DL, Stangoulis, J, Tester, M, Lombi, E, Johnson, AAT. 2014. Localization of iron in rice grain using synchrotron X-ray fluorescence microscopy and high resolution secondary ion mass spectrometry. *Journal of Cereal Science* 59: 173–180.

La Frano, MR, Moura, FF de, Boy, E, Lönnerdal, B, Burri, BJ. 2014. Bioavailability of iron, zinc, and provitamin A carotenoids in biofortified staple crops. *Nutrition reviews* 72: 289–307.

Li, S, Zhou, X, Huang, Y, Zhu, L, Zhang, S, Zhao, Y, Guo, J, Chen, J, Chen, R. 2013. Identification and characterization of the zinc-regulated transporters, iron-regulated transporter-like protein (ZIP) gene family in maize. *BMC plant biology* 13: 114.

Liberato, SC, Singh, G, Mulholland, K. 2015. Zinc supplementation in young children. A review of the literature focusing on diarrhoea prevention and treatment. *Clinical nutrition (Edinburgh, Scotland)* 34: 181–188.

Liu, D, Liu, Y, Zhang, W, Chen, X, Zou, C. 2017. Agronomic Approach of Zinc Biofortification Can Increase Zinc Bioavailability in Wheat Flour and thereby Reduce Zinc Deficiency in Humans. *Nutrients* 9. 465.

Lohse, M, Bolger, AM, Nagel, A, Fernie, AR, Lunn, JE, Stitt, M, Usadel, B. 2012. RobiNA: a user-friendly, integrated software solution for RNA-Seq-based transcriptomics. *Nucleic Acids Research* 40: W622-7.

Lombi, E, Smith, E, Hansen, TH, Paterson, D, Jonge, MD, Howard, DL, Persson, DP, Husted, S, Ryan, C, Schjørring, JK. 2011. Megapixel imaging of (micro)nutrients in mature barley grains. *Journal of experimental botany* 62: 273–282.

Lonergan, PF, Pallotta, MA, Lorimer, M, Paull, JG, Barker, SJ, Graham, RD. 2009. Multiple genetic loci for zinc uptake and distribution in barley (*Hordeum vulgare*). *The New phytologist* 184: 168–179.

Lung'aho, MG, Mwaniki, AM, Szalma, SJ, Hart, JJ, Rutzke, MA, Kochian, LV, Glahn, RP, Hoekenga, OA. 2011. Genetic and physiological analysis of iron biofortification in maize kernels. *PLOS ONE* 6: e20429.

Ma, JF, Higashitani, A, Sato, K, Takeda, K. 2004. Genotypic variation in Fe concentration of barley grain. *Soil Science and Plant Nutrition* 50: 1115–1117.

Mamo, BE, Barber, BL, Steffenson, BJ. 2014. Genome-wide association mapping of zinc and iron concentration in barley landraces from Ethiopia and Eritrea. *Journal of Cereal Science* 60: 497–506.

Mascher, M, Gundlach, H, Himmelbach, A, Beier, S, Twardziok, SO, Wicker, T, Radchuk, V, Dockter, C, Hedley, PE, Russell, J, Bayer, M, Ramsay, L, Liu, H, Haberer, G, Zhang, X-Q, Zhang, Q, Barrero, RA, Li, L, Taudien, S, Groth, M, Felder, M, Hastie, A, Šimková, H, Staňková, H, Vrána, J, Chan, S, Muñoz-Amatriaín, M, Ounit, R, Wanamaker, S, Bolser, D, Colmsee, C, Schmutzer, T, Aliyeva-Schnorr, L, Grasso, S, Tanskanen, J, Chailyan, A, Sampath, D, Heavens, D, Clissold, L, Cao, S, Chapman, B, Dai, F, Han, Y, Li, H, Li, X, Lin, C, McCooke, JK, Tan, C, Wang, P, Wang, S, Yin, S, Zhou, G, Poland, JA, Bellgard, MI, Borisjuk, L, Houben, A, Doležel, J, Ayling, S, Lonardi, S, Kersey, P, Langridge, P, Muehlbauer, GJ, Clark, MD, Caccamo, M, Schulman, AH, Mayer, KFX, Platzer, M, Close, TJ, Scholz, U, Hansson, M, Zhang, G, Braumann, I, Spannagl, M, Li, C, Waugh, R, Stein, N. 2017. A chromosome conformation capture ordered sequence of the barley genome. *Nature* 544: 427.

Mayo-Wilson, E, Junior, JA, Imdad, A, Dean, S, Chan, XHS, Chan, ES, Jaswal, A, Bhutta, ZA. 2014. Zinc supplementation for preventing mortality, morbidity, and growth failure in children aged 6 months to 12 years of age. *The Cochrane database of systematic reviews* 5: CD009384.

Meharg, AA, Norton, G, Deacon, C, Williams, P, Adomako, EE, Price, A, Zhu, Y, Li, G, Zhao, F-J, McGrath, S, Villada, A, Sommella, A, Silva, PMCS de, Brammer, H, Dasgupta, T, Islam, MR. 2013. Variation in rice cadmium related to human exposure. *Environmental science & technology* 47: 5613–5618.

Mendiburu, F de. 2013. agricolae: Statistical Procedures for Agricultural Research. R package version 1.1-6. http://CRAN.R-project.org/package=agricolae.

Morgounov, A, Gómez-Becerra, HF, Abugalieva, A, Dzhunusova, M, Yessimbekova, M, Muminjanov, H, Zelenskiy, Y, Ozturk, L, Cakmak, I. 2007. Iron and zinc grain density in common wheat grown in Central Asia. *Euphytica* 155: 193–203.

Murgia, I, Arosio, P, Tarantino, D, Soave, C. 2012. Biofortification for combating 'hidden hunger' for iron. *Trends in plant science* 17: 47–55.

Murgia, I, Gara, L de, Grusak, MA. 2013. Biofortification. How can we exploit plant science and biotechnology to reduce micronutrient deficiencies? *Frontiers in plant science* 4: 429.

Muthayya, S, Rah, JH, Sugimoto, JD, Roos, FF, Kraemer, K, Black, RE. 2013. The global hidden hunger indices and maps. An advocacy tool for action. *PLoS ONE* 8: e67860.

Myers, SS, Zanobetti, A, Kloog, I, Huybers, P, Leakey, Andrew D B, Bloom, AJ, Carlisle, E, Dietterich, LH, Fitzgerald, G, Hasegawa, T, Holbrook, NM, Nelson, RL, Ottman, MJ, Raboy, V, Sakai, H, Sartor, KA, Schwartz, J, Seneweera, S, Tausz, M, Usui, Y. 2014. Increasing CO_2 threatens human nutrition. *Nature* 510: 139–142.

Nanda, AK, Pujol, V, Wissuwa, M. 2017. Patterns of stress response and tolerance based on transcriptome profiling of rice crown tissue under zinc deficiency. *Journal of experimental botany* 68: 1715–1729.

Newton, AC, Flavell, AJ, George, TS, Leat, P, Mullholland, B, Ramsay, L, Revoredo-Giha, C, Russell, J, Steffenson, BJ, Swanston, JS, Thomas, William T. B., Waugh, R, White, PJ, Bingham, IJ. 2011. Crops that feed the world 4. Barley: a resilient crop? Strengths and weaknesses in the context of food security. *Food Security* 3: 141–178.

Norton, GJ, Douglas, A, Lahner, B, Yakubova, E, Guerinot, ML, Pinson, Shannon R M, Tarpley, L, Eizenga, GC, McGrath, SP, Zhao, F-J, Islam, MR, Islam, S, Duan, G, Zhu, Y, Salt, DE, Meharg, AA, Price, AH. 2014. Genome wide association mapping of grain arsenic, copper, molybdenum and zinc in rice (*Oryza sativa* L.) grown at four international field sites. *PLOS ONE* 9: e89685.

Oatway, L, Vasanthan, T, Helm, JH. 2007. PHYTIC ACID. *Food Reviews International* 17: 419–431.

Olsen, LI, Hansen, TH, Larue, C, Østerberg, JT, Hoffmann, RD, Liesche, J, Krämer, U, Surblé, S, Cadarsi, S, Samson, VA, Grolimund, D, Husted, S, Palmgren, M. 2016. Mother-plant-mediated pumping of zinc into the developing seed. *Nature Plants* 2: 16036.

Ozturk, L, Yazici, MA, Yucel, C, Torun, A, Cekic, C, Bagci, A, Ozkan, H, Braun, H-J, Sayers, Z, Cakmak, I. 2006. Concentration and localization of zinc during seed development and germination in wheat. *Physiologia plantarum* 128: 144–152.

Palmgren, MG, Clemens, S, Williams, LE, Krämer, U, Borg, S, Schjørring, JK, Sanders, D. 2008. Zinc biofortification of cereals: problems and solutions. *Trends in plant science* 13: 464–473.

Pan, J, Plant, JA, Voulvoulis, N, Oates, CJ, Ihlenfeld, C. 2010. Cadmium levels in Europe: implications for human health. *Environmental geochemistry and health* 32: 1–12.

Peleg, Z, Saranga, Y, Yazici, A, Fahima, T, Ozturk, L, Cakmak, I. 2008. Grain zinc, iron and protein concentrations and zinc-efficiency in wild emmer wheat under contrasting irrigation regimes. *Plant and Soil* 306: 57–67.

Peris-Peris, C, Serra-Cardona, A, Sánchez-Sanuy, F, Campo, S, Ariño, J, San Segundo, B. 2017. Two NRAMP6 Isoforms Function as Iron and Manganese Transporters and Contribute to Disease Resistance in Rice. *MPMI* 30: 385–398.

Persson, DP, Bang, TC de, Pedas, PR, Kutman, UB, Cakmak, I, Andersen, B, Finnie, C, Schjoerring, JK, Husted, S. 2016. Molecular speciation and tissue compartmentation of zinc in durum wheat grains with contrasting nutritional status. *New Phytologist* 211: 1255–1265.

Persson, DP, Hansen, TH, Laursen, KH, Schjørring, JK, Husted, S. 2009. Simultaneous iron, zinc, sulfur and phosphorus speciation analysis of barley grain tissues using SEC-ICP-MS and IP-ICP-MS. *Metallomics* 1: 418.

Pfeiffer, WH, McClafferty, B. 2007. HarvestPlus: Breeding Crops for Better Nutrition. *Crop Science* 47: S 88.

Phuke, RM, Anuradha, K, Radhika, K, Jabeen, F, Anuradha, G, Ramesh, T, Hariprasanna, K, Mehtre, SP, Deshpande, SP, Anil, G, Das, RR, Rathore, A, Hash, T, Reddy, BVS, Kumar, AA. 2017. Genetic Variability, Genotype × Environment Interaction, Correlation, and GGE Biplot Analysis for Grain Iron and Zinc Concentration and Other Agronomic Traits in RIL Population of Sorghum (*Sorghum bicolor* L. Moench). *Frontiers in Plant Science* 8: 712.

Pinson, S, Tarpley, L, Yan, W, Yeater, K, Lahner, B, Yakubova, E, Huang, X-Y, Zhang, M, Guerinot, ML, Salt, DE. 2015. Worldwide Genetic Diversity for Mineral Element Concentrations in Rice Grain. *Crop Science* 55: 294.

Pongrac, P, Kreft, I, Vogel-Mikuš, K, Regvar, M, Germ, M, Vavpetič, P, Grlj, N, Jeromel, L, Eichert, D, Budic, B, Pelicon, P. 2013. Relevance for food sciences of quantitative spatially resolved element profile investigations in wheat (*Triticum aestivum*) grain. *Journal of The Royal Society Interface* 10: 20130296.

Pongrac, P, Vogel-Mikuš, K, Jeromel, L, Vavpetič, P, Pelicon, P, Kaulich, B, Gianoncelli, A, Eichert, D, Regvar, M, Kreft, I. 2013. Spatially resolved distributions of the mineral elements in the grain of tartary buckwheat (*Fagopyrum tataricum*). *Food Research International* 54: 125–131.

Prasad, AS. 2013. Discovery of human zinc deficiency. Its impact on human health and disease. *Advances in nutrition (Bethesda, Md.)* 4: 176–190.

R Core Team. 2013. R: A language and environment for statistical computing. *R Foundation for Statistical Computing, Vienna, Austria.* http://www.R-project.org/.

Ricachenevsky, FK, Menguer, PK, Sperotto, RA, Williams, LE, Fett, JP. 2013. Roles of plant metal tolerance proteins (MTP) in metal storage and potential use in biofortification strategies. *Frontiers in Plant Science* 4: 144.

Ruel-Bergeron, JC, Stevens, GA, Sugimoto, JD, Roos, FF, Ezzati, M, Black, RE, Kraemer, K. 2015. Global Update and Trends of Hidden Hunger, 1995-2011. The Hidden Hunger Index. *PLoS ONE* 10: e0143497.

Ryan, CG. 2000. Quantitative trace element imaging using PIXE and the nuclear microprobe. *International Journal of Imaging Systems and Technology* 11: 219–230.

Saisho, D, Takeda, K. 2011. Barley: emergence as a new research material of crop science. *Plant & cell physiology* 52: 724–727.

Sales, PM, Souza, PM, Simeoni, LA, Silveira, D. 2012. α-Amylase inhibitors: a review of raw material and isolated compounds from plant source. *Journal of pharmacy & pharmaceutical sciences* 15: 141–183.

Sandstead, H. 1991. Zinc deficiency. A public health problem? *American Journal of Diseases of Children*: 853–859.

Schlemmer, U, Frølich, W, Prieto, RM, Grases, F. 2009. Phytate in foods and significance for humans: food sources, intake, processing, bioavailability, protective role and analysis. *Molecular nutrition & food research* 53 Suppl 2: S330-75.

Second International Conference on Nutrition. 2014. Conference Outcome Document. Rome Declaration on Nutrition. Rome.

Senoura, T, Sakashita, E, Kobayashi, T, Takahashi, M, Aung, MS, Masuda, H, Nakanishi, H, Nishizawa, NK. 2017. The iron-chelate transporter OsYSL9 plays a role in iron distribution in developing rice grains. *Plant molecular biology* 95: 375–387.

Shahzad, Z, Rouached, H, Rakha, A. 2014. Combating Mineral Malnutrition through Iron and Zinc Biofortification of Cereals. *Comprehensive Reviews in Food Science and Food Safety* 13: 329–346.

Shi, J, Li, L, Pan, G. 2009. Variation of grain Cd and Zn concentrations of 110 hybrid rice cultivars grown in a low-Cd paddy soil. *Journal of Environmental Sciences* 21: 168–172.

Singh, BR, Timsina, YN, Lind, OC, Cagno, S, Janssens, K. 2018. Zinc and Iron Concentration as Affected by Nitrogen Fertilization and Their Localization in Wheat Grain. *Frontiers in Plant Science* 9: 307.

Singh, SP, Vogel-Mikuš, K, Vavpetič, P, Jeromel, L, Pelicon, P, Kumar, J, Tuli, R. 2014. Spatial X-ray fluorescence micro-imaging of minerals in grain tissues of wheat and related genotypes. *Planta* 240: 277–289.

Slamet-Loedin, IH, Johnson-Beebout, SE, Impa, S, Tsakirpaloglou, N. 2015. Enriching rice with Zn and Fe while minimizing Cd risk. *Frontiers in Plant Science* 6: 121.

Smith, MR, Myers, SS. 2018. Impact of anthropogenic CO_2 emissions on global human nutrition. *Nature Climate Change* 8: 834–839.

Solé, VA, Papillon, E, Cotte, M, Walter, P, Susini, J. 2007. A multiplatform code for the analysis of energy-dispersive X-ray fluorescence spectra. *Spectrochimica Acta Part B: Atomic Spectroscopy* 62: 63–68.

Sreenivasulu, N, Graner, A, Wobus, U. 2008. Barley genomics: An overview. *International journal of plant genomics* 2008: 486258.

Stomph, TJ, Choi, EY, Stangoulis, J C R. 2011. Temporal dynamics in wheat grain zinc distribution: is sink limitation the key? *Annals of botany* 107: 927–937.

Suzuki, M, Bashir, K, Inoue, H, Takahashi, M, Nakanishi, H, Nishizawa, NK. 2012. Accumulation of starch in Zn-deficient rice. *Rice (New York, N.Y.)* 5: 9.

Täufel, A, Böhm, H, Flamme, W. Protein Inhibitors of Alpha-amylase in Mature and Germinating Grain of Rye (*Secale cereale*). *Journal of Cereal Science* 1997: 267–273.

Tauris, B, Borg, S, Gregersen, PL, Holm, PB. 2009. A roadmap for zinc trafficking in the developing barley grain based on laser capture microdissection and gene expression profiling. *Journal of Experimental Botany* 60: 1333–1347.

Tulchinsky, TH. 2010. Micronutrient Deficiency Conditions. Global Health Issues. *Public Health Reviews* 32: 243–255.

Uraguchi, S, Fujiwara, T. 2012. Cadmium transport and tolerance in rice: perspectives for reducing grain cadmium accumulation. *Rice (New York, N.Y.)* 5: 5.

Villafort Carvalho, MT, Pongrac, P, Mumm, R, van Arkel, J, van Aelst, A, Jeromel, L, Vavpetič, P, Pelicon, P, Aarts, MGM. 2015. *Gomphrena claussenii*, a novel metal-hypertolerant bioindicator species, sequesters cadmium, but not zinc, in vacuolar oxalate crystals. *New Phytologist*.

Vogel-Mikuš, K, Simcic, J, Pelicon, P, Budnar, M, Kump, P, Necemer, M, Mesjasz-Przybyłowicz, J, Przybyłowicz, WJ, Regvar, M. 2008. Comparison of essential and non-essential element distribution in leaves of the Cd/Zn hyperaccumulator *Thlaspi praecox* as revealed by micro-PIXE. *Plant, cell & environment* 31: 1484–1496.

Vogel-Mikuš, K, Pongrac, P, Pelicon, P. 2014. Micro-PIXE elemental mapping for ionome studies of crop plants. *International Journal of PIXE* 24: 217–233.

VSN International. 2013. GenStat for Windows 17th edition. Hemel Hempstead, UK: VSN International.

Wang, KM, Wu, JG, Li, G, Zhang, DP, Yang, ZW, Shi, CH. 2011. Distribution of phytic acid and mineral elements in three indica rice (*Oryza sativa* L.) cultivars. *Journal of Cereal Science* 54: 116–121.

Warnes, GR, Bolker, B, Bonebakker, L, Gentleman, R, Huber, W, Liaw, A, Lumley, T, Mächler, M, Magnusson, A, Möller, S, Schwartz, M, Venables, B. 2016. gplots: Various R programming tools for plotting data. *R package version 3.0.1.* https://CRAN.R-project.org/package=gplots.

Waters, BM, Chu, H-H, Didonato, RJ, Roberts, LA, Eisley, RB, Lahner, B, Salt, DE, Walker, EL. 2006. Mutations in *Arabidopsis yellow stripe-like1* and *yellow stripe-like3* reveal their roles in metal ion homeostasis and loading of metal ions in seeds. *Plant Physiology* 141: 1446–1458.

Waters, BM, Sankaran, RP. 2011. Moving micronutrients from the soil to the seeds. Genes and physiological processes from a biofortification perspective. *Plant Sci.* 180: 562–574.

Wessells, KR, Brown, KH. 2012. Estimating the global prevalence of zinc deficiency. Results based on zinc availability in national food supplies and the prevalence of stunting. *PLoS ONE* 7: e50568.

White, PJ, Broadley, MR. 2005. Biofortifying crops with essential mineral elements. *Trends in plant science* 10: 586–593.

White, PJ, Broadley, MR. 2009. Biofortification of crops with seven mineral elements often lacking in human diets—iron, zinc, copper, calcium, magnesium, selenium and iodine. *New Phytologist* 182: 49–84.

WHO. 2002. The world health report 2002. Reducing Risks, Promoting Healthy Life. Geneva, Switzerland: World Health Organization.

WHO. 2009. Global health risks. Mortality and burden of disease attributable to selected major risks. Geneva, Switzerland: World Health Organization.

WHO, Regional Office Europe, ed. 2015. European food and nutrition action plan 2015-2020. Copenhagen: World Health Organization, Regional Office for Europe.

Wu, D, Sato, K, Ma, JF. 2015. Genome-wide association mapping of cadmium accumulation in different organs of barley. *New Phytologist*.

Xu, Y, An, D, Li, H, Xu, H. 2011. Review. Breeding wheat for enhanced micronutrients. *Canadian Journal of Plant Science* 91: 231–237.

Xue, Y-F, Eagling, T, He, J, Zou, C-Q, McGrath, SP, Shewry, PR, Zhao, F-J. 2014. Effects of nitrogen on the distribution and chemical speciation of iron and zinc in pearling fractions of wheat grain. *Journal of agricultural and food chemistry* 62: 4738–4746.

Yang, M, Lu, K, Zhao, F-J, Xie, W, Ramakrishna, P, Wang, G, Du, Q, Liang, L, Sun, C, Zhao, H, Zhang, Z, Liu, Z, Tian, J, Huang, X-Y, Wang, W, Dong, H, Hu, J, Ming, L, Xing, Y, Wang, G, Xiao, J, Salt, DE, Lian, X. 2018. Genome-Wide Association Studies Reveal the Genetic Basis of Ionomic Variation in Rice. *The Plant cell* 30: 2720–2740.

Zhang, T, Sun, H, Lv, Z, Cui, L, Mao, H, Kopittke, PM. 2018. Using Synchrotron-Based Approaches To Examine the Foliar Application of $ZnSO_4$ and ZnO Nanoparticles for Field-Grown Winter Wheat. *Journal of agricultural and food chemistry* 66: 2572–2579.

Zhang, Y, Shi, R, Rezaul, KM, Zhang, F, Zou, C. 2010. Iron and zinc concentrations in grain and flour of winter wheat as affected by foliar application. *Journal of agricultural and food chemistry* 58: 12268–12274.

Zhao, C-R, Ikka, T, Sawaki, Y, Kobayashi, Y, Suzuki, Y, Hibino, T, Sato, S, Sakurai, N, Shibata, D, Koyama, H. 2009. Comparative transcriptomic characterization of aluminum, sodium chloride, cadmium and copper rhizotoxicities in *Arabidopsis thaliana*. *BMC plant biology* 9: 32.

Zhao, F-J, McGrath, SP. 2009. Biofortification and phytoremediation. *Current opinion in plant biology* 12: 373–380.

Zhao, F-J, Moore, KL, Lombi, E, Zhu, Y-G. 2014. Imaging element distribution and speciation in plant cells. *Trends in plant science* 19: 183–192.

Zhao, F-J, Su, YH, Dunham, SJ, Rakszegi, M, Bedo, Z, McGrath, SP, Shewry, PR. 2009. Variation in mineral micronutrient concentrations in grain of wheat lines of diverse origin. *Journal of Cereal Science* 49: 290–295.

Zschiesche, W, Barth, O, Daniel, K, Böhme, S, Rausche, J, Humbeck, K. 2015. The zinc-binding nuclear protein HIPP3 acts as an upstream regulator of the salicylate-dependent plant immunity pathway and of flowering time in *Arabidopsis thaliana*. *New Phytologist* 207: 1084–1096.

2 Publikationen und Eigenanteil

2.1 Spatially resolved analysis of variation in barley (*Hordeum vulgare*) grain micronutrient accumulation

Detterbeck, A., Pongrac, P., Rensch, S., Reuscher, S., Pečovnik, M., Vavpetič, P., Pelicon, P., Holzheu, S., Krämer, U. und Clemens, S. (2016). *The New phytologist* **211**: 1241–1254. DOI:10.1111/nph.13987.

Die Konzeption der Forschungsidee und des Versuchsdesigns entstanden durch A. Detterbeck, S. Rensch, P. Pongrac, U. Krämer und S. Clemens. Hierbei lag ein Hauptaugenmerk auf der Analyse der natürlichen Variation und der räumlichen Verteilung von Zink, Eisen, Mangan und Kupfer in Körnern von Gerste. Die Pflanzenanzucht zur Analyse der Mikronährstoff-Gehalte wurden von A. Detterbeck und S. Rensch in Bayreuth sowie zur Analyse der Cadmium-Akkumulation von S. Reuscher in Bochum durchgeführt. Die Analyse der Metallgehalte ganzer Körner erfolgte durch A. Detterbeck und S. Rensch. Die Samenzerlegung in einzelne Bestandteile wie Embryo, Perikarpgewebe und Endosperm wurde vollständig von A. Detterbeck ausgeführt. Ebenso erfolgte die Probenaufbereitung und Probenanalyse via ICP-OES durch A. Detterbeck. Die Probenvorbereitung für die µ-PIXE Analyse wurde unter Anleitung von P. Pongrac vollständig von A. Detterbeck ausgeführt. Die Vermessung der vorbereiteten Schnitte erfolgte im Jožef Stefan Institute in Ljubljana von M. Pečovnik, P. Vavpetič, und P. Pelicon. Die Analyse der Verteilungskarten über PyMca, die Kalkulation der einzelnen gewebespezifischen Konzentrationen und die Co-Lokalisations-analyse erfolgte ausschließlich durch A. Detterbeck nach fachlicher Anleitung von P. Pongrac. A. Detterbeck wertete die Daten aus. Ebenso wurden die statistischen Analysen, wie Korrelationsanalysen, Genotyp-Umwelt-Analysen und Signifikanztests von A. Detterbeck ausgeführt. Hierbei erfolgte eine statistische Beratung durch S. Holzheu. A. Detterbeck erstellte die Abbildungen und Tabellen des Manuskriptes, recherchierte Literatur und verfasste das Manuskript, das nach konstruktiver Diskussion von S. Clemens überarbeitet wurde.

Spatially resolved analysis of variation in barley (*Hordeum vulgare* L.) grain micronutrient accumulation

Amelie Detterbeck[1], Paula Pongrac[1], Stefan Rensch[1], Stefan Reuscher[2], Matic Pečovnik[3], Primož Vavpetič[3], Primož Pelicon[3], Stefan Holzheu[4], Ute Krämer[2], Stephan Clemens[1,4]

[1]Department of Plant Physiology, University of Bayreuth, Universitätsstr. 30, 95447 Bayreuth, Germany; [2]Department of Plant Physiology, Ruhr University Bochum, Universitätsstr. 150, 44801 Bochum, Germany; [3]Jožef Stefan Institute, Jamova 39, SI-1000 Ljubljana, Slovenia; [4]Bayreuth Center for Ecology and Environmental Research, University of Bayreuth, Dr.-Hans-Frisch-Str. 1-3, 95440 Bayreuth, Germany

Author for correspondence:
Stephan Clemens
Tel: +49 921 552630
Email: stephan.clemens@uni-bayreuth.de

SUMMARY

• Genetic biofortification requires knowledge on natural variation and underlying mechanisms of micronutrient accumulation. We therefore studied diversity in grain micronutrient concentrations and spatial distribution in barley (*Hordeum vulgare* L.), a genetically tractable model cereal and an important crop with widespread cultivation.

• We assembled a diverse collection of barley cultivars and landraces and analysed grain micronutrient profiles in genebank material and after three independent cultivations. Lines with contrasting grain Zn accumulation were selected for in-depth analysis of micronutrient distribution within the grain by micro-particle-induced X-ray emission (μ-PIXE). Also, we addressed association with grain Cd accumulation.

• The analysis of more than 120 lines revealed substantial variation especially in grain Zn concentrations. A large fraction of this variation is due to genetic differences. Grain dissection and μ-PIXE analysis of contrasting lines showed that differences in grain Zn accumulation apply to all parts of the grain including the endosperm. Cd concentrations exceeded the Codex Alimentarius threshold in most of the representative barley lines after cultivation in a slightly Cd-contaminated agricultural soil.

• Two important conclusions for biofortification are: first, high Zn grains contain more Zn also in the consumed parts of the grain; second, higher micronutrient concentrations are strongly associated with higher Cd accumulation.

Key words: barley (Hordeum vulgare L.), biofortification, grain, metal, micronutrient accumulation, μ-PIXE, natural variation

INTRODUCTION

The dissection of micronutrient accumulation in plants has increasingly come into focus of studies aiming to aid in tackling the problems of malnutrition in humans. In the Rome Declaration on Nutrition, over 170 countries stated the necessity to overcome all forms of malnutrition, including micronutrient deficiencies, and made a commitment to action (Second International Conference on Nutrition, 2014). Iodine, iron (Fe), vitamin A and zinc (Zn) deficiencies are the most prevalent deficiency burdens especially in developing countries and affecting mostly children and pregnant women (Black *et al.*, 2008). About two billion people worldwide are estimated to suffer from Fe or Zn deficiency, mainly caused by a diet dominated by cereals low in bioavailability of these two mineral elements (Sandstead, 1991; International Nutritional Anemia Consultative Group *et al.*, 1998; Wessells & Brown, 2012). A major consequence of Zn deficiency is higher vulnerability to diseases such as diarrhea, respiratory tract infections, or malaria. More than five hundred thousand deaths per year and about 1 % of all disability-adjusted life years are attributed globally to Zn deficiency. Affected are mostly low income countries (WHO, 2009). Supplementation of diets with Zn has repeatedly been demonstrated to significantly reduce the incidence of infectious diseases in children (Mayo-Wilson *et al.*, 2014; Liberato *et al.*, 2015). Thus, enabling an improved micronutrient status especially of people living in developing countries has become a major objective globally. Different strategies are being pursued (Murgia *et al.*, 2012). They include the use of food supplements, the systematic fortification of staple food (e.g. wheat flour), the modification of food processing and preparation habits (e.g. polishing of cereal grains), as well as biofortification of staple crops (Gómez-Galera *et al.*, 2010). Biofortification refers to the development of crops with higher density of bioavailable micronutrients (White & Broadley, 2005). It offers several advantages over supplementation. Infrastructure demands are much lower and the risk of overdosing is smaller (Murgia *et al.*, 2012; Clemens, 2014). Biofortification can be achieved through agronomic strategies, e.g. Zn fertilization (Cakmak, 2008), or through the development of crop varieties with higher levels of bioavailable micronutrients. The path to biofortified varieties can proceed via classic breeding or via engineering approaches (Borrill *et al.*, 2014). A prerequisite for both is the exploration of natural variation in micronutrient accumulation to assess breeding potential and to enable approaches aiming at a mechanistic understanding of micronutrient loading into edible plant organs (Cakmak *et al.*, 2004; Palmgren *et al.*, 2008; Lung'aho *et al.*, 2011; Waters & Sankaran,

2011; Xu *et al.*, 2011; Huang & Han, 2014; Shahzad *et al.*, 2014). Accordingly, a number of studies has documented the degree of variation in the accumulation of Fe, Zn and other micronutrients in several crop species (Pfeiffer & McClafferty, 2007; SHI *et al.*, 2009; White & Broadley, 2009; Zhao *et al.*, 2009; Xu *et al.*, 2011; Bashir *et al.*, 2014; Bashir *et al.*, 2014; Baxter *et al.*, 2014). Following predominantly classic breeding strategies, existing natural variation in micronutrient density has been exploited for the development of biofortified varieties within the HarvestPlus program (Bouis & Welch, 2010). For instance, Fe- and Zn-biofortified pearl millet was shown to provide significantly more bioavailable Fe and Zn for children (Kodkany *et al.*, 2013).

Efforts within HarvestPlus are focused on staple foods such as wheat, rice, maize, sweet potato, and pearl millet that are important calorie sources in countries with a high incidence of Fe and/or Zn deficiency in humans (Pfeiffer & McClafferty, 2007). Barley (*Hordeum vulgare* L.) is not included in these biofortification attempts, even though it is one of the most important crops worldwide, ranking fourth in grain production (Food and Agriculture Organization of the United Nations. FAOSTAT., 2014). While barley grains are mostly used as animal feed and for brewing, this species nonetheless offers considerable potential for biofortification. Extensive genetic variation, a sequenced genome (International Barley Genome Sequencing *et al.*, 2012), self-fertilization and diploidy render barley a promising model system to unravel the molecular mechanisms underlying cereal grain micronutrient accumulation traits (Sreenivasulu *et al.*, 2008; Saisho & Takeda, 2011). An efficient way to explore natural variation in crop micronutrient accumulation lies in the screening of worldwide germplasm collections representing a broad variety of genetic backgrounds. With about 1600 accessions available at the moment (Genebank department of the Leibniz Institute of Plant Genetics and Crop Plant Research, Gatersleben), the International Barley Core Collection (BCC) is one of the largest barley collections representing the diversity of barley germplasm in the world (Bothmer, 2003). Thus, one major objective of this study was to investigate the genetic potential of micronutrient accumulation in barley grains by analysing a subset of the BCC.

Furthermore, we asked to what extent higher Zn concentration of grains coincides with stronger accumulation of Cd. Plant-derived food and especially cereal grains represent the major source of human Cd intake (Clemens *et al.*, 2013). Recent risk assessments indicate an urgent need to reduce chronic human Cd exposure (European Food Safety Authority, 2009). It is therefore an important consideration in the development of biofortified crops to limit the accumulation of Cd. Accordingly, grain elemental profiles were analysed in selected extreme barley lines after cultivation in a native agricultural soil with Cd contamination.

The third objective was to gain mechanistic insights into micronutrient accumulation by analysing element interactions and by studying the distribution of elements in grains of lines exhibiting contrasting Zn accumulation traits. Distribution was analysed through micronutrient analysis of dissected grains and with techniques providing in situ spatial distribution information, namely micro-particle-induced X-ray emission (μ-PIXE). The spatial distribution is important because it influences the degree of mineral losses during polishing and grain processing (Hansen *et al.*, 2012; Atungulu & Pan, 2014). Moreover, the chemical environment of micronutrients is far from uniform across a grain (Persson *et al.*, 2009; Clemens, 2014; Eagling *et al.*, 2014).

MATERIALS AND METHODS

Plant material and growth conditions

Barley (*Hordeum vulgare* L.) grains were supplied by the Genebank department of the IPK Gatersleben (Germany), where specific information on all lines is available online (http://gbis.ipk-gatersleben.de/GBIS_I/).

Initially, grain micronutrient profiles of the 136 lines (Tab. S1) were directly measured from five grains supplied by the genebank. Subsequently 102 to 125 lines (as determined by the availability of viable grains with satisfactory germination rates) were grown in soil (pH 6.7; for elemental composition see Table S2) in three different cultivation rounds in three different years in the glasshouse under long day conditions (16h:8h, light:dark), with supplementary lighting (total light intensity 100 - 150 μmol s^{-1} m^{-2}). Total Zn of the soil used for the exploration of natural variation was 82 mg kg^{-1}, which is representative for European topsoils with a mean of 68.1 mg kg^{-1} (FOREGS Geochemical Atlas of Europe, http://weppi.gtk.fi/publ/foregsatlas/). Cultivar Pasadena was included in all experiments as control line in five to six replicates. For all lines, five plants were cultivated in 4 L pots. If needed, plants were sprayed with non-metal based fungicides against powdery mildew. Mature grains were harvested and five grains from five different ears as well as from five different positions within these ears were pooled and oven dried at 60 °C for 3 days. Five grains sampled in this way were found to provide reliable data since the variation between grains and between different positions in the ears was small (Fig. S1).

For the characterization of grain metal accumulation on a contaminated soil, a subset of nine BCC lines (32, 35, 54, 431, 434, 601, 604, 605, 1369) and cultivar Pasadena (seven

replicate individuals each) were cultivated to maturity in a heavy metal-contaminated agricultural soil mix. The soil (pH 7.5; for elemental composition, see Table S3) was collected (with permission from the local authority in charge of this site, the Lower Saxony *Landesamt für Bergbau, Energie und Geologie*, LBEG, Hanover, Germany) from the margin of an agricultural field in the flood plain of the river Oker, which rises in the Harz Mountains, a major historical mining region in Central Germany. To prepare the soil mix, 135 L of air-dried contaminated soil were mixed thoroughly with 50 L of fine Sahara sand and 150 g fertilizer 'Osmocote start 6 weeks', and the mix was used to fill pots with 0.5-0.6 L soil per pot. Addition of sand to this loamy soil was necessary to improve its physical properties for barley cultivation. The metal contamination of the soil did not elicit any toxicity symptoms in the plants. Positions of pots were randomized, and the experimental plant stand was surrounded by a row of filler plants (cv Scarlett) to avoid edge effects. Plants were grown in a glasshouse under long day conditions (16h:8h, light:dark) and with supplementary lighting (total light intensity 80 - 110 µmol s^{-1} m^{-2}). Mature grains were harvested, and husks were manually removed after incubation at 150 °C for 1 h. For each plant, a pool of five randomly chosen grains was digested for multi-element analysis.

Grain dissection

After glasshouse cultivation mature grains were soaked in bidistilled water for 4 h at 4 °C. Dissection was performed with plastic forceps to prevent metal contamination of the samples. Grains were dissected under a stereomicroscope to separate husk (including bran, epidermal cell layers and testa), endosperm (including parts of the aleurone layer) and embryo tissues. For elemental analysis tissues from five grains per line were pooled and oven dried at 60 °C for 3 days.

Inductively Coupled Plasma–Optical Emission Spectroscopy (ICP-OES)

For ICP-OES analysis, oven-dried grains were wet-digested in a microwave (START 1500; MLS GmbH) with 2 ml bidistilled water, 2 ml 30 % H_2O_2 (w/w) and 4 ml 65 % HNO_3 (w/w) for 12 min at 180 °C. Endosperm tissues from dissected grains were digested in the same way. Dissected husk and embryo tissues were microwave digested with only 1 ml bidistilled water, 1 ml 30 % H_2O_2 (w/w) and 2 ml 65 % HNO_3 (w/w) in smaller vessels.

Total metal content of soils was determined upon extracting 0.25 g of air-dried soil (2 mm particle size) in 0.75 mL concentrated HNO_3 (65 % w/w) and 2.25 mL concentrated HCl (37 % w/w). The suspension was heated to 160 °C within 15 min, maintained at 160 °C for

15 min and left to cool to room temperature in a microwave-assisted chemical digestion system (Mars Express, CEM GmbH, Kamp-Lintford, Germany). Each digest was filled up to 10 mL final volume with ultrapure water and filtered through Whatman No. 595½ paper before analysis by ICP-OES. The exchangeable fraction was determined upon shaking 1 g of soil in 10 mL of 0.01 M $BaCl_2$ at 150 rpm and room temperature overnight. Samples were then filtered, followed by the addition of 1 mL 65 % HNO_3 (w/w) before analysis by ICP-OES.

Concentrations were measured with an iCAP 6500 (Thermo Scientific) at wavelengths of 213.8 nm (Zn), 238.2 nm (Fe), 257.6 nm (manganese, Mn) and 324.7 nm (copper, Cu).

Inductively Coupled Plasma–Mass Spectrometry (ICP-MS)

For the analysis of Cd in grains received from the genebank, ICP-MS analysis was performed by the Central analytical lab of BayCEER (Bayreuth Center for Ecology and Environmental Research). ICP-MS has lower Cd detection limits compared to ICP-OES. Five grains per line were pooled and ground with a ball mill MM2 to particles of less than 60 µm size. Afterwards 100 mg ground material were digested with a mixture of 1 ml 65 % HNO_3 (w/w) and 100 µl 30 % HCl (w/w) at 170 °C for 7 h. Cooled digests were diluted to 10 ml with bidistilled water and measured with ICP-MS Agilent 7500ce/Cetac ASX-510.

Micro-Proton-Induced X-Ray Emission (µ-PIXE) analysis

Grains of two lines with contrasting Zn accumulation and the reference line were soaked in distilled water for three hours at 4 °C. Soaking enabled us to obtain flat surfaces (sectioning dry grains can result in uneven surface due to crumbly endosperm). This is important for elemental mapping as non-flat surfaces can cause geometrical artefacts (Hatam *et al.*, 2012). Grains (n=4 for each line) were hand-cut transversely under a stereomicroscope using new stainless steel razor blades and immediately frozen in liquid nitrogen. Sections were made in such a way that the embryo was cut in half. Cross-sections comprised radicles, scutellum, endosperm and the outer parts of the grains. These cross sections were freeze-dried (Alpha 2-4, Christ, Germany) in a temperature gradient (temperature gradually increased from -180 °C to -25 °C, and a pressure of 0.08 mbar, for 3 days) and afterwards checked for their integrity. For µ-PIXE analysis samples were mounted and analysed as described previously (Vogel-Mikus *et al.*, 2008; Klančnik *et al.*, 2014) The size of the beam was 0.8 µm, with pixel size of 7.81 µm. Quantitative spatial distribution maps were generated with PyMca vers. 5.0.0 (Solé *et al.*, 2007) based on numerical matrices generated with GEOPIXEII software (Ryan, 2000) and mean micronutrient concentrations were calculated by selecting specific areas using

the ROI manager tool in ImageJ (Abràmoff *et al.*, 2004). For each section the following tissues were distinguished: aleurone, endosperm, husk and embryo tissues (including the scutellum).

Statistical analysis

In order to show variation in micronutrient concentrations box plots displaying the median, the upper and lower quartile as well as outliers were generated. For comparing the relationship of micronutrients in barley grains and correlations of different cultivation rounds, micronutrient concentrations were subjected to regression analysis, and Pearson product moment correlation coefficients were computed with SigmaPlot (vers. 11.0) and squared in order to specify the coefficient of determination (r^2). For the calculation of genotype or round effects on different micronutrients and their contribution to the total variance, a two-way ANOVA was conducted with R (R Core Team, vers. 3.0.1) using package 'multcomp' (Hothorn *et al.*, 2008). Only lines grown in all three independent rounds of cultivation were taken into account (n=87). Testing for significance ($P \leq 0.05$) was performed with ANOVA and Tukey's HSD posthoc test with R (R Core Team, vers. 3.0.1) using packages 'multcomp' (Hothorn *et al.*, 2008) and 'agricolae' (Mendiburu, 2013). For pairwise comparison, differences were tested by t-test based on a level of significance of $P \leq 0.05$ with SigmaPlot (vers. 11.0).

RESULTS

Assembly of the barley collection

In order to capture as much diversity as possible with respect to elemental profiles in barley grains, we assembled a subset of accessions from the BCC. Selection was based on soil type in the region of origin (calcic soils with high pH, saline soils, heavy soils with low pH, low Zn soils, heavy soils with high pH) according to the FAO soil atlas (Food and Agriculture Organization of the United Nations, 2012) and aimed at maximizing the number of soil types included. Other criteria were country of origin, row-type, and the representation of both cultivated and wild varieties. In total, 136 lines from five different continents and 21 different countries were chosen (Tab. S1). Lines (98 bred varieties and 38 landraces) included two-rowed and six-rowed ear types and two different *H. vulgare* L. convarieties with 15 different subtaxa. Plants varied in shape and height, but none of them showed micronutrient deficiency symptoms in leaves during the glasshouse cultivation.

Variation of grain micronutrient concentrations

First, grains derived from genebank material were analysed (sample set IPK). Second, plants were then grown under glasshouse conditions in three independent cultivation rounds to assess the natural variation in grain Zn, Fe, Mn and Cu accumulation. Median Zn concentration differed between the genebank material (24.8 mg kg^{-1} DW) and the grains harvested after glasshouse cultivation. Mean values also differed within the latter (48.1, 63.4, 46.1 mg kg^{-1} DW) (Fig. 1a).

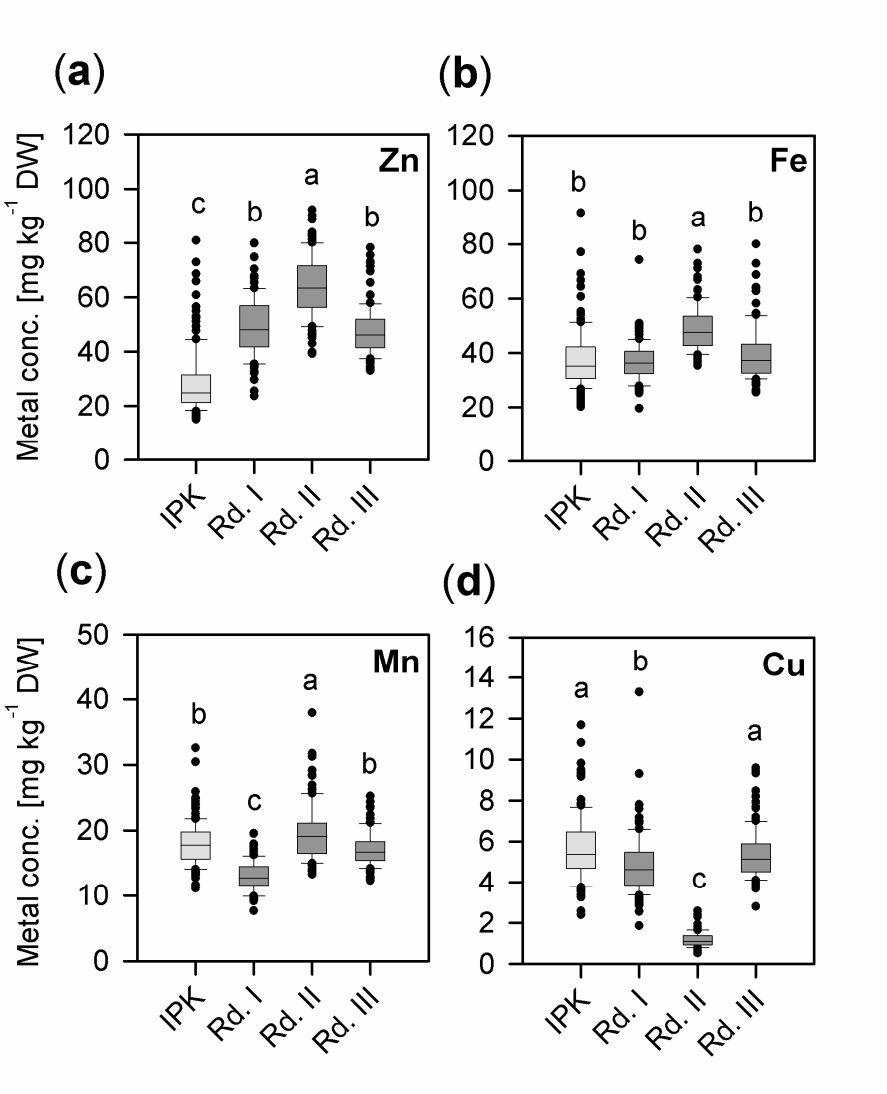

Fig. 1: Variation of grain micronutrient concentrations within a selection of 136 barley lines from the Barley Core Collection. Grain metal concentrations were either measured in material obtained from the genebank (IPK) directly or from plants grown in the glasshouse in three different cultivation rounds over three years (Rd. I, Rd. II, Rd. III); box plots of Zn (**a**), Fe (**b**), Mn (**c**) and Cu (**d**) concentrations for the 4 sample sets, displaying the median, the upper and lower quartile as well as extremes. The minimum number of lines analysed per sample set was 102. Statistical differences were calculated using ANOVA/Tukey's HSD post hoc test and are indicated with small letters ($P \leq 0.05$).

In contrast, the degree of variation between accessions was similar for the sample sets (IPK: 15.1 to 80.9, round I: 23.7 to 79.9, round II: 39.2 to 92.3 and round III: 33.1 to 78.3 mg kg^{-1} DW). Median grain Fe and Mn levels ranged from 35.1 (IPK) over 36.3 (round I) and 37.3 (round III) to 47.5 (round II) and from 12.7 (round I) over 16.7 (round III) and 17.7 (IPK) to 19.1 (round II) mg kg^{-1} DW, respectively (Fig. 1b,c). Max-min ratios of the 4 sample sets for Fe were between 2.2 and 4.5, for Mn between 2 and 2.9. Grains from IPK as well as from the rounds I and III showed similar Cu concentrations (median: 4.6 (round I), 5.1 (round III) and 5.4 (IPK) mg kg^{-1} DW) while grains grown in round II had a much lower median value of 1.1 mg kg^{-1} DW. Cu concentrations of the second cultivation round ranged near the lower detection limit. Max-min ratios for Cu ranged between 3.4 (round III) and 7.1 (round I) (Fig. 1d).

In order to detect possible patterns in grain Zn variation we grouped the accessions and compared median Zn values. Neither country groups nor the sorting based on prevalent soil type in the region of origin revealed significant differences. For instance, lines from regions with a high proportion of low Zn soils on average only marginally differed in their grain Zn from lines originating from areas with average soil Zn levels. Interestingly, even a comparison between cultivars and landraces did not reveal any significant differences (Fig. S2).

Correlation of Zn, Fe, Mn and Cu concentrations

Associations between micronutrients can be informative with respect to pathways involved in accumulation (Baxter, 2009). We conducted correlation analyses to reveal such associations. Across the three independent cultivations, the strongest correlation between the micronutrients analysed was found between Zn and Fe (Fig. 2a; for separate correlation analyses of individual experiments see Fig. S3). The correlations between Zn or Fe and Mn varied strongly depending on cultivation (from no significant difference to correlation coefficients of 0.742 and 0.62, respectively; Tab. S4), which resulted in overall coefficients of determination of 0.277 (Zn-Mn) and 0.232 (Fe-Mn). Because of the extremely divergent Cu concentrations of grains harvested in round II this sample set was eliminated from the regression analysis for Cu associations with Zn, Fe or Mn (Fig. 2b; for an analysis including data from all rounds see Fig. S4). Coefficients of determination were the highest for Cu-Zn (r^2=0.337). The respective values for Cu-Fe and Cu-Mn were 0.251 and 0.161.

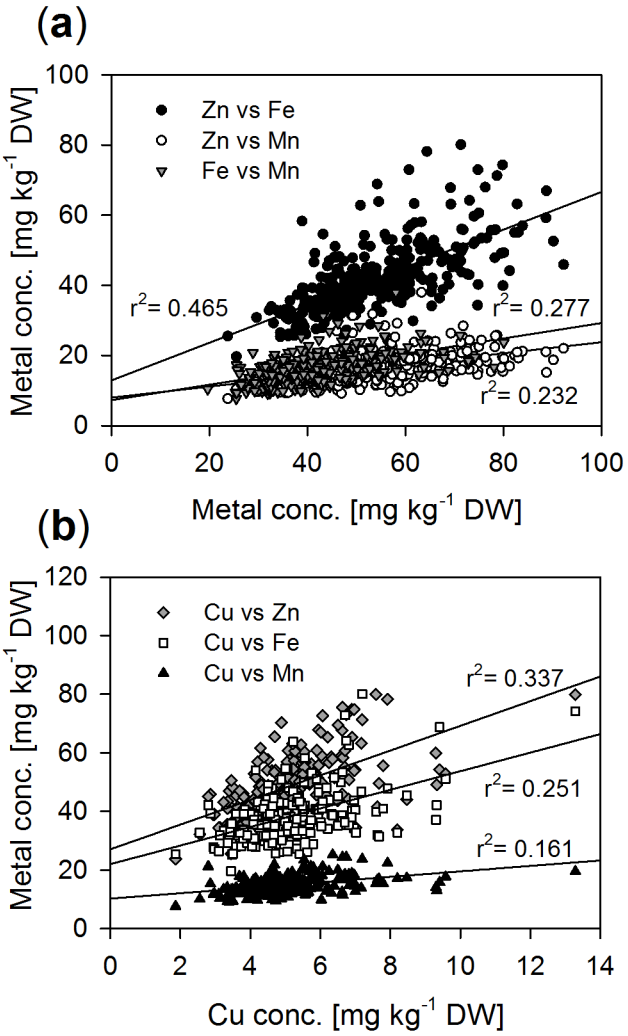

Fig. 2: Regression analysis of barley grain micronutrient concentrations. (**a**)**:** Regression plots of Zn vs Fe (closed circles), Zn vs Mn (open circles) and Fe vs Mn (triangles). Regression plots are including data from all three glasshouse cultivations (total number of samples=321). (**b**)**:** The regression plots of Cu vs Zn (diamond), Fe (squares) and Mn (triangles) of the first and third cultivation round (total number of samples=219). All displayed coefficients of determination were significant.

Genotype and cultivation round effects on grain micronutrient concentrations

The contributions of cultivation year and genotype to variation in grain micronutrient concentrations were determined through an ANOVA (Tab. 1). It revealed a highly significant contribution of 41.5 % to total variability for Zn by the cultivar. In comparison, the cultivar influence for Fe concentration was 29.3 %, for Mn 24 % and for Cu 13.2 %. Conversely, the effects of the cultivation rounds were 33.2 % for Zn, 29.3 % for Fe, 41.7 % for Mn and 73.9 % for Cu. Hence, this analysis showed genetic influence on grain mineral concentrations in the order Zn > Fe > Mn. For Cu accumulation, the apparent small genotype influence is at least in

part due to the drastic differences between the data obtained in the second cultivation and all other data sets and was therefore not considered further.

Tab. 1 ANOVA table for comparisons of genotype and cultivation round effects on grain Zn, Fe, Mn and Cu concentrations. 87 different genotypes were grown in three different cultivation rounds under glasshouse cultivation for the analysis.

Micronutrient	Source	Df	Sum Sq	Mean Sq	F value	*P* value	Contribution to variation [%]
Zn	Genotype	86	18405	214	3.286	< 0.001	41.5
	Round	2	14695	7347	112.811	< 0.001	33.2
	Residuals	172	11202	65			
Fe	Genotype	86	7578	88	1.417	< 0.05	29.3
	Round	2	7558	3779	60.771	< 0.001	29.3
	Residuals	172	10695	62			
Mn	Genotype	86	1086	12.6	1.403	< 0.05	24.0
	Round	2	1887	943.7	104.847	< 0.001	41.7
	Residuals	172	1548	9			
Cu	Genotype	86	170.3	2	2.041	< 0.001	13.2
	Round	2	956	478	492.782	< 0.001	73.9
	Residuals	172	166.8	1			

Grain Zn and Cd concentrations upon cultivation in contaminated soil

Enhanced Cd accumulation represents an imminent risk of biofortification via breeding of more micronutrient-dense crop varieties. In order to address the extent of correlation between grain Zn and Cd accumulation under near-natural conditions, we grew contrasting barley lines on mining-impacted contaminated agricultural soil. Because the strongest and most robust variation was found for Zn, the selection of lines targeted those showing consistent low, intermediate and high accumulation of Zn. Shown in Fig. 3a is a representation of Zn accumulation across the three different rounds of cultivation (respective displays of the Fe, Mn and Cu data are shown in Fig. S5). We chose lines 601, 604 and 605 as strong Zn accumulators, the reference line cv Pasadena and line 1369 as weak Zn accumulators and lines 32, 35, 54, and 434 as intermediate Zn accumulators. High Zn accumulating lines contained 68.4±17.4 (601), 72.1±14.8 (605) and 74.6±9.8 (604) mg kg^{-1} DW in the grains, while the control line cv Pasadena and line 1369 showed consistently low Zn concentrations in the grain (44.7±7.2 and 40.3±5.4 mg kg^{-1} DW, respectively). Most of the cultivated lines had Zn concentrations at a medium level, of which lines 32, 35, 54, and 434 (53±4.9, 52.7±4.9, 52.4±4.2 mg kg^{-1} DW and

59.1±11.6 mg kg^{-1} DW, respectively) were chosen as intermediate lines. The Zn accumulation behavior was also reflected in our ionome data generated for genebank material, underlining the suitability of the chosen lines to represent the range of barley grain Zn concentrations (Fig. 3b). Line 431, harvested only twice and therefore not represented in Fig. 3a, was added to the group of high Zn lines (70.6±9 mg kg^{-1} DW).

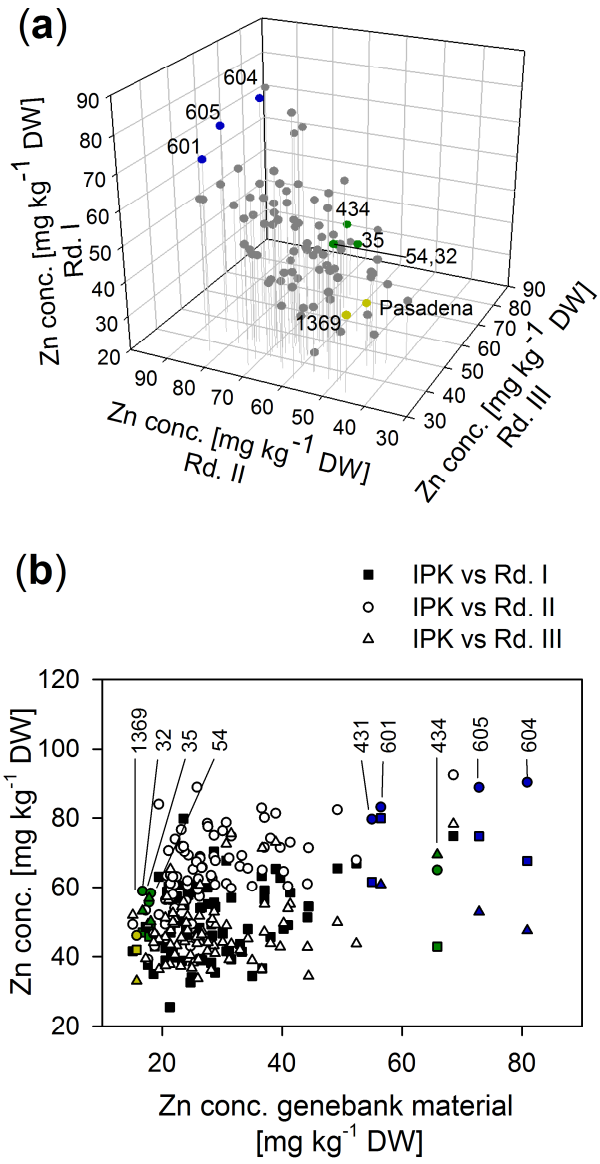

Fig. 3 Comparison of grain Zn concentrations of all analysed Barley Core Collection lines over different cultivation rounds. Grain Zn concentrations of lines grown in all three cultivation rounds (**a**) and of lines grown in all three cultivation rounds in comparison to the grain Zn concentrations in the samples measured from the genebank material directly (**b**). Lines selected as representing those showing consistently low (blue), medium (green) or high (yellow) Zn concentrations in all cultivation rounds and the genebank material are marked (n=87) (squares: IPK vs Rd. I, circles: IPK vs Rd. II, triangles: IPK vs Rd: III).

Upon cultivation in the contaminated soil, overall Zn accumulation was higher than after cultivation in regular soil with mean values between 68±15.6 and 166.7±29 mg kg^{-1} DW (see above and Figs. 3,4a). The relative differences in grain Zn accumulation were confirmed for most but not all of the lines. The line 434 was not among the best Zn accumulating lines in non-contaminated soil, while in contaminated soil it showed the highest level of Zn accumulation (166.7±29 mg kg^{-1} DW).

Cd concentrations in these grains revealed pronounced variation of >8fold with significant differences between the lines (Fig. 4b). The highest mean concentrations were found in line 604 with 0.6±0.3 mg kg^{-1} DW, the lowest in the reference line cv Pasadena with 0.07±0.03 mg kg^{-1} DW.

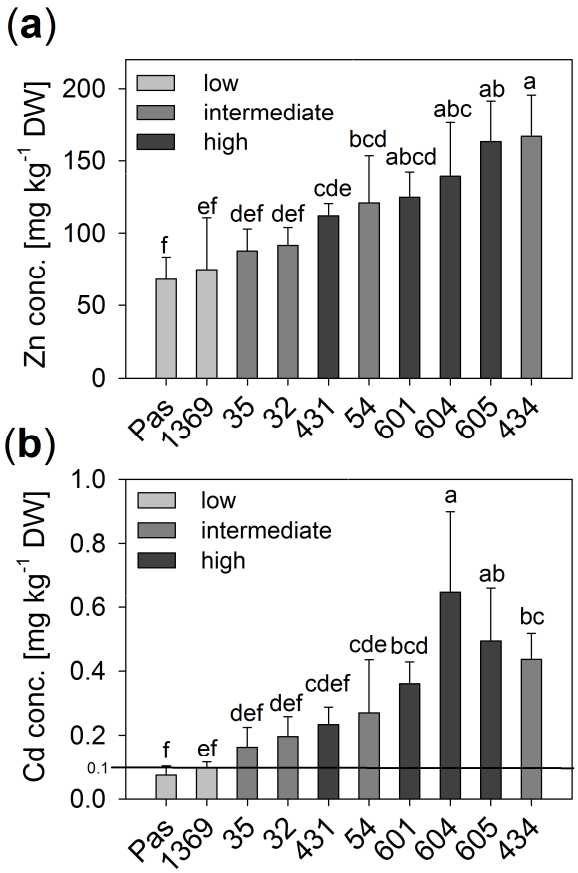

Fig. 4 Zn and Cd concentrations of lines grown on contaminated soil. Grain Zn (**a**) and Cd (**b**) concentrations of nine representative barley core collection lines (1369, 35, 32, 431, 54, 601, 604, 605, 434) and the reference line cv Pasadena grown on metal-contaminated agricultural soil. The threshold of 0.1 mg kg^{-1} DW Cd established by the Codex Alimentarius for cereals (Joint FAO/WHO Codex Alimentarius Commission, 1995) is indicated by a black line. Values are means + SD (n=7). Statistical differences were calculated using ANOVA/Tukey's HSD post hoc test and are displayed as letters ($P \leq 0.05$).

Grain Cd concentration correlated strongly with grain Zn concentration and also with concentrations of the other micronutrients analysed (Tab. 2). The coefficient of determination for Zn and Cd was highest (0.623), followed by the coefficients of Mn and Cd (0.514), Cu and Cd (0.448), and Fe and Cd (0.192). When comparing the Zn/Cd ratios, however, there was detectable variation in spite of the correlation between Zn and Cd. The low Zn lines showed the most favorable Zn/Cd ratio (Fig. S6). Among the high Zn lines, 431 accumulated less Cd than 604 and 605.

Tab. 2 Coefficients of determination of Zn, Fe, Mn and Cu concentrations in barley grains from plants grown on contaminated soil. 73 individuals of 9 cultivars were grown in a pot experiment on native agricultural soil with metal contamination: *, $P < 0.05$; **, $P < 0.01$; ***, $P < 0.001$.

	Fe	**Mn**	**Cu**	**Cd**
Zn	0.366 ***	0.850 ***	0.381 ***	0.623 ***
Fe		0.436 ***	0.134 ***	0.192 ***
Mn			0.340 ***	0.514 ***
Cu				0.448 ***

Because low-level anthropogenic Cd contamination is widespread, Cd is found in the majority of grain samples even after crop cultivation in soil without notably increased Cd concentrations (European Food Safety Authority, 2009). Therefore, we decided to also analyse grain Cd in the field-grown genebank material of these lines. For this the more sensitive ICP-MS analysis was applied. Cd was clearly detectable in all grain samples in a range from 0.011 to 0.099 mg kg^{-1} DW (Fig. S7). With the exception of line 434 the data confirmed the rank of lines as observed in the experiment on Cd-contaminated soil.

Grain dissection

Next, we investigated whether variation in grain micronutrients applies to all tissues of the grain uniformly or rather is due to enrichment in distinct parts. For this analysis the set of representative lines was made slightly smaller and included grains of three high (601, 604, 605), two intermediate (32 and 35) and two low Zn lines (cv Pasadena and 1369) (Fig. 5a).

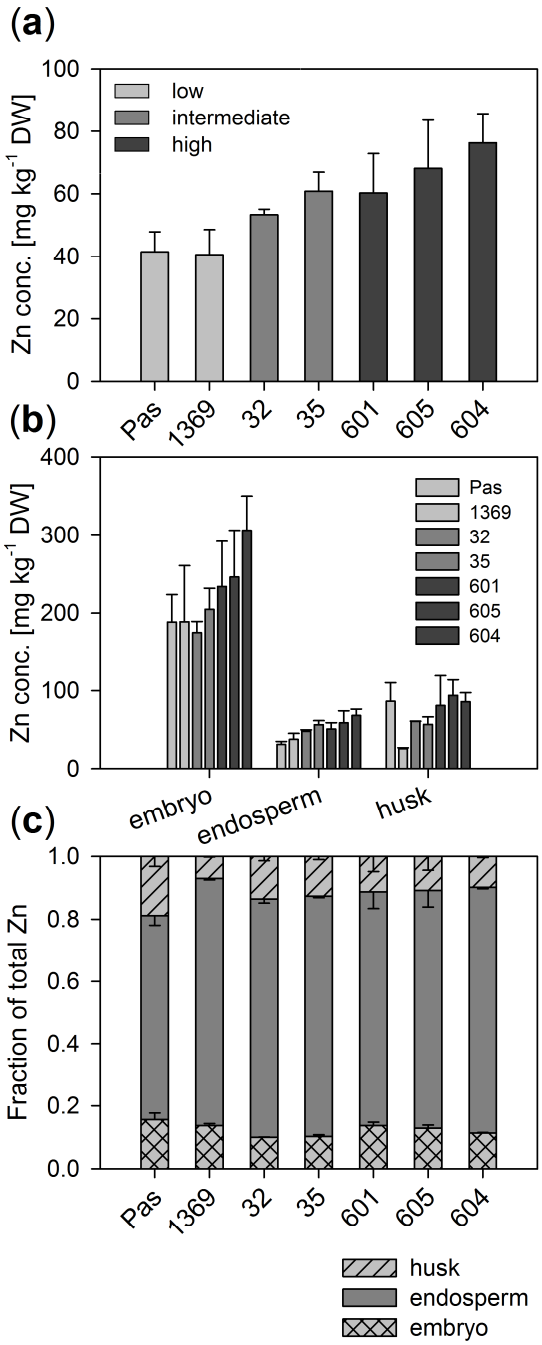

Fig. 5: Analysis of grain Zn distribution by grain dissection. (**a**)**:** Grain Zn concentrations of two low (Pas=cv Pasadena, 1369), two intermediate (32, 35) and three high Zn (601, 605, 604) barley lines. (**b**)**:** Zn concentrations of separate grain parts (embryo, endosperm and husk) for the lines described in (a). (**c**)**:** Contributions of dissected tissues (embryo, endosperm and husk) to the total amount of Zn per grain. For each sample five grains per line and cultivation round were pooled. Values are means + SD (n=2-3). Statistical analysis with ANOVA/Tukey's HSD post hoc test ($P \leq 0.05$) did not reveal any significant differences.

Average grain weights deviated by more than 10 % from the mean only for lines 1359 (22 % lower) and 35 (19 % higher). Embryo tissues had the highest levels of Zn (174.9±14.3 to 306.4±43.7 mg kg^{-1} DW), followed by the husk (25.6±1.2 to 94±20.1 mg kg^{-1} DW) and the endosperm (31±3.9 to 68±8.3 mg kg^{-1} DW) (Fig. 5b). Despite these differences in Zn concentration between the grain parts, however, the comparison across the contrasting lines showed largely the pattern observed in total grain Zn. High Zn lines had higher Zn concentration than low Zn lines in all grain parts. Only cv Pasadena as a low Zn line showed Zn concentrations comparable to those of the high Zn lines in the husk. When taking the weight percentage into account, the endosperm contributed the most (65.5 to 79.3 %, Fig. 5c) to the absolute amount of Zn per grain in all lines. Husk and embryo tissues made comparable low contributions to the total Zn (7 to 18.9 % and 10 to 15.6 %, respectively). No obvious pattern emerged with respect to the relative importance of grain parts (Fig. 5c). Fe, Mn and Cu concentrations showed similar levels in all the lines. Hence, these micronutrients were also the highest in embryo tissue, followed by husk and endosperm. Relative contributions of the different parts to grain Fe concentration were comparable to Zn, while for Mn and Cu higher variability was observed (Fig. S8).

µ-PIXE analyses

For a more detailed picture of the micronutrient distribution in low vs. high Zn barley grains, line 1369 (low Zn), line 604 (high Zn) and cv Pasadena as the reference line were subjected to quantitative mapping using µ-PIXE. Four grains per line were sectioned in a way that reveals four tissues, namely the embryo with the cross-sectioned root primordia and including the scutellum, aleurone, endosperm and husk (Fig. S9). Representative quantitative distribution maps of Zn, Fe and Mn are shown in Fig. 6 (for all Zn maps obtained see Fig. S10, for Fe Fig. S11, and for Mn Fig. S12). Cu was below the detection limit of the technique. From these maps, the tissue-specific concentrations were calculated and results are consistent with higher overall Zn concentrations of the high Zn line 604 compared to the low Zn line 1369 and to cv Pasadena (Fig. 6b). Fine-scale analysis showed the highest Zn concentrations in aleurone tissue of line 604 with 783.5±299.7 mg kg^{-1} DW in comparison to 410.7±134.4 (cv Pasadena) and 321.2±87 mg kg^{-1} DW (1369 line), followed by embryo (404.4±61 compared to 214.6±29.2 and 241.1±47.6 mg kg^{-1} DW, respectively) and endosperm tissue (165.8±64.3 compared to 60.8±33.5 and 88.3±65 mg kg^{-1} DW, respectively). For the husk, the same trends as seen in the grain dissection were found (Fig. 6c) with cv Pasadena having Zn concentrations (173.3±102.9 mg kg^{-1} DW) comparable to the high Zn accumulating line 604 (122.2±61.9 mg kg^{-1} DW).

Regardless of the line, Zn was mainly found in aleurone and embryo tissues with the highest concentrations in a transition zone between aleurone and embryo tissue. In the endosperm, a band representing higher Zn concentrations than surrounding cells was apparent near the scutellum/embryo tissues in all lines. Fe was mainly found in aleurone and embryo tissues. This was also seen in sections stained with Perl's stain (Fig. S13). Mn was concentrated in a layer of root primordia, especially in the reference line Pasadena and the high Zn accumulating line 604.

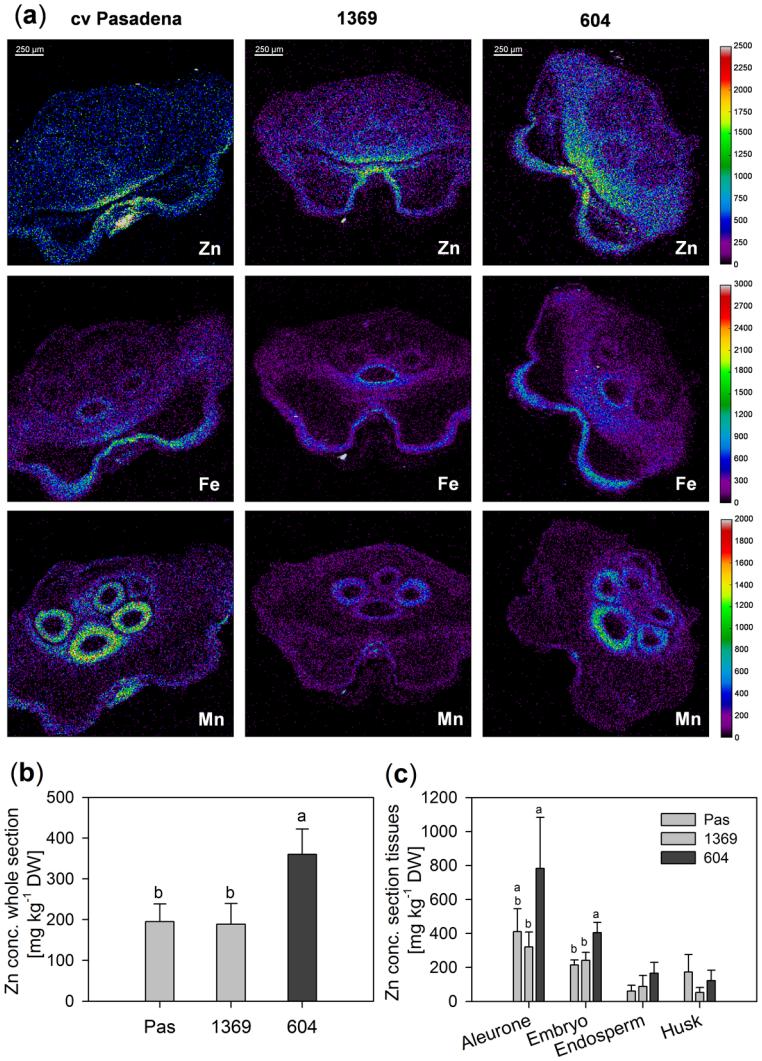

Fig. 6: Distribution maps of Zn, Fe and Mn obtained by quantitative µ-PIXE for grains of lines representing the variation in grain Zn accumulation. (**a**)**:** µ-PIXE maps for Zn, Fe and Mn of barley grain sections of the reference line cv Pasadena, the low Zn line 1369 and the high Zn line 604. Mature grains were transversely sectioned at the position of the embryo as indicated in Fig. S8. (**b**)**:** Zn concentrations averaged over µ-PIXE maps of four sections per line. (**c**)**:** Zn concentrations of different tissues (aleurone, embryo, endosperm and husk) derived from µ-PIXE maps of four sections per line. Values are means + SD. Statistical differences in grain tissue concentrations between the lines were calculated using ANOVA/Tukey's HSD post hoc test and are displayed as letters ($P \leq 0.05$).

Co-localization maps of Zn, Fe and Mn with P and S (as proxies for phytic acid and thiol ligands, respectively) are shown in Fig. 7. P was mainly found in embryo and aleurone tissue, whereas S was detected with nearly equal intensity in the root primordia and in the endosperm. Within the latter a gradient from the sub-aleurone layer to the inner part of the endosperm was apparent. Total grain P and S concentrations calculated based on the µ-PIXE maps showed no differences between the lines (Fig. S14).

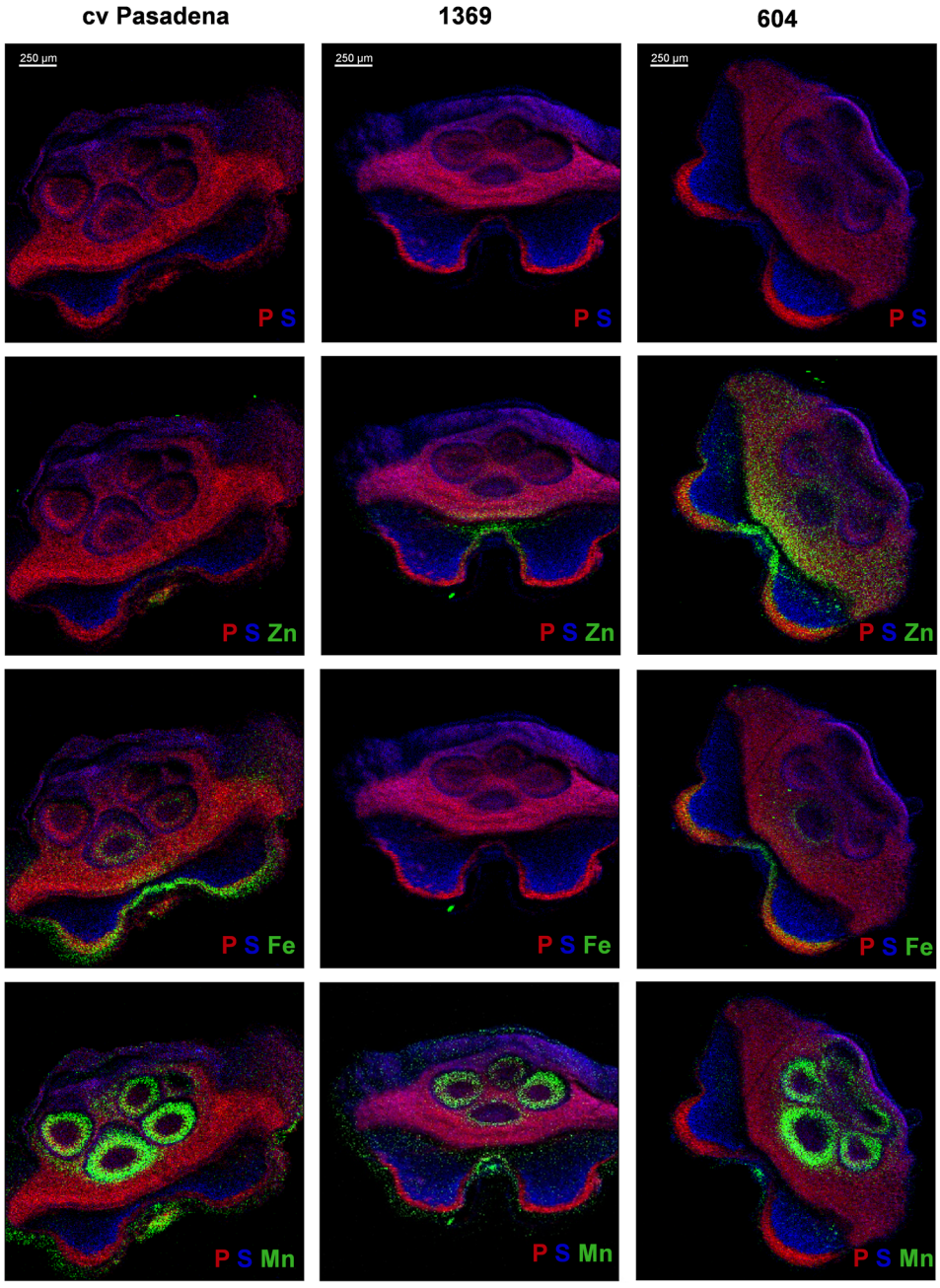

Fig. 7 Co-localization of P and S with Zn, Fe and Mn. µ-PIXE co- localization maps for Zn, Fe or Mn (shown in green) with P (red) and S (blue) in barley grain sections of the reference line cv Pasadena, the low Zn line 1369 and the high Zn line 604.

DISCUSSION

The potential for breeding of biofortified cereals depends on the magnitude and exploration of phenotypic diversity in grain micronutrient density. Accordingly, we first investigated the diversity in barley grain micronutrient accumulation. Barley represents a very valuable model for cereals, in particular wheat (Brenchley *et al.*, 2012). Furthermore, the use of barley as a human food may well expand with rising interest in health-promoting components of barley grains such as β-glucans. Also, because of the wide range of environments barley is adapted to (Dawson *et al.*, 2015), it is part of a staple diet in some areas of the world such as mountainous regions in Asia, Africa and South America (Newton *et al.*, 2011). However, little is known to date about variation in barley grain micronutrient density.

During the course of breeding for modern high-yielding cultivars, crop species including barley went through a genetic bottleneck that led to the loss of potentially desirable traits (Dawson *et al.*, 2015). It is therefore important to access as much of the genetic diversity within cultivated barley and wild *Hordeum* species as possible. We chose both cultivars and landraces from the BCC. Unable to include all of the ca. 1600 varieties in the analysis we used the FAO world soil atlas to maximize the number of edaphic environments represented.

The two biofortification target micronutrients Zn and Fe as well as the two other main micronutrients Mn and Cu were analysed. Across the glasshouse cultivations mean values differed by a factor of 1.3 to 1.5 for Zn, Mn, and Fe (Fig. 1 a,b,c), reflecting variation in growth conditions such as temperature and humidity. A comparison with the few published data sets on barley grain micronutrient compositions showed very good agreement for Fe concentrations. Ma *et al.* (2004) found mean values of around 39 and 48 mg kg^{-1} in two different sets of accessions. Zn concentrations were similar to the ones reported recently for barley landraces from Ethiopia and Eritrea (between 30.7 and 48.5 mg kg^{-1} in different sample sets; Mamo *et al.*, 2014). Thus, it appears that barley grains are on average slightly more Zn-dense than wheat grains based on data compiled by White & Broadley (2009) and Xu *et al.* (2011), while there is no difference in Fe density. Interestingly, unlike in wheat (Zhao *et al.*, 2009; Xu *et al.*, 2011) there appears to be no overall difference in micronutrient density between landraces and modern accessions (Fig. S2). Relative to whole (unmilled) rice grains, barley grains show about 2fold higher mean Zn concentrations (Norton *et al.*, 2014; Pinson *et al.*, 2015) and >3fold higher Fe concentrations (Pinson *et al.*, 2015).

The maximum/minimum quotients for Fe and Zn concentrations of cereal grains show remarkable similarity across a wide range of experiments. In the majority of studies with wheat or rice values between 1.5 and 4 were determined for Fe and Zn (White & Broadley, 2009; Xu *et al.*, 2011). Our analysis revealed a comparable degree of variation in barley after cultivation in a soil with average total Zn levels.

A considerable fraction of the observed variation is explained by genetic differences according to our ANOVA. This applies to grain Zn concentrations in particular. Genetic influence on grain Zn is supported by the detection of QTLs for grain Zn in a doubled haploid mapping population (Lonergan *et al.*, 2009) and the heritability recently found in the Ethiopian and Eritrean Barley Collection (Mamo *et al.*, 2014). Strong genotype effects are further supported by the fact that the ranking based on grain Zn was confirmed for many accessions even in genebank material, which was multiplied on different fields in different years. Taken together, the degree of variation and the genotype influence on this variation indicate that there is breeding potential for barley with higher Zn and also Fe concentrations.

Well-characterized processes such as root uptake, symplastic mobility, xylem loading, xylem-to-phloem transfer, or remobilization from leaves influence the accumulation of essential and non-essential metals in grains (Palmgren *et al.*, 2008; Zhao & McGrath, 2009). Distribution pathways for the different elements are shared or intersect in various ways. Thus, analysis of correlations can help building hypotheses about grain metal accumulation mechanisms. The strongest correlation was found between Zn and Fe with 46.5 % of the variation in Fe concentration being explained by the Zn concentration of the grain. These strong correlations have been reported before for wheat and pearl millet grains (Cakmak *et al.*, 2004; Jiang *et al.*, 2007; Morgounov *et al.*, 2007; Peleg *et al.*, 2008; Zhao *et al.*, 2009; Chatzav *et al.*, 2010) and could be attributable to the limited specificity of transporters and metal ligands for either Zn or Fe (Tauris *et al.*, 2009; Li *et al.*, 2013; Borrill *et al.*, 2014; Slamet-Loedin *et al.*, 2015).

More in-depth analyses had to be focused on small subsets of lines. Since there were no lines that showed consistently high grain concentrations of both Zn and Fe, we selected lines with contrasting grain concentrations of Zn. Grain Zn showed more pronounced variation and a higher genotype influence than grain Fe. Moreover, grain Mn and Cu concentrations are of less interest in the context of biofortification. Correlation analysis for the three glasshouse cultivations (Fig. 3a) as well as between glasshouse cultivations and the genebank material (Fig. 3b) revealed several accessions with robust differences in grain Zn.

Of particular relevance is the association between grain micronutrient concentrations and the concentrations of Cd. Cereal consumption represents the major source of Cd intake (Clemens *et al.*, 2013; Meharg *et al.*, 2013). Cd is highly toxic and accumulates in the human body for 10 to 30 years. Recent assessments of the health threat through chronic exposure to low levels of Cd have led the EFSA to recommend a lowering of the provisional tolerable weekly intake (European Food Safety Authority, 2009). One of the strategies towards reaching this goal is the development of low grain Cd cultivars. This strategy is most advanced in rice (Uraguchi & Fujiwara, 2012). However, since uptake and accumulation of the non-essential metal Cd are strongly influenced by micronutrient status of a plant and assumed to be mediated by pathways for Zn, Fe, and Mn (Clemens, 2006; Slamet-Loedin *et al.*, 2015), the breeding of more micronutrient-dense crops is associated with the risk of inadvertently increasing the Cd burden. We therefore tested a representative set of lines on a metal-contaminated genuine agricultural soil. Total Cd of 10 mg kg^{-1} in this soil is within the range and close to the upper limit of 14 mg kg^{-1} documented for European topsoils in the FOREGS Geochemical Atlas of Europe (Pan *et al.*, 2010), the total Zn of 3200 mg kg^{-1} is slightly above the upper limit of 2900 mg kg^{-1} (http://weppi.gtk.fi/publ/foregsatlas/). All but one of the mean grain Cd levels exceeded the threshold of 0.1 mg kg^{-1} DW established by the Codex Alimentarius for barley (Joint FAO/WHO Codex Alimentarius Commission, 1995), demonstrating the problems arising from Cd contamination of soils. The about 8fold variation in grain Cd was confirmed in a re-analysis of genebank material both with respect to magnitude and the ranking of accessions (Fig. 4 and Fig. S7). It agrees well with a recent study that revealed pronounced variation in barley grain Cd (Wu *et al.*, 2015). For other cereals, e.g. rice, wide variation in Cd accumulation is documented too (e.g. Meharg *et al.*, 2013; Pinson *et al.*, 2015). Correlation of grain Cd was strongest with Zn, followed by Mn, Cu and Fe (Tab. 2). Strongest correlation with Zn was found in Wu *et al.* (2015) as well. The correlation with Mn is confirming data reported by Chen *et al.* (2007). Overall, these results indicate the involvement of Zn and Mn homeostasis factors in Cd accumulation. Importantly though, there is evidence for variation in Zn/Cd ratios, indicating potential to breed both for low Cd barley and for high Zn/low Cd barley.

The bioavailability of grain micronutrients for absorption by the human gut is influenced first by how much of the micronutrients remain after processing of the grains and second by the binding environment (speciation) within the grain (Hansen *et al.*, 2012; Eagling *et al.*, 2014). It is therefore of utmost importance to obtain detailed knowledge on micronutrient localization within the grain, and whether there is variation in this respect between genotypes with contrasting micronutrient concentrations (Pongrac *et al.*, 2013). We addressed this question

following two approaches, namely elemental analysis after mechanical grain dissection and μ-PIXE. In agreement with many previous studies we found much higher micronutrient concentrations in the embryo and to a lesser extent in the husk than in the endosperm. For instance, a detailed analysis of Zn accumulation in wheat grains (Stomph *et al.*, 2011) found around 8-fold higher Zn concentrations in the embryo relative to the endosperm, which is very close to the ratios we observed (Fig. 5 b,c). This was qualitatively confirmed with much higher resolution through synchrotron-based X-ray fluorescence microscopy (Ajiboye *et al.*, 2015). Validation of our grain dissection comes also from a comparison with data reported for fractionation of barley grains (Lombi *et al.*, 2011). The 13 % of total grain Zn determined for the embryo of the reference cultivar Golden Promise is similar to the values around 15 % we determined for our selection of cultivars. Overall, the distribution of the four analysed micronutrients within the barley grain differs. Relative to Zn the embryo contains less Fe and more Mn (Fig. S8). Still, the endosperm always contributes the most to the total micronutrient content of a grain. Importantly, the differences in total grain Zn between the contrasting lines were observed in all analysed parts. With the exception of relatively high Zn concentrations in the husk of cv Pasadena grains, the relative contributions were found to be rather stable. This indicates that in high Zn barley lines transfer of Zn to the endosperm is as efficient as in low Zn barley lines. The additional Zn is not deposited at higher rates in the outer layers of the grain. Similar observations were reported for the grains of wheat that were agronomically biofortified by Zn fertilization (Pongrac *et al.*, 2013).

Even more informative than elemental profiles of grain fractions are elemental maps obtained by advanced spectroscopic techniques (Lombi *et al.*, 2011; Zhao *et al.*, 2014). Using μ-PIXE we obtained the first quantitative high-resolution maps for barley grains with contrasting Zn accumulation. Patterns were consistent across the biological replicates (Figs. S10-S12). Zn showed a more diffuse distribution than Fe and Mn. Similar to high-definition synchrotron X-ray fluorescence analysis of the barley reference cultivar Golden Promise (Lombi *et al.*, 2011), Zn extended more into the endosperm while Fe was mostly detected in the outer layers of the grain (in particular the aleurone cells, as clearly seen in Perl's stained sections; Fig. S13) and like Mn in the layer of cells surrounding the provasculature in embryonic roots. A similar microelement distribution pattern was also seen in grains of different wheat cultivars (Singh *et al.*, 2014). Generally, a growing number of recent studies has demonstrated differential localization of Zn and Fe in cereal grains (e.g. Kyriacou *et al.*, 2014; Ajiboye *et al.*, 2015).

It is not possible to directly compare the quantitative data obtained after grain dissection and μ-PIXE analysis because the latter is performed on a section through the embryo and therefore does not represent concentration gradients such as apparent for the endosperm. Nonetheless, stability of higher Zn accumulation in line 604 was confirmed for all tissue-specific Zn concentrations. The only exception was high Zn concentration in the husk of cv Pasadena grains. This once more suggests considerable transfer of Zn into the endosperm in high Zn accessions, which should favor the development of lines with higher Zn bioavailability. Low Fe concentrations and high Mn concentrations in the embryo are in good agreement with the grain dissection analysis too. It will be very interesting to integrate such distribution maps with high-resolution molecular analysis, enabled, for instance, by laser capture microdissection (e.g. Tauris *et al.*, 2009). Ideally such analyses would be combined with information on the speciation of micronutrients and the distribution of macromolecules. Co-localization of Zn, Fe and Mn with P and S provide first hints. Within the endosperm much less P was detected than in other tissues while S was more evenly distributed. Thus, endosperm Zn may in barley grains well be complexed with S ligands as suggested by SEC-ICP-MS and enzymatic digestion (Persson *et al.*, 2009).

ACKNOWLEDGEMENTS

We are most grateful to the team of the genebank at the IPK in Gatersleben for providing the barley grains. We thank Erika Szakács for cultivation of plants on metal-contaminated soil, the Department of Biology, University of Ljubljana for assisting with sample holder preparations for μ-PIXE, and the BayCEER analytical facility at the University of Bayreuth for ICP-MS analyses. This work was financially supported by the European Union through its Sixth Framework Program for RTD (contract no FOOD-CT-2006- 016253) (SC and UK) and a postdoctoral fellowship by the Alexander von Humboldt foundation to PP.

REFERENCES

Abràmoff MD, Magalhães PJ, Ram SJ. 2004. Image Processing with ImageJ. Biophotonics International 11: 36–42.

Ajiboye B, Cakmak I, Paterson D, de Jonge, Martin D, Howard DL, Stacey SP, Torun AA, Aydin N, McLaughlin MJ. 2015. X-ray fluorescence microscopy of zinc localization in wheat grains biofortified through foliar zinc applications at different growth stages under field conditions. Plant and Soil 392: 357–370.

Alloway BJ. 2008. Zinc in soils and crop nutrition (2nd ed.). Brussels, Belgium: International Zinc Association; Paris: International Fertilizer Industry Association.

Atungulu GG, Pan Z. 2014. Rice industrial processing worldwide and impact on macro- and micronutrient content, stability, and retention. Annals of the New York Academy of Sciences 1324: 15–28.

Baxter I. 2009. Ionomics: studying the social network of mineral nutrients. Current Opinion in Plant Biology 12: 381–386.

Baxter I, Ziegler G, Lahner B, Mickelbart MV, Foley R, Danku J, Armstrong P, Salt DE, Hoekenga OA. 2014. Single-kernel ionomic profiles are highly heritable indicators of genetic and environmental influences on elemental accumulation in maize grain (*Zea mays*). PloS ONE 9: e87628.

Black RE, Allen LH, Bhutta ZA, Caulfield LE, Onis M de, Ezzati M, Mathers C, Rivera J. 2008. Maternal and child undernutrition: global and regional exposures and health consequences. The Lancet 371: 243–260.

Borrill P, Connorton JM, Balk J, Miller AJ, Sanders D, Uauy C. 2014. Biofortification of wheat grain with iron and zinc: integrating novel genomic resources and knowledge from model crops. Frontiers in Plant Science 5: 53.

Bothmer Rv. 2003. Diversity in barley (*Hordeum vulgare*). Amsterdam, Boston: Elsevier.

Bouis HE, Welch RM. 2010. Biofortification - a sustainable agricultural strategy for reducing micronutrient malnutrition in the global south. Crop Science 50: 20-32.

Brenchley R, Spannagl M, Pfeifer M, Barker, Gary L A, D'Amore R, Allen AM, McKenzie N, Kramer M, Kerhornou A et al. 2012. Analysis of the bread wheat genome using whole-genome shotgun sequencing. Nature 491: 705–710.

Cakmak I. 2008. Enrichment of cereal grains with zinc: agronomic or genetic biofortification? Plant and Soil 302: 1–17.

Cakmak I, Turun A, Millet E, Feldman M, Fahima T, Korol A, Nevo E, Braun HJ, Ozkan H. 2004. Triticum dicoccoides: an important genetic resource for increasing zinc and iron concentration in modern cultivated wheat. Soil Science and Plant Nutrition 50: 1047–1054.

Chatzav M, Peleg Z, Ozturk L, Yazici A, Fahima T, Cakmak I, Saranga Y. 2010. Genetic diversity for grain nutrients in wild emmer wheat: potential for wheat improvement. Annals of Botany 105: 1211–1220.

Chen F, Dong J, Wang F, Wu F, Zhang G, Li G, Chen Z, Chen J, Wei K. 2007. Identification of barley genotypes with low grain Cd accumulation and its interaction with four microelements. Chemosphere 67: 2082–2088.

Clemens S. 2006. Toxic metal accumulation, responses to exposure and mechanisms of tolerance in plants. Biochimie 88: 1707–1719.

Clemens S. 2014. Zn and Fe biofortification: the right chemical environment for human bioavailability. Plant science 225: 52–57.

Clemens S, Aarts MG, Thomine S, Verbruggen N. 2013. Plant science: the key to preventing slow cadmium poisoning. Trends in Plant Science 18: 92–99.

Dawson IK, Russell J, Powell W, Steffenson B, Thomas WT, Waugh R. 2015. Barley: a translational model for adaptation to climate change. New Phytologist 206: 913–931.

Eagling T, Neal AL, McGrath SP, Fairweather-Tait S, Shewry PR, Zhao F. 2014. Distribution and speciation of iron and zinc in grain of two wheat genotypes. Journal of Agricultural and Food Chemistry 62: 708–716.

European Food Safety Authority (EFSA). 2009. Scientific Opinion of the Panel on Contaminants in the Food Chain on a request from the European Commission on cadmium in food. EFSA Journal: 1–139.

Food and Agriculture Organization of the United Nations. 2012. FAO GEONETWORK. Digital Soil Map of the World (GeoLayer). URL http://www.fao.org/soils-portal/soil-survey/soil-maps-and-databases/faounesco-soil-map-of-the-world/en/.

Food and Agriculture Organization of the United Nations. FAOSTAT. 2014. FAOSTAT (Database). URL http://data.fao.org/ref/262b79ca-279c-4517-93de-ee3b7c7cb553.html?version=1.0 [accessed January 30 2015].

Gómez-Galera S, Rojas E, Sudhakar D, Zhu C, Pelacho AM, Capell T, Christou P. 2010. Critical evaluation of strategies for mineral fortification of staple food crops. Transgenic Research 19: 165–180.

Hansen TH, Lombi E, Fitzgerald M, Laursen KH, Frydenvang J, Husted S, Boualaphanh C, Resurreccion A, Howard DL, Jonge MD de et al. 2012. Losses of essential mineral nutrients by polishing of rice differ among genotypes due to contrasting grain hardness and mineral distribution. Journal of Cereal Science 56: 307–315.

Hatam EG, Pelicon P, Lamehi-Rachti M, Vavpetic P, Kakuee O, Grlj N, Cekada M, Fathollahi V. 2012. Surface topography reconstruction by stereo-PIXE. Journal of Analytical Atomic Spectrometry 27: 834–840.

Hothorn T, Bretz F, Westfall P. 2008. Simultaneous inference in general parametric models. Biometrical journal. Biometrische Zeitschrift 50: 346–363.

Huang X, Han B. 2014. Natural variations and genome-wide association studies in crop plants. Annual Review of Plant Biology 65: 531–551.

International Barley Genome Sequencing Consortium, Mayer KF, Waugh R, Brown JW, Schulman A, Langridge P, Platzer M, Fincher GB, Muehlbauer GJ, Sato K et al. 2012. A physical, genetic and functional sequence assembly of the barley genome. Nature 491: 711–716.

Jiang SL, Wu JG, Feng Y, Yang XE, Shi CH. 2007. Correlation analysis of mineral element contents and quality traits in milled rice (*Oryza sativa* L.). Journal of Agricultural and Food Chemistry 55: 9608–9613.

Joint FAO/WHO Codex Alimentarius Commission. 1995. General Standard For Contaminants And Toxins In Food And Feed (CODEX STAN 193-1995). Adopted in 1995. Revised in 1997, 2006, 2008, 2009. Amendment 2010, 2012, 2013, 2014, 2015. URL http://www.codexalimentarius.org/standards/list-of-standards/en/?provide=standards&orderField=fullReference&sort=asc&num1=CODEX [accessed October 29 2015]

Khan MA, Castro-Guerrero N, Mendoza-Cozatl DG. 2014. Moving toward a precise nutrition: preferential loading of seeds with essential nutrients over non-essential toxic elements. Frontiers in Plant Science 5: 51.

Klančnik K, Vogel-Mikuš K, Kelemen M, Vavpetič P, Pelicon P, Kump P, Jezeršek D, Gianoncelli A, Gaberščik A. 2014. Leaf optical properties are affected by the location and type of deposited biominerals. Journal of Photochemistry and Photobiology. B: Biology 140: 276–285.

Kodkany BS, Bellad RM, Mahantshetti NS, Westcott JE, Krebs NF, Kemp JF, Hambidge KM. 2013. Biofortification of pearl millet with iron and zinc in a randomized controlled trial increases absorption of these minerals above physiologic requirements in young children. The Journal of Nutrition 143: 1489–1493.

Kyriacou B, Moore KL, Paterson D, Jonge MD de, Howard DL, Stangoulis J, Tester M, Lombi E, Johnson AA. 2014. Localization of iron in rice grain using synchrotron X-ray fluorescence microscopy and high resolution secondary ion mass spectrometry. Journal of Cereal Science 59: 173–180.

Li S, Zhou X, Huang Y, Zhu L, Zhang S, Zhao Y, Guo J, Chen J, Chen R. 2013. Identification and characterization of the zinc-regulated transporters, iron-regulated transporter-like protein (ZIP) gene family in maize. BMC Plant Biology 13: 114.

Liberato SC, Singh G, Mulholland K. 2015. Zinc supplementation in young children: a review of the literature focusing on diarrhoea prevention and treatment. Clinical nutrition (Edinburgh, Scotland) 34: 181–188.

Lombi E, Smith E, Hansen TH, Paterson D, Jonge MD de, Howard DL, Persson DP, Husted S, Ryan C, Schjørring JK. 2011. Megapixel imaging of (micro)nutrients in mature barley grains. Journal of Experimental Botany 62: 273–282.

Lonergan PF, Pallotta MA, Lorimer M, Paull JG, Barker SJ, Graham RD. 2009. Multiple genetic loci for zinc uptake and distribution in barley (*Hordeum vulgare*). New Phytologist 184: 168–179.

Lung'aho MG, Mwaniki AM, Szalma SJ, Hart JJ, Rutzke MA, Kochian LV, Glahn RP, Hoekenga OA. 2011. Genetic and physiological analysis of iron biofortification in maize kernels. PloS ONE 6: e20429.

Ma JF, Higashitani A, Sato K, Takeda K. 2004. Genotypic variation in Fe concentration of barley grain. Soil Science and Plant Nutrition 50: 1115–1117.

Mamo BE, Barber BL, Steffenson BJ. 2014. Genome-wide association mapping of zinc and iron concentration in barley landraces from Ethiopia and Eritrea. Journal of Cereal Science 60: 497–506.

Mayo-Wilson E, Junior JA, Imdad A, Dean S, Chan, Xin Hui S, Chan ES, Jaswal A, Bhutta ZA. 2014. Zinc supplementation for preventing mortality, morbidity, and growth failure in children aged 6 months to 12 years of age. The Cochrane Database of Systematic Reviews 5: CD009384.

Meharg AA, Norton G, Deacon C, Williams P, Adomako EE, Price A, Zhu Y, Li G, Zhao F, McGrath S et al. 2013. Variation in rice cadmium related to human exposure. Environmental Science & Technology 47: 5613–5618.

Mendiburu F de. 2013. agricolae: statistical procedures for agricultural research. R package version 1.1-6. URL http://CRAN.R-project.org/package=agricolae [accessed February 18 2014].

Morgounov A, Gómez-Becerra HF, Abugalieva A, Dzhunusova M, Yessimbekova M, Muminjanov H, Zelenskiy Y, Ozturk L, Cakmak I. 2007. Iron and zinc grain density in common wheat grown in Central Asia. Euphytica 155: 193–203.

Murgia I, Arosio P, Tarantino D, Soave C. 2012. Biofortification for combating 'hidden hunger' for iron. Trends in Plant Science 17: 47–55.

Newton AC, Flavell AJ, George TS, Leat P, Mullholland B, Ramsay L, Revoredo-Giha C, Russell J, Steffenson BJ, Swanston JS et al. 2011. Crops that feed the world 4. Barley: a resilient crop? Strengths and weaknesses in the context of food security. Food Security 3: 141–178.

Norton GJ, Douglas A, Lahner B, Yakubova E, Guerinot ML, Pinson SRM, Tarpley L, Eizenga GC, McGrath SP, Zhao F et al. 2014. Genome wide association mapping of grain arsenic, copper, molybdenum and zinc in rice (*Oryza sativa* L.) grown at four international field sites. PloS ONE 9: e89685.

Palmgren MG, Clemens S, Williams LE, Krämer U, Borg S, Schjørring JK, Sanders D. 2008. Zinc biofortification of cereals: problems and solutions. Trends in Plant Science 13: 464–473.

Pan J, Plant JA, Voulvoulis N, Oates CJ, Ihlenfeld C. 2010. Cadmium levels in Europe: implications for human health. Environmental Geochemistry and Health 32: 1–12.

Peleg Z, Saranga Y, Yazici A, Fahima T, Ozturk L, Cakmak I. 2008. Grain zinc, iron and protein concentrations and zinc-efficiency in wild emmer wheat under contrasting irrigation regimes. Plant and Soil 306: 57–67.

Persson DP, Hansen TH, Laursen KH, Schjørring JK, Husted S. 2009. Simultaneous iron, zinc, sulfur and phosphorus speciation analysis of barley grain tissues using SEC-ICP-MS and IP-ICP-MS. Metallomics 1: 418-426.

Pfeiffer WH, McClafferty B. 2007. HarvestPlus: breeding crops for better nutrition. Crop Science 47: 88-105.

Pinson S, Tarpley L, Yan W, Yeater K, Lahner B, Yakubova E, Huang X, Zhang M, Guerinot ML, Salt DE. 2015. Worldwide genetic diversity for mineral element concentrations in rice grain. Crop Science 55: 294-311.

Pongrac P, Kreft I, Vogel-Mikuš K, Regvar M, Germ M, Vavpetič P, Grlj N, Jeromel L, Eichert D, Budic B et al. 2013. Relevance for food sciences of quantitative spatially resolved element profile investigations in wheat (*Triticum aestivum*) grain. Journal of The Royal Society Interface 10: 20130296.

R Core Team. R: A language and environment for statistical computing. R Foundation for Statistical Computing, Vienna, Austria. URL http://www.R-project.org/ [accessed October 10 2013].

Ryan CG. 2000. Quantitative trace element imaging using PIXE and the nuclear microprobe. International Journal of Imaging Systems and Technology 11: 219–230.

Saisho D, Takeda K. 2011. Barley: emergence as a new research material of crop science. Plant & Cell Physiology 52: 724–727.

Sandstead H. 1991. Zinc deficiency: a public health problem? American Journal of Diseases of Children: 853–859.

Second International Conference on Nutrition. 2014. Conference Outcome Document: Rome Declaration on Nutrition. Rome.

Shahzad Z, Rouached H, Rakha A. 2014. Combating mineral malnutrition through iron and zinc biofortification of cereals. Comprehensive Reviews in Food Science and Food Safety 13: 329–346.

Shi J, Li L, Pan G. 2009. Variation of grain Cd and Zn concentrations of 110 hybrid rice cultivars grown in a low-Cd paddy soil. Journal of Environmental Sciences 21: 168–172.

Singh SP, Vogel-Mikuš K, Vavpetič P, Jeromel L, Pelicon P, Kumar J, Tuli R. 2014. Spatial X-ray fluorescence micro-imaging of minerals in grain tissues of wheat and related genotypes. Planta 240: 277–289.

Slamet-Loedin IH, Johnson-Beebout SE, Impa S, Tsakirpaloglou N. 2015. Enriching rice with Zn and Fe while minimizing Cd risk. Frontiers in Plant Science 6: 121.

Solé VA, Papillon E, Cotte M, Walter P, Susini J. 2007. A multiplatform code for the analysis of energy-dispersive X-ray fluorescence spectra. Spectrochimica Acta. Part B: Atomic Spectroscopy 62: 63–68.

Sreenivasulu N, Graner A, Wobus U. 2008. Barley genomics: an overview. International Journal of Plant Genomics 2008: 486258.

Stoltzfus RJ, Dreyfuss ML. 1999. Guidelines for the use of iron supplements to prevent and treat iron deficiency anemia. Washington, DC: ILSI Pr.

Stomph TJ, Choi EY, Stangoulis JC. 2011. Temporal dynamics in wheat grain zinc distribution: is sink limitation the key? Annals of Botany 107: 927–937.

Tauris B, Borg S, Gregersen PL, Holm PB. 2009. A roadmap for zinc trafficking in the developing barley grain based on laser capture microdissection and gene expression profiling. Journal of Experimental Botany 60: 1333–1347.

Uraguchi S, Fujiwara T. 2012. Cadmium transport and tolerance in rice: perspectives for reducing grain cadmium accumulation. Rice (New York, N.Y.) 5: 5.

Vogel-Mikuš K, Simcic J, Pelicon P, Budnar M, Kump P, Necemer M, Mesjasz-Przybyłowicz J, Przybyłowicz WJ, Regvar M. 2008. Comparison of essential and non-essential element distribution in leaves of the Cd/Zn hyperaccumulator Thlaspi praecox as revealed by micro-PIXE. Plant, Cell & Environment 31: 1484–1496.

Waters BM, Sankaran RP. 2011. Moving micronutrients from the soil to the seeds: genes and physiological processes from a biofortification perspective. Plant Science 180: 562–574.

Wessells KR, Brown KH. 2012. Estimating the global prevalence of zinc deficiency: results based on zinc availability in national food supplies and the prevalence of stunting. PloS ONE 7: e50568.

White PJ, Broadley MR. 2005. Biofortifying crops with essential mineral elements. Trends in Plant Science 10: 586–593.

White PJ, Broadley MR. 2009. Biofortification of crops with seven mineral elements often lacking in human diets - iron, zinc, copper, calcium, magnesium, selenium and iodine. New Phytologist 182: 49–84.

WHO. 2009. Global health risks. Mortality and burden of disease attributable to selected major risks. Geneva, Switzerland: World Health Organization.

Wu D, Sato K, Ma JF. 2015. Genome-wide association mapping of cadmium accumulation in different organs of barley. New Phytologist 208: 817-829.

Xu Y, An D, Li H, Xu H. 2011. Review: breeding wheat for enhanced micronutrients. Canadian Journal of Plant Science 91: 231–237.

Zhao F, McGrath SP. 2009. Biofortification and phytoremediation. Current Opinion in Plant Biology 12: 373–380.

Zhao F, Moore KL, Lombi E, Zhu Y. 2014. Imaging element distribution and speciation in plant cells. Trends in Plant Science 19: 183–192.

Zhao F, Su YH, Dunham SJ, Rakszegi M, Bedo Z, McGrath SP, Shewry PR. 2009. Variation in mineral micronutrient concentrations in grain of wheat lines of diverse origin. Journal of Cereal Science 49: 290–295.

2.2 Temporal and spatial pattern of zinc and iron accumulation during barley (*Hordeum vulgare*) grain development

Detterbeck, A., Pongrac, P., Persson. D. P., Vogel-Mikuš, K., Mitja, K., Vavpetič, P., Pelicon, P., Arčon, I., Husted, S., Schjoerring, J. K., Clemens, S. (Status: Manuskript)

Die Konzeption der Forschungsidee und des Versuchsdesigns entstanden durch A. Detterbeck, P. Pongrac, D. Persson, S. Husted, J.K. Schjoerring und S. Clemens. Hierbei lag ein Hauptaugenmerk auf der Analyse der Zink- und Eisen-Gehalte während der Kornentwicklung in zwei kontrastierenden Gerstelinien. Die Pflanzenanzucht zur Analyse der Mikronährstoff-Gehalte wurde von A. Detterbeck in Bayreuth und in Kopenhagen durchgeführt. Die Probenaufbereitung und Analyse der Metallgehalte via ICP-OES erfolgte durch A. Detterbeck. Die Ernte von Proben 7, 15, 27 Tage nach Befruchtung und bei Reife erfolgte durch A. Detterbeck. Für die µ-PIXE Analyse wurden die Proben zudem vollständig von A. Detterbeck vorbereitet. Hierfür erfolgte ein Erfahrungsaustausch mit P. Pongrac. Zusätzlich wurden Proben, die 7 Tage nach Befruchtung von A. Detterbeck geerntet wurden, von K. Vogel-Mikuš durch Mikrodissektion vorbereitet. Die Vermessung der vorbereiteten Schnitte erfolgte im Jožef Stefan Institute in Ljubljana von K. Mitja, P. Vavpetič, P. und P. Pelicon. Die Analyse der Verteilungskarten über PyMca, die Kalkulation der einzelnen gewebespezifischen Konzentrationen und die Co-Lokalisationsanalyse erfolgte ausschließlich durch A. Detterbeck. Zeilen-Scans wurden von P. Pongrac durchgeführt. Die Probenanzucht und Proben-vorbereitung für LA-ICP-MS Analysen wurde von A. Detterbeck ausgeführt. Die Vermessung erfolgte durch D. Persson. Die Datenauswertung erfolgte vollständig durch A. Detterbeck und für die LA-ICP-MS Messung durch D. Persson. A. Detterbeck stellte das Probenmaterial für die XANES-Analyse zur Verfügung, die von K. Vogel-Mikuš am Elettra-Synchrotron (Triest, Italien) durchgeführt und von I. Arčon ausgewertet wurde. Die statistischen Analysen wurden von A. Detterbeck ausgeführt. A. Detterbeck erstellte die Abbildungen und Tabellen des Manuskriptes, recherchierte Literatur und verfasste das Manuskript, das nach konstruktiver Diskussion von D. P. Persson, P. Pongrac und S. Clemens überarbeitet wurde.

Temporal and spatial pattern of zinc and iron accumulation during barley (*Hordeum vulgare*) grain development

Amelie Detterbeck[1], Paula Pongrac[1,2], Daniel P. Persson[3], Katarina Vogel-Mikuš[2,4], Mitja Kelemen[2], Primož Vavpetič[2], Primož Pelicon[2], Iztok Arčon[2,4], Søren Husted[3], Jan Kofod Schjørring[3], Stephan Clemens[1]

[1]Department of Plant Physiology, Bayreuth Center of Ecology and Environmental Research, University of Bayreuth, Universitätsstr. 30, 95447 Bayreuth, Germany; [2]Jožef Stefan Institute, Jamova 39, SI-1000 Ljubljana, Slovenia, [3]Department of Plant and Environmental Sciences, University of Copenhagen, Thorvaldsensvej 40, 1871 Frederiksberg C, Denmark; [4]University of Nova Gorica, Nova Gorica, Slovenia

Author for correspondence:

Stephan Clemens

Tel: +49 921 552630

Email: stephan.clemens@uni-bayreuth.de

ABSTRACT

Low concentrations of micronutrients in the diet cause mineral malnutrition, also known as hidden hunger. To breed nutritionally enriched crops, a better understanding of micronutrient accumulation during grain development and micronutrient localization in the grain is needed. We studied temporal and spatial patterns of micronutrient accumulation in barley (*Hordeum vulgare* L.). Grains of a low and a high zinc (Zn) accumulating barley line were analyzed 7, 15, 27 days after pollination (dap) and at maturity with micro-Proton-Induced X-Ray Emission (μ-PIXE) and Laser-Ablation-Inductively Coupled Plasma–Mass Spectroscopy (LA-ICP-MS). Differences in Zn accumulation between the two lines mainly appeared at maturity, and at this stage the high Zn accumulating line had higher Zn concentration in the endosperm. By contrast, iron (Fe) concentration in endosperm did not differ between the two barley lines studied. In the high Zn accumulating line, Zn was gradually decreasing from the aleurone to the inner endosperm, whereas Fe concentrations sharply decreased from aleurone to the outer endosperm. At different positions of the grain, the low and high Zn line showed contrasting Zn and Fe concentrations in the aleurone and crease tissue. In these tissues, the high Zn line had higher Zn and Fe concentrations at the position of the embryo, whereas at the middle of the grain the low Zn line had higher concentrations. X-ray Absorption Near Edge Structure (XANES) analysis on the embryo revealed more Zn bound to phosphorus (P) in the high Zn accumulating line than in the low Zn accumulating line. Proportions of Zn and Fe were co-localized with sulphur, especially in the sub-aleurone layer in mature sections of the high Zn accumulating line.

Key words: *barley (Hordeum vulgare L.), grain, development, zinc, iron; biofortification, μ-PIXE, LA-ICP-MS, XANES*

INTRODUCTION

Worldwide over two billion people are estimated to suffer from micronutrient deficiencies (WHO, 2002; Tulchinsky, 2010). Herein, iron (Fe) and zinc (Zn) deficiency cause 1.4 and 1.5 % of deaths, meaning almost 1 million deaths per year (WHO, 2002, 2009). Highly prevalent in low- and middle-income countries, mineral malnutrition can be caused by monotonous diets mainly based on staple crops such as cereals and legumes, which often lack sufficient amounts of micronutrients (WHO, 2009; Bewley & Black, 2013). In addition, rising CO_2 levels could lead to reduced micronutrient concentrations in staple foods, putting an additional 175 million people at risk of Zn deficiency (Myers *et al.*, 2014; Dietterich *et al.*, 2015; Smith & Myers, 2018). Lack of sufficient amounts of Zn and Fe in the diet, lead to stunting, increased risk of infectious diseases and anemia, which especially affect children and women (Singh, 2004; Black *et al.*, 2008; WHO, 2009; Wessells & Brown, 2012). In order to improve the nutritional value of staple crops, two basic requirements have to be met: First, staple crops need to contain sufficiently high micronutrient concentrations in edible parts and second, the micronutrients need to be bioavailable for human digestion. Hence, a detailed understanding of micronutrient loading, localization and speciation in the edible parts of the crop, most often grain and seeds, is needed. Barley (*Hordeum vulgare* L.) is a model organism for investigating these aspects in cereals, since diverse barley germplasm collections with extensive genetic variation and a reference genome assembly are available (Bothmer 2003; Sreenivasulu et al. 2008; International Barley Genome Sequencing et al. 2012; Ullrich 2011; Mascher et al. 2017).

Zinc and Fe are heterogeneously distributed throughout the cereal grain, with the highest concentrations in the aleurone and embryo tissues in wheat (Cakmak *et al.*, 2010; Pongrac *et al.*, 2013; Eagling *et al.*, 2014; Singh *et al.*, 2014b; Brier *et al.*, 2016; van Malderen *et al.*, 2017; Singh *et al.*, 2018), maize (Cheah *et al.*, 2019), rice (Lu *et al.*, 2013) and barley (Lombi *et al.*, 2011; Detterbeck *et al.*, 2016). Comparably, micronutrient concentrations in the endosperm are much lower than e.g. the embryo, which has about 8-fold higher Zn concentrations (Stomph *et al.*, 2011; Detterbeck *et al.*, 2016). For human consumption, cereal grains are processed to sequentially remove outer parts of the grain by different milling steps to obtain pure endosperm, i.e. white flour (Slavin *et al.*, 2001; Atungulu & Pan, 2014). As a result of these procedures, white flour from cereals contains substantially less Zn and Fe compared to whole grain flour especially in wheat and rice (Liu *et al.*, 2008; Tang *et al.*, 2008; Hansen *et al.*, 2012). However,

the patterns of Zn or Fe loading and distribution leading to natural variation in Zn or Fe concentrations in the grain remain elusive. Especially, knowledge on Zn and Fe distribution in the grain during development and its impact on their resulting concentrations in mature grain is scarce. Grain development includes different stages, including cell division, extension and morphogenesis, storage and desiccation (Sreenivasulu *et al.*, 2010; Bewley & Black, 2013). In barley, the transition from the cell division to storage phase takes place at 7 to 10 days after flowering (Sreenivasulu *et al.*, 2006), while maturation takes place 21 to 40 days after pollination (Evers & Millar, 2002). During wheat grain development, Zn concentration was shown to remain stable from about 20 days after anthesis until maturity (Ozturk *et al.*, 2006; Stomph *et al.*, 2011). Zinc localization analysis using micro X-ray fluorescence (μ-XRF) in rice revealed a highly dynamic pattern of Zn distribution during grain development, with Zn spreading from the aleurone layer into the endosperm after 10 days after flowering (Iwai *et al.*, 2012).

In addition to the concentration and localization of Zn or Fe in the grain, the binding environment is equally important, since the bioavailability of micronutrients is affected by their interactions with binding ligands. In this context, sulphur (S)-containing proteins or phosphorus (P) in form of phytic acid (myo-inositol phosphate; IP_6) are major players (Clemens, 2014). A range of essential minerals, including Fe and Zn, were long believed to be mainly bound to IP_6, which cannot be digested in humans and non-ruminant animals due to the absence of degrading enzymes such as phytases (Oatway *et al.*, 2007; Gupta *et al.*, 2015). However, speciation analyses by inductively coupled plasma-mass spectrometry (ICP-MS) techniques on pea seeds, barley and wheat grains revealed a more complex chemical environment of different ligands (Clemens, 2014). In extracts of barley embryo, Fe co-eluted mainly with P, whereas Zn co-eluted mainly with S (Persson *et al.*, 2009), suggesting that Zn was primarily bound to peptides, and not to IP_6, which would possibly indicate a higher bioavailability for humans. Investigations in wheat also revealed different binding environments for Fe and Zn in different milling fractions (Eagling *et al.*, 2014; Xue *et al.*, 2016). Here, the metal chelators nicotianamine (NA) and deoxymugenic acid (DMA) were the potential Zn-binding partners identified. By X-ray absorption near-edge spectroscopy (XANES) analyses, Fe was found to be bound in a chemical environment of oxygen, P and S in intact wheat grains (Singh *et al.*, 2013). More detailed analyses on Zn and Fe speciation were performed on tissue level, where these micronutrients were differentially bound to P, NA and S in the aleurone, embryo and nucellar projection (Brier *et al.*, 2016). The authors showed that Fe was bound to phytate in aleurone

tissue and was rather associated with NA than phytate in the nucellar projection. In the embryo, Zn was concentrated in the shoot and root primordia and associated with S, showing overall different binding environments of one micronutrient in single grain tissues.

In this study, we aimed to elucidate the differences leading to natural variation in Zn and Fe concentrations in barley grain by analyzing their concentrations during grain development. First, we analyzed Zn and Fe concentrations at four different developmental stages in whole ears in a low and a high Zn accumulating barley line, previously identified (Detterbeck *et al.*, 2019). To determine how the observed differences in bulk Zn or Fe concentrations are reflected in their spatial distribution, we analyzed grain sections of the two barley lines at different developmental stages using micro-particle-induced X-ray emission (μ-PIXE). Based on the μ-PIXE maps, nutrient concentrations of different grain tissues were established and compared in order to assess differences between the two lines during grain development. In addition to the μ-PIXE analyses, we performed Laser Ablation Inductively Coupled Plasma Mass Spectrometry (LA-ICP-MS) analysis at different positions in the grain for further in-depth analysis. In addition, XANES analyses on the embryo were performed to obtain insights in the Zn binding environments in the two contrasting barley lines.

MATERIAL AND METHODS

Plant material and growth conditions

Two barley (*Hordeum vulgare subsp. vulgare convar. vulgare*) landraces, previously identified to differ in Zn accumulation ability (Detterbeck *et al.*, 2019) were used for all the experiments. The two barley lines were ICARDA_IG #128160 from Pakistan, the low Zn accumulating line (henceforth referred to as LAL) and #37726 from Tunisia, the high Zn accumulating line (henceforth referred to as HAL). Plants were grown in pots under controlled conditions as described in detail by (Detterbeck *et al.*, 2019). The plants were not sprayed with pesticides or fungicides and only healthy plants were included in sampling.

Sample preparation for bulk element analysis

Whole ears and flag leaves were harvested at three different developmental stages (7, 15, 27 days after pollination [dap], for exemplar pictures see Suppl. Fig. S1) always at the same time of the day. These time-points covered the end of cell division and elongation phase (7 dap) followed by early and late stages of grain filling (15 and 27 dap). Developmental stages were determined by examining the developmental status of one grain positioned at the bottom of the ear. Especially from three to 10 dap the development time of the grains can more easily be determined and ears were therefore marked at those time points for future harvesting on 7, 15 and 27 dap. At harvest, awns and undeveloped grains were removed from whole ears and all the material was immediately frozen in liquid nitrogen. Whole ears and flag leaves were ground separately in liquid nitrogen using porcelain pestles and mortars and stored at -80 °C.

Inductively Coupled Plasma–Optical Emission Spectroscopy (ICP-OES)

Prior to ICP-OES analysis, mature grains were dried at 60 °C for 3 days. Ground material of whole ears and flag leaves of three to five plants was pooled and freeze- dried for three days in a temperature gradient, which increased from -180 °C to - 25 °C, at a constant pressure of 0.08 mbar (Alpha 2-4, Christ, Osterode am Harz, Germany). Dried plant material was wet digested in a microwave (START 1500; MLS GmbH) with 2 ml bidistilled water, 2 ml 30 % H_2O_2 and 4 ml 65 % HNO_3 for 12 min at 180 °C. Element concentrations were measured with an iCAP 6500 (Thermo Scientific, Waltham, MA, USA) at wavelengths of 213.8 nm (Zn) and 238.2 nm (Fe).

Micro-Proton-Induced X-Ray Emission (µ-PIXE) analysis

For µ-PIXE analysis, mature grains and grains harvested 7, 15 and 27 dap of the two lines with contrasting Zn accumulation were sectioned. Grains of 7, 15, and 27 dap were harvested and kept on ice during harvesting. After harvesting, grains were frozen in isopentane cooled with liquid-nitrogen and freeze-dried, as described above. Before cutting, grains were soaked in distilled water for one, two, three and four hours at 4 °C (7, 15, 27 dap and mature, respectively). Grains (n=3 for 15, 27 dap and mature grains and n=4 for 7 dap grains) were hand-cut transversely at the embryo location indicated in Fig. S1c, always using new stainless

steel platinum-coated razor blades (Science Services GmbH, München, Germany) and immediately frozen in liquid nitrogen. In all the cross-sections of grains 15, 27 dap and mature grains, the embryo, scutellum, endosperm and the husk were visible. Because of the softness of the 7 dap grains, which contained large amounts of water, these grains could not be prepared by hand-sectioning. Therefore, these grains were prepared in a way typical for leaf sectioning as described previously (Vogel-Mikuš *et al.*, 2014). In short, grains were placed into stainless-steel needles, cryo-fixed in liquid propane, cryo-sectioned to 50 µm, freeze-dried, sandwiched between two Pioloform (SPI supplies, West Chester, PA, USA) foils and checked for their integrity. Dried grain cross-sections were analyzed as described previously (Klančnik *et al.*, 2014; Vogel-Mikuš *et al.*, 2014). µ-PIXE spectra were processed using GEOPIXEII software (Ryan, 2000) and quantitative spatial distribution maps of P, S, Fe and Zn and element co-localization maps were generated using PyMca version 5.0 (Solé *et al.*, 2007). Mean concentrations in particular grain tissues were calculated by selecting specific areas in the quantitative spatial distribution maps using the Region of Interest (ROI) manager tool in ImageJ (Abràmoff MD, Magalhães PJ, Sunanda RJ, 2004). For each cross-section the following tissues were distinguished: aleurone, crease, endosperm, husk and embryo tissues (including the scutellum), except for the 7 dap grain, where crease and aleurone could not be discerned.

Microscope photographing

All sections for µ-PIXE analysis were photographed, to assist in defining the different tissues. Hand-cut sections of 15, 27 dap and mature grains were photographed with a stereomicroscope M50 (Leica microsystems, Wetzlar, Germany), camera DP26 and software cellSens Dimension 1.11 (Olympus, Shinjuku, Japan) and the cryo-sectioned samples were photographed with a stereomicroscope MZFLII, camera DFC450c and software Application Suite V4.0 (Leica microsystems, Wetzlar, Germany). The settings were: brightness 55 %, gain 5.3 %, saturation 0.9, gamma 1.06.

Laser-ablation-Inductively Coupled Plasma–Mass Spectroscopy (LA-ICP-MS)

Mature grains were transversely sliced with a cryotome to achieve an even surface at the middle of the grain as indicated in Suppl. Fig. S1. From here, cross sections were prepared from 3 different grains, using the Kawamoto cryo-tape method (Kawamoto & Kawamoto,

2014). The LA-ICP-MS analyses were carried out with a nanosecond LA unit (NWR 193; New Wave Research, Fremont, CA, USA) which has an ArF excimer laser source operating at 193 nm. The following settings were used: energy: 1.4 J cm^{-2}, scan speed: 400 µm s^{-1}, repetition rate: 40 Hz and spot size 20 µm. The elements were detected with an Agilent 7900 ICP-MS, operated in H_2 mode (1.5 mL min^{-1}), where the key parameters were: RF power: 1500 V, sample depth: 3.5 mm and carrier gas flow: 0.89 L min^{-1}. The isotopes analyzed were ^{13}C, ^{31}P, ^{34}S, ^{56}Fe, ^{66}Zn, ^{55}Mn and ^{44}Ca. The integration times were 0.1 s for ^{13}C and 0.04 s for all of the other elements.

Line profiles across grain sections

Line scans with LA-ICP-MS were taken as indicated in Suppl. Fig. S1, scanning the side of the cross-section from the crease side to the opposite side. The lines were between 800-1200 µm long. Three lines immediately next to each other were analyzed per grain. Data was processed and presented using SigmaPlot 13.

Line profiles with µ-PIXE, across aleurone and endosperm, were extracted from each analyzed mature grain using PyMca version 5.0.0 (Solé *et al.*, 2007). The transects were ten pixels wide and 60 pixels long. Data were smoothed using the smoothing function in the Scan window five times. Because the source data of the distribution maps is a matrix, the angle at which the transect is taken will affect the absolute transect length, the relative distances were calculated. At each pixel the average concentration (n=3) and standard error were calculated and plotted on a relative scale to depict the concentration gradient across the tissues of interest.

Zinc ligand environment in the grain embryo

Zinc and potassium (K) distribution maps and the Zn K-edge X-ray Absorption Near Edge Structure (XANES) spectra of the reference Zn complexes and of the grain tissues were recorded at the XRF beamline of Elettra-Synchrotron (Trieste, Italy). Reference Zn complexes were prepared as described previously (Terzano *et al.*, 2008) by mixing $ZnCl_2$ with relevant ligand at room temperature at selected pH, freezing the solution in liquid nitrogen and freeze-drying from −20 °C to the room temperature (Alpha 2–4 LSC, Christ, Osterode am Harz, Germany) for three days. The following complexes were prepared: Zn citrate (6.7 mM $ZnCl_2$

was mixed with 27 mM citric acid at pH 6.5), Zn histidine (6.7 mM $ZnCl_2$ was mixed with 80 mM histidine at pH 7.0), Zn cysteine (7.0 mM $ZnCl_2$ was mixed with 70 mM cysteine at pH 7.0), Zn proline (7.0 mM $ZnCl_2$ was mixed with 70 mM cysteine at pH 7.0), Zn acetate (7.0 mM $ZnCl_2$ was mixed with 70 mM acetic acid at pH 6.5), Zn phytate (7.0 mM $ZnCl_2$ was mixed with 70 mM phytic acid at pH 7) and Zn malate (7.0 mM $ZnCl_2$ was mixed with 70 mM malic acid at pH 6.5). The freeze-dried complexes were pressed into homogeneous pellets. Grain tissues were exposed by longitudinally cutting the mature grain using a stainless-steel scalpel and Zn distribution was mapped with the beam size of 0.05 x 0.125 mm and dwell time of 2s per pixel at excitation energy of 10.5 keV. The Zn K-edge XANES spectra were recorded in fluorescence detection mode at room temperature. The optimal total absorption thickness of about 2 above the investigated absorption edge was obtained. The details of the beamline have been described previously (Karydas *et al.*, 2018). About 1 eV energy resolution at Zn K-edge was used. Exact energy calibration was obtained with measurement of Zn K-edge on Zn reference metal foils. The absorption spectra were measured within the interval [−250 eV to 150 eV] relative to the Zn absorption edge and equidistant energy steps of 0.25 eV were used. In cases of low Zn concentration, the absorption spectra of two or three identical runs for each sample were superimposed to improve the signal-to-noise ratio and to check the stability and reproducibility of the detection system. The Zn K-edge XANES spectra were analysed using the IFEFFIT package (Ravel & Newville, 2005). Co-localization maps were generated using PyMca version 5.0.0 (Solé *et al.*, 2007).

Statistical analysis

Testing for significant differences was done based on 95 % confidence interval with ANOVA/Tukey's HSD in whole ears comparing developmental stages, lines and their interactions with with R vers. 3.0.1 (R Core Team) using packages 'multcomp' (Hothorn *et al.*, 2008) and 'agricolae' (Mendiburu, 2013). Testing for significant differences on data extracted from µ-PIXE maps was done based on 95 % confidence interval with ANOVA/Holm Sidak comparing differences within each line at different developmental stages and between lines at every single developmental stage with SigmaPlot (vers. 14.0).

RESULTS

Zn and Fe concentrations in whole ears during grain development

The contrasting barley lines differed in whole-grain Zn concentration at maturity, where the HAL had Zn concentrations of 78.5 ± 11.7 mg kg^{-1} dry weight (DW) compared to the LAL with 57.1 ± 14.1 mg kg^{-1} DW (Fig. 1). During development, the Zn concentrations of the high Zn accumulating line were slightly higher for all analyzed time points (7, 15 and 27 dap) compared to those of the LAL, but this difference was not significant. When considering the Zn concentrations within each barley line only, the concentration remained stable from 7 dap to maturity, although there was a slight tendency for higher Zn concentrations in the HAL at maturity. The concentrations during development ranged from 37.5 ± 12.1 mg kg^{-1} DW (15 dap) to 57.1 ± 14.1 mg kg^{-1} DW (maturity) in the LAL and 57.1 ± 8.0 mg kg^{-1} DW (27 dap) to 78.5 ± 11.7 mg kg^{-1} DW (maturity) in the HAL.

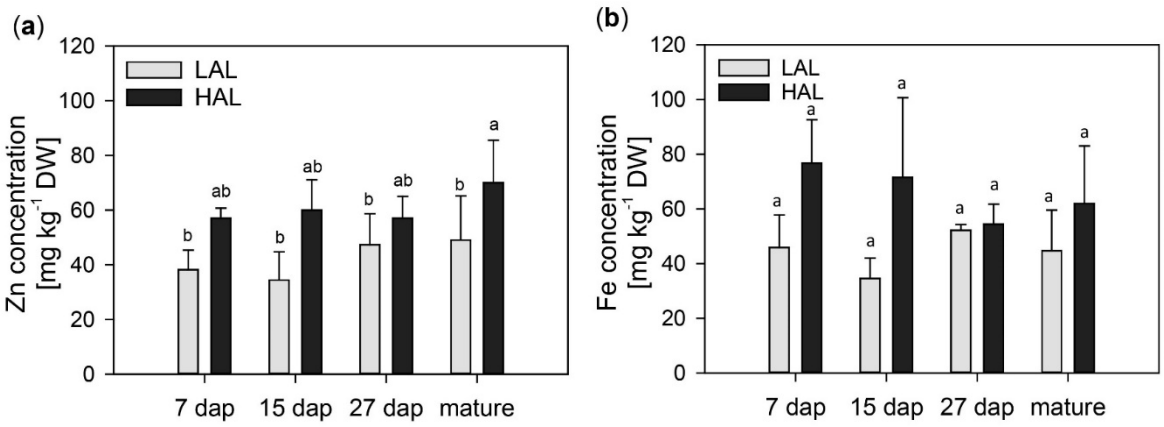

Fig. 1 Zinc (Zn) and iron (Fe) concentration at different developmental stages of two contrasting barley lines in whole ears and mature grains. Whole ear Zn **(a)** and Fe **(b)** concentrations at 7 days after pollination (dap), 15 dap, 27 dap and in mature grains in a low (LAL) and high (HAL) Zn accumulating barley line. 7 and 27 dap: n=3, 15 dap and mature grains: n=5 (7, 15 and 27 dap: 3-5 plants were pooled, mature grains: 5 grains per sample were pooled; 3-5 samples analyzed per cultivation round). Values are means + standard deviation. Statistical differences were calculated using ANOVA/Tukey's HSD post hoc test and are displayed as different letters ($P \leq 0.05$); DW, dry weight.

The HAL tended to have higher Fe concentrations than the LAL, but no statistical differences were apparent. At maturity, Fe concentrations ranged between 51.9 ± 9.4 mg kg^{-1} DW for the LAL and 72.9 ± 8.7 mg kg^{-1} DW for the HAL. During development, Fe concentrations were comparable within each barley line. During development Fe concentrations ranged from 38.8 ± 6.9 mg kg^{-1} DW (15 dap) to 52.2 ± 2.12 mg kg^{-1} DW (27 dap) in the LAL and 54.5 ± 7.3 mg kg^{-1} DW (27 dap) to 87.0 ± 28.0 mg kg^{-1} DW (15 dap) in the HAL.

µ-PIXE analysis – Zn concentrations during development

Four different developmental stages of two contrasting barley lines were analyzed by µ-PIXE. Representative quantitative distribution maps of Zn and microscopic pictures of the corresponding sections are shown in Figure 2. At 7 dap, the endosperm and husk tissues were visible and the embryo tissue was differentiating, while aleurone and crease could not yet be discerned. At this developmental stage, apart from some hotspots in the vascular tissue and within the developing embryo, Zn was evenly distributed.

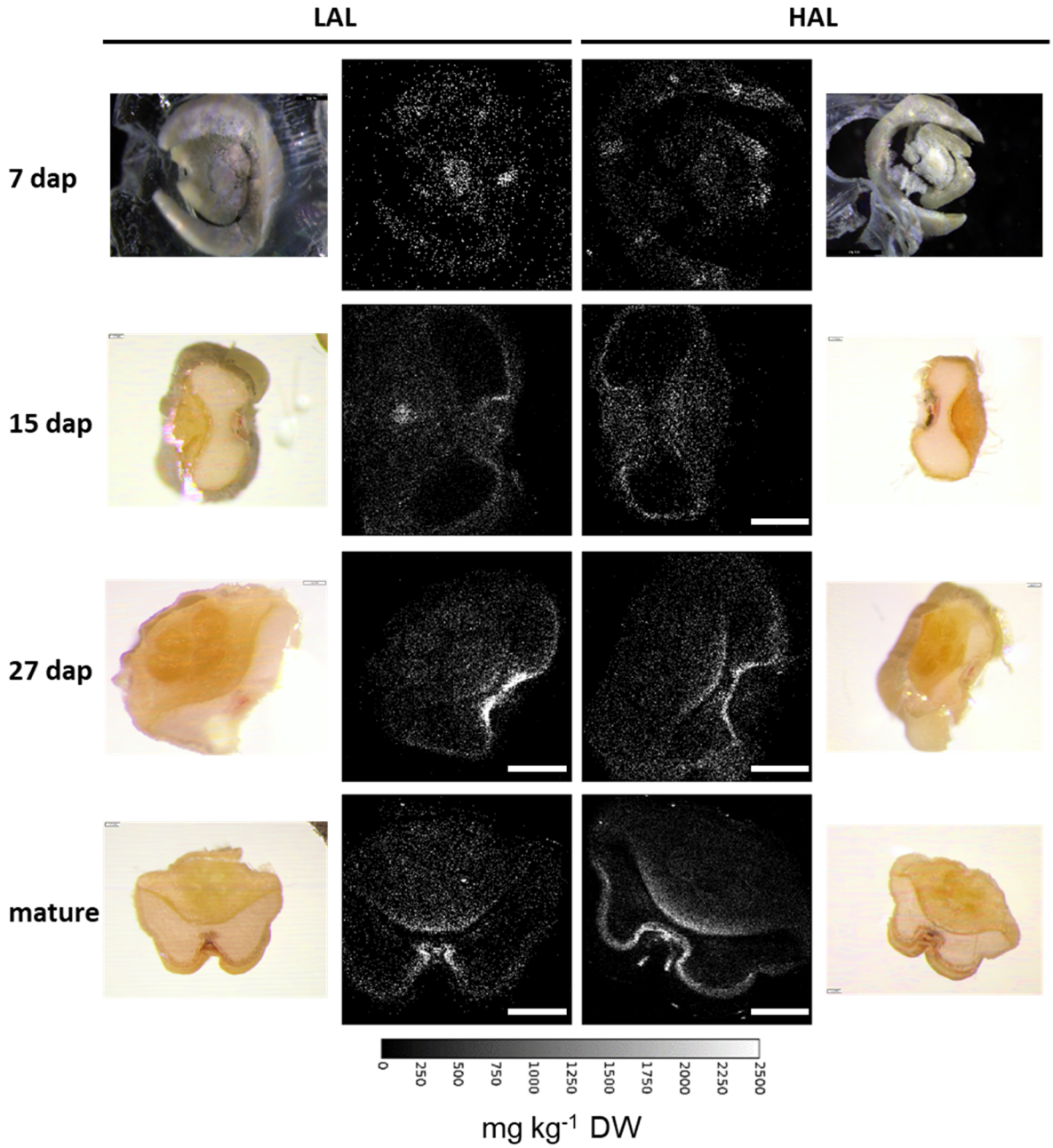

Fig. 2 Distribution maps of zinc (Zn) obtained by quantitative µ-PIXE for grains of two contrasting barley lines at different developmental stages. µ-PIXE maps for Zn of barley grain sections (shown on the left and the right hand side of the corresponding distribution maps) of the low (LAL) and high (HAL) Zn accumulating lines at different developmental stages (7 days after pollination (dap), 15 dap, 27 dap and mature). Grains were transversely sectioned at the position of the embryo as indicated in Fig. S1. Scale bars indicate 62.5 µm (7 dap) and 500 µm (15, 27 dap and mature). DW, dry weight.

At 15 dap, the embryo was distinguishable from the surrounding tissues and aleurone and crease were differentiated. At this stage, the endosperm had lower Zn concentrations

compared to all the other tissues in both barley lines. At 27 dap all tissues were fully differentiated and in the embryo, root primordia and scutellum were visible. Aleurone and crease had highest Zn concentrations, particularly in the crease region. This difference appeared to be higher in the LAL compared to the HAL. In both barley lines, the endosperm tissue contained more Zn at this developmental stage, compared to the 15 dap grains. At maturity, the Zn distribution was similar to the 27 dap grains, with higher Zn concentrations in the HAL than in the LAL across the whole section. Higher concentrations appeared especially in the transition zone from aleurone and crease in direction of the scutellum/embryo. Based on all analyzed maps, the Zn concentrations were quantified for the whole section, endosperm, embryo, aleurone, husk and crease (Fig. 3). Average Zn concentrations in the whole sections differed between the two barley lines at maturity with 297.42 ± 25.71 mg kg^{-1} DW (HAL) compared to 197.7 ± 8.72 mg kg^{-1} DW (LAL) in the whole sections (Fig. 3a). Differences could also be seen in the endosperm (HAL: 243.81 ± 62.36 mg kg^{-1} DW and LAL: 118.52 ± 17.76 mg kg^{-1} DW) and in the aleurone (HAL: 845.26 ± 81.5 mg kg^{-1} DW and LAL: 450.66 ± 33.81mg kg^{-1} DW) at maturity (Fig. 3b, d). At 27 dap, the HAL showed significantly lower Zn concentrations in the aleurone (HAL: 876.8 ± 109.62 mg kg^{-1} DW and LAL: 1132.65 ± 124.21 mg kg^{-1} DW) and crease (HAL: 219.21 ± 17.15 mg kg^{-1} DW and LAL: 500.27 ± 122.66 mg kg^{-1} DW) compared to the LAL (Fig. 3d, f). Within each line, similar Zn concentrations were apparent during development in the endosperm, the embryo and the husk (Fig. 3b, c, e). In contrast, the HAL showed higher Zn concentrations in the aleurone tissue at 27 dap and in the aleurone and crease tissue at maturity compared to the LAL. Zinc concentrations in the LAL differed in the aleurone tissue at 27 dap compared to 15 dap and maturity (1132.65 ± 124.21 mg kg^{-1} DW, 450.66 ± 33.81mg kg^{-1} DW and 465.73 ± 71.83 mg kg^{-1} DW, respectively). Overall, the highest Zn concentrations were found in aleurone, crease and embryo in both barley lines and at all developmental stages.

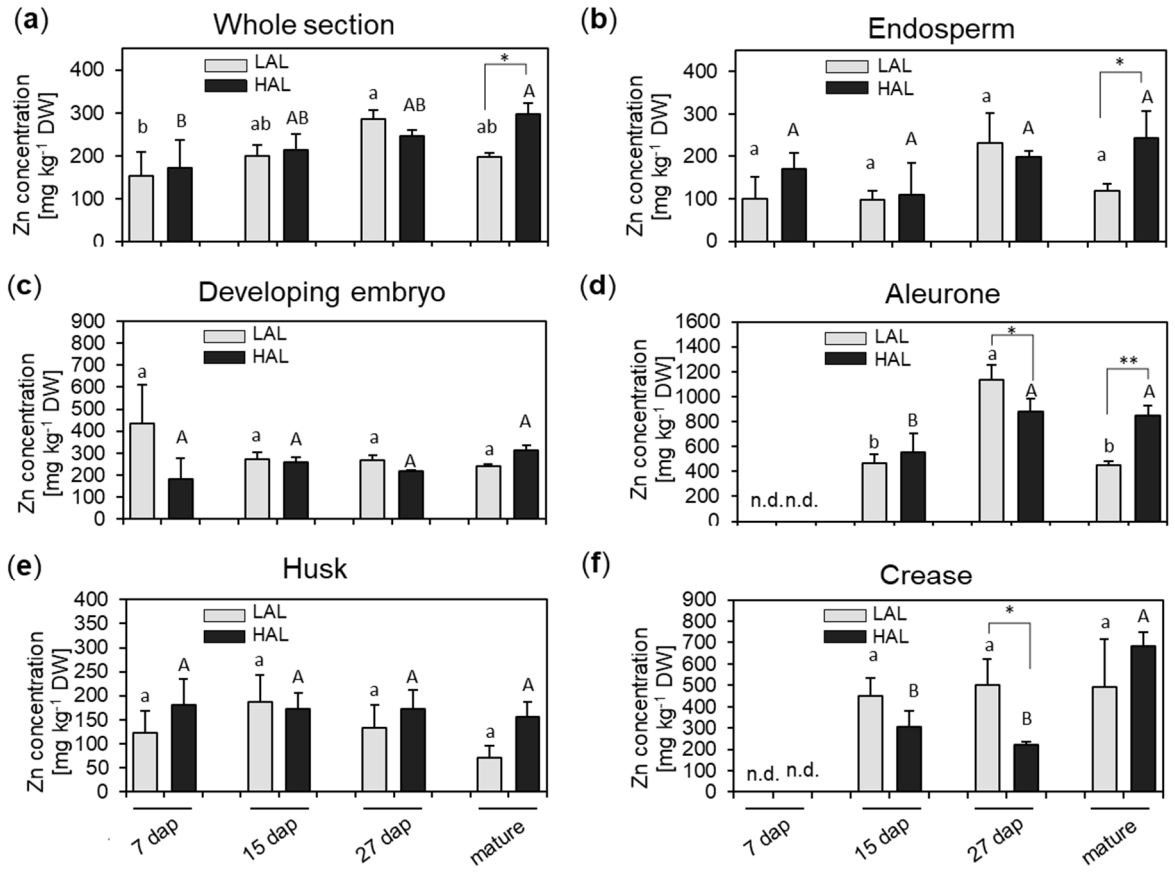

Fig. 3 Zinc (Zn) concentration in different parts of the grain of two contrasting barley lines at four developmental stages extracted from µ-PIXE maps. Zinc concentrations averaged over µ-PIXE maps of three sections per line in the whole section (**a**), endosperm (**b**), embryo (**c**), aleurone (**d**), husk (**e**) and crease (**f**) in a low (LAL) and high (HAL) Zn accumulating barley line. At 7 days after pollination (dap) aleurone and crease were not yet differentiated (indicated n.d.). Values are means + standard deviation (n=3). Statistical differences in Zn concentrations between the lines at different developmental stages were calculated using ANOVA/Sidak Holm post hoc test and are displayed as different letters ($P \leq 0.05$) for comparing developmental differences within each line (LAL: small letters, HAL: capital letters) and asterisks for comparison of the two different lines within one developmental stage (*: $P \leq 0.05$, **: $P \leq 0.01$, ***: $P \leq 0.001$). DW, dry weight.

µ-PIXE analysis – Fe concentrations during development

Distribution maps for Fe from the four different developmental stages are shown in Figure 4. At 7 dap, Fe was evenly distributed over the different tissues in both barley lines. At 15 dap, the aleurone contained higher concentrations of Fe than the other tissues, in both barley lines, whereas the Fe concentration was lower in the endosperm compared to all other tissues.

This pattern was also visible for sections at 27 dap and at maturity. In addition, there were higher Fe concentrations around the root primordia in both barley lines compared to the surrounding embryo.

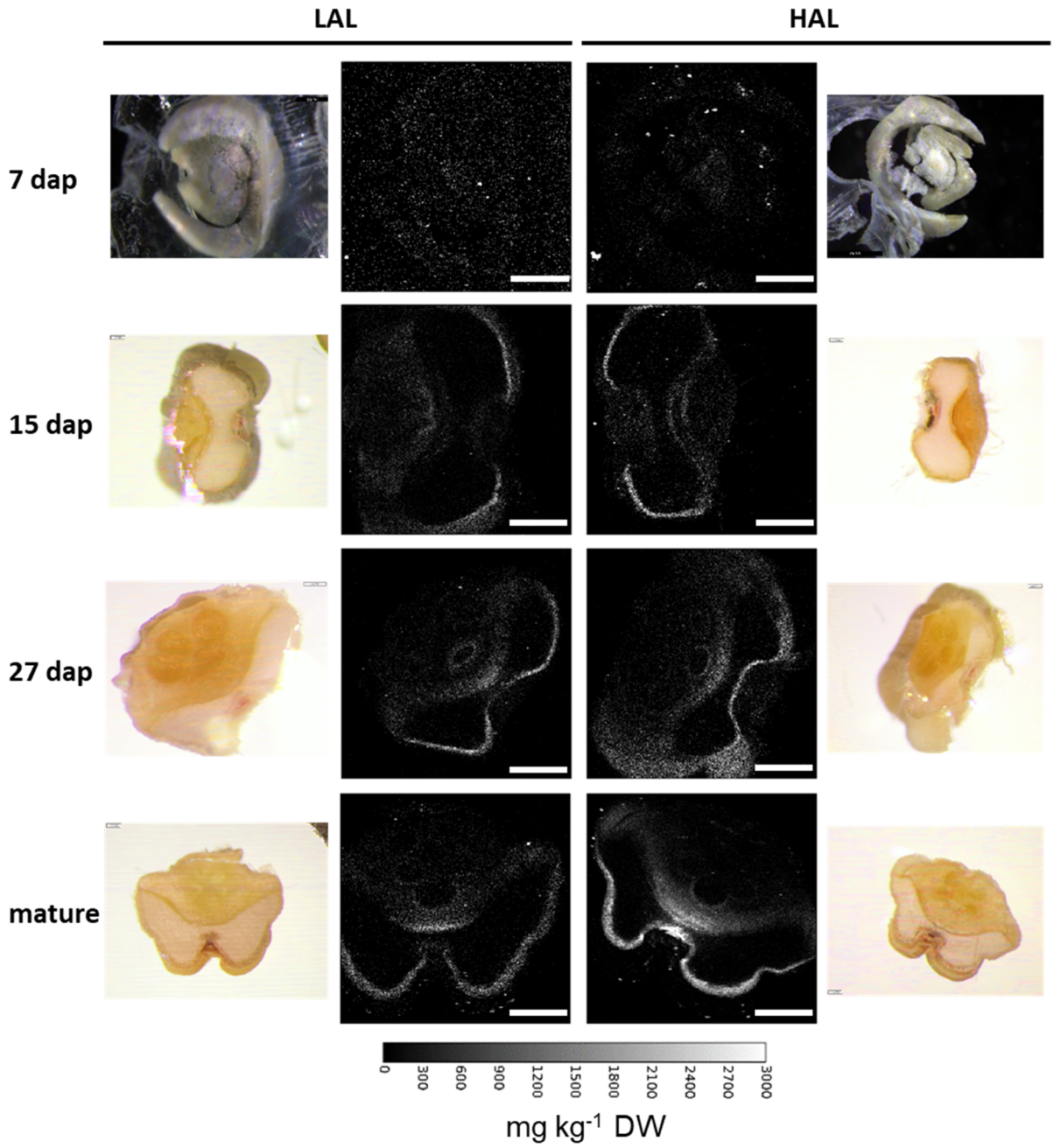

Fig. 4 Distribution maps of iron (Fe) obtained by quantitative µ-PIXE for grains of two contrasting barley lines at different developmental stages. µ-PIXE maps for Fe of barley grain sections of (shown on the left and the right hand side of the corresponding distribution maps) the low and high Zn accumulating lines at different developmental stages (7 days after pollination (dap), 15 dap, 27 dap and mature). Grains were transversely sectioned at the position of the embryo as indicated in Fig. S1. Scale bars indicate 62.5 µm (7 dap) and 500 µm (15, 27 dap and mature). DW, dry weight.

Especially at maturity, the HAL showed higher Fe concentrations in the aleurone and crease than LAL. Similar to the distribution of Zn, Fe was more concentrated in the transition zone between the crease and scutellum in the HAL compared to the LAL. In contrast to Zn, there were no differences in Fe concentration in the endosperm of the two barley lines at maturity. Average Fe concentrations differed in the whole sections between the two contrasting barley lines at maturity, with higher Fe concentrations of 336.72 ± 32.90 mg kg^{-1} DW in the HAL compared to 190.59 ± 19.55 mg kg^{-1} DW in the LAL (Fig. 5a).

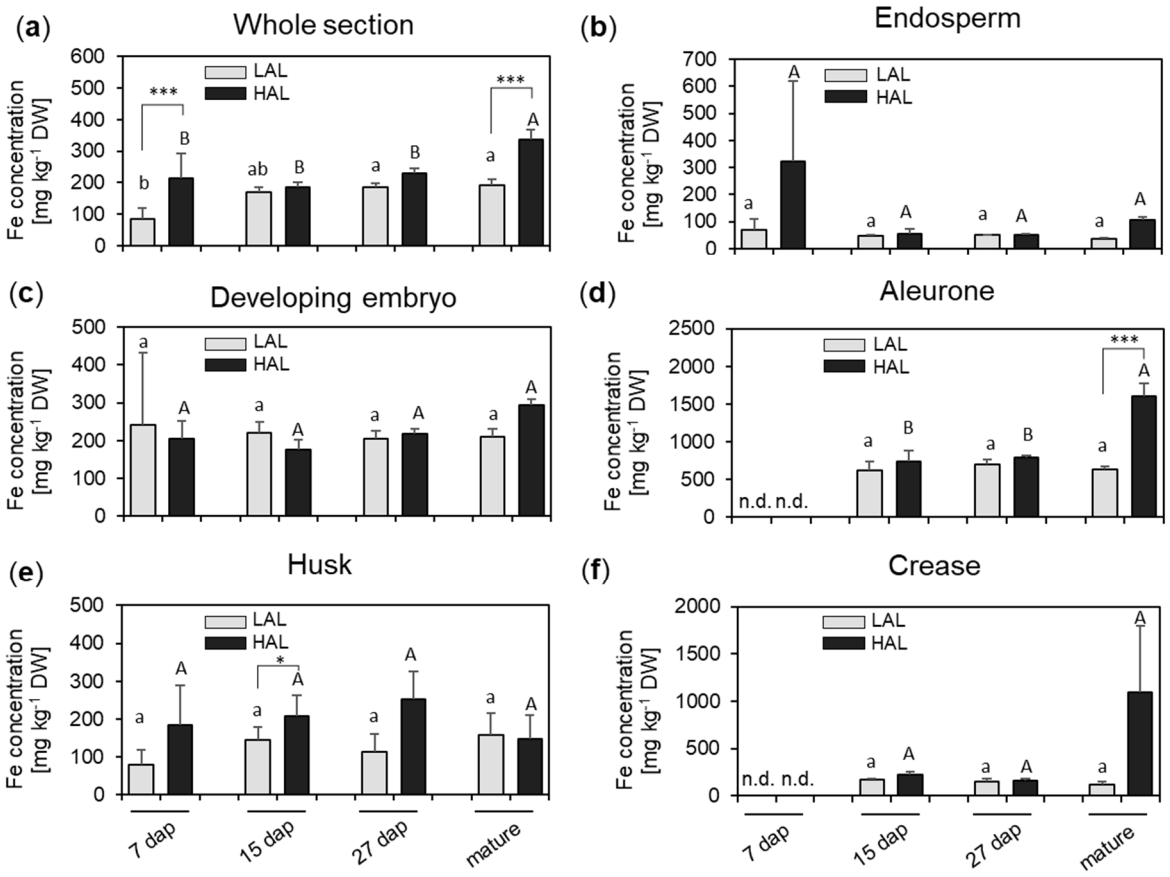

Fig. 5 Iron (Fe) concentration in different parts of the grain of two contrasting barley lines at four developmental stages extracted from µ-PIXE maps. Iron concentrations averaged over µ-PIXE maps of three sections per line in the whole section (**a**), endosperm (**b**), embryo (**c**), aleurone (**d**), husk (**e**) and crease (**f**). At 7 days after pollination (dap) aleurone and crease were not yet differentiated (indicated n.d.). Values are means + standard deviation (n=3). Statistical differences in grain tissue concentrations between the lines at different developmental stages were calculated using ANOVA/Sidak Holm post hoc test and are displayed as different letters ($P \leq 0.05$) for comparing developmental differences within each line (LAL: small letters, HAL: capital letters) and asterisks for comparison of the two different lines within one developmental stage (*: $P \leq 0.05$, **: $P \leq 0.01$, ***: $P \leq 0.001$). DW, dry weight.

This difference was also apparent in aleurone at maturity (HAL: 1605.17 ± 173.01 mg kg^{-1} DW and LAL: 630.36 ± 39.13 mg kg^{-1} DW) (Fig. 5d). In addition, Fe concentrations of the two barley lines differed significantly in whole sections at 7 dap (HAL: 214.18 ± 77.32 mg kg^{-1} DW and LAL: 85.39 ± 34.44 mg kg^{-1} DW) and in the husk at 15 dap (LAL: 207.32 ± 55.36 mg kg^{-1} DW and LAL: 145.05 ± 34.03 mg kg^{-1} DW) (Fig. 5a, e). Within each barley line, similar Fe concentrations were apparent during development in the endosperm, the embryo, the husk and crease (Fig. 5b, c, e, f). In aleurone, the HAL showed higher Fe concentrations at maturity compared to the other developmental stages (1605.17 ± 173.01 mg kg^{-1} DW compared to 795.09 ± 20.10 (27 dap) and 737.31 ± 141.46 mg kg^{-1} DW (15 dap)). The highest Fe concentrations were found in aleurone of both barley lines being on average 1605.17 ± 173.01 mg kg^{-1} DW (HAL at maturity) and 698.89 ± 71.51 mg kg^{-1} DW (LAL at 27 dap).

µ-PIXE analysis – S and P concentrations during development and co-localization analysis

In endosperm tissue, S concentrations were significantly higher in the HAL at maturity (3134.26 ± 420.06 mg kg^{-1} DW compared to 2236.38 ± 155.76 mg kg^{-1} DW in LAL (Suppl. Fig. S2 b)). Within each line, S concentrations increased in the endosperm during the development, reaching up to 2236.38 ± 155.76 mg kg^{-1} DW (LAL) and 3134.26 ± 420.06 mg kg^{-1} DW (HAL) at maturity. In contrast, S concentrations decreased in the aleurone during development to 1497.47 ± 125.76 mg kg^{-1} DW (LAL) and 1890.99 ± 303.47 mg kg^{-1} DW (Suppl. Fig. S2 d). The HAL had higher P concentrations in whole sections (HAL: 14126.7 ± 699.24 mg kg^{-1} DW and LAL: 12486.7 ± 541.35 mg kg^{-1} DW) and the embryo (HAL: 21709.6 ± 1716.7 mg kg^{-1} DW and LAL: 19307.2 ± 870.5 mg kg^{-1} DW) at maturity (Suppl. Fig S3 a, c). Differences were also apparent at 27 dap in the husk (HAL: 8787.9 ± 1178.9 mg kg^{-1} DW and LAL: 4336.1 ± 1413.7 mg kg^{-1} DW) (Suppl. Fig. S3 e). Phosphorus concentrations were comparable in endosperm, aleurone and crease, in both barley lines (Suppl. Fig S3 b, d, f). The lowest concentrations were found in the endosperm (from 2093.21 ± 675.26 mg kg^{-1} DW at 7 dap in the LAL to 4804.24 ± 856.51 mg kg^{-1} DW at 15 dap in HAL).

Co-localization maps of Zn or Fe with P and S are shown in Suppl. Fig. S4 and S5, respectively. At 7 dap, P and S were evenly distributed within the grain. At later developmental stages, the highest P concentrations were mainly found in aleurone and embryo tissue, whereas S was mainly found in the embryo (especially root primordia) and endosperm. In both barley

lines, S was distributed in a decreasing gradient from the sub-aleurone layer towards the inner endosperm. Zinc and Fe showed co-localization with S in the sub-aleurone in mature sections of the HAL. Zinc and Fe were not solely co-localized with S or P throughout the section, but Zn was co-localized partially with P in the scutellum, whereas Fe was co-localized with P in the scutellum and aleurone tissue.

µ-PIXE and LA-ICP-MS line scans

Line-scans from the outer part of the grain into the endosperm were extracted from µ-PIXE maps of mature grains (Fig. 6). The HAL had higher Zn concentrations throughout the whole transect, from the aleurone to the inner parts of the endosperm (Fig. 6a). Zinc concentrations were highest in the aleurone tissue for both barley lines and decreasing in direction of the endosperm. Endosperm Zn concentrations varied to some extent in direction of the inner part of the section, but were always higher in the HAL compared to LAL.

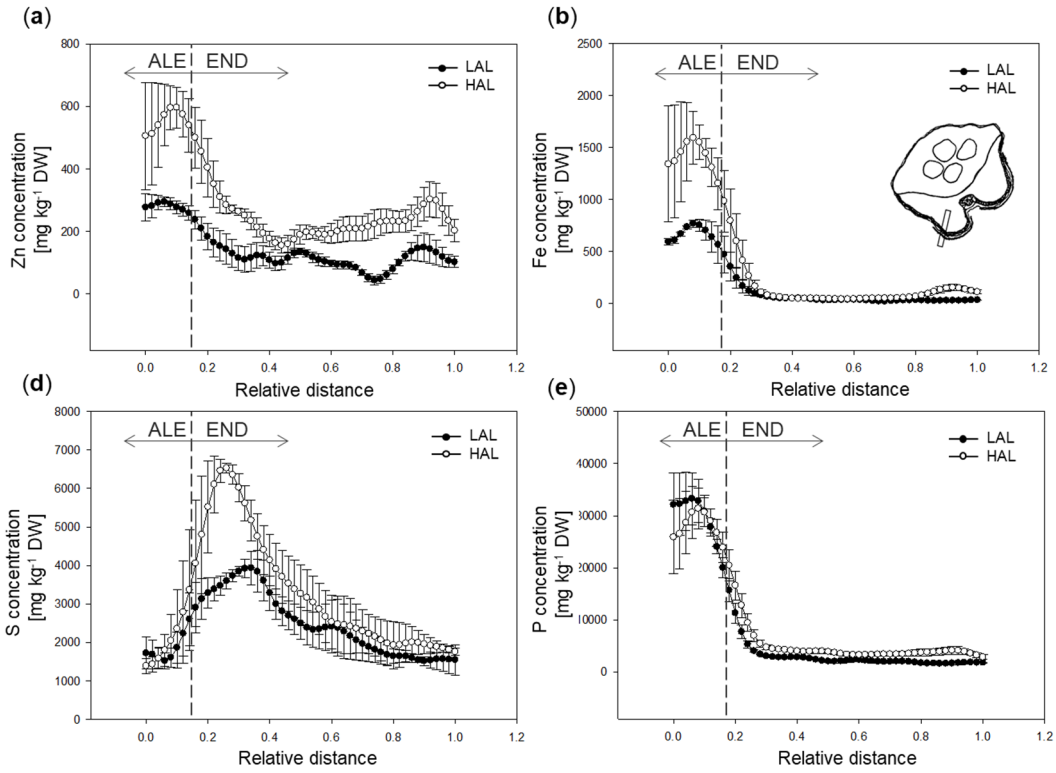

Fig. 6 Extracted line scans from µ-PIXE maps. Zinc (Zn, **a**), iron (Fe, **b**), sulphur (S, **c**) and phosphorus (P, **d**) concentrations extracted from three different grain sections of a low (LAL) and high (HAL) Zn accumulating barley line at maturity. Line scans transversed the aleurone (ALE) and the endosperm (END) tissue as indicated in (**b**). DW, dry weight. *n*=3.

For Fe, aleurone concentrations were higher in the HAL compared to LAL (Fig. 6b). The Fe concentrations of the barley lines were not different in the endosperm tissue. In both barley lines, the S concentrations increased from the aleurone to the sub-aleurone region and decreased in direction of the inner parts of the endosperm (Fig. 6c). The HAL showed higher S concentrations in the sub-aleurone layer compared to the LAL, but the S concentrations were similar in the core endosperm. In both barley lines, P concentrations of the line scans were comparable, with the highest concentrations in the aleurone followed by a sharp decrease in the endosperm (Fig. 6e). Line scans of Fe and P showed similar distribution patterns.

In addition to µ-PIXE distribution maps, line scans were performed on cross-sections from the center of the grain using LA-ICP-MS as shown in Figure 7 and 8. In the endosperm, these line scans showed similar results as described for µ-PIXE analysis, with higher Zn concentrations in the HAL compared to the LAL (Fig. 7a). At this position of the grain, the LAL had higher Zn signals in the aleurone at the crease side than the HAL (Suppl. Tab. 1). LA-ICP-MS images of the line scans affirmed the gradient from aleurone to endosperm tissue shown before (Fig. 7b).

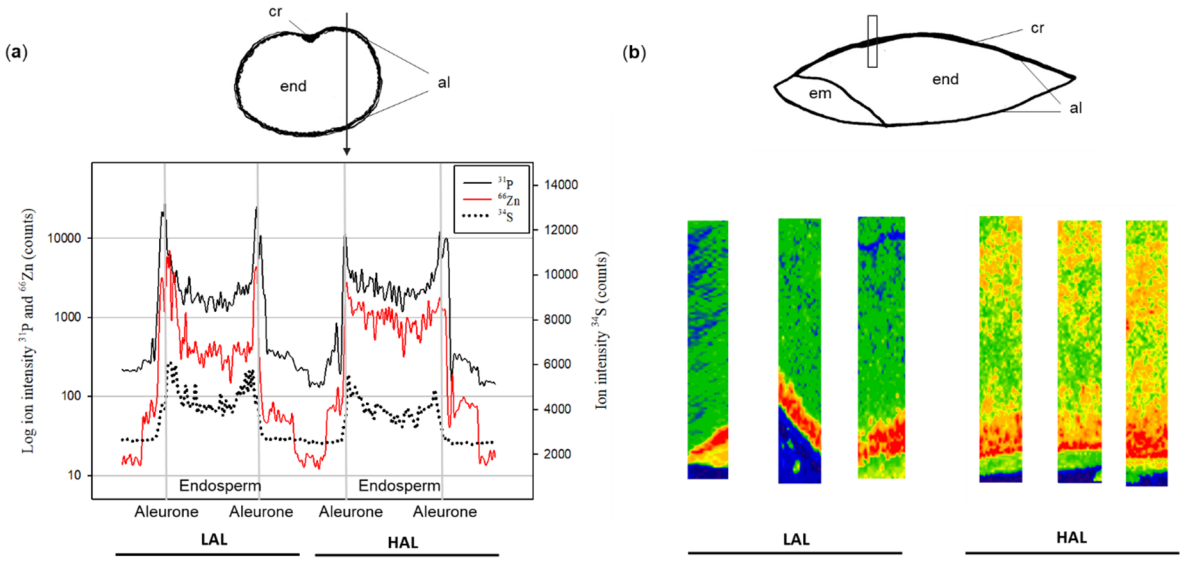

Fig. 7 Line scans and images obtained with LA-ICP-MS for zinc distribution. Zinc (^{66}Zn), sulphur (^{34}S) and phosphorus (^{31}P) intensities (**a**) extracted from three different grain sections of a low (LAL) and high (HAL) Zn accumulating barley line at maturity. Zinc distribution images of scans from three different grains of LAL and HAL at maturity (**b**). Line scans were obtained at the middle of the grain including aleurone (al) and the endosperm (end) tissue as indicated (**a**, transverse section) and (**b**, longitudinal). Position of the embryo (em) and crease (cr) are indicated. *n*=3.

Within the endosperm, the Zn concentration varied to some degree, but Zn concentrations were higher in all measured parts of the endosperm in the HAL compared to the LAL. In both barley lines, Fe was mainly found in the aleurone tissues and significantly less in the endosperm (Fig. 8). Similar to Zn, the LAL had higher Fe concentrations in the aleurone at the crease side of the grain, compared to the HAL (Suppl. Tab. 1). The Fe distribution within the different replicates of the LAL were not as uniform as the replicates of the HAL (Fig. 8b).

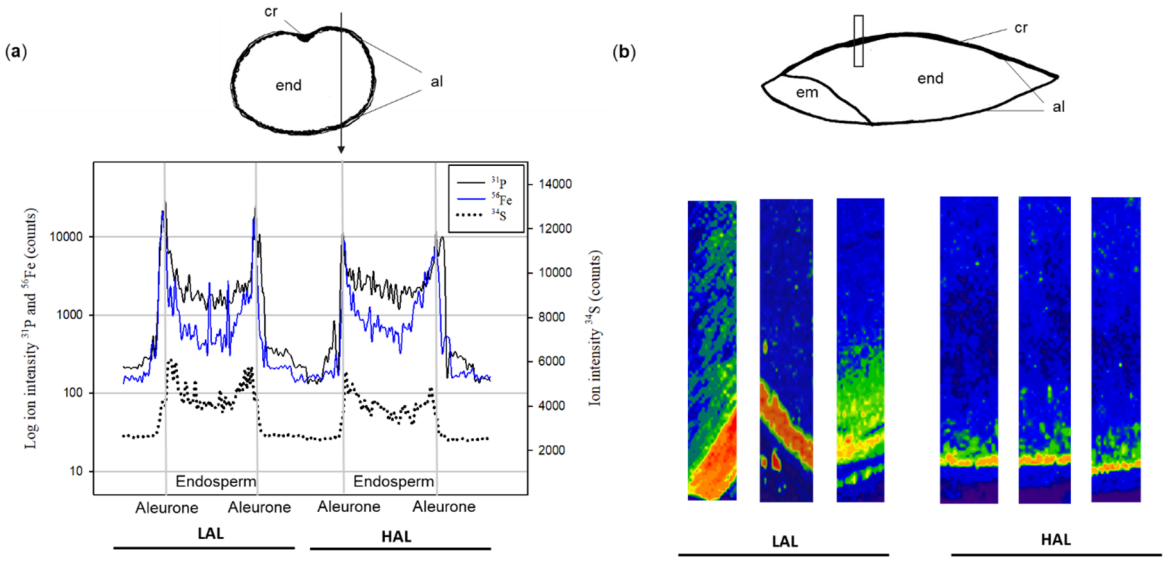

Fig. 8 Line scans and images obtained with LA-ICP-MS for iron distribution. Iron (^{56}Fe), sulphur (^{34}S) and phosphorus (^{31}P) intensities (**a**) extracted from three different grain sections of a low (LAL) and high (HAL) Zn accumulating barley line at maturity. Zinc distribution images of scans from three different grains of LAL and HAL at maturity (**b**). Line scans were obtained at the middle of the grain including aleurone (al) and the endosperm (end) tissue as indicated (**a**, transverse section) and (**b**, longitudinal). Position of the embryo (em) and crease (cr) are indicated. *n*=3.

LA-ICP-MS images of transversal sections at 27 dap

The µ-PIXE maps had shown lower Zn concentrations in the HAL compared to the LAL in the aleurone and crease tissues at 27 dap. To elucidate this difference, LA-ICP-MS images of longitudinally cut grains at 27 dap were made and co-localization maps created to show the distribution of Zn, Fe, S and P from a different angle (Fig. 9, Suppl. Fig. S7). Images of the HAL showed higher Zn concentrations in the crease, the transition zone and scutellum compared to the LAL. Iron distribution showed a similar pattern, but the Fe concentrations were

lower in root and shoot primordia compared to Zn. In the scutellum, Zn was rather located in direction of the endosperm and Fe in direction of the shoot and root primordia. In contrast to the LAL, Zn and Fe were mainly co-localized in the crease in the HAL. In both barley lines, Zn and Fe were partly co-localized in the scutellum.

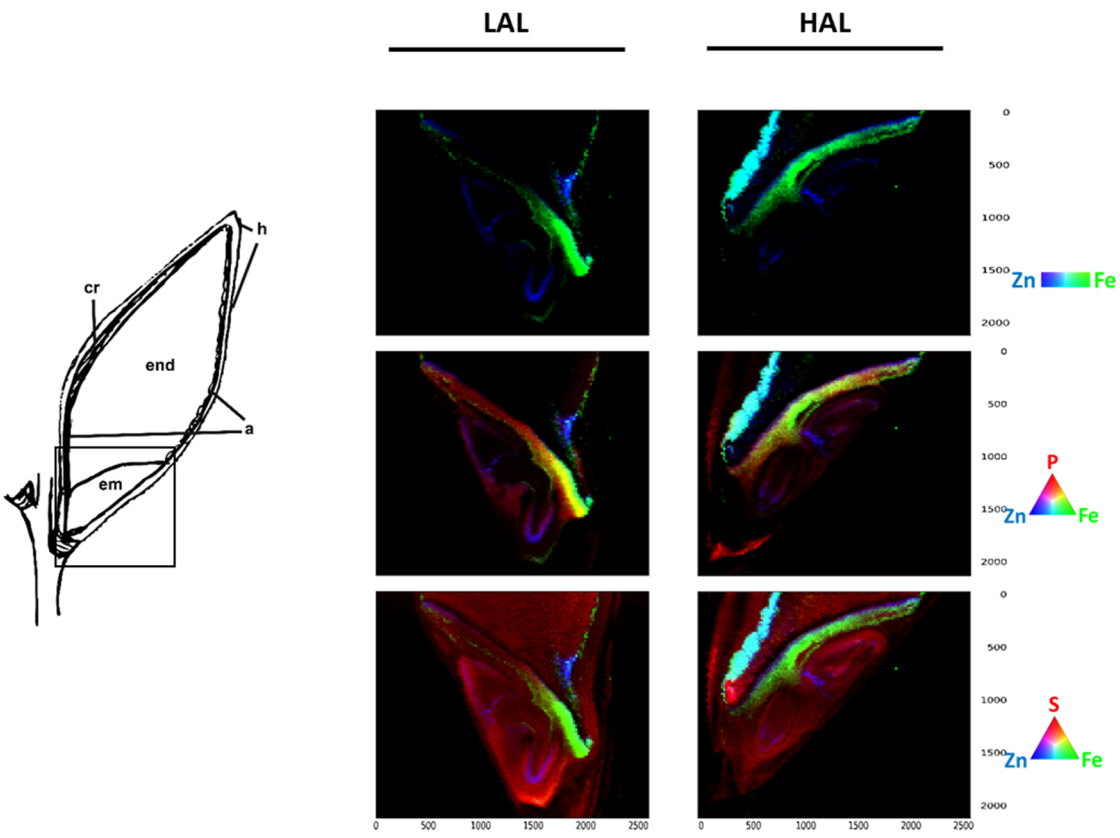

Fig. 9 Co-localization of representative zinc (^{66}Zn), iron (^{56}Fe), sulphur (^{34}S) and phosphorus (^{31}P) in and around the embryo in barley grains 27 days after pollination, analysed by LA-ICP-MS. Elements were analysed in a low (LAL) and high (HAL) Zn accumulating barley line. All signals were normalized to endogenous carbon, measured as ^{13}C. Images were made at longitudinally cut grains including endosperm (end), aleurone (a), crease (cr) and husk (h) as indicated.

Phosphorus was mainly localized in the scutellum and crease. Zinc and P were co-localized in some parts of the shoot and root primordia and in the scutellum. Iron was mainly co-localized with P in the scutellum. Co-localization of Zn and Fe with P was similar for both barley lines. Sulphur showed co-localization with Zn mainly in the shoot and root primordia and in the scutellum. In the HAL, S was also co-localized with Zn in a transition zone between the crease and embryo tissues. There was no obvious pattern of S and Fe co-localization.

Zinc chemical environment in barley grain embryo

The longitudinal cross sections of mature grain were first subjected to fast XRF mapping to identify the highest Zn signal pixels (hot spots; Fig. 10a, b). These pixels were subsequently selected for XANES analysis to ensure best signal to noise ratio in Zn K-edge spectra. Although the largest Zn concentrations occur in the aleurone (Fig. 3), embryo tissue was selected for analysis because the size of the beam was larger than the thickness of the aleurone layers. Due to low Zn concentrations in endosperm, good-quality Zn K-edge XANES spectra could not be recorded here. Each of the embryo-specific Zn K-edge XANES spectra was compared to the spectra of reference Zn complexes, as explained in Materials and Methods. The best fits were obtained with Zn-phytate, Zn-cysteine and Zn-histidine (Fig. 10c, d), as the results indicated the presence of Zn-O-P-(phytate), Zn-S-(cysteine) and Zn-N-(histidine) coordination in the local environment, respectively.

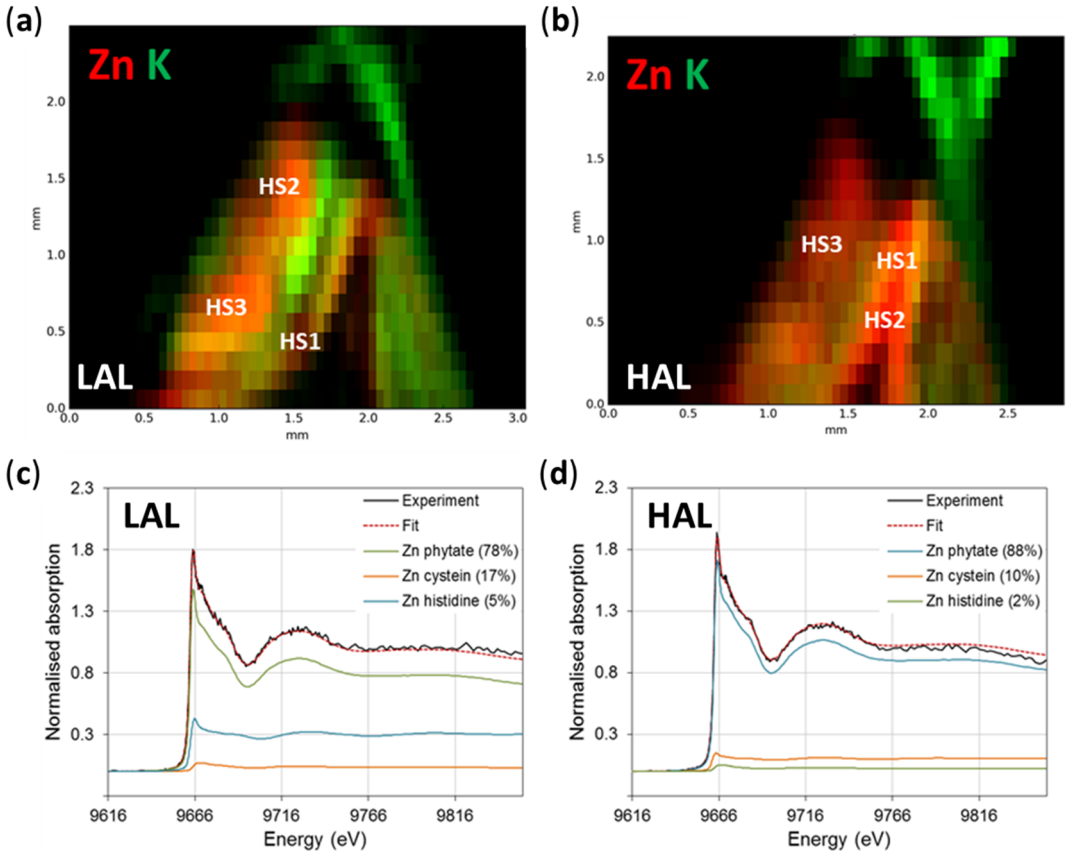

Fig. 10 Potential zinc binding environments in embryos of mature barley grains analysed by XANES. Representative zinc (Zn) and potassium (K) co-localization maps (**a**, **b**) and Zn X-ray absorption near edge spectra ("Experiment"; **c**, **d**) recorded in grain embryo of the low Zn-accumulating (**a**, **c, LAL**) and high Zn-accumulating (**b**, **d, HAL**) barley lines and the best linear combination fit ("Fit") obtained by the spectra of the three reference Zn complexes (Zn phytate, Zn cysteine and Zn histidine). The relative amount of each complexes is given in parenthesis. HS, hotspot; eV, electron volts.

A majority of the Zn in the barley embryo was bound to phytate (78-88 %) and the rest was bound to cysteine and histidine. The LAL had approximately 10 % less Zn bound to phytate, which was reflected in more cysteine and histidine-bound Zn (cysteine 17 % (LAL) compared to 10 % (HAL and histidine 5 % (LAL) compared to 2 % (HAL)).

DISCUSSION

Hidden hunger affects about 2 billion people worldwide, especially children (WHO, 2002, 2009; Tulchinsky, 2010; Muthayya *et al.*, 2013; Ruel-Bergeron *et al.*, 2015). Micronutrient deficiencies lead to severe consequences for public health, e.g. higher vulnerability to diseases, anemia and reduced growth, resulting in higher morbidity and mortality (WHO, 2002; Tulchinsky, 2010). Although the estimated number of stunted children decreased from 198.2 to 149.0 million over the last two decades (2000-2018) (United Nations Children's Fund *et al.*, 2019), rising CO_2 levels are predicted to aggravate the problem with micronutrient deficiencies (Myers *et al.*, 2014; Dietterich *et al.*, 2015; Smith & Myers, 2018). Zinc and Fe are most problematic, mainly due to their insufficient concentrations in the endosperm of cereal grains (Sandstead, 1991; Bewley & Black, 2013; Clemens, 2014). Because most cereals are processed before consumption, the micronutrient distribution within the grain will affect the amount of Zn or Fe in the meal. Milling reduces the amount of Zn and Fe by removing Zn- and Fe-rich aleurone and embryo tissues, resulting in low concentrations remaining in the white flour (Slavin *et al.*, 2001; Lu *et al.*, 2013; Atungulu & Pan, 2014). The loss of micronutrients during milling has been shown to be affected by the micronutrient distribution within the grain and other grain properties, e.g. hardness (Hansen *et al.*, 2012). Therefore, to combat micronutrient deficiencies, it is important to breed cereals with high micronutrient concentrations not only in the whole grain, but especially in the endosperm.

Detailed research has been carried out to understand processes such as root uptake, translocation and storage of micronutrients in plants (Palmgren *et al.*, 2008; Zhao & McGrath, 2009). Nevertheless, mechanisms leading to natural diversity in Zn and Fe accumulation in the grain, especially in the endosperm, are still not well understood. Thus, to explore natural variation as a basis for molecular research and targeted breeding approaches, detailed knowledge on the distribution of micronutrients in the grain and their accumulation pattern during development is needed. Barley is a suitable model crop for studying micronutrient

accumulation in the grain, as it shows a considerable degree of natural variation in Zn and Fe accumulation, ranging from about 1.3 to 3.7 fold and from 1.8 to 9.6 fold, respectively (Ma *et al.*, 2004; White & Broadley, 2009; Detterbeck *et al.*, 2016; Detterbeck *et al.*, 2019). Additionally barley is self-fertilizing, diploid and a genome assembly is available, which facilitate the analysis of molecular mechanisms leading to natural diversity in micronutrient accumulation (Sreenivasulu *et al.*, 2008; Saisho & Takeda, 2011; International Barley Genome Sequencing *et al.*, 2012; Mascher *et al.*, 2017).

We analyzed Zn and Fe concentrations in barley at four different developmental stages, at 7, 15 and 27 dap in whole ears and in mature grains, in a low and a high Zn accumulating barley line. During the early stages of development, Zn and Fe concentrations remained stable for each barley line (Fig. 1 a, b), which is in agreement with reports for wheat, where Zn and Fe concentrations were stable during grain development (Stomph *et al.*, 2011; Singh *et al.*, 2014a). Another study showed, however, decreasing Zn concentrations during the first weeks of wheat grain development, with stable concentrations only from about 27 days after anthesis (Ozturk *et al.*, 2006). In order to study the mechanisms leading to low or high micronutrient accumulation in the grain, basic knowledge on potential temporal dynamics during grain development is needed. On this basis, in depth analyses can be performed on the time-point of occurring differences in micronutrient accumulation. Interestingly, in the two barley lines studied, differences in Zn concentration between the two lines occurred especially at maturity (Fig. 1a), even though the HAL tended to show higher Zn concentrations than the LAL at all analyzed time points. Accordingly, Zn foliar application increased grain Zn concentrations in wheat especially when applied at the late developmental stages (Cakmak *et al.*, 2010). In our study, Fe concentrations did not increase the HAL compared to the LAL at maturity (Fig. 1b). Zinc and Fe accumulation has been shown to be genetically determined to a considerable degree in barley, wheat and rice (SHI *et al.*, 2009; Zhao *et al.*, 2009; Chatzav *et al.*, 2010; Mamo *et al.*, 2014; Pinson *et al.*, 2015). Hence, the processes of Zn loading and distribution within the grain are presumably tightly genetically controlled. Our results suggest that there are temporally regulated mechanisms maintaining specific micronutrient levels during grain development in each line. Changes leading to high Zn concentrations in the grain seem to appear especially at the later stages of grain ripening in barley grains.

To unravel potential differences in mechanistic pathways leading to low or high micronutrient concentrations in the grain, it is important to know how micronutrients are distributed within the grain in contrasting lines (Pongrac *et al.*, 2013). In order to gain a more

detailed insight in nutrient localization, we performed μ-PIXE analysis to determine the spatial distribution of Zn and Fe in grain tissues at four different developmental stages in two contrasting barley lines. The measured concentrations of micronutrients were higher in μ-PIXE quantitative distribution maps compared to the quantitative measurements obtained by ICP-OES analysis of whole ears. This is contributable to the position of the section, which contains mostly the embryo and does not reflect distribution gradients within the grain. In addition, we hypothesize that especially the endosperm, which is closely positioned between the aleurone and embryo at this part of the grain, is enriched in micronutrients as high amounts of nutrients need to be loaded into the embryo. Regardless of total Zn concentrations measured, the pattern of stable Zn accumulation during early stages of development within each line was reconfirmed by the μ-PIXE measurements of the endosperm, the embryo and the husk (Fig. 2 and 3). Our analysis revealed differences in Zn localization and concentration in the different grain tissues during grain development in the two barley lines. In agreement with several previous studies, we found much higher micronutrient concentrations in the aleurone, crease and embryo tissues than in the endosperm (Lombi *et al.*, 2011; Stomph *et al.*, 2011; Ajiboye *et al.*, 2015). We found that differences in Zn concentration of the two barley lines appeared mainly in the endosperm and aleurone tissues at maturity. Hence, it is a promising finding for future breeding approaches that the mechanisms leading to high Zn accumulation in the HAL also affected endosperm Zn concentrations.

Several other studies found a correlation between grain Zn and Fe concentrations of barley, wheat, rice and pearl millet, suggesting similar distribution pathways or metal ligands (Cakmak *et al.*, 2004; Jiang *et al.*, 2007; Zhao *et al.*, 2009; Chatzav *et al.*, 2010; Bashir *et al.*, 2014; Detterbeck *et al.*, 2016). Still, detailed studies of different grain tissues in various cereals have demonstrated differences in Zn and Fe localization within the grain (Kyriacou *et al.*, 2014; Ajiboye *et al.*, 2015). In accordance with these studies, our results show a differentiated pattern of Zn and Fe localization. The HAL showed higher Fe concentrations in the aleurone and crease tissues at maturity compared to the LAL, which was in agreement with observations for Zn concentration (Fig. 4, 5). In contrast to Zn, however, there was less Fe in the endosperm at all developmental stages analyzed in both barley lines. This was also shown for rice grain (Iwai *et al.*, 2012), in mature grains of barley cv Golden Promise (Lombi *et al.*, 2011) and wheat grain (Singh *et al.*, 2018). In contrast, other studies in wheat have shown similar distribution patterns of Fe and Zn in the endosperm, which was influenced by genotypic influences or fertilization approaches (Pongrac *et al.*, 2013; Singh *et al.*, 2013; Singh *et al.*, 2018). Our results suggest

that Zn and Fe loading from the crease to the aleurone tissues and subsequently to the endosperm are more efficient in the HAL compared to the LAL near the embryo. Additionally, there seem to be genetically determined processes regulating different Zn unloading and transport efficiencies into the endosperm for Zn and Fe in both barley lines.

Co-localization analyses with P or S can indicate potential binding environments such as phytate or proteins. In our analyses, the HAL had higher S concentrations in the endosperm and higher P concentrations in the embryo compared to the LAL at maturity (Suppl. Fig. S2 and S3). Proportions of Zn and Fe were co-localized with S especially in the sub-aleurone layer in mature sections of the HAL. Hence, it is difficult to compare the localization and concentrations of the different nutrients based on the µ-PIXE maps. Therefore, we extracted line-scans from µ-PIXE measurements, where the high Zn line showed higher Zn concentrations throughout the line scan compared to the low Zn line (Fig. 6a). Interestingly, Fe and P concentrations decreased largely following the way from aleurone to endosperm (Fig. 6b, d). In contrast, Zn concentrations were decreasing to a smaller degree, reaching with comparably higher concentrations into the endosperm. Similar patterns were previously reported in rice (Kyriacou *et al.*, 2014) and barley (Hansen *et al.*, 2012). However, analyses in wheat found a more similar localization pattern of Zn compared to Fe (Brier *et al.*, 2016). The Zn and Fe localization has been shown to be distributed in a gradient within the grain and this is why the position of sectioning can highly influence the absolute concentrations reported (Lombi *et al.*, 2011; Kyriacou *et al.*, 2014). Therefore, we decided to perform LA-ICP-MS measurements in the middle of the grain, to gain insights in distribution differences in this part of the grain. Similar to the sections near the embryo, Zn concentrations were significantly higher in the endosperm in the HAL compared to the LAL (Fig. 7). In contrast to the µ-PIXE sections, P concentrations in the endosperm were significantly higher and S concentrations significantly lower in the HAL than in the LAL (Suppl. Tab. 1). Interestingly, both Zn and Fe concentrations were higher in the aleurone of the LAL than in the HAL, but only at the crease side (Fig. 7 and 8). These results are comparable to analyses in wheat, where Zn levels in the crease could be raised to high Zn levels by fertilization, whereas endosperm Zn concentrations did not alter correspondingly (Stomph *et al.*, 2011). The authors of this study suggested that there is a rate-limiting process of Zn transfer in between the crease and inner endosperm. Our results also indicate a more efficient unloading of Zn and Fe from the aleurone tissue to the endosperm in the HAL in the middle of the grain, especially at the crease side, than in the LAL. Theoretically, this could be influenced by differences in structure or transfer capacity of

endosperm transfer cells, which are positioned along the crease in barley (Olsen, 2004; Lopato *et al.*, 2014).

Differences in Zn concentrations of aleurone and crease tissues were also visible in μ-PIXE measurements during development. Comparably to LA-ICP-MS measurements in the middle of the grain at maturity, the LAL showed higher Zn concentrations at 27 dap in crease and aleurone tissue at the position of the embryo than LAL. As the crease and aleurone tissues are most important for Zn loading into the grain, differences in micronutrient concentration at different developmental stages could lead to the hypothesis of different temporal dynamics of Zn loading in the two barley lines. Therefore we created LA-ICP-MS images of transversal sections at 27 dap to visualize the nutrient distribution from a different position at the embryo. The LA-ICP-MS images of a grain analyzed 27 dap showed that the low Zn line showed higher Zn concentrations in crease and aleurone at 27 dap at this position of the grain. Even though a clear differentiation between the crease and aleurone tissues was not possible in the LA-ICP-MS images, the HAL line clearly had more Zn and Fe in these tissues compared to the LAL (Fig. 9). This difference between μ-PIXE and LA-ICP-MS measurements could be attributable to the different positions of the sections. As such, these results show how important it is to analyze different angles and positions of a grain for probative discussion of results. Hence, the LA-ICP-MS images supported the findings of partially different localization of Zn and Fe and co-localization with P and S, especially in the embryo (Fig. 9), where, Zn co-localized with S in parts of the root and shoot primordia and scutellum, whereas in the scutellum Fe was mainly co-localized with P. In agreement with our results, Zn was found to concentrate in the root and shoot primordia of wheat embryos, with co-occurring to S (Brier *et al.*, 2016). In addition, Fe was found to be primarily located in scutellum and to be co-localized with P.

Though the co-localization of μ-PIXE maps and LA-ICP-MS images can give hints regarding the binding environment, an identification of the binding species in different tissues is not possible. Therefore, we performed XANES analysis on the contrasting barley lines in order to identify the chemical binding forms of Zn. Due to low Zn concentrations in the endosperm, XANES analysis was not possible in this tissue and therefore, we analyzed the embryo instead. The best linear combination fits were found for Zn-phytate, Zn-cysteine and Zn-histidine, with the highest amounts of Zn bound to phytate (Fig. 10c, d). These results are in contrast to previous findings in barley embryos, where Zn co-eluted mainly with S in the soluble fraction, indicating that protein-bound Zn (Persson *et al.*, 2009). In our study, the HAL had proportionally more Zn bound to phytate and less to cysteine and histidine in the embryo

compared to the LAL. However, the exact binding forms of Zn in endosperm (both soluble and insoluble forms) remains unresolved. Interestingly, our μ-PIXE and LA-ICP-MS measurements revealed that especially in the HAL, proportions of Zn and Fe were co-localized with S especially in the sub-aleurone layer in mature sections. This result could indicate that Zn speciation is differentially altered in different parts of the grain in the HAL.

To our knowledge, this study contributes the first temporal and spatial patterns of Zn and Fe in a low and a high Zn accumulating line in barley grains. Our results indicate that differences in Zn accumulation occur especially at late stages of development and affect endosperm concentrations. Hence, more in depth analyses on the binding environment of micronutrients especially in the endosperm are needed to investigate how changes in Zn accumulation affect the binding environment of Zn.

ACKNOWLEDGEMENTS

We thank Stefan Geimer, Department of Electron Microscopy, University of Bayreuth, for the help with pioloform foil preparation. We are grateful to Mimoza Naseska for initial μ-PIXE spectra processing and to the Department of Animal Ecology, University of Bayreuth, for the possibility of taking microscopic pictures. We thank Christiane Meinen, Pia Schuster and Silke Matros for their expert technical assistance.

FUNDING

This work was in part financially supported by a postdoctoral fellowship by the Alexander von Humboldt foundation to PPo. Financial support from the Slovenian Research Agency (ARRS) through programmes P1-0212 and P1-0112 and projects N7-077, J7-9418, J7-9398 and N1-0105 s gratefully acknowledged.

AUTHOR CONTRIBUTION

AD, PPo, DPP, KVM, MK, PV, PPe and IA performed experiments; AD, PPo, DPP, KVM, SH, JKS and SC planned experiments and analyzed data. AD, PPo, DPP and SC wrote the paper. All authors approved the final version.

COMPETING INTERESTS

The Authors declare that there are no competing interests associated with the manuscript.

REFERENCES

Abràmoff MD, Magalhães PJ, Sunanda RJ. 2004. Image Processing with ImageJ. *Biophotonics Int*: 36–42.

Ajiboye, B, Cakmak, I, Paterson, D, Jonge, MD de, Howard, DL, Stacey, SP, Torun, AA, Aydin, N, McLaughlin, MJ. 2015. X-ray fluorescence microscopy of zinc localization in wheat grains biofortified through foliar zinc applications at different growth stages under field conditions. *Plant and Soil* 392: 357–370.

Atungulu, GG, Pan, Z. 2014. Rice industrial processing worldwide and impact on macro- and micronutrient content, stability, and retention. *Annals of the New York Academy of Sciences* 1324: 15–28.

Bashir, EMA, Ali, AM, Ali, AM, Ismail, MI, Parzies, HK, Haussmann, BIG. 2014. Patterns of pearl millet genotype-by-environment interaction for yield performance and grain iron (Fe) and zinc (Zn) concentrations in Sudan. *Field Crops Research* 166: 82–91.

Bewley, JD, Black, M. 2013. Seeds. Physiology of Development and Germination: Springer US.

Black, RE, Allen, LH, Bhutta, ZA, Caulfield, LE, Onis, M, Ezzati, M, Mathers, C, Rivera, J. 2008. Maternal and child undernutrition. Global and regional exposures and health consequences. *The Lancet* 371: 243–260.

Brier, N de, V Gomand, S, Donner, E, Paterson, D, Smolders, E, Delcour, JA, Lombi, E. 2016. Element distribution and iron speciation in mature wheat grains (*Triticum aestivum* L.) using synchrotron X-ray fluorescence microscopy mapping and XANES imaging. *Plant, Cell & Environment*. 39 (8). 1835-1847.

Cakmak, I, Kalayci, M, Kaya, Y, Torun, AA, Aydin, N, Wang, Y, Arisoy, Z, Erdem, H, Yazici, A, Gokmen, O, Ozturk, L, Horst, WJ. 2010. Biofortification and localization of zinc in wheat grain. *Journal of Agricultural and Food Chemistry* 58: 9092–9102.

Cakmak, I, Turun, A, Millet, E, Feldman, M, Fahima, T, Korol, A, Nevo, E, Braun, HJ, Ozkan, H. 2004. Triticum dicoccoides. An important genetic resource for increasing zinc and iron concentration in modern cultivated wheat. *Soil Science and Plant Nutrition* 50: 1047–1054.

Chatzav, M, Peleg, Z, Ozturk, L, Yazici, A, Fahima, T, Cakmak, I, Saranga, Y. 2010. Genetic diversity for grain nutrients in wild emmer wheat. Potential for wheat improvement. *Annals of botany* 105: 1211–1220.

Cheah, ZX, Kopittke, PM, Harper, SM, O'Hare, TJ, Wang, P, Paterson, DJ, Jonge, MD de, Bell, MJ. 2019. In situ analyses of inorganic nutrient distribution in sweetcorn and maize kernels using synchrotron-based X-ray fluorescence microscopy. *Annals of botany* 123: 543–556.

Clemens, S. 2014. Zn and Fe biofortification: the right chemical environment for human bioavailability. *Plant science: an international journal of experimental plant biology* 225: 52–57.

Detterbeck, A, Nagel, M, Rensch, S, Weber, M, Börner, A, Persson, DP, Schjoerring, JK, Christov, V, Clemens, S. 2019. The search for candidate genes associated with natural variation of grain Zn accumulation in barley. *The Biochemical journal*.

Detterbeck, A, Pongrac, P, Rensch, S, Reuscher, S, Pecovnik, M, Vavpetic, P, Pelicon, P, Holzheu, S, Kramer, U, Clemens, S. 2016. Spatially resolved analysis of variation in barley (*Hordeum vulgare*) grain micronutrient accumulation. *The New phytologist* 211: 1241–1254.

Dietterich, LH, Zanobetti, A, Kloog, I, Huybers, P, Leakey, ADB, Bloom, AJ, Carlisle, E, Fernando, N, Fitzgerald, G, Hasegawa, T, Holbrook, NM, Nelson, RL, Norton, R, Ottman, MJ, Raboy, V, Sakai, H, Sartor, KA, Schwartz, J, Seneweera, S, Usui, Y, Yoshinaga, S, Myers, SS. 2015. Impacts of elevated atmospheric CO_2 on nutrient content of important food crops. *Scientific data* 2: 150036.

Eagling, T, Neal, AL, McGrath, SP, Fairweather-Tait, S, Shewry, PR, Zhao, F-J. 2014. Distribution and Speciation of Iron and Zinc in Grain of Two Wheat Genotypes. *Journal of Agricultural and Food Chemistry* 62: 708–716.

Evers, T, Millar, S. 2002. Cereal Grain Structure and Development: Some Implications for Quality. *Journal of Cereal Science* 36: 261–284.

Gupta, RK, Gangoliya, SS, Singh, NK. 2015. Reduction of phytic acid and enhancement of bioavailable micronutrients in food grains. *Journal of food science and technology* 52: 676–684.

Hansen, TH, Lombi, E, Fitzgerald, M, Laursen, KH, Frydenvang, J, Husted, S, Boualaphanh, C, Resurreccion, A, Howard, DL, de Jonge, Martin D., Paterson, D, Schjoerring, JK. 2012. Losses of essential mineral nutrients by polishing of rice differ among genotypes due to contrasting grain hardness and mineral distribution. *Journal of Cereal Science* 56: 307–315.

Hothorn, T, Bretz, F, Westfall, P. 2008. Simultaneous inference in general parametric models. *Biometrical journal. Biometrische Zeitschrift* 50: 346–363.

International Barley Genome Sequencing, Mayer, KF, Waugh, R, Brown, JWS, Schulman, A, Langridge, P, Platzer, M, Fincher, GB, Muehlbauer, GJ, Sato, K, Close, TJ, Wise, RP, Stein, N. 2012. A physical, genetic and functional sequence assembly of the barley genome. *Nature* 491: 711–716.

Iwai, T, Takahashi, M, Oda, K, Terada, Y, Yoshida, KT. 2012. Dynamic changes in the distribution of minerals in relation to phytic acid accumulation during rice seed development. *Plant Physiology* 160: 2007–2014.

Jiang, SL, Wu, JG, Feng, Y, Yang, XE, Shi, CH. 2007. Correlation analysis of mineral element contents and quality traits in milled rice (*Oryza stavia* L.). *Journal of Agricultural and Food Chemistry* 55: 9608–9613.

Karydas, AG, Czyzycki, M, Leani, JJ, Migliori, A, Osan, J, Bogovac, M, Wrobel, P, Vakula, N, Padilla-Alvarez, R, Menk, RH, Gol, MG, Antonelli, M, Tiwari, MK, Caliri, C, Vogel-Mikuš, K, Darby, I, Kaiser, RB. 2018. An IAEA multi-technique X-ray spectrometry endstation at Elettra Sincrotrone Trieste: benchmarking results and interdisciplinary applications. *Journal of synchrotron radiation* 25: 189–203.

Kawamoto, T, Kawamoto, K. 2014. Preparation of thin frozen sections from nonfixed and undecalcified hard tissues using Kawamot's film method (2012). *Methods in molecular biology (Clifton, N.J.)* 1130: 149–164.

Klančnik, K, Vogel-Mikuš, K, Kelemen, M, Vavpetič, P, Pelicon, P, Kump, P, Jezeršek, D, Gianoncelli, A, Gaberščik, A. 2014. Leaf optical properties are affected by the location and type of deposited biominerals. *Journal of photochemistry and photobiology. B, Biology* 140: 276–285.

Kyriacou, B, Moore, KL, Paterson, D, Jonge, MD de, Howard, DL, Stangoulis, J, Tester, M, Lombi, E, Johnson, AAT. 2014. Localization of iron in rice grain using synchrotron X-ray fluorescence microscopy and high resolution secondary ion mass spectrometry. *Journal of Cereal Science* 59: 173–180.

Liu, Z, Wang, H, Wang, X-E, Xu, H, Gao, D, Zhang, G, Chen, P, Liu, D. 2008. Effect of wheat pearling on flour phytase activity, phytic acid, iron, and zinc content. *LWT - Food Science and Technology* 41: 521–527.

Lombi, E, Smith, E, Hansen, TH, Paterson, D, Jonge, MD, Howard, DL, Persson, DP, Husted, S, Ryan, C, Schjoerring, JK. 2011. Megapixel imaging of (micro)nutrients in mature barley grains. *Journal of experimental botany* 62: 273–282.

Lopato, S, Borisjuk, N, Langridge, P, Hrmova, M. 2014. Endosperm transfer cell-specific genes and proteins: structure, function and applications in biotechnology. *Frontiers in plant science* 5: 64.

Lu, L, Tian, S, Liao, H, Zhang, J, Yang, X, Labavitch, JM, Chen, W. 2013. Analysis of metal element distributions in rice (*Oryza sativa* L.) seeds and relocation during germination based on X-ray fluorescence imaging of Zn, Fe, K, Ca, and Mn. *PLoS ONE* 8: e57360.

Ma, JF, Higashitani, A, Sato, K, Takeda, K. 2004. Genotypic variation in Fe concentration of barley grain. *Soil Science and Plant Nutrition* 50: 1115–1117.

Mamo, BE, Barber, BL, Steffenson, BJ. 2014. Genome-wide association mapping of zinc and iron concentration in barley landraces from Ethiopia and Eritrea. *Journal of Cereal Science* 60: 497–506.

Mascher, M, Gundlach, H, Himmelbach, A, Beier, S, Twardziok, SO, Wicker, T, Radchuk, V, Dockter, C, Hedley, PE, Russell, J, Bayer, M, Ramsay, L, Liu, H, Haberer, G, Zhang, X-Q, Zhang, Q, Barrero, RA, Li, L, Taudien, S, Groth, M, Felder, M, Hastie, A, Šimková, H, Staňková, H, Vrána, J, Chan, S, Muñoz-Amatriaín, M, Ounit, R, Wanamaker, S, Bolser, D, Colmsee, C, Schmutzer, T, Aliyeva-Schnorr, L, Grasso, S, Tanskanen, J, Chailyan, A, Sampath, D, Heavens, D, Clissold, L, Cao, S, Chapman, B, Dai, F, Han, Y, Li, H, Li, X, Lin, C, McCooke, JK, Tan, C, Wang, P, Wang, S, Yin, S, Zhou, G, Poland, JA, Bellgard, MI, Borisjuk, L, Houben, A, Doležel, J, Ayling, S, Lonardi, S, Kersey, P, Langridge, P, Muehlbauer, GJ, Clark, MD, Caccamo, M, Schulman, AH, Mayer, KFX, Platzer, M, Close, TJ, Scholz, U, Hansson, M, Zhang, G, Braumann, I, Spannagl, M, Li, C, Waugh, R, Stein, N. 2017. A chromosome conformation capture ordered sequence of the barley genome. *Nature* 544: 427.

Mendiburu, F. 2013. agricolae. Statistical Procedures for Agricultural Research. R package version 1.1-6.

Muthayya, S, Rah, JH, Sugimoto, JD, Roos, FF, Kraemer, K, Black, RE. 2013. The global hidden hunger indices and maps. An advocacy tool for action. *PLoS ONE* 8: e67860.

Myers, SS, Zanobetti, A, Kloog, I, Huybers, P, Leakey, Andrew D B, Bloom, AJ, Carlisle, E, Dietterich, LH, Fitzgerald, G, Hasegawa, T, Holbrook, NM, Nelson, RL, Ottman, MJ, Raboy, V, Sakai, H, Sartor, KA, Schwartz, J, Seneweera, S, Tausz, M, Usui, Y. 2014. Increasing CO_2 threatens human nutrition. *Nature* 510: 139–142.

Oatway, L, Vasanthan, T, Helm, JH. 2007. PHYTIC ACID. *Food Reviews International* 17: 419–431.

Olsen, O-A. 2004. Nuclear endosperm development in cereals and *Arabidopsis thaliana*. *The Plant cell* 16: S214-27.

Ozturk, L, Yazici, MA, Yucel, C, Torun, A, Cekic, C, Bagci, A, Ozkan, H, Braun, H-J, Sayers, Z, Cakmak, I. 2006. Concentration and localization of zinc during seed development and germination in wheat. *Physiologia Plantarum* 128: 144–152.

Palmgren, MG, Clemens, S, Williams, LE, Krämer, U, Borg, S, Schjørring, JK, Sanders, D. 2008. Zinc biofortification of cereals: problems and solutions. *Trends in plant science* 13: 464–473.

Persson, DP, Hansen, TH, Laursen, KH, Schjoerring, JK, Husted, S. 2009. Simultaneous iron, zinc, sulfur and phosphorus speciation analysis of barley grain tissues using SEC-ICP-MS and IP-ICP-MS. *Metallomics* 1: 418.

Pinson, S, Tarpley, L, Yan, W, Yeater, K, Lahner, B, Yakubova, E, Huang, X-Y, Zhang, M, Guerinot, ML, Salt, DE. 2015. Worldwide Genetic Diversity for Mineral Element Concentrations in Rice Grain. *Crop Science* 55: 294.

Pongrac, P, Kreft, I, Vogel-Mikus, K, Regvar, M, Germ, M, Vavpetic, P, Grlj, N, Jeromel, L, Eichert, D, Budic, B, Pelicon, P. 2013. Relevance for food sciences of quantitative spatially resolved element profile investigations in wheat (*Triticum aestivum*) grain. *Journal of The Royal Society Interface* 10: 20130296.

R Core Team. R: A language and environment for statistical computing. *R Foundation for Statistical Computing, Vienna, Austria.* http://www.R-project.org/.

Ravel, B, Newville, M. 2005. ATHENA, ARTEMIS, HEPHAESTUS: data analysis for X-ray absorption spectroscopy using IFEFFIT. *Journal of synchrotron radiation* 12: 537–541.

Ruel-Bergeron, JC, Stevens, GA, Sugimoto, JD, Roos, FF, Ezzati, M, Black, RE, Kraemer, K. 2015. Global Update and Trends of Hidden Hunger, 1995-2011. The Hidden Hunger Index. *PLoS ONE* 10: e0143497.

Ryan, CG. 2000. Quantitative trace element imaging using PIXE and the nuclear microprobe. *International Journal of Imaging Systems and Technology* 11: 219–230.

Saisho, D, Takeda, K. 2011. Barley: emergence as a new research material of crop science. *Plant & cell physiology* 52: 724–727.

Sandstead, H. 1991. Zinc deficiency. A public health problem? *American Journal of Diseases of Children*: 853–859.

Shi, J, Li, L, Pan, G. 2009. Variation of grain Cd and Zn concentrations of 110 hybrid rice cultivars grown in a low-Cd paddy soil. *Journal of Environmental Sciences* 21: 168–172.

Singh, BR, Timsina, YN, Lind, OC, Cagno, S, Janssens, K. 2018. Zinc and Iron Concentration as Affected by Nitrogen Fertilization and Their Localization in Wheat Grain. *Frontiers in plant science* 9: 307.

Singh, M. 2004. Role of micronutrients for physical growth and mental development. *Indian journal of pediatrics* 71: 59–62.

Singh, SP, Jeet, R, Kumar, J, Shukla, V, Srivastava, R, Mantri, SS, Tuli, R. 2014a. Comparative transcriptional profiling of two wheat genotypes, with contrasting levels of minerals in grains, shows expression differences during grain filling. *PLoS ONE* 9: e111718.

Singh, SP, Vogel-Mikus, K, Arcon, I, Vavpetic, P, Jeromel, L, Pelicon, P, Kumar, J, Tuli, R. 2013. Pattern of iron distribution in maternal and filial tissues in wheat grains with contrasting levels of iron. *Journal of Experimental Botany* 64: 3249–3260.

Singh, SP, Vogel-Mikuš, K, Vavpetič, P, Jeromel, L, Pelicon, P, Kumar, J, Tuli, R. 2014b. Spatial X-ray fluorescence micro-imaging of minerals in grain tissues of wheat and related genotypes. *Planta* 240: 277–289.

Slavin, JL, Jacobs, D, Marquart, L. 2001. Grain processing and nutrition. *Critical reviews in biotechnology* 21: 49–66.

Smith, MR, Myers, SS. 2018. Impact of anthropogenic CO_2 emissions on global human nutrition. *Nature Climate Change* 8: 834–839.

Solé, VA, Papillon, E, Cotte, M, Walter, P, Susini, J. 2007. A multiplatform code for the analysis of energy-dispersive X-ray fluorescence spectra. *Spectrochimica Acta Part B: Atomic Spectroscopy* 62: 63–68.

Sreenivasulu, N, Borisjuk, L, Junker, BH, Mock, H-P, Rolletschek, H, Seiffert, U, Weschke, W, Wobus, U, eds. 2010. Barley Grain Development: Toward an Integrative View: Elsevier.

Sreenivasulu, N, Graner, A, Wobus, U. 2008. Barley genomics. An overview. *International journal of plant genomics* 2008: 486258.

Sreenivasulu, N, Radchuk, V, Strickert, M, Miersch, O, Weschke, W, Wobus, U. 2006. Gene expression patterns reveal tissue-specific signaling networks controlling programmed cell death and ABA- regulated maturation in developing barley seeds. *The Plant journal: for cell and molecular biology* 47: 310–327.

Stomph, TJ, Choi, EY, Stangoulis, J C R. 2011. Temporal dynamics in wheat grain zinc distribution: is sink limitation the key? *Annals of botany* 107: 927–937.

Tang, J, Zou, C, He, Z, Shi, R, Ortiz-Monasterio, I, Qu, Y, Zhang, Y. 2008. Mineral element distributions in milling fractions of Chinese wheats. *Journal of Cereal Science* 48: 821–828.

Terzano, R, Al Chami, Z, Vekemans, B, Janssens, K, Miano, T, Ruggiero, P. 2008. Zinc distribution and speciation within rocket plants (*Eruca vesicaria* L. Cavalieri) grown on a polluted soil amended with compost as determined by XRF microtomography and micro-XANES. *Journal of agricultural and food chemistry* 56: 3222–3231.

Tulchinsky, TH. 2010. Micronutrient Deficiency Conditions. Global Health Issues. *Public Health Reviews* 32: 243–255.

United Nations Children's Fund, World Health Organization, The World Bank Group. 2019. Levels and trends in child malnutrition. Child Malnutrition Estimates Key findings of the 2019 edition. UNICEF, New York, WHO, Geneva, The World Bank, Washington, DC.

van Malderen, SJM, Laforce, B, van Acker, T, Vincze, L, Vanhaecke, F. 2017. Imaging the 3D trace metal and metalloid distribution in mature wheat and rye grains via laser ablation-ICP-mass spectrometry and micro-X-ray fluorescence spectrometry. *J. Anal. At. Spectrom.* 32: 289–298.

Vogel-Mikuš, K, Pongrac, P, Pelicon, P. 2014. Micro-PIXE elemental mapping for ionome studies of crop plants. *International Journal of PIXE* 24: 217–233.

Wessells, KR, Brown, KH. 2012. Estimating the global prevalence of zinc deficiency. Results based on zinc availability in national food supplies and the prevalence of stunting. *PLoS ONE* 7: e50568.

White, PJ, Broadley, MR. 2009. Biofortification of crops with seven mineral elements often lacking in human diets - iron, zinc, copper, calcium, magnesium, selenium and iodine. *New Phytologist* 182: 49–84.

WHO. 2002. The world health report 2002 - Reducing Risks, Promoting Healthy Life. Geneva, Switzerland.

WHO. 2009. Global health risks: Mortality and burden of disease attributable to selected major risks. Mortality and burden of disease attributable to selected major risks. Geneva, Switzerland.

Xue, Y, Zhang, W, Liu, D, Xia, H, Zou, C. 2016. Nutritional Composition of Iron, Zinc, Calcium and Phosphorus in Wheat Grain Milling Fractions as Affected by Fertilizer Nitrogen Supply. *Cereal Chemistry Journal* 39 (6): 543-549.

Zhao, F-J, McGrath, SP. 2009. Biofortification and phytoremediation. *Current opinion in plant biology* 12: 373–380.

Zhao, F-J, Su, YH, Dunham, SJ, Rakszegi, M, Bedo, Z, McGrath, SP, Shewry, PR. 2009. Variation in mineral micronutrient concentrations in grain of wheat lines of diverse origin. *Journal of Cereal Science* 49: 290–295.

2.3 The search for candidate genes associated with natural variation of grain Zn accumulation in barley

Detterbeck, A., Manuela, M, Rensch, S., Weber, M., Börner, A., Persson, D. P., Schjoerring, J. K., Christov, V., Clemens, S. (2019). *The Biochemical journal*. DOI: 10.1042/BCJ20190181. (Status: online veröffentlicht am 04.06.2019)

Die Konzeption der Forschungsidee und des Versuchsdesigns entstanden durch A. Detterbeck, S. Rensch, M. Weber und S. Clemens. Hierbei lag ein Hauptaugenmerk auf der Analyse der natürlichen Variation und der Analyse von Transkriptunterschieden in niedrig und hoch Zink-akkumulierenden Gerstelinien. Die Pflanzenanzucht zur Analyse der Mikronährstoff-Variation in der ausgewählten ICARDA-Kollektion wurde von M. Nagel und A. Börner in Gatersleben durchgeführt. Die Analyse dieser drei Anzuchten auf deren Mikronährstoff-Konzentrationen erfolgte durch S. Rensch. Die Kohlenstoff- und Stickstoff-Gehalte dieser Linien wurden von Daniel Persson und J.K. Schjoerring analysiert. Die genomweite Assoziationsstudie wurde von M. Nagel durchgeführt. A. Detterbeck und M. Nagel führten die Datenbankrecherchen zur Suche nach Marker-assoziierten Genen aus. Die Anzuchten für die Microarray-Analyse wurden vollständig von A. Detterbeck in Bayreuth in Kulturschränken oder im Gewächshaus ausgeführt. Die Analyse der Mikronährstoff-Gehalte in den Microarray-Proben und in den reifen Körnern der entsprechenden Anzuchten erfolgte durch A. Detterbeck. Die Ernte, Probenaufbereitung sowie die RNA-Extraktion und cDNA-Synthese wurde vollständig durch A. Detterbeck durchgeführt. Hierfür wurde von A. Detterbeck ein Extraktionsprotokoll für die effiziente Extraktion von reiner RNA aus Gerstesamen entwickelt. A. Detterbeck amplifizierte zudem die aRNA, die anschließend von V. Christov und A. Simm hybridisiert wurde. Die Samenzerlegung in einzelne Bestandteile wie Embryo, Perikarp-Gewebe und Endosperm wurde vollständig von A. Detterbeck ausgeführt. Ebenso erfolgte die Probenaufbereitung und Probenanalyse via ICP-OES durch A. Detterbeck. Die Datenauswertung inklusive der Analyse der Microarray-Daten mittels RobiNA erfolgte vollständig durch A. Detterbeck. Ebenso wurden die statistischen Analysen, wie Korrelationsanalysen, Genotyp-Umwelt-Analysen und Signifikanztests vollständig von A. Detterbeck ausgeführt. A. Detterbeck erstellte, bis auf die Ergebnisse der GWAS-Analyse (M. Nagel), die Abbildungen und Tabellen des Manuskriptes, recherchierte Literatur und verfasste das Manuskript, das nach konstruktiver Diskussion von S. Clemens und M. Nagel überarbeitet wurde.

This publication was originally published by Amelie Detterbeck, Manuela Nagel, Stefan Rensch, Michael Weber, Andreas Börner, Daniel P. Persson, Jan Kofod Schjoerring, Vesselin Christov and Stephan Clemens in the Biochemical journal (2019), doi:10.1042/BCJ20190181

The search for candidate genes associated with natural variation of grain Zn accumulation in barley

Amelie Detterbeck[1], Manuela Nagel[2], Stefan Rensch[1], Michael Weber[1], Andreas Börner[2], Daniel P. Persson[3], Jan Kofod Schjoerring[3], Vesselin Christov[4], Stephan Clemens[1]

[1]Department of Plant Physiology, University of Bayreuth, Universitätsstr. 30, 95447 Bayreuth, Germany; [2]Department Genebank, Leibniz Institute of Plant Genetics and Crop Plant Research (IPK), Corrensstr. 3, 06466, OT Gatersleben, Seeland, Germany; [3]Department of Plant and Environmental Sciences, Faculty of Science, University of Copenhagen, Thorvaldsensvej 40, 1871 Frederiksberg C, Denmark, [4]Zentrum für Medizinische Grundlagenforschung (ZMG), Medizinische Fakultät der Martin-Luther-Universität Halle-Wittenberg, Universitätsklinikum Halle (Saale), Ernst-Grube-Str. 40, 06097 Halle (Saale), Germany

Author for correspondence:

Stephan Clemens

Tel: +49 921 552630

Email: stephan.clemens@uni-bayreuth.de

ABSTRACT

Combating Hidden Hunger through molecular breeding of nutritionally enriched crops requires a better understanding of micronutrient accumulation. We studied natural variation in grain micronutrient accumulation in barley (*Hordeum vulgare* L.) and searched for candidate genes by assessing marker trait associations (MTAs) and by analyzing transcriptional differences between low and high zinc (Zn) accumulating cultivars during grain filling. A collection of 180 barley lines was grown in three different environments. Our results show a pronounced variation in Zn accumulation, which was under strong genotype influence across different environments. Genome-wide association mapping revealed 13 shared MTAs. Across three environments, the most significantly associated marker was on chromosome 2H at 82.8 cM and in close vicinity to two yellow stripe like (YSL) genes. A subset of two pairs of lines with contrasting Zn accumulation was chosen for detailed analysis. Whole ears and flag leaves were analyzed 15 days after pollination (dap) to detect transcriptional differences associated with elevated Zn concentrations in the grain. A putative alpha-amylase/trypsin inhibitor CMb precursor was decidedly higher expressed in high Zn cultivars in whole ears in all comparisons. Additionally, a gene similar to barley *metal tolerance protein 5* (*MTP5*) was found to be a potential candidate gene.

Abbreviations:

ANOVA, Analysis of variance; BLUEs, best linear unbiased estimates; CT, cycle threshold; DArT^{TM}, Diversity Arrays Technology; DW, dry weight; FT, foil tunnel; GxE, genotype x environment; H^2, heritability; KW, Kirschweg; GWAS, genome-wide association study; ICARDA, International Center for Agricultural Research in the Dry Areas; LSD, least significant difference; MTAs, marker-trait associations; QTLs, quantitative trait loci; REML, Residual Maximum Likelihood; SE, Selkebreite; SMART, Selection with Markers and Advanced Reproductive Technologies; UPGMA, unweighted pair group method with arithmetic average; dap, days after pollination

INTRODUCTION

Hidden hunger, synonymously used for micronutrient malnutrition, represents a major global health burden. Next to iron (Fe), zinc (Zn) is one of the most important undersupplied micronutrients (Sandstead, 1991; WHO, 2009; Wessells & Brown, 2012). Children are particularly affected by Zn deficiency and suffer from developmental defects, mental retardation and an increased susceptibility to infectious diseases (Singh, 2004; WHO, 2009). Monotonous diets based on cereals can cause micronutrient deficiency, which is thus especially prevalent in low- and middle-income countries (WHO, 2009). There, about 70 % of the consumed food is based on seeds, which are often lacking sufficient amounts of bioavailable micronutrients (Bewley & Black, 2013). Elevated atmospheric levels of carbon dioxide (CO_2) are predicted to cause a decrease in grain Zn and Fe concentrations, which would further aggravate the problem (Myers *et al.*, 2014; Dietterich *et al.*, 2015). Hence, besides food supplementation, approaches to enrich micronutrients in edible parts of plants are pursued to tackle the problems of micronutrient deficiency (Palmgren *et al.*, 2008; Murgia *et al.*, 2012; Shahzad *et al.*, 2014). This includes biofortification through foliar application of micronutrient fertilizers and breeding approaches (Darnton-Hill & Nalubola, 2002; Welch, 2002; Gómez-Galera *et al.*, 2010). For the latter, the understanding of molecular mechanisms is essential in order to enable genetic engineering and directed, conventional breeding, e.g. the Selection with Markers and Advanced Reproductive Technologies (SMART) breeding. Thus, there is a strong interest to elucidate mechanisms of micronutrient mobilization and transport into and within the plant, and of processes related to nutrient storage within the edible parts of the plant (Waters & Sankaran, 2011; Schroeder *et al.*, 2013).

A model organism for studying these mechanisms in cereals is barley (*Hordeum vulgare* L.). Barley is an economically important crop, is diploid, self-fertile and diverse germplasm collections are available (Bothmer, 2003; Sreenivasulu *et al.*, 2008; Ullrich, 2011; International Barley Genome Sequencing *et al.*, 2012). The ICARDA (International Center for Agricultural Research in the Dry Areas) (Jilal *et al.*, 2008) germplasm panel represents the world's barley diversity and was genotyped using Diversity Arrays Technology (DArT^{TM}) markers (Varshney *et al.*, 2012; Nagel *et al.*, 2015). In addition, the barley genome was first published by the International Barley Sequencing Consortium in 2012 and, recently, followed by a high-quality reference genome assembly (International Barley Genome Sequencing *et al.*, 2012; Mascher *et al.*, 2017). The genetic information can be linked to phenotypic traits in a genome-wide

association (GWAS) mapping approach to identify candidate genetic loci possibly contributing to variation in e.g. Zn accumulation. A basic requirement for the identification of quantitative trait loci (QTLs) is the variation of the desired trait. Zn accumulation showed considerable variation in barley grains between the genotypes of a mapping panel (Mamo *et al.*, 2014; Detterbeck *et al.*, 2016). Furthermore, transcriptomic approaches may elucidate differences leading to higher Zn concentrations and can help to identify mechanisms involved in micronutrient accumulation in the grain (Cao *et al.*, 2014; Nanda *et al.*, 2017). For example in barley, an analysis of transcripts of *cv.* 'Golden Promise' 20 days after pollination (dap), derived a potential roadmap of Zn trafficking in different tissues (Tauris *et al.*, 2009).

In this study, we aimed to elucidate the molecular mechanisms leading to higher Zn accumulation in barley grains by detecting QTLs and transcriptional differences of low and high Zn accumulating cultivars. The first objective was to perform a phenotypic characterization of Zn accumulation in barley grains and second, to identify potential candidate genes. Grains of 180 lines of the ICARDA germplasm collection grown in three different environments were analyzed for their Zn concentrations. To understand the relationship and overall transport or storage mechanisms for Zn, the concentrations of Fe, manganese (Mn), copper (Cu), carbon (C [%]) and total protein were measured in parallel. Because the micronutrients Fe, Mn and Cu at least partially share distribution pathways with Zn, correlations can help to build hypotheses about mechanisms involved in micronutrient accumulation in the grain. Carbon or total protein contents can indicate major ligand environments of Zn. To identify significant marker-trait associations (MTAs) and genomic regions responsible for micronutrient variations, all nutrients were analyzed by GWAS using 703 DArT markers. Third, to identify general mechanisms leading to high Zn accumulation, we selected two lines each that accumulated consistently lower or higher Zn concentrations in grains across the different environments. Here, we analyzed first the spatial distribution of Zn in different grain tissues to identify potential differences of low and high Zn accumulating lines. Then, the four lines were cultivated and a comparative transcript analysis conducted on whole ears and flag leaves in order to identify putative mechanisms leading to high Zn accumulation.

MATERIALS AND METHODS

Plant material and growth in different environments

Barley (*Hordeum vulgare* L.) grains of the ICARDA germplasm panel were supplied by the Federal *ex situ* Gene Bank at IPK Gatersleben (Germany) (Varshney *et al.*, 2012; Nagel *et al.*, 2015).

To determine variation of Zn accumulation in grains, 180 barley lines (Supporting Information Tab. S1) were cultivated at three different sites [Folientunnel (FT), Selkeweg (SE), Kirschweg (KW)] at IPK. First site: Five replicates of each line were multiplied in a randomized block design in the foil tunnel (FT). In March 2007, grains were sown in pots using standard culture medium (70 % compost soil, 20 % white peat, 10 % sand) with 8.6 mg Zn kg^{-1}, 43 mg Mn kg^{-1}, 1.4 mg Cu kg^{-1} and a pH value of 6.9. In July 2007, grains were harvested and partly used for field experiments in 2008 and partly stored at 20°C and 50 % relative humidity for further usage. Second and third site: field trials were conducted at SE and at KW. At SE soil quality was classified as clayish loam (toniger Lehm) with 4.3 mg Zn kg^{-1}, 12 mg Mn kg^{-1}, 1.2 mg Cu kg^{-1} at a pH of 7.6. At KW, soil was determined as humic loam with 16.6 mg Zn kg^{-1}, 145 mg Mn kg^{-1}, 5.9 mg Cu kg^{-1}, 4.0 % organic matter at a pH of 7.3. Detailed results of soil analysis were provided by AGROLAB Oberdorla (www.agrolab.de) and are shown in Suppl. Tab. S2. In February 2008, at both sites, SE and KW, 100 grains for each line were sown in field plots of 1 m x 1 m, harvested in July 2008 and stored at 20 °C and 50 % relative humidity for further usage. Micronutrient concentrations were analyzed in grains of 150 (KW), 161 (SE) or 162 (FT) lines. The missing lines failed to establish during cultivation.

Plant material and growth conditions for microarray analysis and grain dissection

Grains of the selected lines 140, 154, 143, and 156 were heat treated at 43 °C for 20 min to minimize the risk of infection and to prevent spraying pesticides during cultivation, which could affect gene expression. In three different cultivation rounds, plants were grown in pots in the glasshouse or in a growth chamber under long day conditions (16h:8h, light:dark) at 100 - 150 µmol s^{-1} m^{-2}.

The soil was a mixture of soil type GS90L (Einheitserde Werkverband e.V.), pricking soil (Ökohum GmbH) and vermiculite (Deutsche Vermiculite Dämmstoff GmbH) in a ratio of 3:3:1. Before use, the moistened soil was heat pasteurized for 1.5 hours at 80 °C using a Sterilo1K (Harter Elektrotechnik), to reduce the risk of soil-borne diseases Soil total Zn concentration was 89.7 mg kg^{-1} dry weight (DW), which is representative for European topsoils according to the FOREGS Geochemical Atlas of Europe (http://weppi.gtk.fi/publ/foregsatlas/). For all lines, three (growth chamber) to five (glasshouse) plants were cultivated in 3 L (growth chamber) or 4 L (glasshouse) pots and pooled for analysis. Plants were fertilized once a week with 200 mL 0.2 % Wuxal Super (Wilhelm Haug GmbH & Co. KG) per pot from BBCH 35 on until ripening (BBCH 89). Only healthy plants were sampled. For grain dissection, whole, mature grains were prepared as described by Detterbeck *et al.* (Detterbeck *et al.*, 2016). In brief, grains were soaked in bidistilled water at 4 °C for 4 hours before dissecting husk (including bran, epidermal cell layers and testa), endosperm (including parts of the aleurone layer) and embryo tissues under a stereomicroscope.

For microarray analysis, whole ears and flag leaves were cut 15 days after pollination (dap). The sampling was always done at the same time of the day to eliminate the influence of a circadian rhythm or differences in light conditions. The developmental stage can be determined exactly between 3 and 10 dap and was evaluated for grains positioned at the lower third of the ear on the basis of caryopsis development (Gubatz *et al.*, 2007). Ears were marked at early developmental stages and harvested 15 dap. Excluding awns and poor grains, whole ears and flag leaves including leaf blade and sheath were harvested. After harvest, the samples were immediately frozen in liquid nitrogen. Whole ears and flag leaves were separately ground in liquid nitrogen using porcelain pestles and mortars and stored as powder at -80 °C for further analysis.

Determination of metal concentration

Inductively Coupled Plasma-Optical Emission Spectroscopy (ICP-OES) was used to analyze total metal concentration in grains and in the soil. Oven-dried grains were wet-digested in a microwave (START 1500; MLS GmbH) using 2 ml bidistilled water, 2 ml 30 % H_2O_2 (w/w) and 4 ml 65 % HNO_3 (w/w) at 180 °C for 12 min. Dissected endosperm tissue was digested in the same way. Dissected husk and embryo tissues were microwave digested with only 1 ml bidistilled water, 1 ml 30 % H_2O_2 (w/w) and 2 ml 65 % HNO_3 (w/w) in smaller vessels.

Total metal concentration of soils used for plant growth was determined by adding 2.25 ml conc. HCl (37 %) and 0.75 ml conc. HNO_3 (65 %) to 0.25 g of dried soil. Formed gasses were allowed to dissipate for 30 min and, afterwards, vessels were closed and microwave digested (START 1500; MLS GmbH) with ramping 15 min to 160 °C and holding this temperature for 15 min. The final volume was adjusted to 10 ml using bidistilled water.

Metal concentrations were measured using an iCAP 6500 (Thermo Scientific) at wavelengths of 213.8 nm (Zn), 238.2 nm (Fe), 257.6 nm (Mn) and 324.7 nm (Cu).

Determination of total protein and C [%] content

Carbon and nitrogen concentrations in dried grain tissue (approx. 40 mg) were analyzed by Dumas combustion using a Vario Macro elemental analyzer (Elementar Analysensysteme GmbH, Hanau, Germany). Prior to weighing into tin capsules and analysis, all samples were oven dried at 60 °C for a minimum of 2 h. Data quality was evaluated by analysis of standard reference materials (acetanilide and B2166, National Institute of Standards and Technology, Gaithersburg, MD, USA). Grain protein concentration was calculated as grain N concentration multiplied by 5.4 (Mariotti *et al.*, 2008).

Population structure and GWAS

DArT^{TM} markers and their chromosomal positions were obtained from Triticarte Pty Ltd, Yarralumla, ACT, Australia and comprised 703 markers with average distances of 1.6 cM and a minor allele frequency of 16.6 %.

The population structure was analyzed by the STRUCTURE 2.3.4 software (Pritchard *et al.*, 2000) using the full marker set. By applying the admixture model, a burn-in of 5,000 iterations and a 5,000 Markov Chain Monte Carlo duration, K-values were tested in the range from one to 10 using 10 replicates each. The likely number of sub-populations (Q) present was estimated by a phylogenetic tree based on the DArT marker and unweighted pair group method with arithmetic average (UPGMA) using TASSEL 2.1 software (Bradbury *et al.*, 2007). A phylogenetic tree was drawn using The Tree Drawing Tool ‘FigTree’ version 1.4.3 (http://tree.bio.ed.ac.uk/).

For association analysis, phenotypic data were analyzed using REML (Residual Maximum Likelihood) implemented in GenStat 18 software (VSN International, 2013). The best linear unbiased estimates (BLUEs) of all the genotypes were derived by assuming fixed genotypic and random environment effects and taking into account the genotype x environment (GxE) variance. The broad-sense heritability (H^2) parameter was calculated using the following equation:

$$H^2 = \frac{\sigma^2 G}{\sigma^2 G + \frac{\sigma^2 GE}{E} + \frac{\sigma^2 RGE}{rE} + \frac{\sigma^2 RGET}{rET}}$$

Thereby, σ^2G is the variance of genotypes (G); σ^2GE is the variance component of the interaction G × environment (E), σ^2RGE is the variance component of the interaction replicate (R) × G × E, σ^2RGET is the variance component of the interaction R × G × E ×treatment (T), r is the number of replicates.

Analysis of variance (ANOVA) was applied to genotypes, environments, treatments and the least significance differences at $P \leq 0.05$ (LSD5 %) used for discrimination (VSN International Ltd, UK).

A mixed linear model (MLM) was used to calculate single marker-trait associations (MTA) between 703 genetically mapped DArT™ markers and the estimated phenotypic data (best linear unbiased estimates (BLUEs)). The population structure was corrected by the kinship and associations were regarded as significant when threshold exceeded $-\log(P_M) \geq 2.5$. Non-DArT markers within 0.5 cM and 2.5 cM on either side of MTA loci were in range of the significant LD at $P \leq 0.001$ and at $P \leq 0.05$, respectively, and were used to identify putative functions of the associated markers available at the IPK barley BLAST server, Gatersleben (http://webblast.ipk-gatersleben.de/barley_ibsc/).

RNA extraction and cDNA synthesis

High RNA quality was achieved by a combination of TRIzol Reagent (Thermo Fisher Scientific Life Technologies GmbH) extraction and RNeasy Mini Kit (Qiagen N.V.) (see Suppl. Fig. S1), which prevented the clogging of the silica membrane with starchy endosperm in the columns provided in the RNeasy Mini Kit. One hundred mg powder from whole ears of flag

leaves was mixed with 1 ml TRIzol for 3 min and allowed to set at room temperature for 5 min. To remove remaining plant material including starch, samples were centrifuged at 12,000 x g and 4 °C for 10 min. The supernatant was mixed with 0.2 ml chloroform and 1 ml TRIzol reagent for 15 sec. Again, the mixture was centrifuged at 12,000 x g and 4 °C for 10 min. From this step, the RNeasy Mini protocol described for plants and fungi was applied and the final supernatant was mixed with 1 ml RLC buffer and inverted. Afterwards 0.5 volume ethanol was added to the aqueous phase. Quality and integrity of RNA was checked by agarose gel and NanoPhotometer (Implen GmbH) measurements. RNA samples not meeting purity greater than 1.8 (260/280) or 1.6 (260/230) were subjected to another cleanup step by using RNeasy Mini Kit (Qiagen) RNA Cleanup protocol.

For cDNA synthesis, 500 ng RNA were treated with DNase-I (Life Technologies GmbH) and transcribed with PrimeScript RT MasterMix (Perfect Realtime) (Takara Bio Inc.) following the manufacturer's protocol.

Microarray analysis

The aRNA was amplified following the manufacturer's instruction of the GeneChip 3' IVT Express Kit (Affymetrix Inc.) with 100 ng of RNA and recommended incubation times for microarray hybridization to GeneChip Barley Genome Arrays (Affymetrix Inc.). aRNA purification was performed with RNeasy Mini Kit (Qiagen) following RNA Cleanup protocol. Arrays were hybridized at the Zentrum für Medizinische Grundlagenforschung, Medizinische Fakultät Martin-Luther-Universität Halle-Wittenberg, Universitätsklinikum Halle. Hybridization was done according to the manufacturer's protocol at 45 °C over night. Arrays were stained with biotin and streptavidin using the GeneChip™ Fluidics Station 450 (Thermo Fisher Scientific) and finally scanned with the GeneChip™ Scanner 3000 7G (Thermo Fisher Scientific).

Data analysis was performed with RobiNA software (Version 1.2.4_build656) in basic mode except GcRMA was used for normalization. Clustering and PCA of single experiments was conducted in basic mode. *P*-value correction was performed by Bonferroni Hochberg and multiple testing with nested.F. The *P*-value cutoff was set at 0.05 with a minimal log fold change of one. Heatmaps were created with R package 'gplots' (Warnes *et al.*, 2016) and dendrograms were performed with function 'hclust'.

Database search for metal related genes

Four different strategies were combined to assemble the list of potential metal homeostasis genes. First, a key word search was conducted on ensembl (http://plants.ensembl.org/Hordeum_vulgare/Info/Index) with terms based on known metal related genes (list of keywords see Suppl. Word file S1). Then, sequences of detected MLOC genes were blasted against Affymetrix target sequences (NetAffx BLAST, https://www.affymetrix.com/analysis/netaffx/blast.affx Liu, 2003). Contig hits with an evalue $\leq 1.00E^{-10}$ were selected as related to genes connected to the specific key words. Afterwards, known *Arabidopsis thaliana* metal genes (based on manually curated list of MapMan transition metal homeostasis genes of *A. thaliana*" in (Suryawanshi *et al.*, 2016)) were blasted (BlastP) against exemplar sequences and Contig hits with an evalue $\leq 1.00E^{-10}$ and assigned as genes related to metal homeostasis genes found in *A. thaliana*.

Also, a Gene Ontology (GO) search (http://www.ebi.ac.uk/QuickGO/GSearch?q=metal&what=GO&limit=1000) based on the key word "metal" was conducted to identify genes already assigned to metal homeostasis on the barley gene chip. Contigs assigned to bins related to metal homeostasis or metal related processes were included according to Suppl. Word file S1. After collecting Contigs potentially related to metal homeostasis, all lists were combined and duplicates of Contigs were removed.

Real-time RT-PCR

Transcript quantification was performed on extracted RNA from whole ears of four different lines (140, 154, 143 and 156). To determine a potential change in transcript abundance during grain development, RNA was extracted at three different developmental stages (7, 15 and 27 dap). Similarity of cDNA sequences of all barley lines was analyzed and checked for the absence of polymorphisms in primer binding sites to ensure equal amplification efficiency. Primer sequences were designed based on the exemplar sequence of Contig25867 provided by Affymetrix Inc. (*HvMTP-fw*: GACTTCGAGTTCACACACCG and *HvMTP-rev*: ACTAGTAGTACTTCCCAAGCATCC. *EF1-α* (*TC146566*) was chosen as reference gene (Faccioli *et al.*, 2007). Real-time RT-PCR reactions were performed in 96-well plates (Bio-Rad iCycler, MyiQ real-time PCR detection system) using SYBR Green (Eurogentec). Cycle threshold (CT) values were calculated as described previously (2012).

Statistical analysis

In order to show variation in micronutrient concentrations, box plots displaying the median, the upper and lower quartile as well as outliers were generated. For comparing the relationship of micronutrients in barley grains and of different field sites, micronutrient concentrations were subjected to regression analysis using SigmaPlot (vers. 13.0). The Pearson product moment correlation coefficients were computed and squared in order to specify the coefficients of determination (r^2) with a significance level of $P \leq 0.05$. For the calculation of genotypic or environmental effects (GxE) on different nutrients and their contribution to the total variance, a two-way ANOVA was conducted with R vers. 3.0.1 (R Core Team) using package 'multcomp' (Hothorn *et al.*, 2008). Testing for significance ($P \leq 0.05$) was performed with ANOVA and Tukey's HSD posthoc test with R vers. 3.0.1 (R Core Team) using packages 'multcomp' (Hothorn *et al.*, 2008) and 'agricolae' (Mendiburu, 2013).

RESULTS

Assembly of the barley collection

A subset of 180 lines of the spring barley ICARDA (International Center for Agricultural Research in the Dry Areas) germplasm panel showing higher genetic diversity was selected for analysis. It comprised two- and six-row lines, including 117 landraces and 63 cultivars/breeding lines from 30 different countries (Suppl. Tab. S1). Based on the DArT^{TM} marker results, the assembly clusters into four Q-groups representing predominantly two-row landraces and breeding lines from ICARDA, North Africa and East Asia (Q1), six-row landraces from North Africa (Q2), two-row cultivars from North Africa, Europe and Australia (Q3) and six-row landraces from Asia (Q4) (Suppl. Fig. S2, S3). The cluster structure corresponds to the phylogenetic tree and respective clusters were found for a different subset of the ICARDA collection (Nagel *et al.*, 2015).

Natural variation in grain element concentrations across different environments

A profound variation in grain micronutrient concentrations was found in lines grown in the three different environments FT, SE and KW. The median Zn concentration (Fig. 1a) ranged

from 45.9 mg kg^{-1} dry weight (DW) (SE) to 56.5 mg kg^{-1} DW (FT). In environment FT, the widest range in Zn concentrations was found with 24.8 mg kg^{-1} DW to 91.1 mg kg^{-1} DW, i.e. a 3.7-fold variation. In the other environments, Zn showed a 2.7- (SE) to 3.5- (KW) fold variation. Median values for Fe, Mn and Cu varied from 48.9 to 59.9 mg kg^{-1} DW, 16.0 to 27.0 mg kg^{-1} DW and 5.7 to 7.6 mg kg^{-1} DW, respectively (Suppl. Fig. S4). Median C [%] and total protein contents ranged between 42.6 to 45.0 % and 15.9 to 17.1 %, respectively. Over all three environments and lines, median Zn concentrations for landraces and breeding lines or cultivars were comparable with 50.4 mg kg^{-1} DW for landraces (*n*= 309) and 50.8 mg kg^{-1} DW for cultivars (*n*=164). For the other nutrients Fe, Cu, Mn, C [%] and total protein [%], concentrations were slightly higher in cultivars compared to landraces (Suppl. Tab. S3).

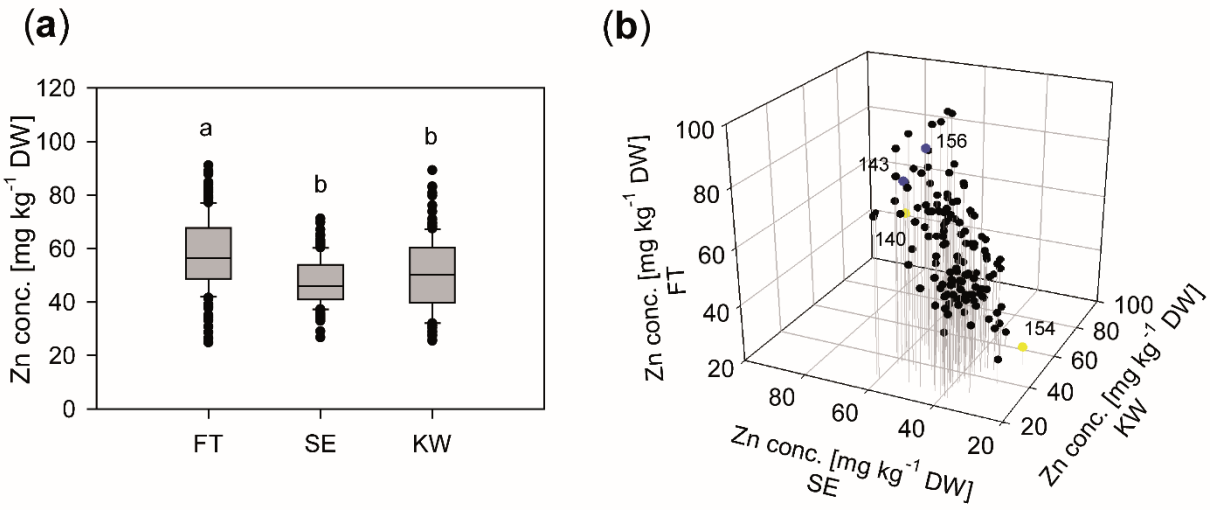

Fig. 1 Variation in zinc (Zn) concentration within a selection of barley accessions from the ICARDA collection. (**a**) Median grain Zn concentrations of barley lines grown in three different environments (FT, SE, KW). Box plots display the median, the upper and lower quartile as well as extremes. The minimum number of accessions analyzed per sample group was 150. (**b**) 3D scatter plot of Zn concentrations for lines grown in the three environments. Lines chosen for further analysis are indicated in blue (high Zn accumulating lines) and yellow (low Zn accumulating lines). *n*=130. DW: Dry weight.

The genotype x environment analyses revealed a strong genotype effect for total protein (77.3 %, Tab. 1), Fe (64.5 %), Zn (58.1 %) and Cu (46.3 %) concentrations. In contrast, Mn (50.8 %) concentrations and C [%] (78.7 %) were more strongly affected by environmental factors. In agreement, H^2 was highest for Fe (0.77) and Zn concentrations (0.73), and lowest for C [%] (0.6) across the three growth environments FT, SE, KW.

Tab. 1 ANOVA table for comparisons of genotype and environment effects on grain zinc (Zn), iron (Fe), manganese (Mn), copper (Cu) concentrations, C [%] and total protein [%]. A set of different barley genotypes were grown in three (Zn, Fe, Mn, Cu, *n*=130) or two (C, total Protein, *n*=146) different environments for the analysis.

Nutrient	Source	Df	Sum Sq	Mean Sq	F value	*P* value	Contribution to variation [%]
Zn	Genotype	129	38891.95	301.49	4.07	≤ 0.001	58.1
	Environment	2	8985.38	4492.69	60.66	≤ 0.001	13.4
	Residuals	258	19109.3	74.07			
Fe	Genotype	129	65839.23	510.38	4.94	≤ 0.001	64.5
	Environment	2	9515.06	4757.53	46.03	≤ 0.001	9.3
	Residuals	258	26667.83	103.36			
Mn	Genotype	129	5190.82	40.24	3.59	≤ 0.001	31.6
	Environment	2	8346.91	4173.45	372.46	≤ 0.001	50.8
	Residuals	258	2890.91	11.21			
Cu	Genotype	129	592.64	4.59	3.11	≤ 0.001	46.3
	Environment	2	306.92	153.46	103.9	≤ 0.001	24.0
	Residuals	258	381.08	1.48			
C	Genotype	145	66.15	0.46	1.96	≤ 0.001	14.1
	Environment	1	370.13	370.13	1591.02	≤ 0.001	78.7
	Residuals	145	33.73	0.23			
Total Protein	Genotype	145	967.8	6.68	5.48	≤ 0.001	77.3
	Environment	1	106.89	106.89	87.72	≤ 0.001	8.5
	Residuals	145	176.68	1.22		≤ 0.001	

The interrelationship between different grain nutrients can provide important information on distribution or storage mechanisms (Fig. 2a, b, Suppl. Tab. S4). Zn was found to be significantly correlated with Fe at r^2=0.58 ($P \leq 0.001$). Regarding correlations of total protein or C [%] and Zn or Fe, correlations were very weak (Fig. 2c, d).

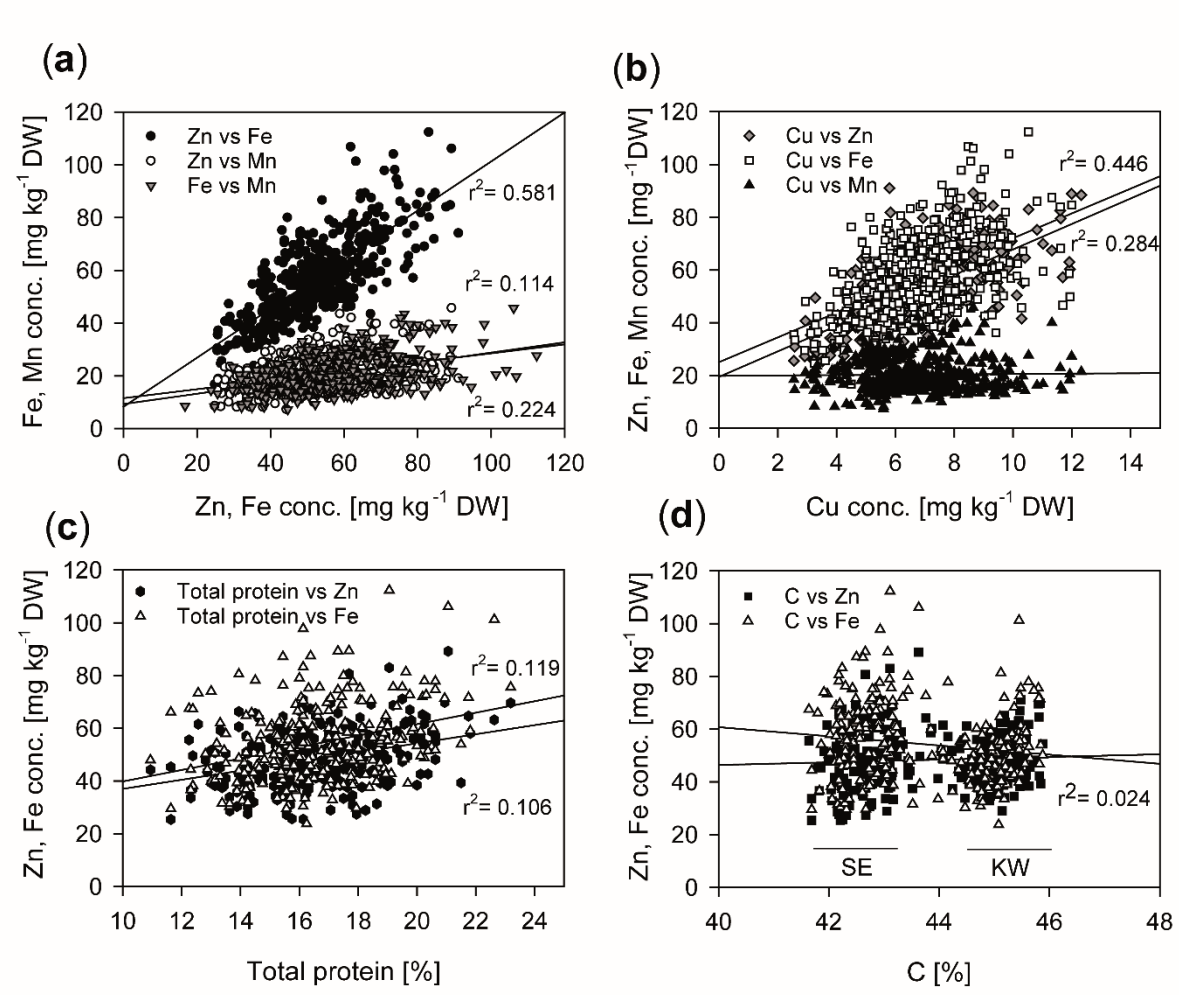

Fig. 2 Correlation of micronutrients, total protein and carbon (C [%]) within the ICARDA collection. (**a**) Regression plots of zinc (Zn) vs iron (Fe), manganese (Mn) and Fe vs Mn (**b**) and regression plots of Cu (copper) vs Zn, Fe and Mn. Regression plots include data from all three environments. (**c**) Regression plots of total protein vs Zn and Fe (**d**) and of C [%] vs Zn and Fe. Regression plots include data from two environments (SE, KW). r^2: coefficient of determination. All displayed coefficients of determination were significant (n=473 (**a**, **b**), n=275 (**c**, **d**)).

For total protein, coefficients of determination were 0.12 ($P \leq 0.001$) and 0.11 ($P \leq 0.001$) for Zn and Fe, respectively. There was a clear clustering of C [%] values for different sites, and only weak correlation (for Fe, coefficient of determination of 0.02 ($P \leq 0.01$))

or no correlation (Zn) with micronutrients. (Fig. 2 d, Suppl. Fig. S5). The correlation between Mn, Cu and total protein was strongly dependent on the environment and coefficients of determination were both higher in SE (Mn: 0.24, $P \leq 0.001$ and Cu: 0.15, $P \leq 0.001$) (Suppl. Fig. S5, Pearson Correlation Coefficients Suppl. Tab. S5, S6). In summary, correlations of Zn and Fe concentrations are stronger and more stable over different environments than correlations between micronutrients and total protein or C [%].

MTAs for micro- and macronutrients varied between different environments

Overall, 76 MTAs were found for the six traits in the three environments and dispersed over 6 of the 7 barley chromosomes (Suppl. Tab. S7, Fig. S6). From grains grown in all environments and BLUEs, 13 MTAs were identified for Zn, 15 MTAs for Cu, 6 MTAs for Fe, 9 MTAs for Mn, 13 MTAs for C [%] and 20 MTAs for protein content. Most MTAs (35) were found on chromosome 2H and were associated with 18 markers. The MTAs found for the different environments FT, SE, KW and BLUEs numbered 10, 20, 25 and 21, respectively. Out of those, 17 markers were significantly associated with more than one trait in the different environments. Most MTAs involving Zn were found on 2H and the most significantly associated markers were 2H │bPb9754 showing an explained phenotypic variation (R^2) of 0.07 in FT, 2H │bPb9199 (R^2 of 0.08 in KW), 2H │bPb1566 (R^2 of 0.03 in SE) and 2H │bPb9754 (R^2 of 0.06 for the BLUEs) (Fig. 3).

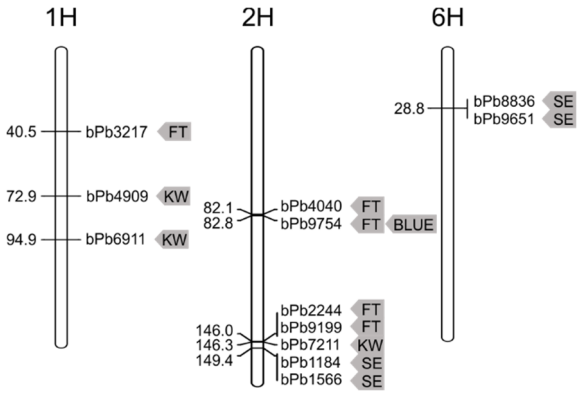

Fig. 3. Significant marker-trait associations (MTAs) for zinc (Zn) concentration in barley seeds grown under different environmental conditions. ICARDA lines were grown in three environments (FT, KW, SE) and data on Zn content in grains were used for GWAS. Best linear unbiased estimates (BLUEs) were calculated across the three environments. All significant MTAs at -log(PM) > 2.5 were mapped on chromosomes 1H, 2H and 6H. Associated DArT markers and marker positions (in cM) are given.

Within ± 0.5 cM of significant MTAs, candidate genes connected to Zn homeostasis were not detected (Suppl. Tab. S8). In close vicinity (± 2.5 cM) of the MTA at 2H │bPb9754 (82.77 cM), we identified two yellow stripe like (YSL) genes. One gene is homologous to *AtYSL2* (*MLOC_40066.*1, position 80.89 cM) and the other one is annotated as *YSL9* (*MLOC_61170.4*, position 80.95 cM) in barley (Suppl. Tab. S9). Both genes, *MLOC_40066.1* and *MLOC_61170.4*, show expression in roots and shoots of seedlings and during grain development (Suppl. Fig. S7).

Over all micronutrients, the marker 2H │bPb4040 revealed highest significant association [-log(P_M) = 3.8 for Cu], whereas for the macronutrients, the marker 2H │bPb2501 at 47 cM achieved highest significance level [-log(P_M) = 5.6] for C [%] of grains grown in KW. The most significant association for protein content was found at 102.4 cM [2H │bPb6194].

In total, eleven pleiotropic loci, i.e. marker loci associated with more than one phenotypic trait, were identified for micronutrients (Suppl. Tab. S8). On chromosome 1H at 72.9 cM, the traits Cu, Mn, Zn were associated with bPb4909. On chromosome 2H between 82.1 and 82.8, Cu and Zn were linked to the same markers bPb4040 and bPb9754 and on chromosome 6H, MTAs for Fe and Zn were associated to bPb8836.

Cultivation under controlled conditions and grain dissection

Based on the broad variation of grain Zn concentrations between 26.4 mg kg^{-1} DW and 83.9 mg kg^{-1} DW in the different environments (Fig. 1b, Suppl. Fig. S8), four lines were selected for further analysis. All lines were six-row barleys and originated from Pakistan (140, 143) or Tunisia (154, 156). Lines 140 and 143 were grouped in subgroup Q4, line 154 in Q3 and line 156 in Q2.

Selected lines were grown under controlled conditions in three different cultivation rounds and ICP-OES measurements on grains confirmed that the selected lines were either low or high Zn accumulating lines (140: 39.4 ± 2.0 mg kg^{-1} DW, 154: 38.4 ± 0.6 mg kg^{-1} DW, 143: 61.2 ± 4.1 mg kg^{-1} DW, 156: 65.3 ± 7.9 mg kg^{-1} DW) (Fig. 4a). Fe concentrations showed significant differences between lines 154 and 156 (Fe: 140: 37.7 ± 4.6 mg kg^{-1} DW, 154: 36.0 ± 0.4 mg kg^{-1} DW, 143: 44.1 ± 2.5 mg kg^{-1} DW, 156: 56.0 ± 10.2 mg kg^{-1} DW) (Fig. 4b). Mn and Cu concentrations in grains of the selected lines were comparable (Fig. 4c, d).

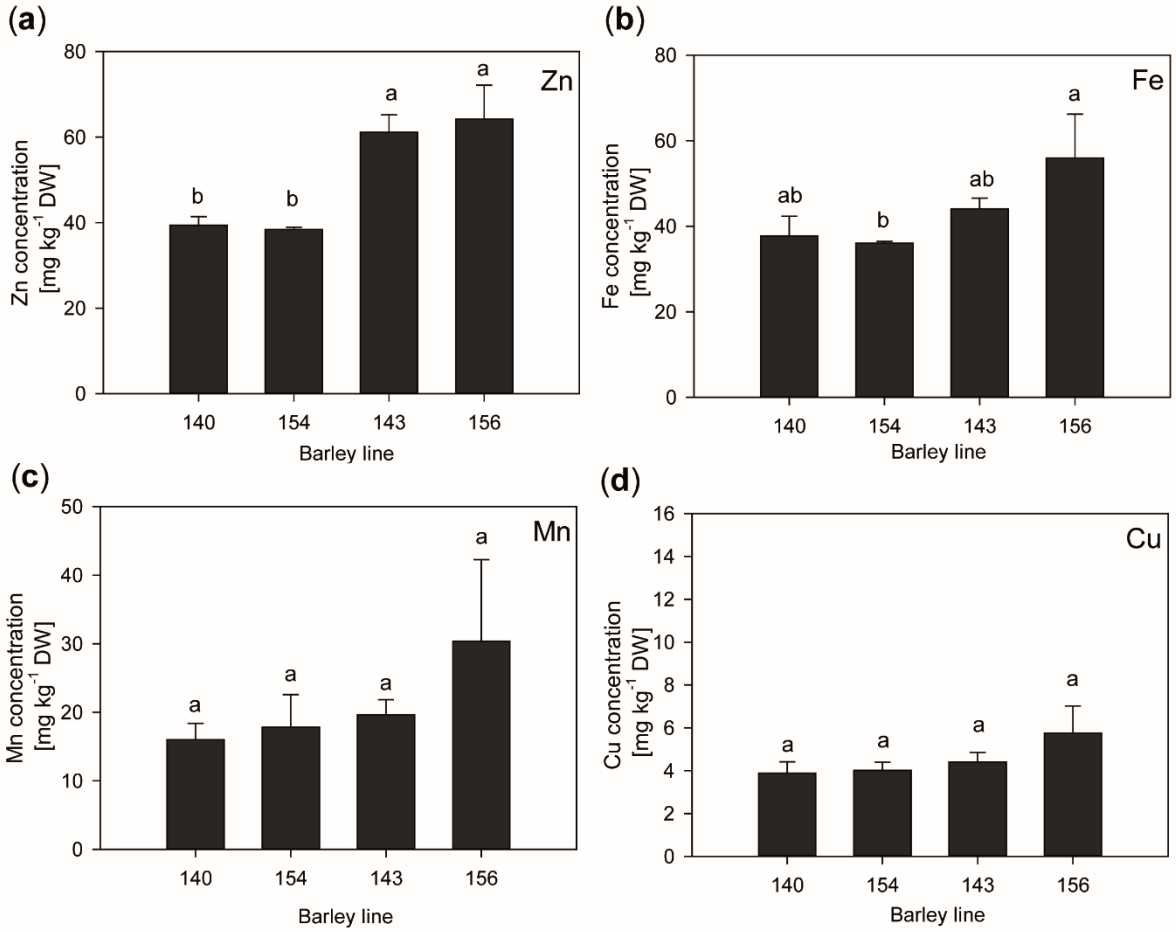

Fig. 4 Zinc (Zn), iron (Fe), copper (Cu) and manganese (Mn) concentration of two contrasting pairs of barley lines in mature grains. (**a**) Grain Zn, (**b**) Fe, (**c**) Mn and (**d**) Cu concentrations of lines 140, 154, 143 and 156 for three different cultivation rounds under controlled conditions in the glasshouse or growth chamber (n=3, 3-5 replicates per cultivation round combined). Values are means + SD. Statistical differences were calculated using ANOVA/Tukey's HSD post hoc test and are displayed as letters ($P \leq 0.05$).

To detect potential hotspots of Zn accumulation in barley grains, whole grains of the selected lines were dissected into embryo, endosperm and husk (Fig. 5). Lines having high Zn concentrations in grains had also elevated Zn concentrations in all separated tissues. Lines showing low Zn concentrations in grains differed significantly from the lines accumulating high Zn concentrations in endosperm tissue (Fig. 5a). The highest Zn concentrations were observed in embryo tissues ranging between 129.0 ± 7.9 mg kg^{-1} DW (154) and 211.8 ± 26.6 mg kg^{-1} DW (143)). Based on the total Zn concentration in the grains, the embryo tissue contributed a

fraction of 0.10 ± 0.02 (154) to 0.13 ± 0.01 (143) while the endosperm comprised a fraction between 0.69 ± 0.02 (156) to 0.77 ± 0.04 (140) (Fig. 5b). Similar patterns were shown for Fe and Cu, whereas for Mn, embryo and husk contributed, taken together, as much to total Mn as the endosperm (Suppl. Fig. S9).

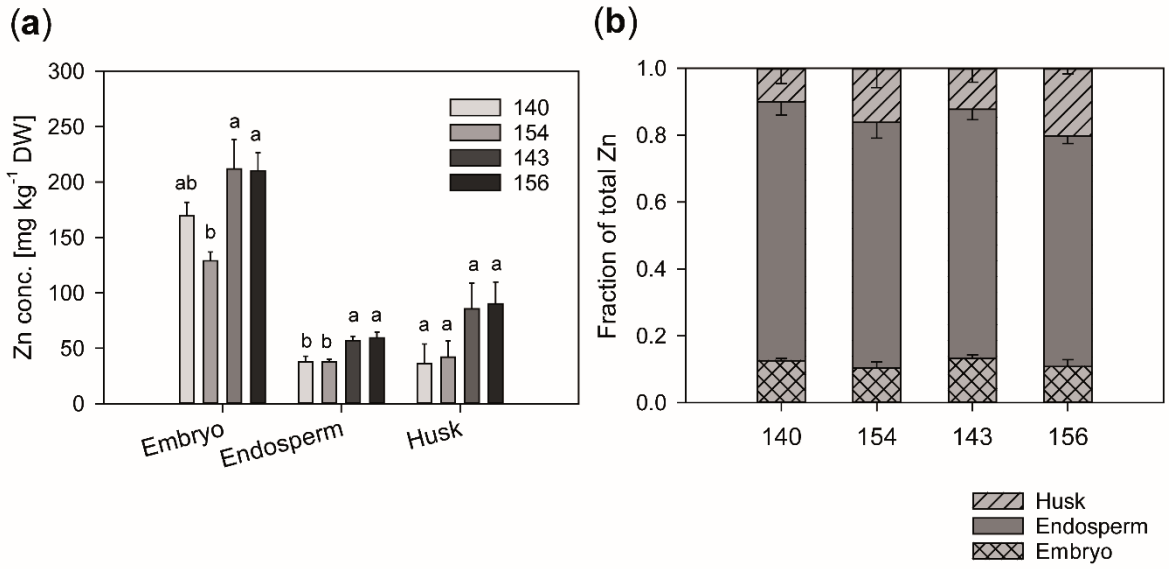

Fig. 5 Zinc (Zn) concentration in different mature seed tissues of two contrasting pairs of barley lines. (**a**) Grain Zn concentrations of embryo, endosperm and husk in four different barley lines (140, 154, 143, 156). (**b**) Fractions of total Zn contributed by different tissues (embryo, endosperm and husk). Fractions were calculated by multiplying the relative weight of each tissue and the corresponding Zn concentration measured for each tissue and referred to the total Zn concentration. Plants were cultivated in three different cultivations in the glasshouse or growth chamber (n=3, 3-5 replicates per cultivation round combined). For each sample, five grains per line and cultivation round were pooled. Values are means + SD. Statistical differences between different lines were calculated for each tissue using ANOVA/Tukey's HSD post hoc test and are displayed as letters ($P \leq 0.05$).

For transcriptome analysis, whole ears and flag leaves were sampled 15 dap and micronutrient concentrations were measured. Zn concentrations of whole ears were mostly consistent with the results for mature grains in the different lines (Fig. 6a). In flag leaves, line 154 showed lower Zn concentrations than the other lines (154: 18.6 ± 1.3 mg kg^{-1} DW, 140: 30.1 ± 10 mg kg^{-1} DW, 143: 40.4 ± 17.5 mg kg^{-1} DW, 156: 50.7 ± 17.9 mg kg^{-1} DW) but this difference was also not significant.

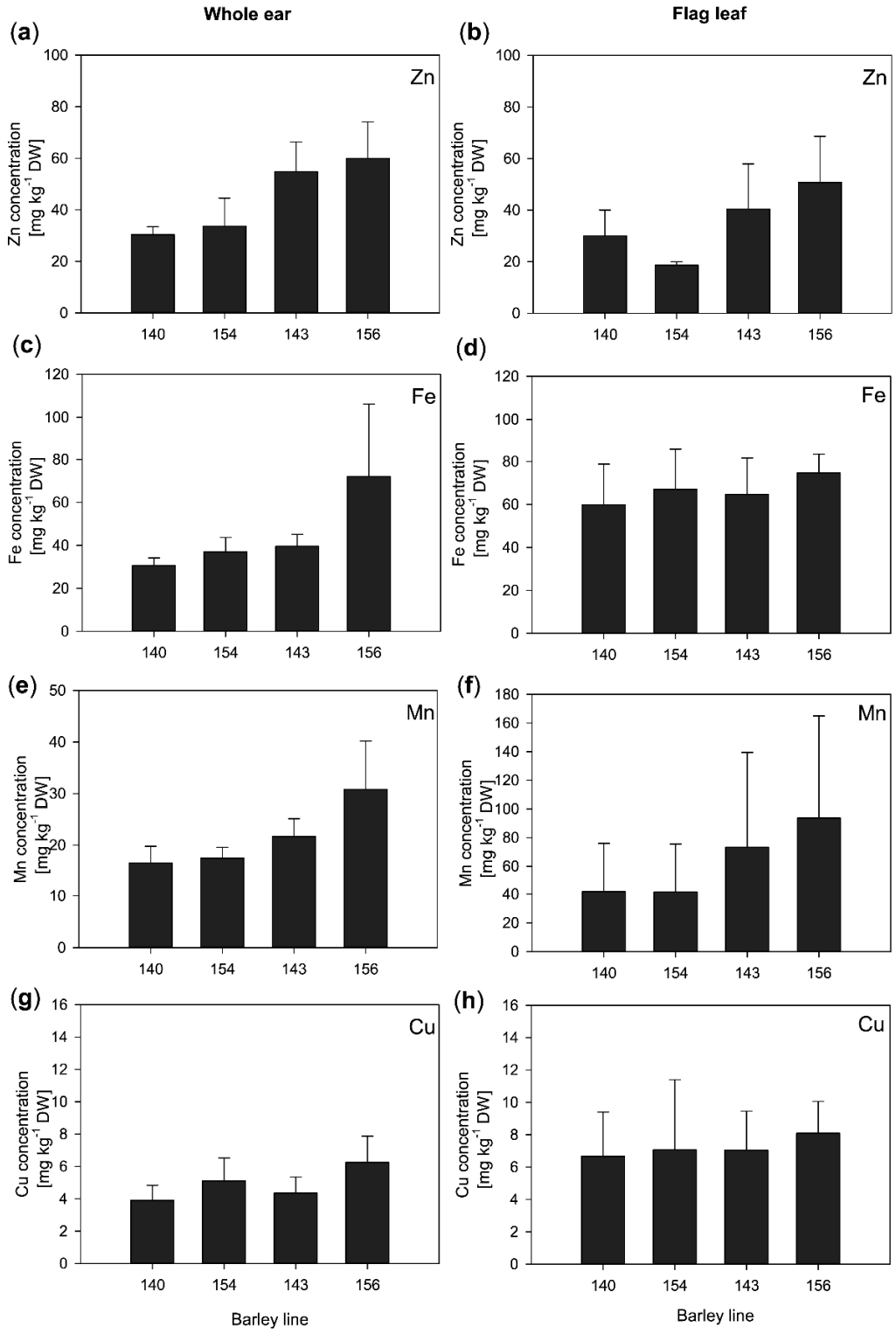

Fig. 6 Zinc (Zn), iron (Fe), copper (Cu) and manganese (Mn) concentrations of two contrasting pairs of barley lines in whole ears and flag leaves 15 days after pollination (dap). (**a**, **c**, **e**, **g**) Metal concentrations in whole ears (**b**, **d**, **f**, **h**) and flag leaves of lines 140, 154, 143 and 156. Plants were cultivated in three different cultivations in the glasshouse or growth chamber (n=3, 3-5 replicates per cultivation round combined). Values are means + SD. Calculation of statistical differences with ANOVA/Tukey's HSD post hoc test ($P \leq 0.05$) did not reveal any significant differences.

For Fe, Mn and Cu, there was a similar pattern between lines in whole ears 15 dap compared to mature grains, but again no significant differences could be detected at 15 dap. Fe and Cu concentrations were comparable between the selected lines in flag leaves at 15 dap, while Mn concentrations were highly variable between the lines. Zn concentrations in whole ears and flag leaves were significantly correlated (r^2: 0.38, P = 0.03, n = 12), whereas Zn concentrations of flag leaves and mature grains were not correlated (r^2=0.17, P = 0.18, n = 12).

Transcriptomic differences in low and high Zn accumulating barley lines

Transcriptome data for independent biological replicates clustered depending on the plant organ sampled (Fig. 7). Lines 140 and 143 clustered for whole ears and were more similar to each other than lines 154 and 156, which is consistent with results obtained in the population structure analysis (Suppl. Fig. S2). Flag leaf transcriptome data clustered depending on cultivation round. Within each cultivation round, lines 140/143 and 154/156 clustered together. In general, PCA of flag leaf transcriptome data indicated a higher variability and a higher influence of external growth factors than found for the transcriptomes of developing ears.

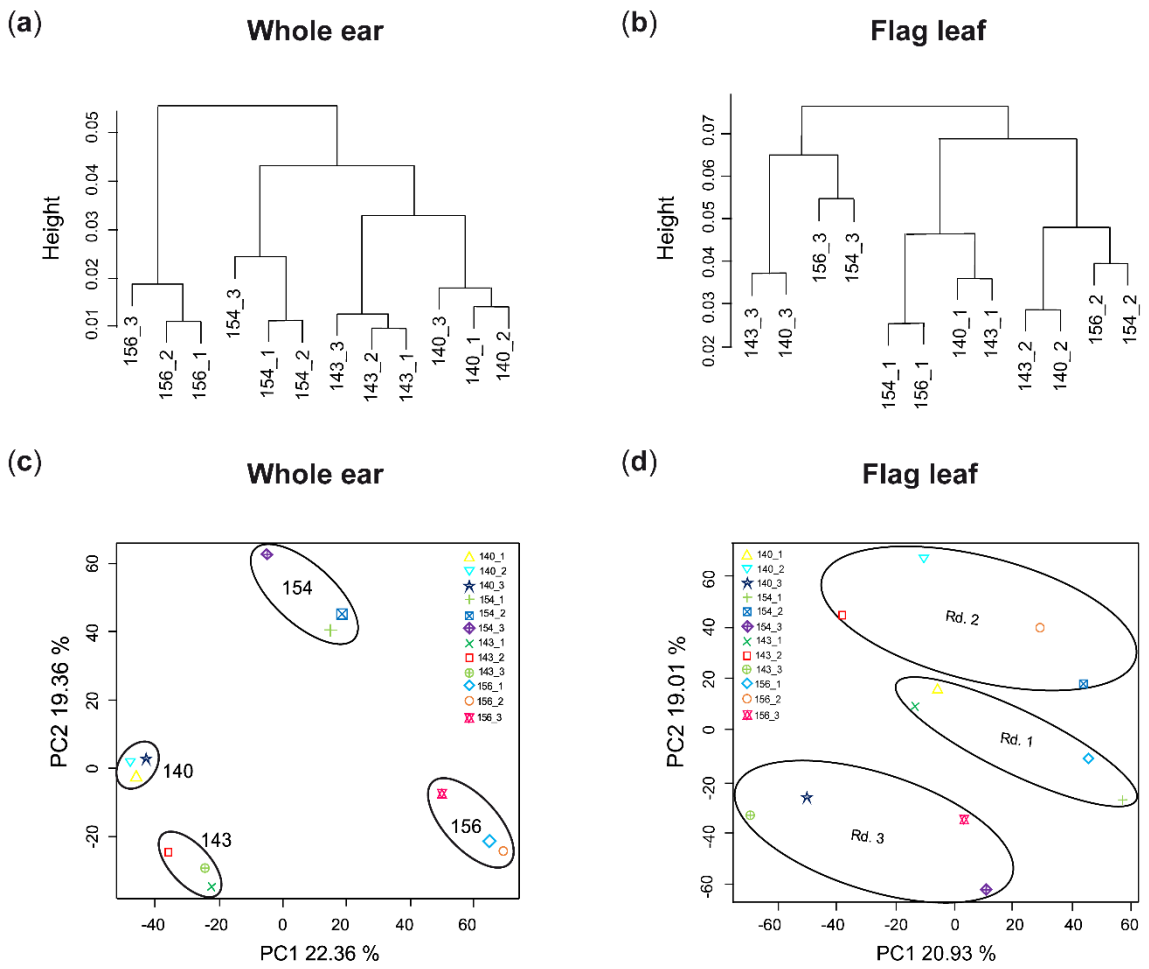

Fig. 7 Clustering of whole ear and flag leaf transcriptomic data. (**a**) Cluster dendrogram of transcripts from whole ears (**b**) and flag leaves. Hclust, method: "pearson". (**c**) Principal component analysis of transcript signals from whole ears (**d**) and flag leaves. *n*=3. Normalization method: GcRMA, *P*-value correction: Bonferroni Hochberg, analysis with RobiNA, multiple testing: nested.F.

Main objective of the transcriptome analyses was to identify genes possibly associated with the differences in grain Zn. Therefore, we searched for transcripts that showed consistent differences in abundance between low Zn cultivars and high Zn cultivars across the four selected cultivars with contrasting grain Zn. Following comparisons of all possible pairs of low vs high Zn cultivars, i.e. 140 vs 143 or 156 and 154 vs, 143 or 156 (Fig. 8), we identified differentially expressed genes shared in all single comparisons.

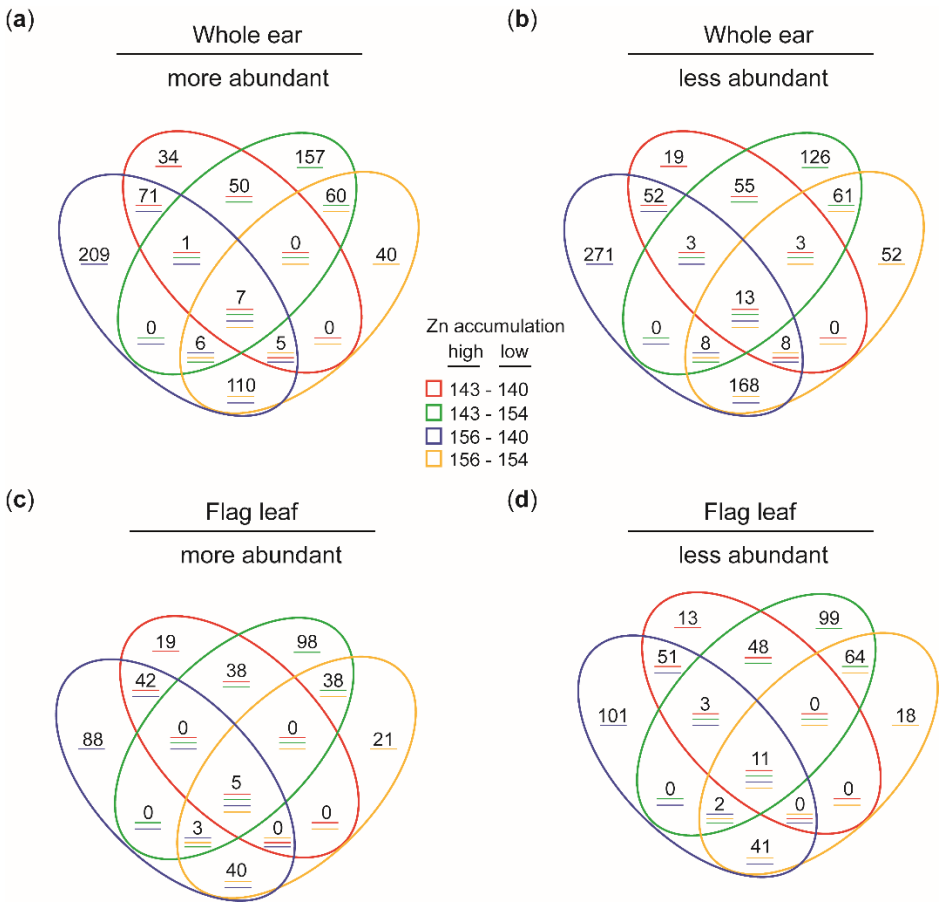

Fig. 8 Differences in transcript abundance between high and low zinc (Zn) lines. (**a**, **b**) Number of genes showing higher or lower transcript abundance in each possible comparison of high Zn (143 and 156) vs low Zn (140 and 154) barley lines 15 days after pollination (dap) in whole ears and (**c**, **d**) flag leaves. Circles are representing comparisons of line 143 vs140 in red, 143 vs 154 in green, 156 vs 140 in blue and 156 vs 154 in light blue. Genes shared between comparisons of different lines are given within circles. Dashes below the corresponding numbers represent the number of single comparisons included (max. 4). Statistical parameters of transcript analysis: *P*-value cutoff: 0.05, log fold change min=1.

In whole ears, 7 genes showed higher and 13 genes lower transcript abundance in high Zn lines compared to low Zn lines. Five and 11 genes with higher and lower transcript abundance, respectively, were found in flag leaves (for full list of genes see Suppl. Tab. S10). The highest difference between transcript levels within one comparison was found for an alpha-amylase/trypsin inhibitor CMb precursor (HB09A04w_s_at) with +8.50 fold higher expression and for an transmembrane protein (similar to *AT5g02160* [*Arabidopsis thaliana*], Contig7943_at) with -7.18 fold lower expression in high compared to low Zn accumulating

lines (Fig. 9). Three genes showed higher transcript abundance in both analyzed tissues in high Zn lines compared to low Zn lines. Through a blastx search, two of the corresponding contigs could be linked to a putative cytochrome P450 and a ribosomal protein S30 homolog, respectively. Conversely, six genes showed lower expression levels in high Zn lines in both tissues. Nineteen out of 26 genes were not assigned to a specific functional category (bin). Blastx searches conducted using exemplar sequences from Affymetrix revealed known conserved domains in nine sequences (Suppl. Tab. S11), adding information to three predicted proteins. This included an exonuclease-endonuclease-phosphatase (EEP) (Contig15482_at), an Ist1 (Contig5646_at) and a DUF247 (Contig10162_s_at) domain superfamily.

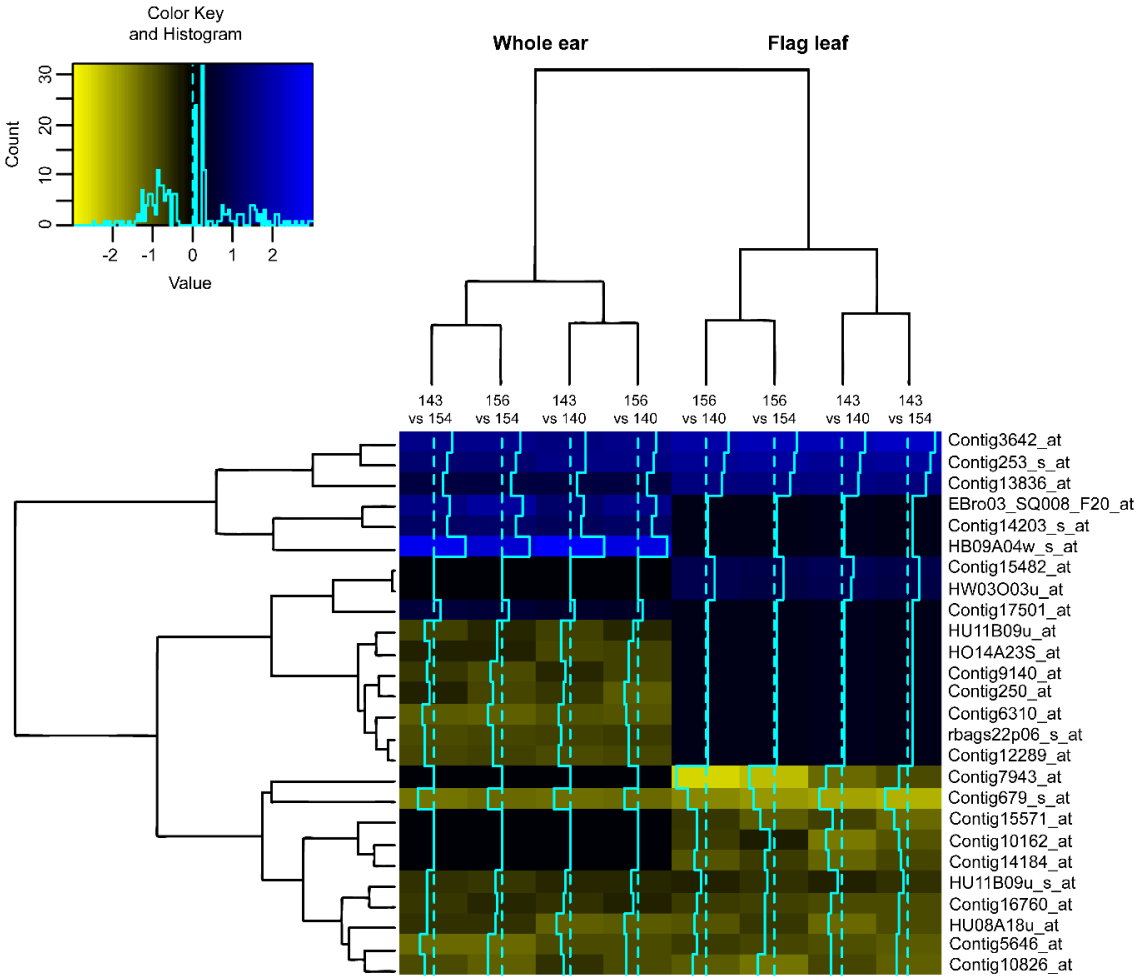

Fig. 9 Heatmap analysis showing differences in transcript abundance in whole ears and flag leaves shared in all possible comparisons of high *vs* low zinc (Zn) lines. Coloured visualization and hierachical clustering of differences in transcript abundance of each comparison of high (143 or 156) vs low (140 or 154) Zn accumulating barley lines 15 days after pollination (dap) in whole ears and flag leaves. Color key displays variation in fold-changes from lower (yellow) to higher (blue) transcript

abundance in high Zn lines compared to low Zn lines. A histogram is shown in light blue. Dendrogram and heatmap were generated with hclust (gplots) in R. Statistical parameters of transcript analysis: *P*-value cutoff: 0.05, log fold change min=1.

Database search for metal related genes

Many of the genes found to show differences in transcript abundance between low and high Zn lines have not yet been assigned a function. Following the roadmap proposed for Zn loading of barley grains (Tauris *et al.*, 2009), we searched for genes that are potentially involved in metal homeostasis and connected those to contigs available on the barley gene chip.

The different searches for putative metal homeostasis genes resulted in 1,447 genes defined by bins, 1,037 by GO terms, 231 by *A. thaliana* blast and 88 genes by ensembl search. 383 of these genes could be identified as or connected to already known metal homeostasis genes (Suppl. Excel file S1). These included barley *YSL* genes (*HvYSL2*, *HvYSL3*, *HvYSL6* and *HvYSL7*). In whole ears and flag leaves none of the putative metal homeostasis genes were differentially expressed in all possible comparisons of high Zn lines with low Zn lines (143 vs 140 or 154 and 156 vs 140 or 154, respectively). We then lowered the stringency of our analysis and included genes that were differentially expressed at least in one comparison between related cultivars with contrasting grain Zn, i.e. when comparing 156 with 154 or 143 with 140. These pairs are more closely related to each other than to the other analyzed cultivars according to the clustering of transcriptome data and assignment to Q-groups. While in flag leaves, none of the defined metal related genes was differentially expressed in any of the single comparisons, Contig25867_at, showed significantly lower transcript abundance in whole ears of both pairwise comparisons of the more related lines (143-140: -1.97 fold and 156-154: -2.04 fold). Blast searches based on the exemplar sequence of the contig revealed high similarity to barley *Metal tolerance protein 5* (*MTP5*: *HORVU1Hr1G071930*, Expect = 7^{e-66}, Identities = 208/252 (82 %). Within the query sequence, a dimerization domain of a zinc transporter was detected (Expect = 1.79^{e-04}). Results of quantitative realtime RT-PCR confirmed data of the microarray analysis with higher relative transcript abundance in low Zn lines compared to high Zn lines within pairs 143-140 and 156-154 (Fig. 10). In addition, analysis of different developmental stages showed that relative transcript abundance of the *MTP5* gene was in all lines higher at 27 dap than at the other two analyzed developmental stages. At 7 dap, no significant difference in relative transcript abundance within each pair was detected, while differences were more pronounced at 27 dap, with significant differences in both pairs. At 27 dap, relative transcript

abundance in low Zn lines was 2.2 fold (154/156) to 2.7 fold (140/143) higher compared to high Zn lines.

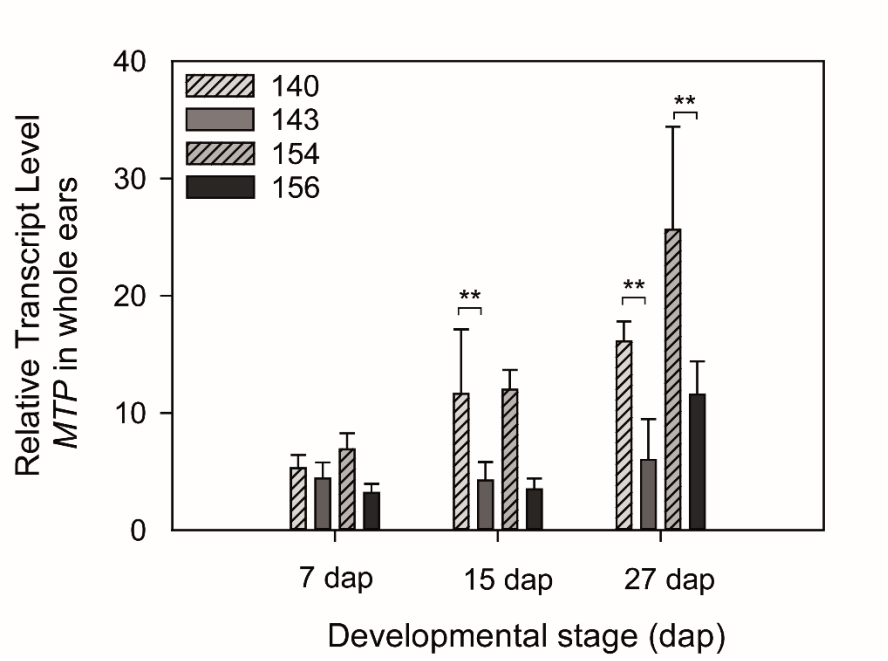

Fig. 10 Transcript levels of the *MTP5* candidate gene at three developmental stages in whole ears of low and high Zn accumulating lines. *MTP5* transcript abundance in whole ears at 7, 15 and 27 days after pollination (dap) in low (140, 154) and high (143, 156) Zn lines. Transcript level was determined relative to *EF1α*. Values are means + SD of three independent experiments (three to five plants of each line were pooled for each data point). Statistical differences were calculated using ANOVA/Tukey's HSD post hoc test on single comparisons of pairs 140/143 and 154/156 and are displayed as asterisks (*, $P \leq 0.05$; **, $P \leq 0.01$; ***, $P \leq 0.001$).

DISCUSSION

Micronutrient deficiencies affect large fractions of the global population (WHO; Muthayya *et al.*, 2013; Ruel-Bergeron *et al.*, 2015). An estimated 2 billion people worldwide are threatened by insufficient Zn supply (Tulchinsky, 2010). Most of them rely on diets that lack diversity and are dominated by cereal grains, which are notoriously poor in bioavailable Zn and also Fe, another undersupplied essential metal (Sandstead, 1991; Clemens, 2014). The ongoing rise in atmospheric CO_2 levels is predicted to further aggravate this problem (Myers *et*

al., 2014; Dietterich *et al.*, 2015). Thus, there is an urgent need to breed for cereals with higher density of bioavailable micronutrients. This has increasingly been realized and drives large-scale programs such as HarvestPlus (www.harvestplus.org). However, modern breeding tools can only be applied when the underlying molecular mechanisms of micronutrient grain loading are known. In crop plants, mechanisms of grain Zn loading are still not well understood. In fact, there are no success stories yet reporting the use of suitable markers to breed for micronutrient enriched cereals (Garcia-Oliveira *et al.*, 2018). While several genes and proteins involved in the uptake, translocation and accumulation of Zn, Fe and other transition metals are known, the factors explaining natural variation in micronutrient density remain unidentified.

The majority of the genes implicated in metal homeostasis of cereals encode metal transporters including members of the Metal Tolerance Protein (MTP) and heavy metal ATPase (HMA) families or enzymes involved in the synthesis of metal chelating molecules (Waters & Sankaran, 2011; Xu *et al.*, 2011; Clemens, 2014; Olsen & Palmgren, 2014). Arguably most advanced is the knowledge for rice. However, rice is predominantly grown in flooded paddy fields, i.e. in conditions with fundamentally altered phytoavailability especially of Fe in the soil. Thus, cereals cultivated in aerated soil need to be studied in detail as well (Reuscher *et al.*, 2016). Barley represents a suitable model system. It is adapted to a wide range of environmental conditions, genetically tractable and shows a wide genetic variation since it has been in cultivation since about 8,000 BC (Zohary *et al.*, 2012). Furthermore, barley seeds are important in Northern Africa and Asia (Grando & Macpherson, 2005). Several studies have already demonstrated a considerable degree of genetically controlled variation in grain micronutrient concentration, i.e. in barley (Ma *et al.*, 2004; Mamo *et al.*, 2014; Detterbeck *et al.*, 2016), wheat (Zhao *et al.*, 2009; Chatzav *et al.*, 2010) and rice (SHI *et al.*, 2009; Pinson *et al.*, 2015). Thus, it appears feasible to identify factors associated with differences in grain Zn concentration.

We selected a representative subset of the ICARDA germplasm for which marker data are available and grew this collection in three different environments to determine the degree of variation in grain micronutrient concentration (Bothmer, 2003; Dawson *et al.*, 2015). The median Zn concentration (Fig. 1a) was similar to other barley collections (Mamo *et al.*, 2014; Detterbeck *et al.*, 2016) while the variation of 3.7 fold was slightly higher than reported for barley germplasm collections grown under controlled conditions (Detterbeck *et al.*, 2016).We found slightly higher median Fe concentrations and with 9.6-fold a higher degree of variation than other studies on different barley panels (Ma *et al.*, 2004; White & Broadley, 2009). Importantly, Fe and Zn concentrations varied little across different environments, resulting in

comparatively high heritability (H^2=0.77 and 0.73, respectively) and a genotype contribution of 64.5 % (Fe) and 58.1 % (Zn) to the total phenotype (Tab. 1). A pronounced heritability for Zn had previously been shown in barley landraces from Ethiopia and Eritrea (H^2=0.65) and in sorghum (H^2=>0.60 for both Zn and Fe) (Mamo *et al.*, 2014; Phuke *et al.*, 2017). Tight genetic control of micronutrient concentration can be interpreted from an evolutionary perspective as arising from the need to provide an adequate supply of nutrients to the progeny via the seed reserves.

Correlations between different macro- and micronutrients may indicate potential overlaps in grain loading pathways. Therefore, we analyzed correlations of Zn with Fe, Mn and Cu as well as with C [%] and total protein (Fig. 2). About 60 % of the variation in Fe concentration could be explained by the Zn concentration in the grain. Comparable findings were reported for barley (Detterbeck *et al.*, 2016), wheat (Cakmak *et al.*, 2004; Morgounov *et al.*, 2007; Peleg *et al.*, 2008; Zhao *et al.*, 2009; Chatzav *et al.*, 2010; Guttieri *et al.*, 2015), rice (Jiang *et al.*, 2007), sorghum (Phuke *et al.*, 2017), pearl millet (Bashir *et al.*, 2014) and black gram (Singh *et al.*, 2017). These results suggest that Zn and Fe are at least partially sharing metal transporters and/or low molecular weight chelators.

The only molecularly understood QTL explaining differences in cereal micronutrient concentration is the Gpc-B1 locus in wheat (Uauy *et al.*, 2006). Allelic variation at this locus, which encodes a transcription factor, affects protein, Fe, and Zn concentration of the grain. On the other hand, there are indications that in wheat grain more Zn than Fe is bound to proteins (Persson *et al.*, 2009; Eagling *et al.*, 2014). Therefore, it is also important to investigate how Zn concentration is correlated with other grain components. Our results suggest that both, Zn and Fe, were correlated with total protein rather than with C [%]. This appears to be similar in wheat, while in rice, a slight, albeit non-significant, negative correlation between Zn or Fe and protein content was found (Anandan *et al.*, 2011). However, correlations were highly affected by different environments in our experiments indicating that other binding environments than storage proteins or C [%] play important roles.

Based on the observed variation in grain Zn we followed two strategies to find candidate genes possibly contributing to differences between barley accessions. First, the available marker data for the analyzed ICARDA collection were used to map loci associated with grain Zn. Second, pairs of contrasting lines were selected for in-depth analysis including transcript analysis of ears and flag leaves.

Zn accumulation is a quantitative inherited trait and was affected by seven loci on chromosomes 1H, 2H, and 6H for grains grown across three different environments (Fig 3). By using 54 introgression lines, Reuscher *et al.* demonstrated that markers in comparable regions such as on chromosome 1H (64.8 – 90.9 cM) and 2H (34.3 – 66.8 cM) were also associated with differences in Zn concentrations (Reuscher *et al.*, 2016). Furthermore, they found a candidate gene on chromosome 2H that showed highest sequence similarity to the *A. thaliana ZIP1* and the rice *OsZIP3* gene, members of the Zinc-regulated transporter Iron-regulated Protein (ZIP) family proposed to be involved in Zn^{2+} uptake (Reuscher *et al.*, 2016). Based on the latest barley genome sequence (Mascher *et al.*, 2017), this gene could be the one now annotated as *Zinc transporter gene 8* (*HORVU2Hr1G025400*). It is located near the centromeric region between 725,227,365 and 725,232,183 bp. The closest marker associated to Zn concentration found in our analysis was bPb4040 at 82.1 cM, which may correspond to a physical position of 663,877,529, indicating that a gene other than the *Zinc transporter gene 8* affects the Zn concentration in the ICARDA panel. Furthermore, by using 336 cultivars of a barley breeding program from ICARDA among others, three QTL regions were identified on chromosomes 2H, 3H and 5H (Gyawali *et al.*, 2017). Again, on chromosome 2H at 87.3 cM, the locus was in close vicinity to the MTAs for Zn concentration in the FT environment and for BLUEs located at 2H│bPb9754 (82.77 cM). Within a range of ±2.5 cM of this most relevant marker on chromosome 2H, two genes were detected that belong to the yellow stripe-like (YSL) transporter family. A few YSL proteins have been shown or hypothesized to transport metals that are bound to nicotianamine (NA) and phytosiderophores (PS) and several family members have been implicated in Fe and Zn transport into grains (Waters *et al.*, 2006; Chu *et al.*, 2010; Conte & Walker, 2012). *HvYSL9* is expressed throughout the grain with exception of the embryo (Tauris *et al.*, 2009). Tauris and colleagues suggested that YSL transporters could play a role in transferring Zn-NA complexes from the endosperm cavity into the apoplast of transfer cells and between testa and aleurone (Tauris *et al.*, 2009). Increased transport capability from maternal to filial tissues could explain the overall higher Zn concentrations in different grain tissues we identified in the high Zn accumulating lines. *AtYSL3* was found to be important for loading of metals into the seeds (Chu *et al.*, 2010). In rice, *YSL9* was found to play an important role in Fe(II)-NA and Fe(III)-deoxymugineic translocation from endosperm to embryo in the seeds, especially at peripheral and inner parts of the endosperm near the embryo (Senoura *et al.*, 2017). We observed elevated Zn in the endosperm near the embryo when barley grains were analyzed by μ-PIXE (Detterbeck *et al.*, 2016). Thus, the locus on chromosome 2H could potentially play an important role in Zn accumulation and the YSL transporters are interesting

candidates for further investigation of Zn grain accumulation differences in barley. Future studies will have to show whether polymorphisms and/or expression differences for the *YSL* genes exist between barley accessions and whether they can be directly associated with grain Zn. Transcriptome analyses of the very limited set of four barley lines did not reveal significant differences.

Several observations indicate that breeding for high yield has selected against micronutrient density, especially in bread wheat cultivars (Fan *et al.*, 2008; Zhao *et al.*, 2009). This and the dilution effect of larger endosperm explains why the nutritional value of bred crops often seems to be lower than of landraces (Hebelstrup, 2017). In our study, however, Zn concentrations varied to the same extent in landraces and barley cultivars with highly comparable median Zn concentrations (Suppl. Tab. S3). Landraces are commonly understood as locally adapted varieties that evolved because of natural and non-targeted human selection. Due to their specific allele combinations, landraces may reveal variations in morphological, quality and yield characteristics and can harbor important genes for plant breeding (Pinheiro de Carvalho, M. A. A. *et al.*, 2013). For example, many barley landraces originate from Zn deficient soils (Reuscher *et al.*, 2016) and could therefore carry alleles supporting higher Zn efficiency. We chose four landraces, two pairs of genetically related lines with contrasting grain Zn across the different environments, for detailed analysis under controlled conditions (Fig. 4).

In the context of biofortification, the distribution of Zn within the grain is relevant because only parts of the grain are consumed. Therefore, we dissected mature barley grains into husk, embryo and endosperm tissues (Fig. 5). Cultivars that show high Zn accumulation have higher Zn concentrations in all grain tissues, including the endosperm, i.e. the part that remains after milling. This result is consistent with a previous study that employed metal imaging via EXAFS (Detterbeck *et al.*, 2016) and was found for wheat as well (Zhang *et al.*, 2010; Eagling *et al.*, 2014; Liu *et al.*, 2017). It suggests that Zn trafficking from maternal to filial tissues including the loading zones of the grain is the major factor causing accumulation differences. Additionally, high Zn lines could have more Zn storage capability across the different grain tissues (Xue *et al.*, 2014; Guttieri *et al.*, 2015). To date no genes have been directly linked to variation in grain micronutrient loading or sink strength. Hence, transgenic approaches aim to analyze mechanisms of micronutrient accumulation in the grain by expressing transporters such as heavy metal ATPase 2 (HMA2) (Palmgren *et al.*, 2008; Tan *et al.*, 2013; Menguer *et al.*, 2017). Functional analysis of *Ta*HMA2 showed an implication in Zn and cadmium (Cd) transport with decreased Zn concentrations in the grains in *TaHMA2* over-expressing rice and

wheat (Tan *et al.*, 2013). Examples like this elucidate the potential of transgenic approaches in gaining mechanistic insights into micronutrient loading of the grain.

Laser dissection-assisted transcript analysis of barley grain tissues had suggested a roadmap of Zn trafficking (Tauris *et al.*, 2009). In order to determine whether genes on or beyond this roadmap can be linked to differences in grain Zn, whole ears and flag leaves were harvested 15 dap and micronutrient concentrations were determined (Fig. 6). At 15 dap, all grain tissues are differentiated and the grain filling process takes place (Sreenivasulu *et al.*, 2010; Pielot *et al.*, 2015). In whole ears, the patterns of low or high Zn lines were the same at 15 dap and maturity. Interestingly, we measured slightly lower micronutrient concentrations at 15 dap compared to mature grains. These results are in contrast to observations made in wheat, where Zn concentrations decreased by 45 % until 27 dap and remained stable until maturity (Ozturk *et al.*, 2006). These results indicate stringent control over micronutrient levels in low or high Zn lines during grain development.

There are two possible pathways for Zn translocation towards the reproductive tissues: Zn is either directly mobilized from the soil and transported to the developing grain or previously stored Zn is remobilized from the flag leaves (Palmgren *et al.*, 2008; Waters *et al.*, 2009; Impa *et al.*, 2013; Sperotto, 2013; Maillard *et al.*, 2015; Hussain *et al.*, 2016; Reuscher *et al.*, 2016). Therefore, flag leaves were included in the analysis. However, in flag leaves, there was no obvious correlation connecting flag leaf micronutrient concentration to grain micronutrient concentration at maturity. Also, analysis of microarray data grouped flag leaf samples based on cultivation round, not genotype (Fig. 7). In contrast, for whole ears, transcriptome data of the single lines clustered together, indicating a stronger influence of environmental factors on gene expression in flag leaves relative to whole ears.

For transcriptome analysis, we first searched for genes differentially expressed in all four possible comparisons between high and low Zn lines. This stringent approach resulted in a relatively small number of differentially expressed genes (DEGs) shared in both groups (Fig.8). Within these DEGs, 19 out of 26 were not assigned yet and could not be connected to any function or annotation. As no genes encoding metal transporters or enzymes involved in the synthesis of Zn ligands were present in our list, we performed further database searches to link more genes of the barley gene chip to metal homeostasis genes. These included well known families such as HMA, YSL, ZIP, CDF (cation diffusion facilitator), Nramp (natural resistance-associated protein), VIT (vacuolar iron transporter), CAX (cation exchanger), NAS

(nicotianamine synthase), ZIF (zinc-induced-facilitator), ZIFL (Zinc induced facilitator-like), MT (metallothionein), NAAT (nicotianamine aminotransferase), PME (pectin methylesterase) or PCS (phytochelatin synthase). A total of 383 genes could be assigned a putative function in metal transport, trafficking or storage based on similarity to already known metal homeostasis related genes (Suppl. Excel file S1/Word File S1). None of these genes was significantly higher or lower expressed in both high Zn lines compared to both low Zn lines. When searching for genes differentially expressed in single related pairs of contrasting lines, a transcript similar to barley *metal tolerance protein 5* (*HvMTP5)* was found to be significantly less abundant in high Zn lines compared to low Zn lines. Blast searches based on the exemplar sequence implicated a function in Zn transport. CDFs, or *in planta* also known as MTPs, are membrane bound transporters involved in Zn efflux from cytoplasm to cellular compartments, e.g. the vacuoles (Ricachenevsky *et al.*, 2013). *Hv*MTP1 was previously identified to transport Zn and cobalt (Co) and to be expressed in phloem and aleurone cells in the grain (Tauris *et al.*, 2009; Podar *et al.*, 2012). Recently, transgenic barley plants expressing *HvMTP1* under control of an endosperm-specific promotor were shown to contain higher Zn concentrations in the grain compared to the reference line *cv.* `Golden Promise`, possibly because sink strength of the endosperm was enhanced. In contrast, we would have to postulate that MTP5 is involved in the trapping of Zn within cells along the loading pathway in maternal tissue and thereby reduce the availability of Zn for transfer to filial tissues. However, at this stage we do not have detailed information on where exactly *MTP5* is expressed. Also, we do not know if expression is responsive to Zn supply. To our knowledge, this study contributes the first transcriptome data exploring natural variation in barley grain Zn accumulation. Our GWAS and transcriptome analyses indicate a potential role of YSL and MTP transporters. Now, more in depth studies such as targeted knockouts of promising transporter genes are needed to investigate the specific involvement of the annotated genes in Zn accumulation.

ACKNOWLEDGEMENTS

We thank Angelika Mustroph, Department of Biology, University of Bayreuth, for the help with blastp searches regarding *A. thaliana* metal homeostasis genes and with microarray data analysis. We are grateful to Stefan Holzheu, Bayreuth Center for Ecology and

Environmental Research, University of Bayreuth, for his advice on statistical analysis, and to Christiane Meinen, Pia Schuster and Silke Matros for their expert technical assistance.

FUNDING

This work was in part financially supported by the European Union through its Sixth Framework Program for RTD (contract no FOOD-CT-2006- 016253). Funding was also supplied from the Independent Research Fund Denmark - Natural Sciences (grant 4002-00181; The molecular Fe and Zn speciation in cereals: Unravelling the chemistry controlling human bioavailability of essential trace elements).

AUTHOR CONTRIBUTION

AD, SR, MW, DPP and VC performed experiments; AD, MN, AB, JKS and SC planned experiments and analyzed data. AD, MN and SC wrote the paper. All authors approved the final version.

COMPETING INTERESTS

The Authors declare that there are no competing interests associated with the manuscript.

REFERENCES

Anandan, A, Rajiv, G, Eswaran, R, Prakash, M. 2011. Genotypic variation and relationships between quality traits and trace elements in traditional and improved rice (*Oryza sativa* L.) genotypes. Journal of food science 76: H122-30.

Bashir, EMA, Ali, AM, Ali, AM, Melchinger, AE, Parzies, HK, Haussmann, BIG. 2014. Characterization of Sudanese pearl millet germplasm for agro-morphological traits and grain nutritional values. Plant Genetic Resources 12: 35–47.

Bewley, JD, Black, M. 2013. Seeds. Physiology of Development and Germination: Springer US.

Bothmer, Rv. 2003. Diversity in barley. (*Hordeum vulgare*). Amsterdam, Boston: Elsevier.

Bradbury, PJ, Zhang, Z, Kroon, DE, Casstevens, TM, Ramdoss, Y, Buckler, ES. 2007. TASSEL: software for association mapping of complex traits in diverse samples. Bioinformatics (Oxford, England) 23: 2633–2635.

Cakmak, I, Turun, A, Millet, E, Feldman, M, Fahima, T, Korol, A, Nevo, E, Braun, HJ, Ozkan, H. 2004. *Triticum dicoccoides*. An important genetic resource for increasing zinc and iron concentration in modern cultivated wheat. Soil Science and Plant Nutrition 50: 1047–1054.

Cao, F, Chen, F, Sun, H, Zhang, G, Chen, Z-H, Wu, F. 2014. Genome-wide transcriptome and functional analysis of two contrasting genotypes reveals key genes for cadmium tolerance in barley. BMC genomics 15: 611.

Chatzav, M, Peleg, Z, Ozturk, L, Yazici, A, Fahima, T, Cakmak, I, Saranga, Y. 2010. Genetic diversity for grain nutrients in wild emmer wheat. Potential for wheat improvement. Annals of botany 105: 1211–1220.

Chu, H-H, Chiecko, J, Punshon, T, Lanzirotti, A, Lahner, B, Salt, DE, Walker, EL. 2010. Successful reproduction requires the function of *Arabidopsis* Yellow Stripe-Like1 and Yellow Stripe-Like3 metal-nicotianamine transporters in both vegetative and reproductive structures. Plant physiology 154: 197–210.

Clemens, S. 2014. Zn and Fe biofortification. The right chemical environment for human bioavailability. Plant Sci. 225: 52–57.

Conte, SS, Walker, EL. 2012. Genetic and biochemical approaches for studying the yellow stripe-like transporter family in plants. Current topics in membranes 69: 295–322.

Darnton-Hill, I, Nalubola, R. 2002. Fortification strategies to meet micronutrient needs: successes and failures. The Proceedings of the Nutrition Society 61: 231–241.

Dawson, IK, Russell, J, Powell, W, Steffenson, B, Thomas, WTB, Waugh, R. 2015. Barley. A translational model for adaptation to climate change. New Phytologist 206: 913–931.

Deinlein, U, Weber, M, Schmidt, H, Rensch, S, Trampczynska, A, Hansen, TH, Husted, S, Schjoerring, JK, Talke, IN, Kramer, U, Clemens, S. 2012. Elevated Nicotianamine Levels in *Arabidopsis halleri* Roots Play a Key Role in Zinc Hyperaccumulation. THE PLANT CELL ONLINE 24: 708–723.

Detterbeck, A, Pongrac, P, Rensch, S, Reuscher, S, Pecovnik, M, Vavpetic, P, Pelicon, P, Holzheu, S, Kramer, U, Clemens, S. 2016. Spatially resolved analysis of variation in barley (*Hordeum vulgare*) grain micronutrient accumulation. The New phytologist 211: 1241–1254.

Dietterich, LH, Zanobetti, A, Kloog, I, Huybers, P, Leakey, ADB, Bloom, AJ, Carlisle, E, Fernando, N, Fitzgerald, G, Hasegawa, T, Holbrook, NM, Nelson, RL, Norton, R, Ottman, MJ, Raboy, V, Sakai, H, Sartor, KA, Schwartz, J, Seneweera, S, Usui, Y, Yoshinaga, S, Myers, SS. 2015. Impacts

of elevated atmospheric CO_2 on nutrient content of important food crops. Scientific Data 2. 150036.

Eagling, T, Neal, AL, McGrath, SP, Fairweather-Tait, S, Shewry, PR, Zhao, F-J. 2014. Distribution and Speciation of Iron and Zinc in Grain of Two Wheat Genotypes. Journal of Agricultural and Food Chemistry 62: 708–716.

Faccioli, P, Ciceri, GP, Provero, P, Stanca, AM, Morcia, C, Terzi, V. 2007. A combined strategy of "*in silico*" transcriptome analysis and web search engine optimization allows an agile identification of reference genes suitable for normalization in gene expression studies. Plant molecular biology 63: 679–688.

Fan, M-S, Zhao, F-J, Fairweather-Tait, SJ, Poulton, PR, Dunham, SJ, McGrath, SP. 2008. Evidence of decreasing mineral density in wheat grain over the last 160 years. Journal of trace elements in medicine and biology: organ of the Society for Minerals and Trace Elements (GMS) 22: 315–324.

Garcia-Oliveira, AL, Chander, S, Ortiz, R, Menkir, A, Gedil, M. 2018. Genetic Basis and Breeding Perspectives of Grain Iron and Zinc Enrichment in Cereals. Frontiers in Plant Science 9: 937.

Gómez-Galera, S, Rojas, E, Sudhakar, D, Zhu, C, Pelacho, AM, Capell, T, Christou, P. 2010. Critical evaluation of strategies for mineral fortification of staple food crops. Transgenic research 19: 165–180.

Grando, S, Macpherson, HG. 2005. Food Barley: Importance, Uses and Local Knowledge. Proceedings of the International Workshop on Food Barley Improvement, 14-17 January 2002, Hammamet, Tunisia. Aleppo, Syria.

Gubatz, S, Dercksen, VJ, Brüss, C, Weschke, W, Wobus, U. 2007. Analysis of barley (*Hordeum vulgare*) grain development using three-dimensional digital models. The Plant Journal 52: 779–790.

Guttieri, MJ, Baenziger, PS, Frels, K, Carver, B, Arnall, B, Waters, BM. 2015. Variation for Grain Mineral Concentration in a Diversity Panel of Current and Historical Great Plains Hard Winter Wheat Germplasm. Crop Science 55: 1035.

Gyawali, S, Otte, ML, Chao, S, Jilal, A, Jacob, DL, Amezrou, R, Verma, RPS. 2017. Genome wide association studies (GWAS) of element contents in grain with a special focus on zinc and iron in a world collection of barley (*Hordeum vulgare* L.). Journal of Cereal Science 77: 266–274.

Hebelstrup, KH. 2017. Differences in nutritional quality between wild and domesticated forms of barley and emmer wheat. Plant Sci. 256: 1–4.

Hothorn, T, Bretz, F, Westfall, P. 2008. Simultaneous inference in general parametric models. Biometrical journal. Biometrische Zeitschrift 50: 346–363.

Hussain, S, Rengel, Z, Mohammadi, SA, Ebadi-Segherloo, A, Maqsood, MA. 2016. Mapping QTL associated with remobilization of zinc from vegetative tissues into grains of barley (*Hordeum vulgare*). Plant and Soil 399: 193–208.

Impa, SM, Morete, MJ, Ismail, AM, Schulin, R, Johnson-Beebout, SE. 2013. Zn uptake, translocation and grain Zn loading in rice (*Oryza sativa* L.) genotypes selected for Zn deficiency tolerance and high grain Zn. Journal of Experimental Botany 64: 2739–2751.

International Barley Genome Sequencing, Mayer, KF, Waugh, R, Brown, JWS, Schulman, A, Langridge, P, Platzer, M, Fincher, GB, Muehlbauer, GJ, Sato, K, Close, TJ, Wise, RP, Stein, N. 2012. A physical, genetic and functional sequence assembly of the barley genome. Nature 491: 711–716.

Jiang, SL, Wu, JG, Feng, Y, Yang, XE, Shi, CH. 2007. Correlation analysis of mineral element contents and quality traits in milled rice (*Oryza stavia* L.). Journal of Agricultural and Food Chemistry 55: 9608–9613.

Jilal, A, Grando, S, Henry, RJ, Lee, LS, Rice, N, Hill, H, Baum, M, Ceccarelli, S. 2008. Genetic diversity of ICARDA's worldwide barley landrace collection. Genetic Resources and Crop Evolution 55: 1221–1230.

Liu, D, Liu, Y, Zhang, W, Chen, X, Zou, C. 2017. Agronomic Approach of Zinc Biofortification Can Increase Zinc Bioavailability in Wheat Flour and thereby Reduce Zinc Deficiency in Humans. Nutrients 9(5): 465.

Liu, G. 2003. NetAffx. Affymetrix probesets and annotations. Nucleic Acids Research 31: 82–86.

Ma, JF, Higashitani, A, Sato, K, Takeda, K. 2004. Genotypic variation in Fe concentration of barley grain. Soil Science and Plant Nutrition 50: 1115–1117.

Maillard, A, Diquélou, S, Billard, V, Laîné, P, Garnica, M, Prudent, M, Garcia-Mina, J-M, Yvin, J-C, Ourry, A. 2015. Leaf mineral nutrient remobilization during leaf senescence and modulation by nutrient deficiency. Frontiers in plant science 6: 317.

Mamo, BE, Barber, BL, Steffenson, BJ. 2014. Genome-wide association mapping of zinc and iron concentration in barley landraces from Ethiopia and Eritrea. Journal of Cereal Science 60: 497–506.

Mariotti, F, Tomé, D, Mirand, PP. 2008. Converting nitrogen into protein - beyond 6.25 and Jones' factors. Critical reviews in food science and nutrition 48: 177–184.

Mascher, M, Gundlach, H, Himmelbach, A, Beier, S, Twardziok, SO, Wicker, T, Radchuk, V, Dockter, C, Hedley, PE, Russell, J, Bayer, M, Ramsay, L, Liu, H, Haberer, G, Zhang, X-Q, Zhang, Q, Barrero, RA, Li, L, Taudien, S, Groth, M, Felder, M, Hastie, A, Šimková, H, Staňková, H, Vrána, J, Chan, S, Muñoz-Amatriaín, M, Ounit, R, Wanamaker, S, Bolser, D, Colmsee, C, Schmutzer, T, Aliyeva-Schnorr, L, Grasso, S, Tanskanen, J, Chailyan, A, Sampath, D, Heavens, D, Clissold, L, Cao, S, Chapman, B, Dai, F, Han, Y, Li, H, Li, X, Lin, C, McCooke, JK, Tan, C, Wang, P, Wang, S, Yin, S, Zhou, G, Poland, JA, Bellgard, MI, Borisjuk, L, Houben, A, Doležel, J, Ayling, S, Lonardi, S, Kersey, P, Langridge, P, Muehlbauer, GJ, Clark, MD, Caccamo, M, Schulman, AH, Mayer, KFX, Platzer, M, Close, TJ, Scholz, U, Hansson, M, Zhang, G, Braumann,

I, Spannagl, M, Li, C, Waugh, R, Stein, N. 2017. A chromosome conformation capture ordered sequence of the barley genome. Nature 544: 427.

Mendiburu, F. 2013. agricolae. Statistical Procedures for Agricultural Research. R package version 1.1-6.

Menguer, PK, Vincent, T, Miller, AJ, Brown, JKM, Vincze, E, Borg, S, Holm, PB, Sanders, D, Podar, D. 2017. Improving zinc accumulation in cereal endosperm using HvMTP1, a transition metal transporter. Plant biotechnology journal.

Morgounov, A, Gómez-Becerra, HF, Abugalieva, A, Dzhunusova, M, Yessimbekova, M, Muminjanov, H, Zelenskiy, Y, Ozturk, L, Cakmak, I. 2007. Iron and zinc grain density in common wheat grown in Central Asia. Euphytica 155: 193–203.

Murgia, I, Arosio, P, Tarantino, D, Soave, C. 2012. Biofortification for combating 'hidden hunger' for iron. Trends in plant science 17: 47–55.

Muthayya, S, Rah, JH, Sugimoto, JD, Roos, FF, Kraemer, K, Black, RE. 2013. The global hidden hunger indices and maps. An advocacy tool for action. PLoS ONE 8: e67860.

Myers, SS, Zanobetti, A, Kloog, I, Huybers, P, Leakey, Andrew D B, Bloom, AJ, Carlisle, E, Dietterich, LH, Fitzgerald, G, Hasegawa, T, Holbrook, NM, Nelson, RL, Ottman, MJ, Raboy, V, Sakai, H, Sartor, KA, Schwartz, J, Seneweera, S, Tausz, M, Usui, Y. 2014. Increasing CO_2 threatens human nutrition. Nature 510: 139–142.

Nagel, M, Kranner, I, Neumann, K, Rolletschek, H, Seal, CE, Colville, L, Fernandez-Marin, B, Borner, A. 2015. Genome-wide association mapping and biochemical markers reveal that seed ageing and longevity are intricately affected by genetic background and developmental and environmental conditions in barley. Plant, cell & environment 38: 1011–1022.

Nanda, AK, Pujol, V, Wissuwa, M. 2017. Patterns of stress response and tolerance based on transcriptome profiling of rice crown tissue under zinc deficiency. Journal of experimental botany 68: 1715–1729.

Olsen, LI, Palmgren, MG. 2014. Many rivers to cross: the journey of zinc from soil to seed. Frontiers in Plant Science 5: 30.

Ozturk, L, Yazici, MA, Yucel, C, Torun, A, Cekic, C, Bagci, A, Ozkan, H, Braun, H-J, Sayers, Z, Cakmak, I. 2006. Concentration and localization of zinc during seed development and germination in wheat. Physiologia plantarum 128: 144–152.

Palmgren, MG, Clemens, S, Williams, LE, Krämer, U, Borg, S, Schjørring, JK, Sanders, D. 2008. Zinc biofortification of cereals: problems and solutions. Trends in plant science 13: 464–473.

Peleg, Z, Saranga, Y, Yazici, A, Fahima, T, Ozturk, L, Cakmak, I. 2008. Grain zinc, iron and protein concentrations and zinc-efficiency in wild emmer wheat under contrasting irrigation regimes. Plant and Soil 306: 57–67.

Persson, DP, Hansen, TH, Laursen, KH, Schjørring, JK, Husted, S. 2009. Simultaneous iron, zinc, sulfur and phosphorus speciation analysis of barley grain tissues using SEC-ICP-MS and IP-ICP-MS. Metallomics 1: 418.

Phuke, RM, Anuradha, K, Radhika, K, Jabeen, F, Anuradha, G, Ramesh, T, Hariprasanna, K, Mehtre, SP, Deshpande, SP, Anil, G, Das, RR, Rathore, A, Hash, T, Reddy, BVS, Kumar, AA. 2017. Genetic Variability, Genotype × Environment Interaction, Correlation, and GGE Biplot Analysis for Grain Iron and Zinc Concentration and Other Agronomic Traits in RIL Population of Sorghum (*Sorghum bicolor* L. Moench). Frontiers in Plant Science 8: 712.

Pielot, R, Kohl, S, Manz, B, Rutten, T, Weier, D, Tarkowská, D, Rolčík, J, Strnad, M, Volke, F, Weber, H, Weschke, W. 2015. Hormone-mediated growth dynamics of the barley pericarp as revealed by magnetic resonance imaging and transcript profiling. Journal of experimental botany 66: 6927–6943.

Pinheiro de Carvalho, M. A. A., Bebeli, PJ, Bettencourt, E, Costa, G, Dias, S, Dos Santos, T. M. M., Slaski, JJ. 2013. Cereal landraces genetic resources in worldwide GeneBanks. A review. Agronomy for Sustainable Development 33: 177–203.

Pinson, S, Tarpley, L, Yan, W, Yeater, K, Lahner, B, Yakubova, E, Huang, X-Y, Zhang, M, Guerinot, ML, Salt, DE. 2015. Worldwide Genetic Diversity for Mineral Element Concentrations in Rice Grain. Crop Science 55: 294.

Podar, D, Scherer, J, Noordally, Z, Herzyk, P, Nies, D, Sanders, D. 2012. Metal selectivity determinants in a family of transition metal transporters. The Journal of biological chemistry 287: 3185–3196.

Pritchard, JK, Stephens, M, Donnelly, P. 2000. Inference of Population Structure Using Multilocus Genotype Data. Genetics 155: 945–959.

R Core Team. R: A language and environment for statistical computing. R Foundation for Statistical Computing, Vienna, Austria. http://www.R-project.org/.

Reuscher, S, Kolter, A, Hoffmann, A, Pillen, K, Krämer, U, Perovic, D. 2016. Quantitative Trait Loci and Inter-Organ Partitioning for Essential Metal and Toxic Analogue Accumulation in Barley. PLOS ONE 11: e0153392.

Ricachenevsky, FK, Menguer, PK, Sperotto, RA, Williams, LE, Fett, JP. 2013. Roles of plant metal tolerance proteins (MTP) in metal storage and potential use in biofortification strategies. Frontiers in Plant Science 4. 144.

Ruel-Bergeron, JC, Stevens, GA, Sugimoto, JD, Roos, FF, Ezzati, M, Black, RE, Kraemer, K. 2015. Global Update and Trends of Hidden Hunger, 1995-2011. The Hidden Hunger Index. PLoS ONE 10: e0143497.

Sandstead, H. 1991. Zinc deficiency. A public health problem? American Journal of Diseases of Children: 853–859.

Schroeder, JI, Delhaize, E, Frommer, WB, Guerinot, ML, Harrison, MJ, Herrera-Estrella, L, Horie, T, Kochian, LV, Munns, R, Nishizawa, NK, Tsay, Y-F, Sanders, D. 2013. Using membrane transporters to improve crops for sustainable food production. Nature 497: 60–66.

Senoura, T, Sakashita, E, Kobayashi, T, Takahashi, M, Aung, MS, Masuda, H, Nakanishi, H, Nishizawa, NK. 2017. The iron-chelate transporter OsYSL9 plays a role in iron distribution in developing rice grains. Plant molecular biology 95: 375–387.

Shahzad, Z, Rouached, H, Rakha, A. 2014. Combating Mineral Malnutrition through Iron and Zinc Biofortification of Cereals. Comprehensive Reviews in Food Science and Food Safety 13: 329–346.

Shi, J, Li, L, Pan, G. 2009. Variation of grain Cd and Zn concentrations of 110 hybrid rice cultivars grown in a low-Cd paddy soil. Journal of Environmental Sciences 21: 168–172.

Singh, J, Kanaujia, R, Srivastava, AK, Dixit, GP, Singh, NP. 2017. Genetic variability for iron and zinc as well as antinutrients affecting bioavailability in black gram (*Vigna mungo* (L.) Hepper). Journal of food science and technology 54: 1035–1042.

Singh, M. 2004. Role of micronutrients for physical growth and mental development. Indian journal of pediatrics 71: 59–62.

Sperotto, RA. 2013. Zn/Fe remobilization from vegetative tissues to rice seeds. Should I stay or should I go? Ask Zn/Fe supply! Frontiers in plant science 4: 464.

Sreenivasulu, N, Borisjuk, L, Junker, BH, Mock, H-P, Rolletschek, H, Seiffert, U, Weschke, W, Wobus, U. 2010. Barley Grain Development. In: Sreenivasulu, N, Borisjuk, L, Junker, BH, Mock, H-P, Rolletschek, H, Seiffert, U, Weschke, W, Wobus, U, eds. Barley Grain Development: Toward an Integrative View: Elsevier, 49–89.

Sreenivasulu, N, Graner, A, Wobus, U. 2008. Barley genomics. An overview. International journal of plant genomics 2008: 486258.

Suryawanshi, V, Talke, IN, Weber, M, Eils, R, Brors, B, Clemens, S, Krämer, U. 2016. Between-species differences in gene copy number are enriched among functions critical for adaptive evolution in *Arabidopsis halleri*. BMC genomics 17.

Tan, J, Wang, J, Chai, T, Zhang, Y, Feng, S, Li, Y, Zhao, H, Liu, H, Chai, X. 2013. Functional analyses of *TaHMA2*, a P(1B)-type ATPase in wheat. Plant biotechnology journal 11: 420–431.

Tauris, B, Borg, S, Gregersen, PL, Holm, PB. 2009. A roadmap for zinc trafficking in the developing barley grain based on laser capture microdissection and gene expression profiling. Journal of Experimental Botany 60: 1333–1347.

Tulchinsky, TH. 2010. Micronutrient Deficiency Conditions. Global Health Issues. Public Health Reviews 32: 243–255.

Uauy, C, Distelfeld, A, Fahima, T, Blechl, A, Dubcovsky, J. 2006. A NAC Gene regulating senescence improves grain protein, zinc, and iron content in wheat. Science 314: 1298–1301.

Ullrich, SE. 2011. Barley, production, improvement, and uses. Chichester, West Sussex, UK, Ames, Iowa: Wiley-Blackwell.

Varshney, RK, Paulo, MJ, Grando, S, van Eeuwijk, FA, Keizer, LCP, Guo, P, Ceccarelli, S, Kilian, A, Baum, M, Graner, A. 2012. Genome wide association analyses for drought tolerance related traits in barley (*Hordeum vulgare* L.). Field Crops Research 126: 171–180.

VSN International. 2013. GenStat for Windows 17th edition. Hemel Hempstead, UK: VSN International.

Warnes, GR, Bolker, B, Bonebakker, L, Gentleman, R, Huber, W, Liaw, A., Lumley, T., Maechler, M, Magnusson, A, Moeller, S, Schwartz, M, Venables, B. 2016. gplots: Various R Programming Tools for Plotting Data. R package version 3.0.1.

Waters, BM, Chu, H-H, Didonato, RJ, Roberts, LA, Eisley, RB, Lahner, B, Salt, DE, Walker, EL. 2006. Mutations in *Arabidopsis yellow stripe-like1* and *yellow stripe-like3* reveal their roles in metal ion homeostasis and loading of metal ions in seeds. Plant Physiology 141: 1446–1458.

Waters, BM, Sankaran, RP. 2011. Moving micronutrients from the soil to the seeds. Genes and physiological processes from a biofortification perspective. Plant Sci. 180: 562–574.

Waters, BM, Uauy, C, Dubcovsky, J, Grusak, MA. 2009. Wheat (*Triticum aestivum*) NAM proteins regulate the translocation of iron, zinc, and nitrogen compounds from vegetative tissues to grain. Journal of experimental botany 60: 4263–4274.

Welch, RM. 2002. Breeding strategies for biofortified staple plant foods to reduce micronutrient malnutrition globally. The Journal of Nutrition 132: 495S–499S.

Wessells, KR, Brown, KH. 2012. Estimating the global prevalence of zinc deficiency. Results based on zinc availability in national food supplies and the prevalence of stunting. PLoS ONE 7: e50568.

White, PJ, Broadley, MR. 2009. Biofortification of crops with seven mineral elements often lacking in human diets—iron, zinc, copper, calcium, magnesium, selenium and iodine. New Phytologist 182: 49–84.

WHO. The world health report 2002 - Reducing Risks, Promoting Healthy Life. Geneva, Switzerland: World Health Organization.

WHO. 2009. Global health risks: Mortality and burden of disease attributable to selected major risks. Mortality and burden of disease attributable to selected major risks. Geneva, Switzerland: World Health Organization.

Xu, Y, An, D, Li, H, Xu, H. 2011. Review. Breeding wheat for enhanced micronutrients. Canadian Journal of Plant Science 91: 231–237.

Xue, Y-F, Eagling, T, He, J, Zou, C-Q, McGrath, SP, Shewry, PR, Zhao, F-J. 2014. Effects of nitrogen on the distribution and chemical speciation of iron and zinc in pearling fractions of wheat grain. Journal of agricultural and food chemistry 62: 4738–4746.

Zhang, Y, Shi, R, Rezaul, KM, Zhang, F, Zou, C. 2010. Iron and zinc concentrations in grain and flour of winter wheat as affected by foliar application. Journal of agricultural and food chemistry 58: 12268–12274.

Zhao, F-J, Su, YH, Dunham, SJ, Rakszegi, M, Bedo, Z, McGrath, SP, Shewry, PR. 2009. Variation in mineral micronutrient concentrations in grain of wheat lines of diverse origin. Journal of Cereal Science 49: 290–295.

Zohary, D, Hopf, M, Weiss, E. 2012. Domestication of plants in the old world. The origin and spread of domesticated plants in South-West Asia, Europe and the Mediterranean basin. Oxford: Oxford Univ. Press.

III Anhang

i. Ergänzendes Material zu Manuskript 1: Spatially resolved analysis of variation in barley (*Hordeum vulgare*) grain micronutrient accumulation.

ii. Ergänzendes Material zu Manuskript 2: Temporal and spatial pattern of zinc and iron accumulation during barley (*Hordeum vulgare*) grain development.

iii. Ergänzendes Material zu Manuskript 3: The search for candidate genes associated with natural variation of grain Zn accumulation in barley.

iv. Stichwortliste zur Suche nach metall-bezogenen Genen zu Manuskript 3: The search for candidate genes associated with natural variation of grain Zn accumulation in barley.

v. Excel-Dokument mit Ergebnissen der Suche zu metall-bezogenen Genen zu Manuskript 3: The search for candidate genes associated with natural variation of grain Zn accumulation in barley.

Der Anhang ist dieser Doktorarbeit in Form einer CD beigelegt.

IV Danksagung

Wüßt ich genau, wie dies Blatt aus seinem Zweig herauskam,
schwieg ich auf ewige Zeit still, denn ich wüßte genug.

- Hugo von Hofmannsthal-

An einem wissenschaftlichen Thema zu arbeiten, bedeutet, sich im Detail mit einer Thematik auseinander setzen zu können, sich neuen Fragestellungen zu widmen und neue Erkenntnisse zu gewinnen. Über die Zeit, die ich mit meiner Doktorarbeit verbringen konnte, bin ich dankbar und denke an viele positive Momente zurück, für die ich meinen Wegbegleitern danken möchte. Ich möchte meinem Doktorvater Prof. Dr. Stephan Clemens danken, der bereits während meines Studiums meine Neugierde an der Forschung und meine Passion für Pflanzen gefördert hat. In zahlreichen Diskussionen und Gesprächen war er stets ein Mentor für mich, dessen Kompetenz und methodische Herangehensweise ich zum Vorbild nehme. Ich möchte des Weiteren Prof. Dr. Angelika Mustroph und Prof. Dr. Stefan Heidmann danken, die mir als Mentoren innerhalb des Graduiertenprogramms BayNAT mit hilfreichen Anregungen zu Seite standen. Für die schöne Zeit danken möchte ich meinen ehemaligen Kolleginnen und Kollegen des Lehrstuhls für Pflanzenphysiologie, darunter insbesondere meinen Labortisch-Nachbarinnen Christiane Meinen und Pia Schuster sowie Ursula Ferrera und Dr. Michael Weber, die immer zur Stelle waren. Besonderer Dank geht auch an meine ehemaligen Kolleginnen Paula Pongrac, Sina Fischer und Tanja Kühnlenz, die während meiner Doktorandinnenzeit zu Freundinnen und geschätzten wissenschaftlichen Ratgeberinnen wurden. Mit Freude denke ich auch an die zahlreichen Kooperationen während meiner Doktorarbeit zurück. Hierbei danke ich insbesondere den Kollegen der Abteilung für Pflanzen- und Umweltwissenschaften an der Universität Kopenhagen für die konstruktive Zusammenarbeit und die schöne Zeit während meines Forschungsaufenthalts.

Ein außerordentliches Dankeschön möchte ich an meine Familie richten. Meinen Eltern Lydia und Rupert danke ich von Herzen für ihre unentwegte und bedingungslose Unterstützung und Liebe. Ich möchte an meine Großeltern erinnern, die in Gedanken immer bei mir sind. Anna, ihrer Familie und meinen Freundinnen Anki und Anni danke ich für die schönen gemeinsamen Momente, die mich von meiner Arbeit ablenken konnten. Ein ganz besonderer Dank gilt meinem Mann Andreas, der mit viel Geduld nicht nur ein partnerschaftlicher, sondern auch ein wissenschaftlicher Berater während der letzten Jahre war. Durch die Geburt unseres Sohnes Valentin ist ein kleiner Sonnenschein in mein Leben getreten, der mir immer wieder hilft, meine Prioritäten im Leben neu zu ordnen. Der Halt und die zeitlichen Freiräume, die mir meine ganze Familie, darunter meine Schwiegereltern Brigitte und Anton, insbesondere in den letzten Jahren gaben, haben diese Doktorarbeit erst ermöglicht.

V (Eidesstattliche) Versicherungen und Erklärungen

(§ 9 Satz 2 Nr. 3 PromO BayNAT)

Hiermit versichere ich eidesstattlich, dass ich die Arbeit selbstständig verfasst und keine anderen als die von mir angegebenen Quellen und Hilfsmittel benutzt habe (vgl. Art. 64 Abs. 1 Satz 6 BayHSchG).

(§ 9 Satz 2 Nr. 3 PromO BayNAT)

Hiermit erkläre ich, dass ich die Dissertation nicht bereits zur Erlangung eines akademischen Grades eingereicht habe und dass ich nicht bereits diese oder eine gleichartige Doktorprüfung endgültig nicht bestanden habe.

(§ 9 Satz 2 Nr. 4 PromO BayNAT)

Hiermit erkläre ich, dass ich Hilfe von gewerblichen Promotionsberatern bzw. -vermittlern oder ähnlichen Dienstleistern weder bisher in Anspruch genommen habe noch künftig in Anspruch nehmen werde.

(§ 9 Satz 2 Nr. 7 PromO BayNAT)

Hiermit erkläre ich mein Einverständnis, dass die elektronische Fassung meiner Dissertation unter Wahrung meiner Urheberrechte und des Datenschutzes einer gesonderten Überprüfung unterzogen werden kann.

(§ 9 Satz 2 Nr. 8 PromO BayNAT)

Hiermit erkläre ich mein Einverständnis, dass bei Verdacht wissenschaftlichen Fehlverhaltens Ermittlungen durch universitätsinterne Organe der wissenschaftlichen Selbstkontrolle stattfinden können.

…….

Ort, Datum, Unterschrift